



UNIVERSITAT DE
BARCELONA

Identifying molecular mechanisms that determine resistance to CDK4/6 inhibitors in HER2-enriched advanced luminal breast cancer

Sara Gregorio Jordán

ADVERTIMENT. La consulta d'aquesta tesi queda condicionada a l'acceptació de les següents condicions d'ús: La difusió d'aquesta tesi per mitjà del servei TDX (www.tdx.cat) i a través del Dipòsit Digital de la UB (diposit.ub.edu) ha estat autoritzada pels titulars dels drets de propietat intel·lectual únicament per a usos privats emmarcats en activitats d'investigació i docència. No s'autoritza la seva reproducció amb finalitats de lucre ni la seva difusió i posada a disposició des d'un lloc aliè al servei TDX ni al Dipòsit Digital de la UB. No s'autoritza la presentació del seu contingut en una finestra o marc aliè a TDX o al Dipòsit Digital de la UB (framing). Aquesta reserva de drets afecta tant al resum de presentació de la tesi com als seus continguts. En la utilització o cita de parts de la tesi és obligat indicar el nom de la persona autora.

ADVERTENCIA. La consulta de esta tesis queda condicionada a la aceptación de las siguientes condiciones de uso: La difusión de esta tesis por medio del servicio TDR (www.tdx.cat) y a través del Repositorio Digital de la UB (diposit.ub.edu) ha sido autorizada por los titulares de los derechos de propiedad intelectual únicamente para usos privados enmarcados en actividades de investigación y docencia. No se autoriza su reproducción con finalidades de lucro ni su difusión y puesta a disposición desde un sitio ajeno al servicio TDR o al Repositorio Digital de la UB. No se autoriza la presentación de su contenido en una ventana o marco ajeno a TDR o al Repositorio Digital de la UB (framing). Esta reserva de derechos afecta tanto al resumen de presentación de la tesis como a sus contenidos. En la utilización o cita de partes de la tesis es obligado indicar el nombre de la persona autora.

WARNING. On having consulted this thesis you're accepting the following use conditions: Spreading this thesis by the TDX (www.tdx.cat) service and by the UB Digital Repository (diposit.ub.edu) has been authorized by the titular of the intellectual property rights only for private uses placed in investigation and teaching activities. Reproduction with lucrative aims is not authorized nor its spreading and availability from a site foreign to the TDX service or to the UB Digital Repository. Introducing its content in a window or frame foreign to the TDX service or to the UB Digital Repository is not authorized (framing). Those rights affect to the presentation summary of the thesis as well as to its contents. In the using or citation of parts of the thesis it's obliged to indicate the name of the author.

Universitat de Barcelona
Facultat de Farmàcia i Ciències de
l'Alimentació
Programa de doctorat en Biomedicina



Institut de Recerca
Biomèdica de Barcelona



Identifying molecular mechanisms that determine resistance to CDK4/6 inhibitors in HER2- enriched advanced luminal breast cancer

Memòria presentada per Sara Gregorio Jordan
per optar al grau de doctora per la Universitat de Barcelona

Barcelona, 2021

Doctoranda:
Sara Gregorio Jordan

Director:
Dr. Roger Gomis Cabré

Tutor:
Dra. Isabel Fabregat Romero

A mis padres,

por darme todas las oportunidades del mundo.

Agradecimientos

Hay mucha gente que quiero agradecer por haber compartido estos 5 años de tesis, con todo lo que ha comportado.

Primero de todo quiero agradecerle a Roger, porque sin aquella oportunidad hace 5 años hoy no sería doctora. De la experiencia en el laboratorio me llevo un gran crecimiento profesional y personal.

Agradecer también a mi tutora Isabel por su constante apoyo, siempre con disposición y amabilidad. Junto con Isabel, agradecer a los demás miembros de mi Comité de evaluación, Ángel y Raúl, por todos sus consejos y las magníficas discusiones sobre los giros de mi proyecto.

A mi colaboradora de proyecto, Fara. Fue una gran suerte compartir este proyecto contigo y haber podido trabajar codo con codo con una gran profesional como tú. Agradecer también a Aleix Prat por su disposición y su ayuda al inicio del proyecto. A Miguel por ayudarme una y otra vez en mis mil peticiones a la hora de analizar el screening. A Frank Supek agradecerle todos los conocimientos sobre el análisis de datos de CRISPR screens.

Uno de los mayores pilares de estos últimos 5 años ha sido mi equipo, el Metlab con todas sus formas. Desde el Metlab del inicio, por 2016, hasta el Metlab del final. Sin todas las risas, charlas y chupitos habría abandonado al segundo mes de tesis. A Alicia, que desde el segundo 1 estuvo en todos los pasos de este camino, quiero agradecerle el ponerme el camino un poquito más fácil, ya fuera con su ejemplo, con sus optimizaciones de protocolos o simplemente con un paseíto para desfogarnos hablando. Hay tantas cosas vividas que estos agradecimientos acabarían siendo tan largos como los de Henry. A Juanmi, el tercer puntito, agradecerle todos y cada uno de los cafés invertidos en cambiar el mundo y en conocernos mejor. No pude tener un mejor compañero de confianzas, fiestas de barrio y karaokes. A Fer agradecerle las risas y Teruel. Sin él acogiendo al 99% de los estudiantes y ayudándonos a los demás en todo lo que estuviera en su mano, el Metlab no habría sido lo mismo. A Mikel, nuestro cantautor particular, siempre con su motivación y sus hipocondrías al 100% agradecerte las risas y los pinchos, pero sobretodo el hit del verano UBE2S. A Marc y Esther, los dos papis del lab, sin vuestro constante apoyo durante estos años habría sido imposible esta tesis. Marc wiwi agradecerte todos y cada uno de los momentos en el estabulario, transformando el aburrimiento de estar ahí abajo en unos bailoteos buenos. Esther agradecerte todos y cada uno de tus consejos de vida, estoy segura que en los años que vengan pensaré mil veces en todo lo que me decías y me reiré mucho (creo). A Anna y Henry que, aunque os fuisteis hace millones de

años del lab parece que sigáis aquí. Me encanta vuestro constante buenrollismo y que estéis en todas. A Sylwia, por ser mi primera mentora y dejarme participar en su proyecto. A Jelena, por su constante calma y amabilidad, hicieron los primeros años de doctorado mucho más agradables. A Cris agradecerle las birris, las recomendaciones culinarias, las confidencias y las risas hablando de nuestras vidas. A Marc Nuñez agradecerle el enseñarme como se podían hacer las cosas de otra manera. Tu confianza en ti mismo y tus actos me han inspirado mucho a seguir mi criterio y confiar un poquito más en él. A Teresa agradecerle el no cansarse nunca de mis millones de interrupciones y siempre estar dispuesta a ayudarme con todo lo que puede. Te agradezco mucho que hayas aceptado seguir mi proyecto, no podría haberme ido así de tranquila si no estuvieras ahí, y creo que hablo en nombre del laboratorio cuando digo que sin ti el lab se hunde. A nos nuevos pipiolos del lab, Irene, Milos y Diogo, ahora el lab es vuestro así que espero que podáis mantener el legado de amistad, risas, chupitos y hablar sin tapujos, que aquí se comparte todo. Me habría gustado compartir más cosas con vosotros y enterarme de la vida de Diogo, pero seguro que seguiremos en contacto. A Aintzane, Xabi, Xavi, Jovana, Miri, Ra, María, Laura, Ieva y Patrizia, cada uno con sus miles de historias que hacían mucho más interesantes las comidas. Espero no dejarme a nadie, aunque seguro que algún estudiante de Fer me estoy olvidando. Cada una de las personas que han pasado por el Metlab durante estos años han dejado una huella bonita en mi corazón y eso no tiene precio.

A todos los compañeros del IRB con los que empecé el doctorado hace una eternidad. He tenido el placer de veros evolucionar, cada uno encontrando su camino poco a poco. Ha sido increíble compartir esta experiencia con vosotros. Chiquitos personajes, nos queda un viaje pendiente. A Marina, con sus ganas y sus incontables movidas, el IRB era mejor encontrándome contigo cada dos por tres por los pasillos. A Joel, podríamos llamarle mi bro del IRB, con saber que siempre tenía un compañero de penurias y cotilleos si lo necesitaba ya era más que suficiente para aguantar los peores momentos. A Isita (Isis para los amigos), desde el primer momento tus bromas y locuras han sido un sitio donde ampararse entre tanto doctorado. A la Lore, por nuestros debates sobre ciencia y sobre la vida. A Enric, por todos los momentos compartidos durante estos años y por saber que siempre tendría un buen amigo. A Edu, por su constante buen humor debido a las power naps. A Marcos y Maria agradecereros vuestro apoyo con las NKs, saber que podía discutir con vosotros mis resultados y mis dudas me dio un gran punto de apoyo para seguir adelante durante los primeros meses. Nuestro Immunology Club fue algo muy bonito que creamos y de lo que estoy muy orgullosa. A Adrian agradecerle su pasión por la ciencia, en parte creo que esa pasión fue uno de los motivos que me decidió a hacer un doctorado en cáncer. A Clara, por todos esos cafés hablando de

ciencia, arte y vida. A Leyre por ser mi punto de referencia durante toda la tesis. Y añadir que una cool off no era lo mismo sin ti. A toda la gente que dedicó un ratito de su tiempo a ayudarme con mis dudas y darme apoyo. Marta y Josep, sin vuestra experiencia poner a punto el CRISPR screen habría costado el triple. Eli y Vero, saber que si me hacía falta cualquier cosa podía ir a mendigaros y que haríais cualquier cosa para ayudar, lo hacía todo mucho más llevadero. Hay muchísimas más personas que me encantaría agradecer individualmente, pero se hace imposible.

A toda la gente de las facilities de estadística, microscopia, genómica, citometría, massas e histología agradeceros las incontables horas que dedicasteis para ayudarme. Sin toda esa ayuda esta tesis no habría podido ver la luz. Especialmente quiero agradecerles a Camille y Jaume por todos sus esfuerzos en comprender lo que quería hacer y brindarme toda su ayuda para que pudiera llegar a conseguirlo.

A mis mindundis, han pasado muchos años y aún seguimos comiendo juntos de vez en cuando, espero que siga siendo así por muchos años más.

A mis otros dos pilares durante esta tesis, Irene y Paula. Por todos esos momentos de desfogue, de consejos, de empatía, os tengo que dar las gracias. A Gemma, que junto a Irene soportaron todos mis altibajos durante tres años de tesis y me apoyaron en todos mis momentos de bajón. Os quiero chicas. A Esther y Llor por compartir sus experiencias y escuchar mis progresos durante la tesis. A Susana, Laura M, Laura R y Marina por animarme a cada paso y darme cada una su punto particular. A Gabri porque, aunque nos veamos poco, siempre has estado y siempre estás ahí. A Samu agradecerle todas las horas de teléfono, los viajes, las risas y el apoyo durante estos años. A Sara agradecerle ser tan bonita y loca, y que cada vez que nos vemos sea como volver a estar juntas viviendo en Utrecht.

A mis padres, por habérmelo dado todo sin pedir nada a cambio. Nunca podré agradeceros suficiente todo el apoyo recibido por vuestra parte. A mi hermana, a la que poco a poco voy conociendo más y con la que puedo hablar de cualquier cosa. Al resto de mi familia por sus constantes ánimos y sobre todo a mis abuelas, por contarle a todo el mundo lo orgullosas que están porque su nieta está curando el cáncer. No habrás podido estar el día de la defensa yaya, pero sé que sigues orgullosa de mí.

A mis pequeños, los tres gatitos más bonitos del universo, por ser tan adorables que me quitan las penas (función crucial durante estos años).

Y a ti Xu, gracias por todo.

Table of contents

Summary	11
Resumen	13
List of abbreviations	17
Introduction	21
1. Breast Cancer.....	23
1.1 Physiopathology of the mammary gland	23
1.1.1 <i>Mammary gland: structure and development</i>	23
1.1.2 <i>Hormone control</i>	25
1.1.3 <i>Estrogen function in homeostasis and BCa</i>	27
1.2 Breast cancer tumorigenesis and progression	28
1.3 Breast cancer classification	29
2 Metastasis.....	33
2.1 The metastatic cascade.....	33
2.2 Metastatic patterns.....	37
2.2.1 <i>Organ specificity</i>	37
2.2.2 <i>Metastatic latency</i>	39
2.2.3 <i>Molecular subtype evolution through metastasis</i>	41
3 Breast Cancer Treatment	43
3.1 Local intervention.....	43
3.2 Systemic interventions.....	44
3.2.1 <i>Chemotherapy</i>	44
3.2.2 <i>Hormone therapy</i>	44
3.2.3 <i>Targeted therapy</i>	46
3.2.4 <i>Immunotherapy</i>	47
4 CDK4/6 inhibitors in Breast Cancer.....	49
4.1 Mechanisms of resistance to CDK4/6 inhibitors	49
4.1.1 <i>Cell cycle specific mechanisms</i>	49

4.1.2	<i>Cell cycle non-specific mechanisms</i>	52
4.2	FGFRs in breast cancer treatment resistance	55
4.2.2	FGFR-driven CDK4/6i resistance	56
4.2.3	Targeting FGFR to overcome CDK4/6i resistance	57
4.3	Molecular subtype in ER+/HER2-negative BCa treatment.....	58
4.3.2	Sensitivity to chemotherapy.....	59
4.3.3	Sensitivity to CDK4/6 inhibitors.....	59
Objectives		63
Methods		65
Materials		79
Results		85
Chapter 1.....		89
Identification of CDK4/6i gene drivers using CRISPR/Cas9 KO screen and clinical data analysis.		89
Chapter 2.....		101
Integration of the CDK4/6i resistance driver candidates from the CRISPR/Cas9 KO screen and clinical data analysis.....		101
Chapter 3.....		107
Validation of XXXX-driven CDK4/6i resistance		107
Chapter 4.....		117
Characterization of the XXXX-driven mechanism that induces CDK4/6i resistance		117
Discussion		125
Conclusions		137
Bibliography		141
Supplementary Tables		177

Summary

Breast Cancer (BCa) is the most prevalent cancer among women worldwide. It is a very heterogeneous disease at the histological, molecular and clinical level. Consequently, different classifications are used for stratifying patients. The histopathological classification is used in patient clinical management. It is based on the expression of three different markers: Estrogen receptor (ER) and progesterone receptor, both hormone receptors, and the human epidermal growth factor receptor 2 (HER2). Recent technical advances have developed a novel classification based on the gene expression profile of the tumors. Four intrinsic molecular subtypes are defined by the expression of 50 specific genes, this gene signature is called PAM50. Accordingly, BCa is classified in Luminal A, Luminal B, HER2-enriched (HER2-E) and Basal-like. These subtypes have critical differences in incidence, survival and response to treatment and have a predictive and prognostic value at the treatment level. The histopathological classification and the molecular classification are independent.

In February 2015, the FDA approved a new drug for postmenopausal women with metastatic ER+/HER2-negative BCa, CDK4/6 inhibitors (CDK4/6i). CDK4/6 are serine-threonine kinases that have a key role in cell cycle regulation by allowing S phase progression. These inhibitors have provided clinical improvement in terms of progression-free survival and overall survival compared with endocrine therapy alone. CDK4/6i are now standard of care for treating metastatic ER+ BCa patients. PAM50 has been used to predict benefit from CDK4/6i in retrospective analysis of clinical trials. According to these retrospective analyses, CDK4/6i are only beneficial in luminal A and B. Thus, HER2-E tumors, which were a big proportion of treated tumors, did not benefit from CDK4/6i.

Understanding mechanisms responsible for primary or secondary resistance to CDK4/6i in advanced ER+ BCa is crucial to improve patient outcome. We aim to identify new candidate genes responsible for resistance to palbociclib (CDK4/6i) treatment in the HER2-E intrinsic subtype of ER+/HER2- BCa by combining an unbiased CRISPR-Cas9-based genome-wide screening approach and the analysis of clinical data.

To approach this question, we characterized CDK4/6i response in ER+ BCa cell lines. We determined ER+ BCa cell lines that are palbo-resistant or palbo-sensitive based on palbociclib IC50. Next, we subjected the palbo-resistant cell lines to CRISPR-cas9 sgRNA pooled genome-wide screening. We identified different genes that confer resistance to palbociclib *in vitro*. In parallel to the unbiased CRISPR/Cas9 knock-out screening, we interrogated which genes were associated with worse response to CDK4/6i using two different patient cohorts (CDK patient cohort and CORALEEN data set). We integrated all

the data and we identified eleven common genes out of the three analyses. Nine out of the eleven genes were related to cell cycle progression machinery such as E2F1 and CCNE1, whereas the other two genes were membrane molecules associated with signal transduction. We selected one of these membrane molecules for further validation based on its tight association with HER2-E molecular subtype.

High expression of this gene was associated with worst progression-free survival and overall survival in the CDK patient cohort. The patients that had progression disease presented a higher mRNA level of this resistance driver. Similar observations were found in samples from the CORALEEN clinical trial. Patients that did not respond to CDK4/6i treatment showed an increased expression of this gene. At the cellular level, different *in vitro* strategies were followed to determine the effect of the expression of this gene in palbociclib response. We developed acquired resistant cell lines from palbo-sensitive MCF7 cells and used them to validate our candidate. Moreover, loss- and gain-of-function approaches confirmed the association of this gene with an increased resistance to palbociclib treatment.

Finally, we study how mechanistically this gene drives resistance to palbociclib. To this end, we interrogated alterations in gene expression of different genes after silencing this membrane protein in different cell lines. We detected reduced CCNE1 expression levels. CCNE1 gene was identified through the CRISPR/Cas9 screen and it was associated with no response and progression disease in both CDK and CORALEEN patient cohorts. Importantly, when we silenced CCNE1 in ZR75 cells we successfully increased CDK4/6i sensitivity. In addition, we optimized a proximity-dependent labeling approach, BioID, in order to describe the interactome of our gene of interest in parental and acquired resistant MCF7 cells. We found interesting downstream signaling transducers to further analyzed as a mechanism of action.

In conclusion, we succeed identifying a new driver of CDK4/6i resistance in ER+/HER2-negative advanced BCa classified as HER2-E molecular subtype.

Resumen

El cáncer de mama es el tipo de cáncer más prevalente en mujeres en todo el mundo. Es una enfermedad heterogénea a nivel histológico, molecular y clínico. En consecuencia, tenemos diferentes clasificaciones para estratificar las pacientes de cáncer de mama. La clasificación histopatológica es una de las más utilizadas en el manejo clínico del paciente. Se basa en la expresión de tres marcadores diferentes: receptor de estrógeno (ER, por sus siglas en inglés) y receptor de progesterona, ambos receptores de hormonas, y el receptor del factor de crecimiento epidérmico humano 2 (HER2, por sus siglas en inglés). Los avances técnicos recientes han desarrollado una clasificación novedosa basada en el perfil de expresión génica de los tumores. Esta clasificación molecular diferencia cuatro subtipos moleculares intrínsecos, definidos por la expresión de 50 genes específicos (firma genética llamada PAM50). En consecuencia, el cáncer de mama se clasifica en Luminal A, Luminal B, HER2-enriched (HER2-E) y Basal-like. Estos subtipos tienen diferencias críticas en incidencia, supervivencia y respuesta al tratamiento y tienen un valor predictivo y pronóstico a nivel de tratamiento. La clasificación histopatológica y la clasificación molecular son independientes.

En febrero de 2015, la FDA aprobó un nuevo fármaco para mujeres posmenopáusicas con cáncer de mama metastásico ER+/HER2-negativo, los inhibidores de CDK4/6 (CDK4 / 6i). CDK4/6 son serina-treonina quinasas que tienen un papel clave en la regulación del ciclo celular al permitir la progresión a la fase S. Estos inhibidores han proporcionado una mejora clínica en la supervivencia de las pacientes en comparación con la terapia endocrina como monoterapia. Los CDK4/6i son ahora un tratamiento estándar para las pacientes con cáncer de mama metastásicos ER+/HER2-negativo. PAM50 se ha utilizado para predecir el beneficio al tratamiento con CDK4/6i en análisis retrospectivos de diferentes ensayos clínicos. Según estos análisis retrospectivos, CDK4/6i solo es beneficioso en tumores con subtipo molecular Luminal A y B. Por lo tanto, los tumores con subtipo molecular HER2-E, que constituyen una gran proporción de los tumores tratados, no se beneficiaron del tratamiento con CDK4/6i.

Comprender los mecanismos responsables de la resistencia a CDK4 / 6i en cáncer de mama metastásico ER+/HER2-negativo es crucial para mejorar el resultado de las pacientes. Nuestro objetivo es identificar nuevos genes responsables de la resistencia al tratamiento con palbociclib (un CDK4/6i) en tumores de cáncer de mama ER+/HER2-negativos con subtipo molecular HER2-E mediante la combinación de un enfoque de cribado de todo el genoma basado en CRISPR-Cas9 y el análisis de datos clínicos.

Para abordar esta pregunta, caracterizamos la respuesta a CDK4/6i en líneas celulares tumores de cáncer de mama ER+. Determinamos qué líneas celulares ER + BCa son palbo-resistentes o palbo-sensibles basandonos en la IC50 de palbociclib. A continuación, sometimos las líneas celulares resistentes a palbociclib a un cribado de todo el genoma usando la tecnología CRISPR-Cas9. Identificamos diferentes genes que confieren resistencia a palbociclib *in vitro*. En paralelo al cribado de CRISPR/Cas9, interrogamos qué genes estaban asociados con una peor respuesta a CDK4/6i utilizando dos cohortes de pacientes diferentes (cohorte de pacientes CDK y conjunto de datos del ensayo clínico CORALEEN). Integramos todos los datos e identificamos once genes comunes de los tres análisis. Nueve de los once genes estaban relacionados con la maquinaria de progresión del ciclo celular, como E2F1 y CCNE1, mientras que los otros dos genes eran moléculas de membrana asociadas con la transducción de señales intracelulares. Seleccionamos una de estas proteínas de membrana para validar su función en generar resistencia a CDK4/6i basándonos en su estrecha asociación con el subtipo molecular HER2-E.

Altos niveles de este gen se asociaron a peor supervivencia en la cohorte de pacientes CDK. Los pacientes que tenían enfermedad en progresión presentaron un nivel de ARNm de este gen más elevado. Se encontraron observaciones similares en muestras del ensayo clínico CORALEEN. Los pacientes que no respondieron al tratamiento con CDK4/6i mostraron un aumento de la expresión de nuestro gen de interés. A nivel celular, se siguieron diferentes estrategias *in vitro* para determinar el efecto de la expresión de este gen en la respuesta de palbociclib. Desarrollamos líneas celulares con resistencia adquirida a palbociclib a partir de células MCF7 sensibles y las usamos para validar nuestro candidato. Además, los enfoques de pérdida y ganancia de función confirmaron la asociación de nuestro candidato con una mayor resistencia al tratamiento con palbociclib.

Finalmente, estudiamos el mecanismo por el cual este gen induce la resistencia a palbociclib. Con este fin, investigamos las alteraciones en la expresión génica de diferentes genes después del silenciamiento del gen en diferentes líneas celulares. Detectamos niveles reducidos de expresión de CCNE1 al silenciar nuestro candidato. El gen CCNE1 se identificó mediante el cribado CRISPR/Cas9 y se asoció con resistencia a CDK4/6i y con progresión de la enfermedad en ambas cohortes de pacientes CDK y CORALEEN. Es importante destacar que cuando silenciamos CCNE1 en células ZR75 aumentamos la sensibilidad a CDK4/6i. Además, optimizamos un enfoque de marcaje por proximidad, BioID, para describir el interactoma del gen que genera resistencia a CDK4/6i en células MCF7 parentales y con resistencia adquirida. Encontramos proteínas interesantes que participan en la

transducción de señales intracelulares. Estos mecanismos tienen que ser analizarlos más a fondo.

En conclusión, logramos identificar un nuevo mecanismo de resistencia a CDK4/6i en cáncer de mama metastásico ER+/HER2-negativo con el subtipo molecular HER2-E.

List of abbreviations

ACT	Adoptive cell transfer
AI	Aromatase inhibitors
ANGPTL4	Angiopoietin-like 4
AP-1	Adaptor Related Protein Complex 1
ATF	Activating Transcription Factor
BBB	Blood-brain barrier
BCa	Breast cancer
BFDR	Bayesian false discovery rate
BioID	Proximity-dependent biotin identification
BRCA1/2	Breast cancer type 1/2 susceptibility protein
CCNE1	G1/S-specific cyclin-E1
CDK	Cyclin-dependent kinase
CDKN2A	Cyclin Dependent Kinase Inhibitor 2A
CNA	Ncopy number alterations
CRC	Colorectal cancer
CSF-1	Colony-stimulating factor-1
CTC	Circulating tumor cell
CTLA-4	Cytotoxic T-lymphocyte-associated protein 4
DTC	Disseminated tumor cell
E2	Estrogen
ECM	Extracellular matrix
EGFR	Epidermal growth factor receptor
EGFR	Epidermal growth factor
EMT	Epithelial-to-mesenchymal
ER	Estrogen receptor
ERE	Estrogen response element
ERK	Extracellular Signal-Regulated Kinase
FDR	False discovery rate
FGFR	Fibroblast growth factor receptor
FISH	Fluorescent <i>in situ</i> hybridization
FOXA1	Hepatocyte nuclear factor 3-alpha
FOXC1	Forkhead box C1
FSH	Follicle-stimulating hormone
GH	Growth hormone
GnRH	Gonadotropin-releasing hormone
GRB2	Growth factor receptor bound 2

GSK3 β	Glycogen Synthase Kinase 3 Beta
HCC	Hepatocellular carcinoma
HDAC	Histone deacetylase
HER2	Human epidermal growth factor 2
HER2-E	HER2-enriched
HNSCC	Head and neck squamous carcinoma
HR	Hormone receptor
HT	Hormone therapy
IFN	Interferon
IGF-I	Insulin-like growth factor-1
IHC	Immunohistochemistry
IL-6/8	Interleukin 6/8
IP	Immunoprecipitation
KLB	Klotho proteins
KRT	Keratine
LH	Luteinizing hormone
LumA	Luminal A
LumB	Luminal B
mAb	Monoclonal antibodies
MAF	v-maf avian musculoaponeurotic fibrosarcoma oncogene homolog
MAPK	Mitogen-Activated Protein Kinase
METABRIC	Molecular Taxonomy of Breast Cancer International Consortium
MMP	Metalloproteinases
MS	Mass spectrometry
mTORC1	Mammalian target of rapamycin complex 1
NK	Natural Killer
OS	Overall survival
PARP	Poly ADP-ribose polymerase
PCG1 α	Peroxisome proliferator-activated receptor-gamma coactivator
PD-L1	Programmed cell death ligand 1
PDX	Patient-derived xenograft
PDX	Patient-derived xenograft
PFS	Progression-free survival
PI3K	Phosphoinositide 3-kinase
	Phosphatidylinositol 4,5-bisphosphate 3-kinase catalytic subunit
PIK3CA	alpha isoform
PLA	Proximity ligation assay
PLC	Phospholipase C
POSTN	Periostin

PR	Progesterone receptor
PTHLH	Parathyroid hormone-related protein
RAF	Rapidly accelerated fibrosarcoma
RARRES3	Retinoic Acid Receptor Responder 3
RAS	Rat Sarcoma Viral Oncogene Homolog
RB	Retinoblastoma Protein
ROR	Risk of relapse
SAM	Significance analysis of microarrays
SERDs	Selective estrogen receptor degraders
SERMs	Selective estrogen receptor modulators
sgRNA	Single guide RNA
shRNA	Short hairpin RNA
SOX2/9	SRY-Box Transcription Factor 2/9
SRC	Proto-oncogene tyrosine-protein kinase Src
STAT3	Signal Transducer and Activator Of Transcription 3
TCGA	The cancer genome atlas
TEB	Terminal end bud
TGF- β	Transforming Growth Factor Beta
TKI	Tyrosine kinase inhibitors
TN	Triple negative
TP53	Cellular tumor antigen p53
UBE2T	Ubiquitin-conjugating enzyme E2 T
VEGF	Vascular Endothelial Growth Factor
WHO	The World Health Organization

- Introduction -

1. Breast Cancer

Breast Cancer (BCa) is the most commonly diagnosed cancer among women worldwide. According to GLOBOCAN2020, female BCa is the leading cause of global cancer incidence in 2020, surpassing lung cancer. It represents 11.7% of all cases with 2.3 million estimated new cases. It is the fifth leading cause of cancer mortality with 6.9%, translated to 685.000 deaths. BCa represents 1 in 4 cancer cases and 1 in 6 cancer deaths among women, with the highest incidence and mortality in most of the countries.

In Spain, 32.953 new cases of BCa were estimated in 2020. One every eight Spanish women will develop BCa (www.Seom.org). Highest incidence is above 50 years old, but around 10% of the cases are diagnosed in women under 40 years old. BCa relative survival after 5 years is 89.2%, hugely influenced by the stage of diagnosis. Early detection and advances in treatment lead to a high survival rate, however when metastasis is present at the time of diagnose (stage IV), the picture is completely different. The survival in tumors diagnosed at stage I is more than 98%, whereas in tumors at stage IV it decreases to 24%. BCa can be detected by physical examination, mammography, ultrasound, magnetic resonance imaging, blood studies and biopsy.

BCa is a complex disease, hugely heterogeneous at various levels, representing a challenge for researchers and clinicians. What determines the aggressiveness of the tumors? Could we find biomarkers that allow us to predict the spread of tumor cells around the body? Which tumors will respond to the treatments and which ones will develop resistance? Many questions are still unsolved and urge to be addressed. In this thesis we aim to tackled some of these in order to better understand why and how some patients develop resistance to specific treatments.

1.1 Physiopathology of the mammary gland

1.1.1 Mammary gland: structure and development

The mammary gland is a glandular tissue responsible for the production and secretion of milk during lactation. Both males and females have a similar glandular tissue within the breasts after birth and during the first years. However, female's mammary gland begins to develop during puberty in response to ovarian hormone signaling, mainly estrogen (E2) and progesterone.

The main structure of the mammary gland consists in a branching duct system and the fat pad tissue that covers the ducts (Figure I1A). Ducts are formed by two layers building a tubular structure: a myoepithelial cell layer surrounding a monolayer of

differentiated luminal epithelial cells that grow forming a tube (Figure I1B). These tubes flow to the terminal end bud (TEB), the proliferative part of the duct that penetrates the fat pad and allows the elongation of the ducts (Robinson, 2007). Mammary gland stem cells are located in this region and allow the dynamic changes that occur during female puberty and pregnancy. TEB consists of 2 cell types arranged in two layers: inner epithelial layer (body cells) and outer undifferentiated

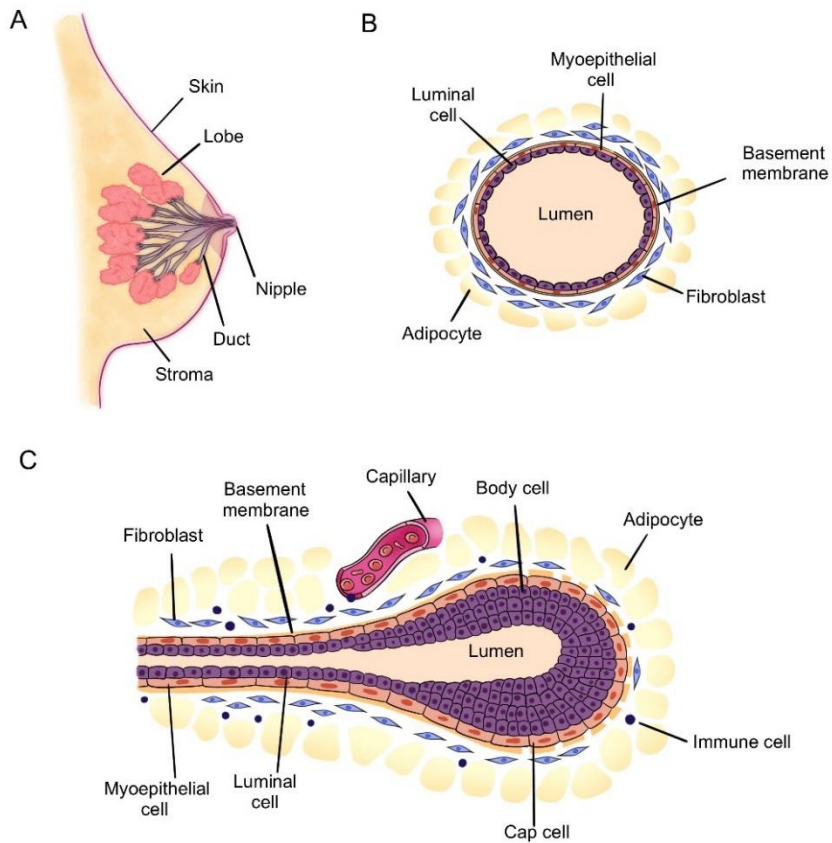


Figure I1. Organization and cellular structure of the mammary gland.

(A) Breast illustration showing the basic structure of the mammary gland. This exocrine gland is formed by 15-20 lobes that produce and secrete milk through a duct system to the nipple. The lobes and the ducts are covered by the mammary fat pad (stroma). (B) Duct section representation. The duct is formed by a monolayer of luminal cells surrounded by a myoepithelial cells layer. This structure is supported by a basement membrane dividing the ducts from the surrounding stroma. The stroma is mainly composed by fibroblasts, adipocytes and cells from the immune system. (C) TEB representation during duct extension. In the TEB the luminal cells that were forming the duct become body cells and the myoepithelial cells, the cap cells. The vasculature is important during mammary gland expansion. Adapted from Ali and Coombes, 2002 and Fu *et al.*, 2020.

cap cells that will develop in myoepithelial cells (Hinck and Silberstein, 2005) (Figure 11C).

Once the branching system has developed after puberty, the mammary glands keep stable with minor changes during menstrual cycle until pregnancy. Pregnancy induces a massive remodeling in the gland: the TEBs extend, generating new branches and developing alveolar buds where the production of milk will occur during lactation (Hennighausen and Robinson, 1998). Alveolar cells produce milk into the lumens, where the contractile force of myoepithelial cells drives the secretion through the ducts. Alveoli group forming lobes and each mammary gland can have between 15 to 20 lobes, that secrete milk to the nipple. During pregnancy and lactation, alveoli can increase 10-fold and new lobes are formed until the whole breast is filled with the epithelial tree (Russo and Russo, 2004). Once the nursing period is finished, the mammary epithelial cells undergo a massive apoptotic process, leading to the involution of the tissue in order to return to a pre-pregnancy state. The dynamism of the mammary gland morphology, including cycles of growth and involution, increases the susceptibility of epithelial cells to acquire new mutations and consequently, experience transformation. Additionally, the ability of the mammary gland to induce angiogenesis makes it suitable for malignant selection. Good vascularization is key to avoid early involution and apoptosis during pregnancy and lactation, leading to an adequate microenvironment for tumor cells to adapt (Ali and Coombes, 2002; Smalley and Ashworth, 2003; Sternlicht, 2006; Warburton *et al.*, 1982; Wiseman and Werb, 2002). The mammary gland stroma is formed by different cell types including fibroblasts, adipocytes, immune cells, hematopoietic cells and neurons (Hennighausen and Robinson, 1998; Hennighausen and Robinson, 2005; Tiede and Kang, 2011). Stromal cells have been found to create a supportive niche used by malignant cells to favor tumor outgrowth, induce vascularization and avoid immune surveillance (Finak *et al.*, 2008).

1.1.2 Hormone control

Development and homeostasis of the mammary gland is under strict hormonal control by both ovarian and pituitary hormones. The menstrual cycle is driven by the hypothalamus-pituitary-ovary axis (Figure 12). First, hypothalamic neurons produce gonadotropin-releasing hormone (GnRH), that activates gonadotropic cells in the pituitary gland to secrete follicle-stimulating hormone (FSH) and luteinizing hormone (LH). These two factors stimulate the release of E2 and progesterone by ovaries, the amount of secreted hormones vary depending on the day of the

menstrual cycle. E2 and progesterone induce the elongation and branching of the duct system through the mammary fat pad.

Growth hormone (GH) produced by the pituitary gland is another important player regulating both ovarian and pituitary hormonal control during pubertal ductal growth. Its function is mainly mediated by IGF-I production in mammary stromal cells. IGF-I affects the surrounding epithelial cells in a paracrine manner triggering the formation of TEB and ductal morphogenesis (Cannata et al., 2010; Kleinberg, 1998; Walden et al., 1998).

During pregnancy, the formation of alveoli is stimulated by progesterone and prolactin secreted by the ovaries and the pituitary gland, respectively. Both hormones are induced by the release of E2 and, at the same time activate the expression of

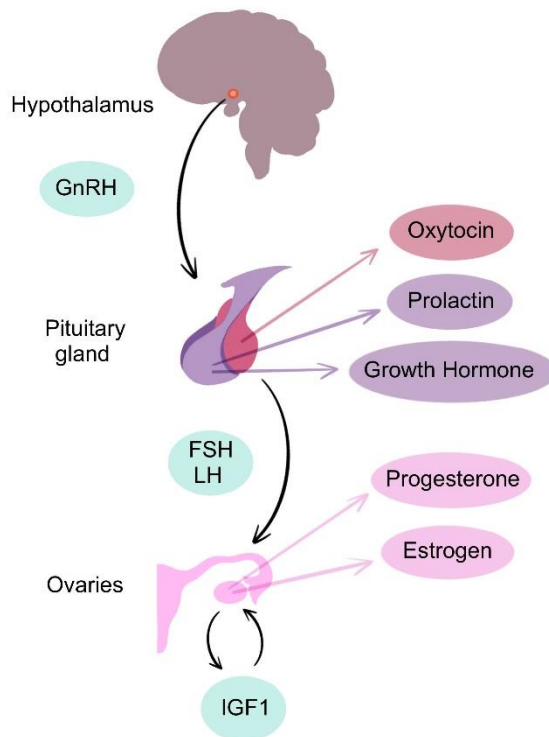


Figure I2. The hypothalamus-pituitary-ovary axis.

Graphic representation of the hormone secretory system during mammary gland development. The hypothalamus secretes GnRH, stimulating the anterior pituitary gland to release FSH and LH. Gonadotropins are responsible for E2 and progesterone production by the ovaries. GH, prolactin and oxytocin are three hormones secreted by the pituitary gland that play a important function during development and pregnancy. Finally, IGF-I induces a paracrine regulation for the ovary secretory function. Adapted from Brisken and O'Malley, 2010.

estrogen receptor (ER), generating a positive feedback loop and enhancing ductal expansion. Until birth, lactation is prevented with progesterone blocking of prolactin signaling. After birth, high progesterone levels start to decrease allowing prolactin function in alveogenesis and milk production. With the suckling of the baby, the pituitary gland secretes oxytocin facilitating the ejection of the milk by contracting myoepithelial cells that surround the ducts and the alveoli (Brisken and O'Malley, 2010). Once the baby stops suckling, prolactin secretion decreases inducing luminal cell death and mammary gland involution to a pre-pregnancy state (Hennighausen and Robinson, 2005; Wagner *et al.*, 1997).

The hormone crosstalk has a key role in proper mammary gland development during puberty and pregnancy. The importance of hormones is not limited to the homeostasis of the normal mammary gland, since they have a huge impact in cell transformation and tumor development. Some BCa tumors develop dependence on hormone function to facilitate their growth and expansion.

1.1.3 Estrogen function in homeostasis and BCa

Mammary epithelial cells need E2 for proper division during development of the gland during puberty and pregnancy. E2 is secreted mainly by the ovaries of premenopausal females, but other tissues have also the capacity to synthesize this hormone. Adipose tissue, bone, vasculature, smooth muscle and the brain can keep the E2 production after menopause, but to a lower extent. Epithelial cells of the mammary gland express two main receptors for E2: ER α and ER β , which are encoded by ESR1 and ESR2, respectively. Although ER β plays a role in organization, adhesion and differentiation of mammary epithelial cells, its expression is not necessary for ductal growth (Förster *et al.*, 2002). ER α is essential for ductal elongation, branching and alveolar formation (Mueller *et al.*, 2002), thus it will be referred as ER during this thesis. E2 is a cholesterol-based molecule that can pass through cellular membranes to bind ER receptors. When the receptor binds to E2 it dimerizes and goes to the nucleus. The complex is recruited to small palindromic DNA motifs called estrogen response elements (ERE) that can be found in many gene promoters and enhancer regions. When ER binds these regions, it facilitates the recruitment of transcription regulatory proteins. Transcription outcome depends on the coactivators or corepressors that partner with ER.

Changes in the hormonal status such as late menopause (Barnard *et al.*, 2015; Howell *et al.*, 2014; Sun *et al.*, 2017), use of birth control contraceptives, menopausal hormone replacement therapy or early menarche have been associated with increased risk of developing BCa (Britt, 2012), which indicates an important role of E2 in BCa

tumorigenesis. Proliferation induced by E2, together with the generation of genotoxic metabolites from E2 metabolism, can result in increased DNA replication damage and mutations that lead to uncontrolled growth (Reviewed in Yager and Davidson, 2006). The overexpression of ER in most of BCa tumors and their dependency in E2 signaling for proliferation and survival make these tumors extremely sensitive to hormonal therapy.

1.2 Breast cancer tumorigenesis and progression

Carcinomas are the result of uncontrolled growth in epithelial cells of the ducts or lobes and they comprise most of the tumors generated in the mammary tissue. Sarcomas develop from mutations in stromal cells such as myofibroblasts and blood vessel cells and they constitute less than 1% of total primary BCa tumors. Clinicians can classify carcinomas based on their invasiveness relative to the primary tumor site, presenting differences in prognosis and treatment. These tumors can be divided into three major subgroups: non-invasive (*in situ*), invasive and metastatic BCa (Veronesi et al., 2005). These groups correspond to the evolution of the tumor through the accumulation of genetic and epigenetic changes. The hyperproliferation of luminal epithelial cells that are confined in a specific location (the duct or the lobe) produces an *in situ* hyperplasia (atypical ductal hyperplasia) that can develop into a pre-neoplastic phase (ductal carcinoma *in situ*) limited by the basal membrane (Figure I3). Eventually, there is a rupture of the basal membrane and the subsequent invasion of the adjacent tissue (invasive ductal carcinoma) (Rivenbark et al., 2013). In the most aggressive tumors, malignant cells can spread through the circulatory system and

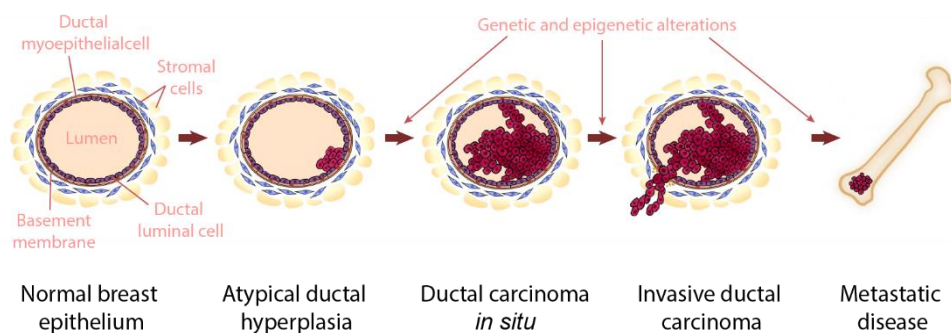


Figure I3. Stages of BCa progression.

Histological stages that BCa undergo to produce a metastatic disease. The acquisition of genetic and epigenetic alterations induces the tumor progression from an early stage called atypical ductal hyperplasia to a ductal carcinoma. First, the carcinoma grows limited by the basement membrane, but eventually cells break the layer towards an invasive phenotype. Ultimately, malignant cells reach a distant tissue and generate a secondary tumor. Adapted from Kothari *et al.*, 2018.

migrate to distant organs generating metastasis (Allison, 2012; Polyak, 2007). The sequential steps presented above when translated to the clinic present a lot of heterogeneity in their histological characteristics. The World Health Organization (WHO) currently classifies pre-malignant lesions and invasive BCa in different histological subtypes defined by their morphology, together with clinical, epidemiological and molecular characteristics (Sinn and Kreipe, 2013).

BCa initiation is normally due to sporadic mutations or genomic alterations in different oncogenes or tumor suppressor genes. However, around 5-10% of BCa tumors are linked to inherited gene mutations. The most common hereditary mutated genes in BCa are *BRCA1* and *BRCA2* genes (Thull and Vogel, 2004). Both genes are tumor suppressor genes that play an essential role in DNA repair by homologous recombination (Narod and Foulkes, 2004). Additionally, *BRCA1* plays a role in other cell processes to maintain genomic integrity during cell cycle. *BRCA1* mutation rises the probability to develop BCa to 55-65%, whereas if *BRCA2* gene is mutated the increase is up to 45% (Kuchenbaecker et al., 2017; Rebbeck et al., 2018).

1.3 Breast cancer classification

The intrinsic clinical and biological heterogeneity of BCa have led clinicians to develop different classifications to stratify patients. In patient clinical management, the expression of hormone receptors (HR) (ER and progesterone receptor (PR)), and Human epidermal growth factor receptor 2 (HER2) are commonly used as biomarkers to assess four main histopathological-based groups: HR- positive and HER2-negative (HR+/HER2-negative), HR-positive and HER2-positive (HR+/HER2+), HR-negative and HER2-positive (HR-negative/HER2+) and triple negative (TN).

In the histopathological classification, the hormonal status of the tumor is determined by the expression of ER and PR assessed by immunohistochemistry (IHC) in tumor samples. Clinicians consider HR+ those tumors with at least 1% of the malignant cells with a positive nucleus for ER or PR staining. The expression of these molecules is crucial to determine if a patient will benefit or not from endocrine therapy (Hammond et al., 2010). They are considered luminal tumors and are the most frequent tumors diagnosed.

The second main histopathological biomarker is HER2. HER2 is an EGFR family member encoded by *ERBB2* proto-oncogene that triggers uncontrolled proliferation. When HER2 IHC staining is positive for more than 10% of the cells, a fluorescent *in situ* hybridization (FISH) is performed to check the copy number of

ERBB2 gene in each nucleus. If the *ERBB2* amplification ratio is more than 6 copies per cell, the tumor is considered HER2+. These tumors are very aggressive, however when monoclonal antibodies against HER2 were developed as a therapeutic strategy, the overall survival (OS) for HER2+ patients completely changed.

TN subtype is a very heterogeneous group, and it includes tumors lacking the expression of HR or the amplification of HER2 signal. TN is the most aggressive subtype with the highest early relapse rate.

Advances in gene expression profiling techniques have allowed a deeper understanding of BCa biology. Parker and colleagues defined a clinically applicable gene expression-based test, called PAM50 that stratified BCa tumors based on their molecular phenotype (Parker et al., 2009). Five different intrinsic molecular subtypes of BCa have been characterized based on the relative expression of 50 genes related to ER function (luminal cluster), HER2 pathway, proliferation and genes associated with the basal phenotype. The five subtypes are Luminal A (LumA), Luminal B (LumB), HER2-Enriched (HER2-E), Basal-like and Claudin-low. They added a sixth group, Normal-like, to include those samples containing few to no tumor cells and therefore discern normal tissue from malignant samples. The five intrinsic subtypes have shown differences in incidence, prognosis and treatment response, providing additional predictive information beyond histopathological classification (Cheang et al., 2012, 2015; Aleix Prat et al., 2013).

At the expression level, **LumA and B** differ from each other specifically in two main biological pathways: cell cycle genes related with proliferation and hormone-regulated pathways. Compared to LumB, LumA shows a lower expression of proliferation genes such as *CCNE1* and *UBE2T* and a higher luminal-related gene profile with genes such as *PR* and *FOXA1*, except for *ER* whose levels are similar in both subtypes. At the DNA level, LumA and B also show a different profile, being LumB the subtype presenting a higher rate of mutations and chromosomal copy number alterations (CNA) (Prat *et al.*, 2015).

HER2-E subtype is defined by the high expression of HER2 signaling-related genes and the proliferation cluster, intermediate expression of luminal-related genes and a low expression of the basal cluster. The DNA of HER2-E tumors present the highest rate of mutations, as an example *TP53* is mutated in 72% of the patients and *PIK3CA* in 39%. Most of HER2-E classified tumors present HER2 amplification (68%), however there are tumors HER2-E according to PAM50 that show no amplification nor overexpression of HER2.

Basal-like tumors show high expression of the proliferative cluster, keratins (KRT) associated with the basal layer of the epithelium (*KRT5*, 14 and 17), medium

expression of HER2-related genes and very low luminal-related gene expression. Basal-like tumors also show a high mutation rate across the genome, being *TP53* the most recurrent mutated gene (80% of the tumors). *BRCAl*-mutated BCa is mainly classified as Basal-like disease and the majority of Basal-like tumors show a global hypomethylation of the genome.

Claudin-low subtype is characterized by the enrichment in epithelial-to-mesenchymal transition (EMT) markers, immune response genes and cancer stem cell-like phenotype, combined with the low to no expression of luminal-related genes. Most of the claudin-low tumors are poor prognosis invasive TN BCa tumors. In the clinical context, it is extensively used the basal-like molecular subtype to define these tumors. Considering the resemblance between the basal-like and claudin-low subtype, in this thesis we consider four intrinsic subtypes when mentioning PAM50 molecular classification.

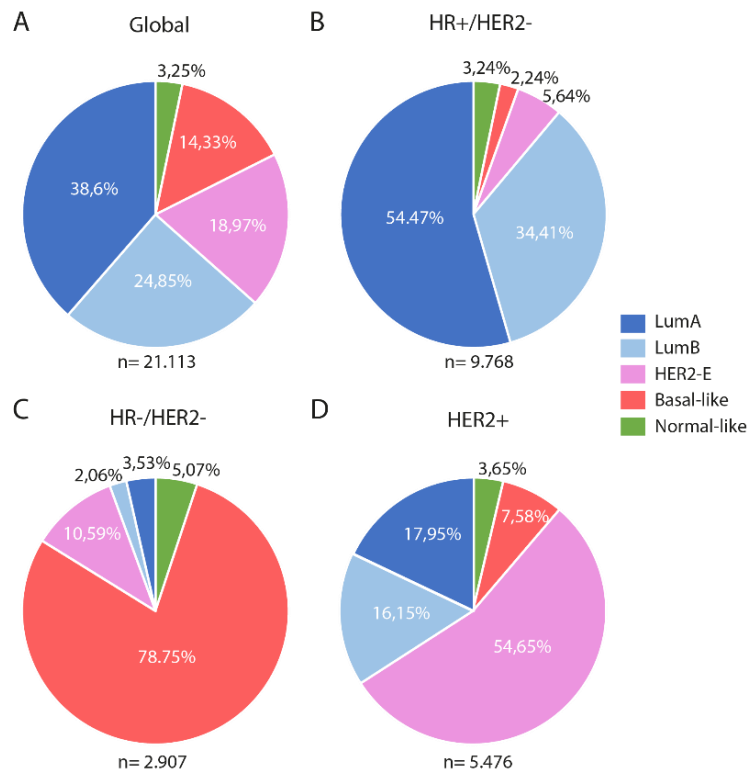


Figure I4. Intrinsic subtype distribution within IHC-based groups.

(A) Molecular subtypes distribution in all the samples of the cohort (21.113 samples). (B) Intrinsic subtypes in HR+/HER2-negative by histopathological classification. (C) Intrinsic subtypes in HR-/HER2-negative by histopathological classification. (D) Intrinsic subtypes in HER2+ (including both HR+/HER2+ and HR-/HER2+) by histopathological classification. Amplified data from Cejalvo *et al.* (2018).

PAM50 has been used to identify the molecular subtypes in a large number of studies. A meta-analysis from 31 independent cohorts (21.113 samples) determined the concordance between histopathological classification (by IHC evaluation for HR and/or FISH for HER2) and intrinsic molecular subtypes (by PAM50). Each tumor was classified with both systems (Figure I4A). Interestingly, this meta-analysis pointed out that both classifications are independent, and they should be considered individually. The four molecular subtypes were found in each histopathological group in different proportions, highlighting the heterogeneity of BCa disease. In the luminal tumors (HR+/HER2-negative), HER2-E (5,64%) and basal-like (2.24%) molecular subtypes were identified (Figure I4B). Similar results were found in TN tumors (HR-/HER2-negative), where HER2-E (10.59%), LumA (3.53%) and LumB (2.06%) were present (Figure I4C). The highest heterogeneity was found in HER2+ tumors (including samples HR+/HER2+ and HR-/HER2+), with only 54.65% of them identified as HER2-E (Figure I4D, Prat *et al.*, 2013).

The majority of BCa tumors that are newly diagnosed are classified as luminal BCa. Thanks to endocrine therapy, these tumors present good prognosis after treatment. However, between 10-15% of them develop resistance and relapse (Dowsett *et al.*, 2010). PAM50 assessment has showed predictive value when determining the benefit that luminal BCa patients have from hormone therapy in adjuvant setting, indicating a new path for a more personalized treatment based of the gene expression of each tumor (Harris *et al.*, 2016).

2 Metastasis

Advances in detection, prevention, risk stratification and therapeutic strategies against BCa primary tumors have prompted important improvements in reducing mortality and cancer relapse. However, overt metastasis persists on being the major cause of cancer-related death (Senkus et al., 2015). Advanced BCa is still an incurable disease and the median OS is around 3 years, with a 5-year survival reached only in 25% of the patients (Cardoso et al., 2018). The metastatic process encompasses a series of stochastic events that lead the malignant cells spread from the primary tumor to a distant organ. The disseminated tumor cells (DTCs) acquire different abilities that enable them to finally produce a clinically detectable metastasis. Biological, genetic and clonal heterogeneity of cancer cells in the primary and secondary tumor, together with the complex tumor-microenvironment interactions are the main limitations that research in metastasis face (Chambers et al., 2002). In addition, the distinct organ-tropism and time-specificity of this sequence of events introduces a new perspective of complexity that needs to be untangled. Addressing the molecular, cellular, genetic and clinical mechanisms underlying metastatic progression is key to develop new therapies to prevent and treat this complex disease.

2.1 The metastatic cascade

Millions of cancer cells are shed into the bloodstream by malignant tumors. However, many patients never experience relapse nor have clinical disease for a long period. Researchers have found a big amount of circulating tumor cells (CTC) in patients' blood at early stages of the disease, but only a fraction of patients will develop an overt metastasis, indicating that the successful rate for distant colonization is very low. This suggests that metastasis is a very inefficient process. The estimation reported in animal models indicates that only the 0,02% of the tumors cells entering circulation will be able to finally form a secondary tumor in a distant tissue (Cameron et al., 2000; Luzzi et al., 1998). DTC will have to confront adverse environments, adapt and colonize the host organ in order to form clinically relevant lesions.

Malignant cells have to overcome a restrictive bottleneck in a process named the metastatic cascade (Gupta and Massagué, 2006; Massagué and Obenauf, 2016; Valastyan and Weinberg, 2011). During the metastatic cascade, only cells phenotypically prepared are able to form an overt metastasis, driving clonal selection. This complex procedure has been simplified in a sequence of basic steps (Figure I5): (1) migration to the adjacent tissue, (2) intravasation into the blood vessels, (3)

immune system avoidance and survival through the circulatory system, (4) arrest at a distant site, (5) extravasation in the new host tissue, (6) survival in a hostile environment (micrometastasis) and (7) formation of a secondary lesion (macrometastasis).

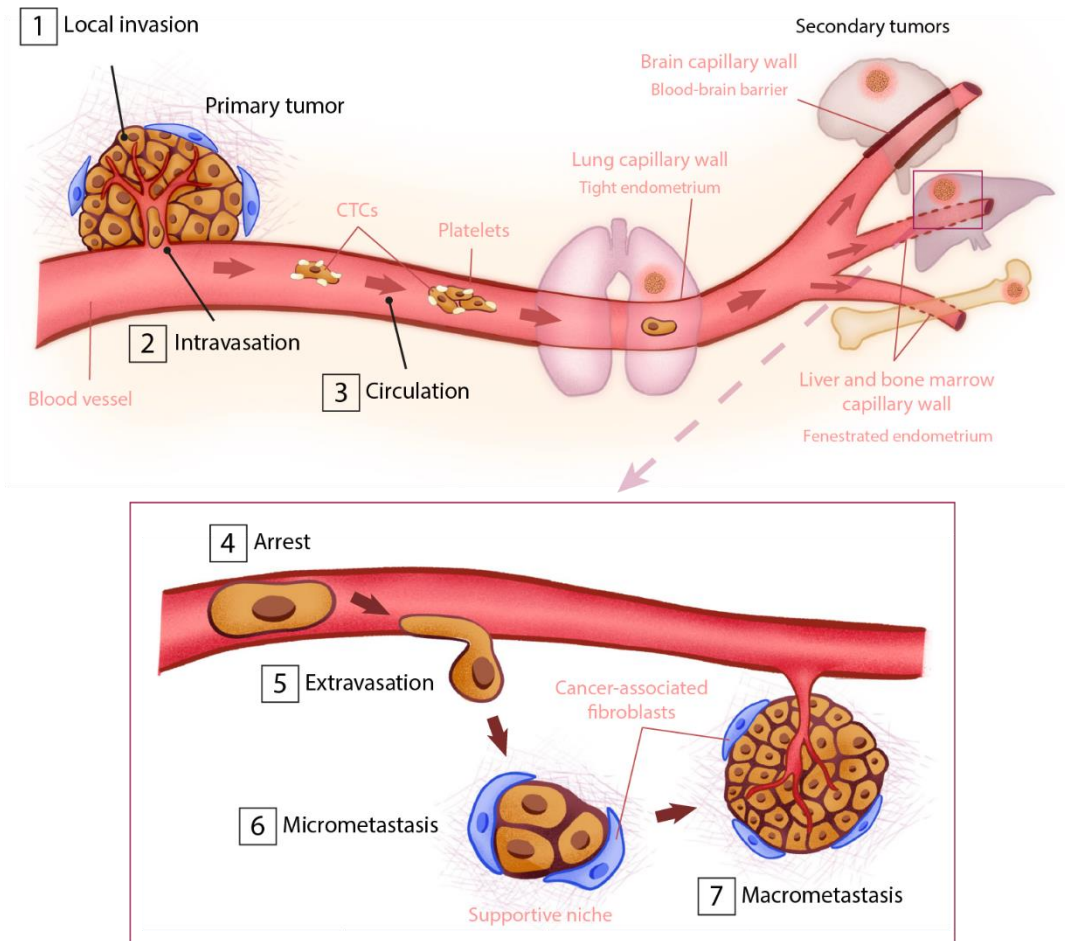


Figure I5. The metastatic cascade.

Schematic representation of the different steps that the malignant cells achieve during the metastatic colonization. Cells from the primary tumor develop migration capacities in order to invade adjacent tissue (1) and intravasate to the circulatory system (2). CTCs survive to the bloodstream mechanical forces and the immune system surveillance (3) to reach different distant organs such as lungs, brain, liver or bones. CTCs get arrested at distant capillaries (4) and extravasate in the new tissue (5). Then, the cell starts growing with the help of the new metastatic niche and form a micrometastasis (6). The final step of this process is the macrometastasis formation (7) after completely adapt to the new environment. Adapted from Massagué and Obenauf, 2016.

Changes in the cellular motility give metastatic cells the advantage to start invading adjacent tissue. The mechanisms that allow the cell to migrate from the primary tumor niche and enter the circulation have been widely studied (Chaffer and Weinberg, 2011; Nguyen *et al.*, 2009). A mixture of cytoskeleton reorganization (Hall, 2009), disruption of adhesive interactions between cells and the secretion of extracellular-matrix (ECM) remodelers like metalloproteinases (MMPs) and cathepsins (Kessenbrock *et al.*, 2010) let the cell infiltrate through the surrounding tissue.

Different migration dynamics used by tumor cells have been reported to influence in this step. Cancer cells can travel as single cells opening a path through the ECM, taking advantage of collagen fibers. They can also migrate as a group forming a tumor invasion front, showing a cooperative behavior (Friedl and Gilmour, 2009). The malignant cells also stimulate the generation of tumor-associated blood microvessels through a process called angiogenesis (Folkman, 2002), allowing the cell to reach more easily the circulatory system.

The tumor-associated stroma, composed by endothelial cells, leukocytes, macrophages, fibroblasts and bone-marrow progenitors, can actively support tumor growth and invasion by promoting neo-angiogenesis, immunosuppression and local inflammation (Kalluri and Zeisberg, 2006; Mantovani *et al.*, 2008; Qian and Pollard, 2010). This cell network have been found to release cell-signaling proteins such as TGF- β , driving malignant cells to undergo EMT (Celià-Terrassa and Jolly, 2020; Giampieri *et al.*, 2009; Seoane and Gomis, 2017). EMT is a development program inactive in differentiated cells that can be exploited by tumor cells. EMT allows malignant cells to change strong adhesions with neighbor cells and switch epithelial polarization in order to gain motility and invasiveness (Celià-Terrassa *et al.*, 2012; Mani *et al.*, 2008; Tsuji *et al.*, 2008). Moreover, EMT can promote the induction of a stem-cell phenotype. The reversion of EMT in the distant organ, named mesenchymal-to-epithelial transition (MET), can promote colonization and growth in the distant organ, maintaining their tumor-initiating ability and stemness (Celià-Terrassa and Kang, 2018). However, some studies suggest that EMT is not necessary for metastasis despite contributing to the aggressiveness by increasing the resistance to different therapies (Fischer *et al.*, 2015; Zheng *et al.*, 2015). Epidermal growth factor (EGF) and colony-stimulating factor (CSF)-1 secreted by perivascular macrophages of the mammary tumor also support tumor cell invasion (Wyckoff *et al.*, 2007).

Once the cancer cell enters the bloodstream, it is exposed to intense mechanical forces, the surveillance of the innate immune system and oxidative stress. There is massive cell death during this step, but CTCs develop different strategies to survive.

It has been shown that CTCs can associate with platelets to trick the innate immunity (Gay and Felding-Habermann, 2011; Gupta and Massagué, 2006; Joyce and Pollard, 2009; Labelle *et al.*, 2011; Malladi *et al.*, 2016). They can also experience reversible metabolic changes to cope with oxidative stress (Le Gal *et al.*, 2015).

CTCs may exit the circulatory system when they get trapped in small capillary beds with insufficient diameter to let them flow through. Tumor cells can either start growing in the lumen to form an embolus that will eventually disrupt the microvessel or penetrate vascular walls in order to extravasate in a distant tissue. Platelets can help supporting extravasation of CTCs to secondary sites (Gay and Felding-Habermann, 2011; Massagué and Obenauf, 2016). Each organ has a particular parenchyma which facilitates or not tumor extravasation. Bone and liver have fenestrated vessels with gaps between cells called sinusoids. In these organs the malignant cells can easily penetrate increasing the incidence of metastasis (Aird, 2007). In organs where the endothelial wall is a physical barrier, the CTC secretes different factors, such as angiopoietin-like-4 (ANGPTL4) or parathyroid hormone-related protein (PTHrP), to increase the permeability of the capillary (Padua *et al.*, 2008; Urosevic *et al.*, 2014). The most difficult organ to access is the brain because of the additional boundary of the blood-brain barrier (BBB) that protects the central neural system from variations in blood composition (Bos *et al.*, 2009). To this, cancer cell may acquire specific functions (Valiente *et al.*, 2014).

Migration through the circulatory system and colonization of the distal organ are pivotal steps of the metastatic cascade where most of the cells die. Unlike the primary tumor niche, the new environment is hostile to CTCs (Cameron *et al.*, 2000), being major players in metastatic blockade cytotoxic T cells and natural killer (NK) cells. In experiments with mice where researchers depleted the immune function of cytotoxic T cells or NK cells, the metastatic outgrowth was increased (Bidwell *et al.*, 2012; Smyth *et al.*, 1999). Therefore, the specific immune-cell composition of an organ can determine the organ's susceptibility to secondary lesions. Consequently, immunotherapy has been reported to have different outcomes depending on which metastatic organ is targeted (Sharma and Allison, 2015).

In order to overcome all the obstacles found in the new organ, CTCs suffer molecular signaling changes such as increasing SRC tyrosine kinase or p38 and ERK MAPK signaling pathways (Aguirre-Ghiso *et al.*, 2003; Zhang *et al.*, 2009) that help them adapt to the new environment. CTCs create a secondary niche by secreting components related with stem-cell niches which allows them to home, survive and finally generate a new tumor. BCa cells that metastasize to the lung have been found to produce tenascin C, an ECM protein that amplifies Notch and Wnt signaling (Oskarsson *et al.*, 2011). Metastasis suppressor genes such as RARRES3 or PCG1 α

repress stem-cell-like phenotype (Morales et al., 2014; Torrano et al., 2016), whereas the expression of genes such as SOX2 and SOX9 transcription factors allows the cells to interact with the microenvironment and increases metastatic burden (Malladi et al., 2016). BCa DTCs can also stimulate the secondary niche stroma (fibroblasts) by means of TGF- β signaling to produce periostin (POSTN), partner of tenascin C, which recruits Wnt molecules and therefore increases Wnt pathway activation in tumor cells (Malanchi et al., 2011). Tumor cells educate the new host stromal cells in order to survive and successfully form a secondary lesion.

The induction of a supporting niche development may occur before the arrival of the malignant cells to the distant organ, the pre-metastatic niche. Experimental models have shown that primary tumor contributes to prime the secondary niche by secreting systemic signals before the CTCs arrive (McAllister and Weinberg, 2014). In diverse cancer types this priming can be achieved through the production of different mediators, such as inflammatory cytokines (Cox *et al.*, 2015; Urosevic *et al.*, 2014, 2020), exosomes (Peinado et al., 2012) and ECM remodelers that recruit bone-marrow-derived cells to pre-condition the tissue for CTCs (Wculek and Malanchi, 2015).

DTCs show different growth dynamics in the new host tissue. Tumor cells with tumor-initiation properties can expand immediately, however others may get arrested and remain dormant for a period of time (days, months or even years) in a process called metastatic latency (Section 2.2.2 Metastatic latency).

In summary, metastasis is a complex, heterogeneous and inefficient process. Although researchers have described many mechanisms used by malignant cells during the metastatic cascade, many details of the process remain unknown.

2.2 Metastatic patterns

The different steps of the metastatic cascade are found, to a certain degree, common in most types of carcinomas. Interestingly, the place to metastasis and the kinetics of the process depends on the primary tumor characteristics.

2.2.1 Organ specificity

Different cancer types show different tropisms when metastasizing. The organ tropism of metastasis has been extensively debated in the cancer field. In 1928, James Ewing pointed at the circulatory system as the factor that determines the malignant cell spread, but the theory could not fully explain the patterns reported in research

and in the clinic (“Neoplastic Diseases: A Treatise on Tumours. By James Ewing, A.M., M.D., Sc.D., Professor of Pathology at Cornell University Medical College, N.Y.; Pathologist to the Memorial Hospital. Third Edition. Royal 8vo. Pp. 1127, with 546 Illustrations. 1928. Phil,” 1928). Organs with comparable vascular and lymphatic circulation presented different colonization behaviors among different tumor types. One hypothesis developed to explain this disparity was the “seed and soil” theory by Stephen Paget. This hypothesis compared the effect of the metastatic site supporting malignant cells growth with the way that fertile soil favors the growth of seeds (Fidler, 2003; Paget, 1989). Intrinsic cancer features and the crosstalk of malignant cells with the microenvironment of the new tissue are factors that Paget proposed to be crucial for the metastatic process. However, even though some environments are less harmful to DTCs than others, all the host tissues are potentially harmful to malignant cells.

Circulation patterns and the structure of the vasculature influence CTCs extravasation. However, in each organ CTCs will find different physical barriers, vascular and nutrient availability and stromal composition (Budczies *et al.*, 2015; Disibio and French, 2008).

Depending on the organ of origin, the metastatic process has a predominant pattern behavior: some cancer types spread preferentially to one organ (e.g. prostate cancer to the bone or pancreatic cancer to the liver); other types have sequential organ-specific colonization (e.g., colorectal cancer (CRC) generally colonize the liver first and then the lungs (Urosevic *et al.*, 2014)). There is a third group that can colonize different organs either sequentially or at the same time, which is the case of BCa, lung cancer or melanoma (Budczies *et al.*, 2015; Chen *et al.*, 2017).

In BCa, different BCa tumor subtypes colonize distinct organs. ER- BCa tumors (basal-like and HER2-E) spread first to extraskelatal tissue and lately to the bone, whereas ER+ BCa tumors (mainly lumA and B) have preference to form bone metastasis, followed by extraskelatal tissues metastasis (Figure I6)(Kennecke *et al.*, 2010; Soni *et al.*, 2015).

Gene expression patterns in the primary tumor have been found to predict the organ where the metastasis will occur. In ER- BCa tumor, the expression of a group of specific genes, called lung metastasis signature, in the primary tumor was associated with increased lung metastatic burden and reduced bone colonization (Minn *et al.*, 2005; Morales *et al.*, 2014). On the other hand, there are gene expression profiles in the primary tumor associated with bone metastasis such as cell adhesion proteins and proteins involved in the FGFR-MAPK signaling pathway (Kang *et al.*, 2003; Smid *et al.*, 2006). 16q23 gain CNA was also associated with bone metastasis after analyzing

primary BCa tumors. Within the amplified region associated with bone metastasis, the v-maf avian musculoaponeurotic fibrosarcoma oncogene homolog (MAF) transcription factor was found to be the driver of bone colonization in ER+ BCa patients (Pavlovic et al., 2015). Additionally, MAF expression levels were found to predict likelihood of benefit from the bisphosphonate treatment zoledronic acid.

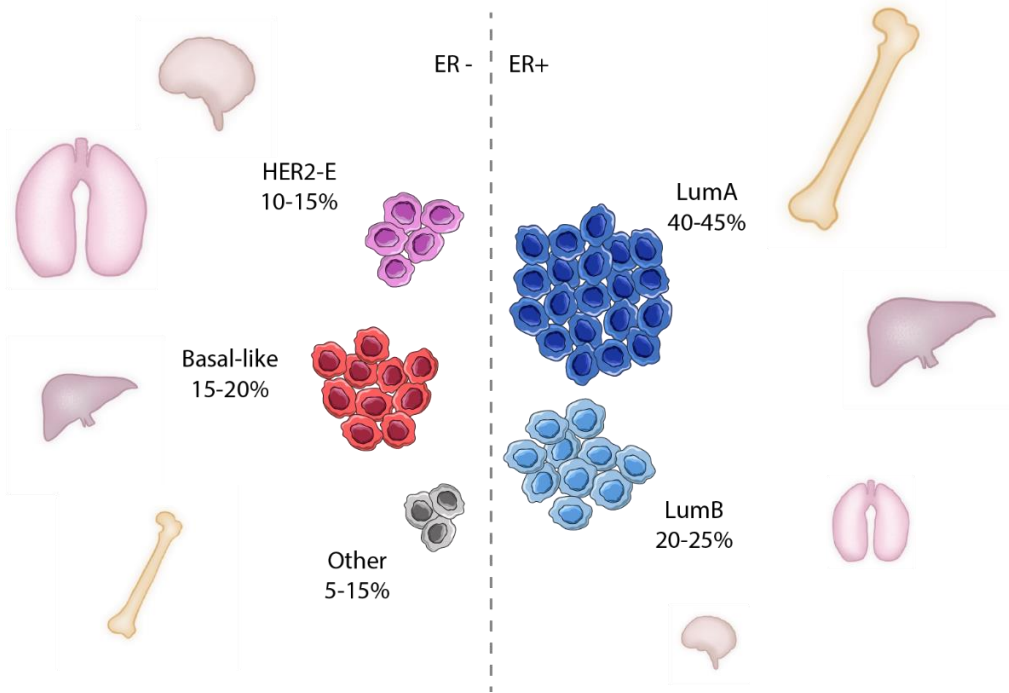


Figure 16. Organ specificity patterns in BCa metastasis.

Depending on the ER status, metastasis appear more frequently in certain organs. In ER- BCa primary tumors, metastasis normally appear in extraskelatal tissues. However, in ER+ BCa primary tumors, metastasis is usually developed in the bone and secondly in extraskelatal tissues. Adapted from Kennecke *et al.*, 2010.

Zoledronic acid is used to inhibit bone resorption in BCa patients, avoiding metastatic niche formation in the bone tissue (Coleman *et al.*, 2017; Coleman *et al.*, 2005; Paterson *et al.*, 2021).

2.2.2 Metastatic latency

Tumor latency or dormancy has been defined as the period of time compressed between the primary tumor detection and the metastatic relapse. When the metastasis will occur highly depends on the tumor type (Gomis and Gawrzak, 2017). Most aggressive cancer types show a short latency period with a high relapse frequency

linked with an increased mortality following diagnosis. Lung cancer is an example of a short metastatic latency. The interval time comprises few weeks, leaving a 2-year survival of 35% (Howlander et al., 2020). This type of tumors acquires metastatic traits fast, leading to massive malignant cell dissemination and multiple distant organ colonization. Medium latency periods are observed in colorectal tumors with a sequential metastasis to liver and lungs. The majority of recurrences in CRC are diagnosed within the first 3 years after treatment in advanced tumors (Nguyen et al., 2009), with a 5-year survival rate of 65% (Siegel *et al.*, 2017). Finally, a known example for long latent cancer type is prostate cancer, with 97% of patients surviving 10-years from diagnose (Siegel *et al.*, 2020). These differences in metastatic time window suggest that how the malignant traits for succeeding in distant organ colonization are acquired may differ among tumor types. Whereas in lung cancer this capacity is probably obtained already in the primary tumor, enabling a rapid overtake of the distant organ; in prostate cancer DTCs need time to adapt and gain the functions that allow tumor initiation and expansion to form overt metastasis in the secondary site. Therefore, in long latent metastasis the microenvironment that the DTC encounters in the new organ will play a very important role in the acquisition of these functions (Gomis and Gawrzak, 2017; Obenauf and Massagué, 2015).

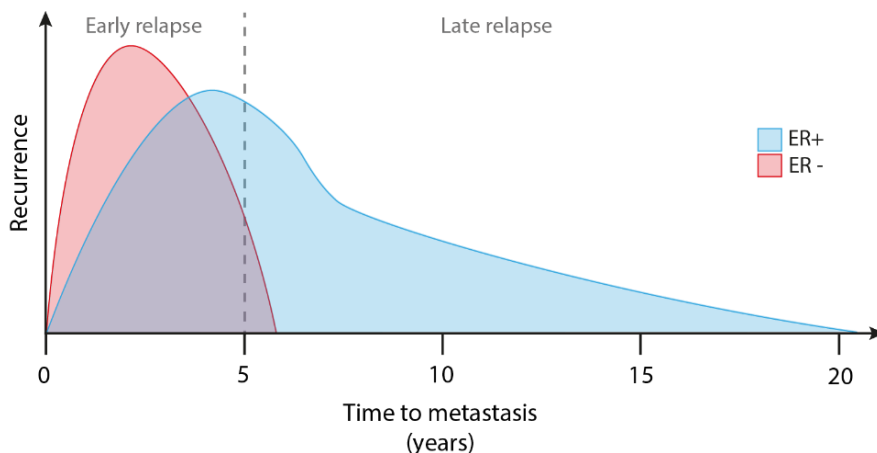


Figure 17. Different time-to-metastasis depending on the hormonal status of the tumor in BCa.

ER- BCa metastasis normally develop in a time window of 5 years (early relapse), whereas ER+ BCa metastasis can relapse early or late (after 5 years from tumor resection and treatment). Dashed line shows the threshold of 5 years between early and late relapse. Adapted from Gomis and Gawrzak, 2017.

BCa metastasis can be considered both medium and long latent disease (Figure I7). Time of diagnose of BCa metastasis after the primary tumor resection can vary. This time window depends on the ER status, volume, stage and molecular subtype of the primary tumor (Gomis and Gawrzak, 2017; Salvador *et al.*, 2019). The lack of ER expression in the primary tumor is associated with a more aggressive spread, with a time to recurrence at around 2 years after diagnosis, however the risk of relapse (ROR) after 5 years is very low (Darby *et al.*, 2011; Hess *et al.*, 2003; Zhang *et al.*, 2013). On the other hand, ER+ tumors have a lower risk of recurrence the first 5 years after detection and half of the metastasis occur after 5 or more years from the detection and removal of the primary tumor. In some patients, the relapse can happen after more than 20 years (Hess *et al.*, 2003). However, some ER+ BCa patients show a rapid metastatic progression, indicating a huge heterogeneity in time-to-relapse patterns (Gomis and Gawrzak, 2017; Salvador *et al.*, 2019).

2.2.3 Molecular subtype evolution through metastasis

The metastatic process is a complex and dynamic process in which cells have to adapt to different obstacles in order to succeed. Many studies have tried to understand how this process affect the phenotype of malignant cells. Additional somatic mutations, copy number alterations (CNA) and genomic alterations occur during the metastasis, yet most of the original genetic alterations were present in the primary tumor (Meric-Bernstam *et al.*, 2014). In contrast, the phenotype that metastatic cells show differs from the primary tumor. When evaluating the expression of the three histopathological biomarkers (ER, PR and HER2) between primary and metastatic tumors, alterations in the expression of these markers were detected: 13-15% conversion for ER, 28-31% for PR and 3-10% for HER2 (de Dueñas *et al.*, 2014; Grinda *et al.*, 2021).

Intrinsic molecular subtype characterization during metastasis showed similar results to the histopathological analysis (Ding *et al.*, 2010; Harrell *et al.*, 2012; Aleix Prat *et al.*, 2011). Interestingly, a group characterized the intrinsic molecular subtype of 123 paired primary and metastatic BCa samples, according to PAM50 (Figure I8A). They showed that BCa tumors present gene expression profile changes during the metastatic process. Consequently, they found molecular subtype switches towards a more aggressive subtype. The higher rate of subtype conversion was detected in LumA tumors (55,3%), followed by LumB (30%), HER2-E (23,1%) and finally Basal-like with a 0% of conversion rate (Cejalvo *et al.*, 2017). The majority of LumA tumors switched towards LumB subtype (40,2%) and 14,3% of LumA and B tumors changed to HER2-E subtype (Figure I8B). Proliferation and migration genes were

enriched in metastatic samples whereas the expression of luminal-related genes was reduced (Figure I8C). These results suggest that tumors adapt during metastasis and acquire more aggressive phenotypes to colonize the distant tissues. This study detected 47 genes differentially expressed comparing the paired samples. In conclusion, although the molecular subtypes are largely maintained through the metastatic process, luminal/HER2-negative BCa tumors switch to a LumB or HER2-E subtype, reflecting the loss of ER-dependency towards tumor evolution.

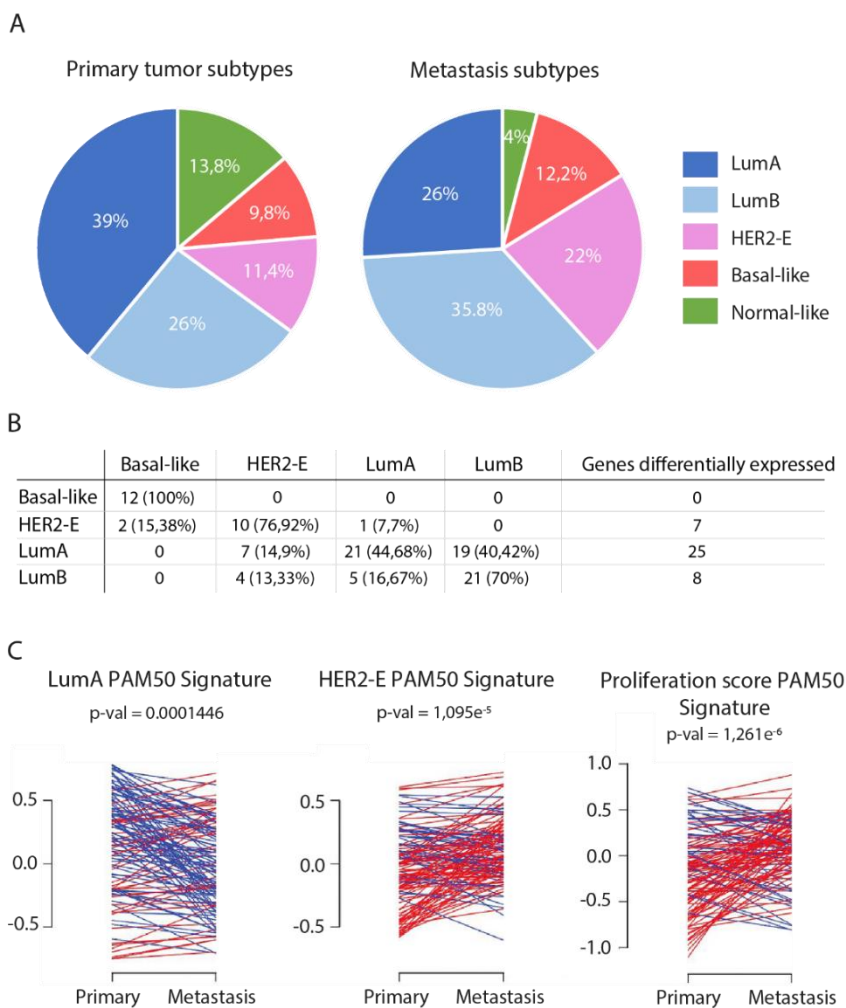


Figure I8. Molecular subtype evolution through metastasis.

(A) PAM50 classification of 123 BCa patient cohort of paired primary tumor samples (left) and metastasis samples (right). (B) Table of subtype concordance comparing primary BCa samples with paired metastatic BCa samples. FDR < 5% for the differentially expressed genes. (C) Expression changes in LumA Signature (left), HER2-E Signature (center) and the proliferation score Signature (right). Statistical analysis was performed with paired *t* test. Adapted figure from Cejalvo *et al.*, 2017.

3 Breast Cancer Treatment

The diagnosis and treatment of BCa involve the collaboration among multiple disciplines. In the diagnosis of BCa, image scanning and tissue biopsies have a key role for establishing localization of the primary tumor and spread to the proximal lymph nodes. BCa treatment can be approached **locally** by chirurgic intervention and radiation of a localized tumor or **systemically** where the whole body is affected and comprises chemotherapy, hormone therapy, targeted therapy and immunotherapy. Surgery is normally combined with adjuvant and/or neoadjuvant treatment. An adjuvant treatment is a local and/or systemic therapy after surgery, given to reduce the risk of primary tumor recurrence or metastasis. On the other hand, neoadjuvant treatment is a systemic approach administered before the surgery to reduce tumor volume and facilitate the local intervention

3.1 Local intervention

The main approach against localized BCa is to resect as much as possible of the primary tumor and the adjacent tissue with a **chirurgic intervention**. Breast-conserving surgery refers to the partial removal of the breast tissue and, depending on the breast area that is resected it can be a lumpectomy, quadrantectomy or partial mastectomy (Matsen and Neumayer, 2013; Waks and Winer, 2019). Mastectomy is the resection of the whole breast and, depending on the tumor spread, the neighboring tissues. Patients can have a breast reconstruction with implants from different materials.

Surgery is normally complemented with post-operative **radiotherapy**, in order to eliminate all the remaining tumor cells adjacent to the primary tumor (Darby et al., 2011). The radiation used is called ionizing radiation because it generates ions that transfer the energy to the cells of the tissues where it passes through. High-energy radiation damages genetic material in the cell nucleus, blocking the ability to replicate. Radiation damages both malignant and normal cells surrounding, therefore one of the main objectives of radiation therapy is to improve the specificity against tumor cells by using targeted drugs (Begg et al., 2011). It has been demonstrated that whole breast radiation therapy reduces the 10-year ROR by 15% and the 15-year risk of BCa-related mortality by 4% (Darby et al., 2011).

3.2 Systemic interventions

3.2.1 Chemotherapy

Chemotherapy refers to the administration of different compounds that target proliferating cells in order to interfere with the cell cycle progression and induce cell death. Patients with more aggressive tumors such as TN and HER2+ subtypes are the ones having a higher benefit from this therapy, because of the increased proliferative rates (Cortazar et al., 2014). Metastasis is also treated with chemotherapy for delaying disease progression. Chemotherapy can be used as a neoadjuvant treatment for big size tumors (Murphy et al., 2018) with the objective of reducing tumor volume before surgery. After surgical intervention, patients are normally administered chemotherapy as an adjuvant approach to eliminate the remaining cells surrounding the tumor or those cells that were able to disseminate.

Cytotoxic agents are classified according to their mechanism of action, including alkylating agents, anti-metabolites, topoisomerase inhibitors, antibiotics, mitotic inhibitors, and protein kinase inhibitors. They can be administered individually, in combination or they can be alternated in order to overcome possible resistance generation to therapy (Andreopoulou and Sparano, 2013). Chemotherapy causes a variety of side effects (nausea, vomiting, immunosuppression, impaired growth of healthy cells, etc.) mainly related with those tissues that have a high renewal rate.

Adversely, some agents can increase the risk of secondary tumor development (Karagiannis et al., 2018; Tarella et al., 2010). Together with radiation, these systemic cytotoxic agents induce an acute inflammatory response that promotes the recruitment of several immune cells to the tumor microenvironment (Karagiannis et al., 2018). As an example, cancer associated fibroblasts (CAFs) and endothelial cells secrete pro-inflammatory molecules such as interleukin-6 and 8 (IL-6/8) (Toste et al., 2016), that affect the activity of myeloid cells promoting tumor immune evasion (David et al., 2016; Ham et al., 2019).

3.2.2 Hormone therapy

BCa tumors that depend on ER to grow (ER+ tumors) are treated with hormone therapy (HT), also known as endocrine therapy. This therapy can be administered in adjuvant setting after surgery or as neoadjuvant treatment to help control the primary tumor before surgery. This treatment is usually maintained for at least 5 to 10 years after surgery. There are several types of endocrine therapy for BCa with the aim of reducing E2 levels or stopping E2 function in BCa cells. The development of drugs that

target ER either directly (tamoxifen) or indirectly (aromatase inhibitors) has led to an improvement in healthcare and BCa prognosis.

Selective ER modulators (SERMs) block E2 function in breast tissue while activates/inhibits other E2-responsive tissues. Tamoxifen selectively binds to ER competing with E2 inside the cells. Tamoxifen was the first hormone-based treatment for both pre- and post-menopausal patients and has been the endocrine therapy of choice for ER+ BCa patients for many years. However, a deeper evaluation of tamoxifen-treated patients revealed significant side effects such as blood clots, endometrial cancer and the development of acquired resistance.

Aromatase inhibitors (AI) are included in the clinic for post-menopausal ER+ BCa patients. These inhibitors target the aromatase enzyme and prevent the conversion of androstenedione to estrone and subsequently estradiol, thus decreasing E2 concentration. Both steroid (exemestane) and non-steroid (letrozole and anastrozole) third-generation AI have shown promising results in a large meta-analysis published in 2006 by Mauri *et al.* compared to Tamoxifen (Mauri et al., 2006). However, the treatment of chose will be decided depending on the menopausal status and adverse effects (Dowsett et al., 2010).

Selective ER degraders (SERDs) are molecules that bind to ER, inducing protein misfolding and accelerating ER degradation. The only SERD approved in the clinic is fulvestrant which is administered in post-menopausal BCa patients. There are other promising SERDs such as SAR439859 in clinical trials for metastatic BCa setting (Tolaney et al., 2020). SERDs lacks E2 agonistic effects, downsizing the adverse effects induced by other drugs such as Tamoxifen.

GnRH analogs are short peptides that cause a strong inhibition of E2 synthesis by suppressing the ovarian function in pre-menopausal women. Moreover, it has been shown that GnRH analogs have a direct anticancer effect over tumor cells by reducing tumor growth and cell invasion (Everest et al., 2001). Triptorelin is a GnRH analog approved by the EMA as an adjuvant HT in combination with Tamoxifen or AI to treat early-stage ER+ BCa patients (Frampton, 2017; Huerta-Reyes et al., 2019). After GnRH analog therapy, patients suffer from an induced menopause-like condition.

3.2.3 Targeted therapy

During the past decades, our understanding of malignant cells biology has grown exponentially. This has allowed the development of drugs directed to block specific signaling cascades used by tumor cells to proliferate and survive. Targeted therapies are systemic approaches that aim to tackle each tumor in a more specific and personalized way.

Tumors that rely on HER2 signaling

HER2 inhibitors were introduced in the clinics in 1998 and changed completely the landscape of HER2+ BCa patients (Drebin et al., 1986). Trastuzumab and pertuzumab are monoclonal anti-HER2 antibodies that target extracellular domains of the HER2 receptor in order to avoid activation and signal transduction. Both antibodies have shown a significant increase in progression-free survival (PFS) and OS in HER2+ BCa patients (Slamon *et al.*, 2001; Swain *et al.*, 2013), however pertuzumab is given to those patients with high ROR due to the higher cost and side effects (Waks and Winer, 2019). Lapatinib and neratinib are tyrosine kinase inhibitors (TKI) that bind to the intracellular domain of HER2 receptor to block the signal pathway. The two inhibitors are mainly administered after previous anti-HER2 treatments in advanced HER2+ BCa (Blackwell et al., 2009; Rabindran et al., 2004). Phase III NALA clinical trial showed that neratinib plus capecitabine (a chemotherapeutic agent) had an improved PFS versus lapatinib plus capecitabine in metastatic HER2+ BCa patients that had already received 2 or more lines of HER2-directed treatments (Saura et al., 2020).

In 2013, the FDA approved a new treatment for metastatic HER2+ BCa patients. This new treatment consists in the chemical combination of the trastuzumab antibody with the chemotherapeutic drug emtansine or DM1 (Phillips *et al.*, 2008). This T-DM1 antibody-drug conjugate not only blocks the activity of HER2 receptor but also delivers emtansine directly to tumor cells. In 2019, the FDA expanded the approval to treat early stage HER2+ BCa patients in adjuvance. The new approval was based on the results from the KATHERINE clinical trial that compared the effect of T-DM1 with trastuzumab as adjuvant treatments (von Minckwitz et al., 2018). In the trial, T-DM1 treated patients showed a 50% reduced risk of invasive disease or death compared with patients treated with trastuzumab alone (von Minckwitz et al., 2018).

Advanced ER+ HER2-negative tumors

In ER+ BCa tumors, HT is the first line of treatment with very good results. However, some patients can present intrinsic resistance to HT or develop resistance

after an initial response, which is called acquired resistance. The first clinical strategy to overcome this resistance is to combine or alternate different therapeutic drugs (Waks and Winer, 2019).

Different drugs have been developed to target signaling cascades associated with proliferation and survival of malignant cells. Phosphatidylinositol 3-kinase/protein kinase B (AKT)/mechanistic target of rapamycin complex 1 (PI3K/AKT/mTORC1) pathway controls many cellular functions and has been found altered in some BCa patients (Janku et al., 2018). Aberrant signaling through this cascade has been found associated with endocrine resistance (Crowder et al., 2009; Miller et al., 2010, 2011). Alpelisib is the only **PI3K inhibitor** approved in combination with endocrine therapy for advanced *PIK3CA* mutated HR+/HER2-negative BCa tumors (André et al., 2019). Everolimus is an **mTORC1 inhibitor** that, in combination with AI, has become a standard treatment for patients with metastatic HR+/HER2-negative BCa resistant to prior HT (Baselga et al., 2012). A comparative study of alpelisib and everolimus clinical trials showed that alpelisib is only effective in patients with *PIK3CA*-mutated tumors, while everolimus improves AI therapy independently of *PIK3CA* mutational status (Vernieri et al., 2020).

Other strategies to overcome HT resistance include **Poly (ADP-ribose) polymerase inhibitors (PARPi)** which impair the function of the PARP protein. PARP is a key player in the repair of DNA single-strand breaks. This treatment is administered to HR+/HER2-negative advanced BCa with *BRCA1/2* mutations, being the first clinically approved drug designed to take advantage of synthetic lethality. Tumors carrying mutations in *BRCA1/2* are sensitive to PARPi because they already have a DNA repair machinery malfunctioning, thus the amount of DNA damage is unbearable for the cell and enters in apoptosis (Lord and Ashworth, 2017).

Cyclin-dependent kinase 4/6 inhibitors (CDK4/6i) are small molecules that target CDK4/6 proteins which are key players for cell cycle progression, therefore inducing cellular arrest in malignant cells. The approval of abemaciclib, palbociclib and ribociclib for advanced ER+/HER2-negative BCa treatment represents a milestone in target-directed therapies. The three inhibitors have shown a significantly improved PFS when combined with endocrine therapy in different clinical trials (Section 4 CDK4/6 inhibitors in breast cancer).

3.2.4 Immunotherapy

One of the most important obstacles that tumor cells have to bypass is the immune system. Taking the premise that malignant cells use different mechanisms to avoid

immune surveillance, researchers have developed strategies to tackle these mechanisms and stimulate the immune system of the patient against the tumor cells. Clinical immune-oncology treatments can be broadly grouped into checkpoint inhibitors, vaccines and cell-based therapies. **Checkpoint inhibitors** are monoclonal antibodies that block the interaction of checkpoint molecules with their ligands. Immune checkpoints are proteins on the surface of immune cells, such as T cells, that help modulate the function of the immune response. Two immune checkpoints expressed by malignant cells to overcome and inactivate the immune response are programmed cell death ligand 1 (PD-L1) and cytotoxic T-lymphocyte-associated protein 4 (CTLA-4) (He and Xu, 2020). In the clinical context, the benefits in BCa treatment with checkpoint inhibitors are more modest than in other tumor types such as melanoma, and they are limited to TN BCa. Currently approved therapies are pembrolizumab and atezolizumab, immune checkpoint inhibitors that are administrated with chemotherapy in previously untreated, locally recurrent unresectable or metastatic PD-L1+ TN BCa (Cortes et al., 2020; Schmid et al., 2018, 2020).

Other studies show promising results concerning the effect of the **vaccines** in TN BCa in animal models (Niavarani et al., 2020; Pack et al., 2020). Recently, a clinical trial has been started to test the effect of α -lactalbumin vaccine in TN BCa patients (NCT04674306).

Adoptive cell transfer (ACT) therapies involve the isolation of patients' lymphocytes and *ex vivo* activation and expansion to attack malignant cells. ACT has shown positive results for treating several malignancies. How to improve the design, feasibility and ease of manufacturing is under active research. However, BCa treatment with ACT showed to be limited by the lack of known neoantigens that can be targeted.

4 CDK4/6 inhibitors in Breast Cancer

CDK4/6i development is possibly one of the most important recent innovation for ER+/HER2-negative advanced BCa. There are three CDK4/6i approved to treat patients: palbociclib (Ibrance®), ribociclib (Kisqali®) and abemaciclib (Verzenio™). These inhibitors prevent malignant cells proliferation and induce cell cycle arrest. CDK4/6i are administered in combination with AI, fulvestrant or as monotherapy (abemaciclib). Up to the present, many Phase II and III clinical trials have assessed CDK4/6i benefit in ER+/HER2-negative metastatic BCa treatment. Palbociclib was evaluated in three randomized clinical trials: PALOMA-1 (Richard S Finn *et al.*, 2015), PALOMA-2 (Finn *et al.*, 2016, 2020) and PALOMA-3 (Cristofanilli *et al.*, 2016; Turner *et al.*, 2018). Ribociclib was evaluated in MONALEESA-2 (Hortobagyi *et al.*, 2018), MONALEESA-3 (Slamon *et al.*, 2018) and MONALEESA-7 (Tripathy *et al.*, 2018), and abemaciclib in MONARCH 1 (Dickler *et al.*, 2017), MONARCH 2 (Sledge *et al.*, 2017) and MONARCH 3 (Goetz *et al.*, 2017). Together, these clinical trials reported the beneficial effect of adding CDK4/6i to HT in terms of PFS in ER+/HER2-negative metastatic BCa patients compared with HT alone (Di Leo *et al.*, 2018; Gao *et al.*, 2020). Prolonged OS was also observed for CDK4/6i treatment arm in some of these clinical trials. Recently, different meta-analysis including these clinical trials have further established the improvement in PFS and OS of CDK4/6i combined with HT compared to HT alone (Kunwor *et al.*, 2020; Li *et al.*, 2020; Piezzo *et al.*, 2020; Schettini *et al.*, 2020).

4.1 Mechanisms of resistance to CDK4/6 inhibitors

PFS in advanced ER+ BCa patients has been significantly prolonged thanks to CDK4/6i, however not all the patients respond to these inhibitors and most of the patients that responded at the beginning will eventually develop acquired resistance. Cells adapt through different mechanisms and bypass the cytostatic effect of CDK4/6i. In this section, I will shortly explore the different biomarkers that have been described associated with resistance to CDK4/6i in advanced ER+ BCa. We can classify them in two groups: cell cycle specific and cell cycle non-specific mechanisms.

4.1.1 Cell cycle specific mechanisms

The main regulator of the G1-S phase transition of the cell cycle is the cyclin D – CDK4/6 – INK4 – RB axis (Choi and Anders, 2014). Proliferation signals activate cyclin D, allowing the formation of a complex with CDK4/6 kinases. The active complex phosphorylates RB, promoting the dissociation of RB from the inactive

E2F. The release of E2F induces an early transcription cascade, which is required for DNA replication and the progression to the S phase (Weinberg, 1995). The cyclin D-CDK4/6 complex is inhibited by p16INK4A, a protein from the INK4 family of cell cycle inhibitors, through the blockage of CDK4 catalytic activity (McConnell et al., 1999). Other important inhibitors of the complex are p21 and p27 from the Cip/Kip family proteins (Denicourt and Dowdy, 2004). Some mechanisms that affect this axis and its interacting network are summarized hereunder.

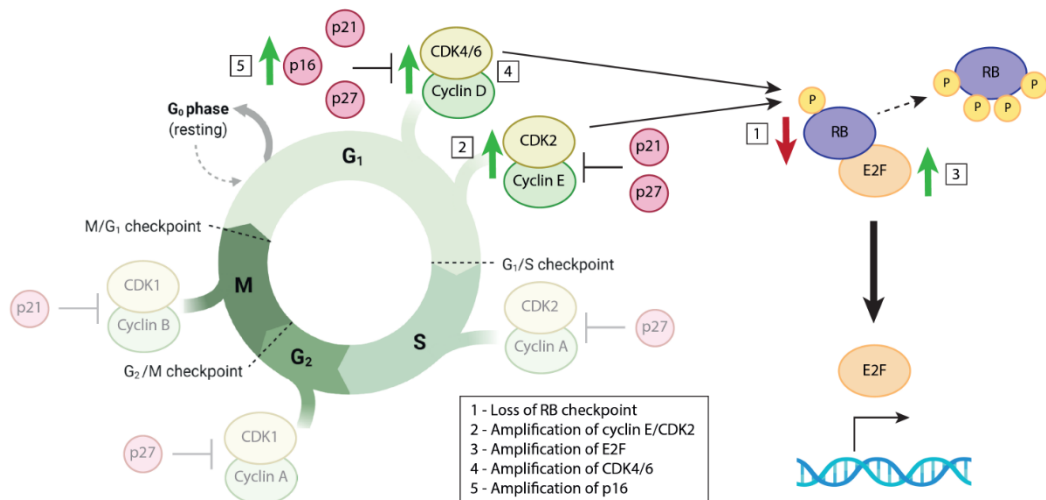


Figure I9. Cell cycle specific mechanisms for CDK6/6i resistance.

Different molecules that regulate cell cycle are involved in CDK6/6i resistance. The loss of CDK4/6i target genes, such as RB (1) is one of the main mechanisms. The overexpression of cyclin E/CDK2 (2), E2F (3) or CDK4/6 (4), which are genes that induced cell cycle progression, is also associated with increased CDK4/6i resistance. The amplification of p16 (5), a molecule that inhibits CDK4/6 complex, reduces the target for CDK4/6i and generates resistance. Adapted from Pandey *et al.*, 2019.

Loss of RB checkpoint

RB is a tumor suppressor protein that avoids E2F release and therefore maintains the cell in G1. When it is phosphorylated and subsequently inactivated by CDK4/6, E2F can proceed with cell cycle progression (Weinberg, 1995). Hence, the loss of RB is one of the most important causes that drives resistance to the CDK4/6i (Figure I9-1). In preclinical and clinical studies, mutations in RB have been reported to cause CDK4/6i resistance (Cen et al., 2012; Condorelli et al., 2018). A gene

expression signature of RB loss (RBsig) showed prognostic value between palbociclib-sensitive and resistant BCa cell lines (Malorni et al., 2016). RB was also associated with sensitivity to abemaciclin in the neoMONARCH clinical trial (Hurvitz et al., 2020). After RB loss, the cell starts depending on cyclin E-CDK2 complex to keep proliferating, which introduces a new therapeutic approach.

Amplification of cyclin E1/2-CDK2 axis

The complex cyclin E-CDK2 has a similar function to cyclin D-CDK4/6 in G1/S phase transition. CDK2 upon complex formation and activation can phosphorylate RB protein and allow E2F function (Gladden and Diehl, 2003). Many studies demonstrated that *CCNE1* overexpression (cyclin E gene) is associated with CDK4/6i resistance in cancer cell lines and in the clinic (Figure I9-2) (Chandarlapaty and Razavi, 2019; Guarducci *et al.*, 2017, 2018; Taylor-Harding *et al.*, 2015; Turner *et al.*, 2019).

Amplification of E2F

The RB-E2F complex is essential for the proper regulation of G1-S phase transition. E2F release enhance the transcription of different key proteins for this process, including cyclin E1, starting a positive feedback loop (Morris et al., 2000; Ohtani et al., 1995). Overexpressing E2F allows the cell to bypass the inhibition by CDK4/6i and depend on other cell cycle pathways instead of cyclin D-CDK4/6 (Figure I9-3)(Dean et al., 2010). Moreover, E2F has many other functions such as the activation of AKT signaling cascade through Gab2, which may contribute to the resistance (Chaussepied and Ginsberg, 2004).

Amplification of CDK4 and CDK6

Gene amplifications, mutations and epigenetic alterations may activate cyclin D-CDK4/6 complex, forcing the pathway activity and limiting the efficiency of the inhibitors. Overexpression of CDK4 has been reported to happen in many cancer types (Wu *et al.*, 2011) and has been linked with resistance to CDK4/6i (Figure I9-4)(Cen et al., 2012; Olanich et al., 2015). Similarly, CDK6 overexpression was observed to drive CDK4/6i resistance in preclinical models (Yang et al., 2017). Additionally to the kinase function, CDK6 plays a role in the transcription of different genes such as p16 when STAT3 and cyclin D are present or VEGF-A in the presence of c-Jun (Kollmann et al., 2013; Tigan et al., 2016). This gives new mechanisms of action through which CDK6 could be driving resistance to CDK4/6i.

Amplification of p16

P16 is a tumor suppressor molecule in charge of inhibiting CDK4 function. The tumor suppressor function of this gene requires from the proper activity of RB molecule. However, p16 is overexpressed during oncogenic stress independently of the RB presence. It has been observed that p16 overexpression, even with functional RB protein, leads to resistance to CDK4/6i because of the reduction of CDK4/6i target CDK4 (Figure I9-5)(Romagosa et al., 2011).

Alternative cell cycle specific mechanisms that have been observed in CDK4/6i resistance are the overexpression of CDK7 (Guarducci *et al.*, 2019), that has a similar function as CDK6 but in G2/M phase transition. Overexpression of WEE1, which is an important protein involved in G2/M checkpoint (Matheson et al., 2016). Overexpression of the p53 inhibitor MDM2 which disrupts the senescence associated phenotype induced by CDK4/6i, causing a resistance to CDK4/6i (Efeyan et al., 2007; Laroche-Clary et al., 2017). Histone deacetylases (HDACs) are proteins that remove acetyl groups from histone lysins and regulate the expression of many genes. One of these genes is p21, a CDK inhibitor, which is suppressed due to HDAC regulation (Zupkovitz et al., 2010). This function could lead to resistance, however the specific mechanism that drive HDAC activation to CDK4/6i resistance is still unknown. These mechanisms are some of the most important pathways associated with cell cycle related resistance to CDK4/6i.

4.1.2 Cell cycle non-specific mechanisms

Additionally, to cell cycle key players, there are many other proteins that have been reported to be implicated in CDK4/6i resistance. I shortly described some of these cell cycle non-specific mechanisms below. FGFR signaling cascade which is one of these alternative resistance drivers will be more extendedly described in Section 4.2 FGFRs in BCa treatment resistance.

MAPK pathway activation

MAPK cascade has been demonstrated to regulate cyclin D1 expression and considered as a therapy with synergistic function with CDK4/6i (Figure I10-2) (Meloche and Pouyssegur, 2007; Yamamoto *et al.*, 2006). In preclinical research MAPK pathway inhibition through RAF inhibitors, revealed a combinational effect with abemaciclib in xenograft mouse models mutated in KRAS, NRAS or BRAF (Chen *et al.*, 2018). MEK inhibitors were also reported to affect CDK4/6i-resistant cell lines, which opens the door to a promising combination treatment (de Leeuw et

al., 2018). All the ongoing clinical trials involving CDK4/6 and MAPK dual blockade are summarized in the review Scheiblecker *et al.*, 2020.

PI3K/AKT/mTOR pathway activation

In 30% of BCa tumors PI3K/AKT/mTOR signaling cascade is activated, especially in ER+ tumors (Herrera-Abreu *et al.*, 2016; Takeshita *et al.*, 2018). As commented previously (Section 3.2.3 Targeted therapies), mutations in this pathway are associated with endocrine therapy resistance. Recently, this pathway has also been reported to be associated to CDK4/6i resistance (Figure I10-3)(Herrera-Abreu *et al.*, 2016; Iida *et al.*, 2018; Jansen *et al.*, 2017; O'Brien *et al.*, 2017). As an example, BCa cell lines resistant to CDK4/6i relied on this pathway more than on ER function (Iida *et al.*, 2018). In ribociclib-resistant BCa cell lines it was reported that CDK4/6i activate this pathway through AKT phosphorylation. This phosphorylation was PDK1-specific. PDK1 phosphorylated AKT in a residue reported to be CDK2-dependent phosphorylation target (Jansen *et al.*, 2017). Moreover, preclinical results showed that inhibiting mTORC1/2 blocked pRB/E2F progression in CDK4/6i-resistant cell lines, restoring the inhibitors sensitivity (Michaloglou *et al.*, 2018). A study reported that treating different BCa cell lines with PI3K inhibitors decrease cyclin D1 expression and prevents early adaptation to CDK4/6i (Herrera-Abreu *et al.*, 2016). In addition, this group demonstrated that combined therapy of CDK4/6i plus PI3Ki showed complete tumor progression compared to single treatments in a CDK4/6i-sensitive PDX model (Herrera-Abreu *et al.*, 2016). These studies suggest that adding PI3K/AKT/mTOR inhibition to CDK4/6i would increase the therapeutic benefits in overcoming CDK4/6i resistance.

ER loss

In ER+ BCa, ER is a key activator of cyclin D-CDK4/6-RB axis. However, the loss of dependence on ER signaling is normally associated with a more aggressive phenotype. Clinical and preclinical studies have suggested that the loss of ER and the subsequent decrease of estrogen-regulated genes, together with a reduced sensitivity to endocrine therapy can induce CDK4/6i acquired resistance development (Figure I10-4)(Iida *et al.*, 2020; Pancholi *et al.*, 2020; Yang *et al.*, 2017). Changes in ER dependence would lead the cells to escape CDK4/6i action, suggesting that taking a similar approach to the ER- BCa tumors' treatment could benefit those patients with CDK4/6i acquired resistance.

AP-1 increased activity

AP-1 family of transcription factors, which encompasses Jun, Fos, ATF and MAF sub-families, regulates the correct transcription of many genes, including cyclin

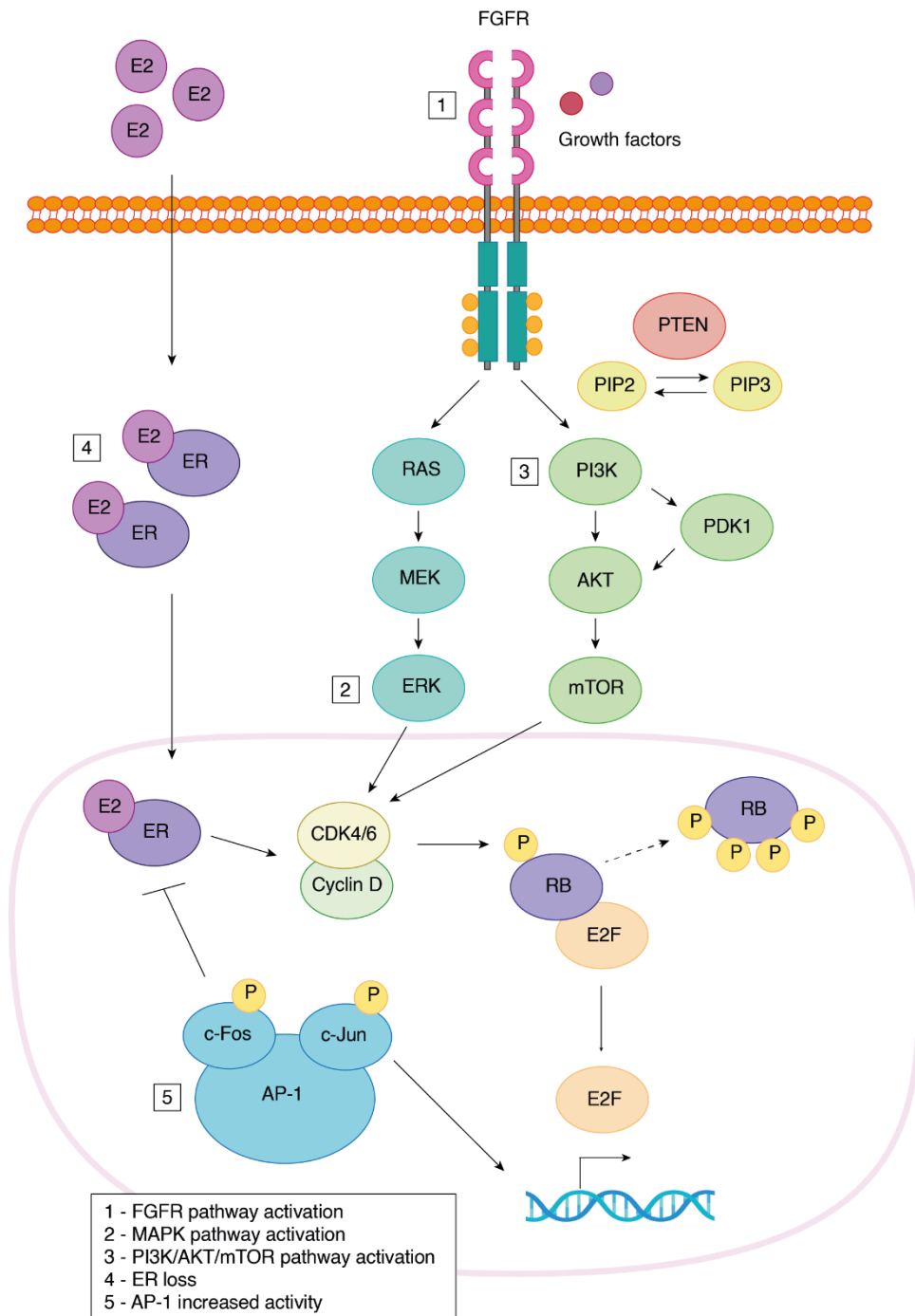


Figure I10. Cell cycle non-specific mechanisms for CDK6/6i resistance.

The hyperactivation or overexpression of proteins involved in signaling cascades upstream cell cycle such as FGFR (1), MAPK (2), PI3K/AKT/mTOR pathway (3) and AP-1 (5), can push cell cycle progression, increasing the resistance of CDK4/6i. The reduction of ER dependency (4) leads to CDK4/6i resistance. Adapted from Pandey *et al.*, 2019.

D1 (Shaulian and Karin, 2001). These transcription factors have been found altered in different BCa tumors and some of them have been associated with treatment resistance (Figure I10-5). In MCF7 cells, c-Jun was described to contribute to HT resistance (Smith *et al.*, 1999). Furthermore, MCF7 with acquired resistance to palbociclib and tamoxifen showed increased activity of AP-1 and higher levels of c-Fos (De Angelis *et al.*, 2018). How AP-1 is associated with resistance to CDK4/6i is still unknown. However, different theories have pointed out c-Jun function in suppressing ER activity (Smith *et al.*, 1999) or overexpressing cyclin D1 as mechanisms of CDK4/6i resistance. Genetic suppression of c-Jun, together with palbociclib led to a combined lethality on BCa cells (De Angelis *et al.*, 2018). The blockade of AP-1 has been found to have a synergistic effect when added to palbociclib and fulvestrant, showing an increased efficiency than the single treatments or the combination of palbociclib plus fulvestrant. Much effort is being made in the development of AP-1 inhibitors (Brennan *et al.*, 2020; Ye *et al.*, 2014), but at the moment only one c-Fos/AP-1 inhibitor is in clinical trials (Makino *et al.*, 2017).

Many **alternative cell cycle non-specific mechanisms** have been described to be associated with CDK4/6i resistance: the EMT process, suppression of Smad3 by cyclinE-CDK2, activation of autophagy, immune-related pathways such as IFN α and IFN β , among other mechanisms. Studying each individual tumor setting with the help of specific biomarkers would lead researchers to better understand CDK4/6i resistance, allowing clinicians to choose the appropriate therapeutic strategy in each situation.

4.2 FGFRs in BCa treatment resistance

FGFR family contains four members (FGFR1-4) with a single-pass transmembrane and an intracellular tyrosine kinase domain. Their ligands are FGF molecules, which bind to three immunoglobulin (ig)-like domains exposed in the extracellular domain. The first group of ligands contain 15 canonical FGFs (FGF1-14/18) that require binding to heparan sulfate proteoglycans to function as a paracrine signal. The second group of FGFR ligands are endocrine FGFs (FGF19/21/23), which bind to Klotho proteins (KLB) to help stabilizing the ligand-receptor interaction. FGFs from this second group are able to diffuse to the bloodstream and act as hormones (Katoh, 2019). Tissue-specific expression, the ligands availability and the alternative splicing variants of the four FGFRs would determine the specific cellular outcome. FGF-FGFR signaling regulates many physiological processes such as tissue development, homeostasis, metabolism, tissue repair and angiogenesis. The downstream activation

of pathways involved in cell proliferation, cellular survival and differentiation make FGFR susceptible proteins to be associated with malignancy acquisition.

Aberrant FGFR activation induced by genetic alterations have been widely associated with tumor development and progression in different cancer types such as breast, liver and lung among others (Kato, 2019). Interestingly, a study characterized the genetic alterations of FGFRs in 4853 tumors and they found alterations in 7,1% of the tumors, mainly amplifications and point mutations. FGFR1 was the most frequently mutated (3,5% of the patients), followed by FGFR3 (2%), FGFR2 (1,5%) and FGFR4 (0,5%)(Helsten et al., 2016).

[Eliminated section - confidential information]

4.2.2 FGFR-driven CDK4/6i resistance

As mentioned previously, FGFRs are involved in proliferation, differentiation and survival, mechanisms that lead to tumor formation and progression (Turner and Grose, 2010). FGFR1 and 2 have been associated with HT resistance and CDK4/6i resistance. There are two mutations in *FGFR2* gene (M538I and N550K) that have been related with palbociclib and/or fulvestrant resistance in HT-resistant ER+ advanced BCa patients (Mao et al., 2020).

FGFR1 amplification activates PI3K-AKT and MAPK signaling pathways in malignant cells resistant to HT (Turner *et al.*, 2010). Clinical data analysis also supported these findings. Through the analysis of blood samples from patients included in the MONALEESA-2 clinical trial, researchers could detect *FGFR1/2* amplifications or mutations in 41% of the patients that progressed after CDK4/6i therapy (ribociclib plus fulvestrant treatment) (Formisano et al., 2019).

[Eliminated figure - confidential information]

Reduced PFS was associated with *FGFR1* amplification in circulating DNA samples from these MONALEESA-2 patients compared with wild-type *FGFR1* (Formisano et al., 2019). Other studies showed that FGFR1 amplification, together with *TP53* mutation, showed worse survival in a cohort of 521 ER+/HER2-negative advanced BCa after palbociclib plus fulvestrant treatment (O'Leary et al., 2019).

Moreover, molecules involved in FGFR signaling cascade have been associated with CDK4/6i resistance. In a recent report presented at ASCO 2020 meeting, the analysis of MONALEESA-2/3/7 patients pointed out potential ribociclib plus letrozole resistance biomarkers: *YYYY*, *MDM2*, *PRKCA*, *AKT*, *BRCA1/2* and *ERBB2* (O'Leary et al., 2019). Additionally, another study showing the alterations enriched in CDK4/6i resistance highlighted PI3K/AKT, *RB1*, Hippo signaling genes, *CDKN2A* and *FGFR1* (Razavi et al., 2019). In summary, all these studies show the key role of the FGF/FGFR axis during CDK4/6i resistance.

4.2.3 Targeting FGFR to overcome CDK4/6i resistance

The importance of FGFR deregulation in tumor progression and CDK4/6i resistance, indicates a new therapeutic target to explore. Formisano and colleagues showed the effect of the TKI lucitanib, which targets FGFR among other tyrosine kinases, in reversing the CDK4/6i plus fulvestrant acquired resistance in FGFR1-overexpressing ER+ BCa cells (Formisano et al., 2019). They also developed a patient-derived xenograft model (PDX) with ER+ metastatic BCa cells with FGFR1 amplification. When the selective FGFR TKI erdafitinib was added to palbociclib and fulvestrant treatment, established tumors were reduced more 50% in their size (Formisano *et al.*, 2019). NanoString expression analysis in patients treated with palbociclib plus fulvestrant showed a reduction of most of cell cycle genes, whereas the expression of FGFR1/2/3 and genes of the MAPK cascade were increased (Formisano et al., 2019). Collectively, these results indicate that cell proliferation is maintained with a CDK4/6-independent mechanism during CDK4/6 inhibition combined with HT and points towards a role of the FGFR-MAPK signaling in this process. At the moment, a phase Ib clinical trial is evaluating the combined effect of fulvestrant, palbociclib and erdafitinib in ER+/HER2-negative advanced BCa patients with any amplification at FGFR1-4 genes (NCT03238196). All the information concerning the latest developed treatments and clinical trials targeting FGFR has been recently reviewed in Krook *et al.*, 2021.

In lung cancer cells resistant to palbociclib, the inhibition of FGFRs by LY2874455 reduced the expression of CDK6, cyclin D1, and cyclin D3 (Haines et al., 2018). The induced effect of FGFR inhibitor was similar to MEK and mTOR inhibitors in these cells. In the same study, the authors showed that FGF2 secretion was able to promote palbociclib resistance and MEK sensitivity by activating FGFR1 cascade through ERK1/2 activation. Remarkably, FGF2-stimulated cells showed no changes in their cell cycle expression profile with palbociclib presence. These results suggest

that FGFR activity induces cell cycle progression independently of CDK4/6 activation (Haines et al., 2018).

In conclusion, many studies point at FGFR pathway as a promising therapeutic target to overcome CDK4/6i resistance.

4.3 HER2-E molecular subtype in ER+/HER2-negative breast cancer

Increasing evidence has shown clinical value from stratifying patients according to PAM50 classification. Differences in treatment response between the non-luminal (HER2-E and Basal-like) and luminal subtypes (LumA and B) have been observed in ER+/HER2-negative tumors. A considerable proportion of ER+/HER2-negative patients are classified as non-luminal subtype. Basal-like molecular subtype represents a small proportion of non-luminal classified ER+/HER2-negative BCa patients, however HER2-E subtype can represent around the 19% of this patients (Figure I11, Finn *et al.*, 2016) Further, it is important to consider the changes in molecular subtype that tumors acquire during the metastatic process. HER2-E subtype frequency have been found to double from 5% to 10% in metastatic ER+/HER2-negative BCa compared to early disease. This molecular subtype switch can be due to patient selection, tumor evolution through metastasis and treatment bottleneck. Some genetic alterations can be acquired during the tumor cells spread to a secondary location, but metastatic lesions share most of the genetic alterations with their primary tumor. Thus, the phenotypical adaptation found in secondary tumor is mainly due to changes at the transcription level, which is captured with gene expression analysis such as PAM50. ER+/HER2-negative BCa patients classified as HER2-E showed a higher likelihood of relapsing than the luminal subtypes when treated with HT (Finn *et al.*, 2018a; Prat *et al.*, 2012, 2016). Therefore, patients that have relapsed are enriched in HER2-E intrinsic subtype compared to early BCa patients. In line with this observations, the analysis of 123 paired primary and advanced BCa samples, around 13-15% of LumA or LumB primary tumors switch towards a HER2-E molecular expression profile during the metastatic evolution, despite being HER2-negative (Section 2.2.3 Molecular subtype evolution through metastasis, Cejalvo *et al.*, 2017). In conclusion, changes towards HER2-E intrinsic subtype might show an increased estrogen-independent profile in tumors that were luminal in the early disease. The phenotypical differences between HER2-E and luminal subtypes are translated in different treatment outcomes, even though these tumors are all histopathologically classified as ER+/HER2-negative.

4.3.1 ER dependency and chemotherapy sensitivity

Different studies evaluated changes in Ki67 expression level before and after different treatment lines including HT in ER+/HER2-negative tumors (Dunbier et al., 2011; Ellis et al., 2011; Ma et al., 2017). Tumors PAM50 classified as HER2-E subtype showed little changes in Ki67 expression levels after endocrine therapy compared with luminal tumors, despite being classified as ER+ by IHC.

On the other hand, many studies have reported the increased sensitivity to chemotherapy of HER2-E subtype compared with luminal tumors (Fujii *et al.*, 2017; Prat *et al.*, 2016) in ER+/HER2-negative BCa. A recent retrospective study evaluated the chemotherapy effect in ER+/HER2-negative BCa tumors (Prat *et al.*, 2015). In this study, 451 ER+/HER2-negative BCa patients treated with neoadjuvant multi-agent chemotherapy were classified by PAM50. Pathological complete response (pCR) rates varied through the different intrinsic subtypes: LumA (6%), LumB (16%), HER2-E (37%) and Basal-like (38%) (Prat *et al.*, 2015). Compared to luminal tumors (8.9% pCR), non-luminal tumors (HER2-E and Basal-like subtypes) showed a 30% pCR after chemotherapy treatment (Prat *et al.*, 2015). In another study that included 180 biopsies from ER+/HER2-negative BCa patients treated with neoadjuvant chemotherapy (Prat *et al.*, 2016). PAM50 intrinsic subtypes were correlated with pathologic response such as residual cancer burden. There was variability found between subtypes: residual cancer burden 0/1 in LumA was 9.3% rate, LumB 20%, HER2-E 14.3% and Basal-like 50%. Moreover, SOLTI-NEOERIBULIN phase II clinical trial showed HER2-E subtype ER+/HER2-negative BCa patients to have the highest benefit from eribulin chemotherapeutic agent (Prat *et al.*, 2017).

Globally, these studies suggest that HER2-E subtype, which represents an important proportion of ER+/HER2-negative BCa tumors, shows a lower sensitivity to HT and an increased sensitivity to chemotherapy (Prat *et al.*, 2017).

4.3.2 CDK4/6 inhibitors sensitivity

Sensitivity to palbociclib varies depending on the luminal status of BCa cell lines. Non-luminal cell lines showed less sensitivity to the drug *in vitro* compared to luminal cells (Finn *et al.*, 2016). At the 2017 San Antonio Breast Cancer Symposium (SABCS), Finn and colleagues presented an exploratory retrospective analysis of the PALOMA-2 clinical trial, stratifying with PAM50 455 patients. In the analyzed samples, 80% of the ER+/HER2-negative BCa tumors were LumA or B, 19% of were HER2-E and <1% of Basal-like molecular subtype (Figure I11A). The median PFS of the palbociclib plus letrozole arm was 27,6 months compared with 14,5 months of the letrozole alone (Finn *et al.*, 2016). The intrinsic subtypes that benefit

from the combined treatment were LumA (30.4 months vs 17 months) and LumB (19.6 months vs 11 months). Non-luminal subtypes (20% of the total population) showed little to any benefit from palbociclib plus letrozole compared with letrozole monotherapy: Notably, HER2-E showed little benefit from palbociclib plus letrozole (13.8 months vs 11 months) (Figure I12, Finn *et al.*, 2018).

Interestingly, in a recent study Brasó-Maristany and colleagues explored changes in molecular subtype after anti-HER2 therapies in HER2+ BCa cell lines (HER2-E PAM50 molecular subtype) (Brasó-Maristany *et al.*, 2020). The inhibition of HER2 pathway switches the HER2-E molecular subtype towards a low-proliferative LumA phenotype both in patient’s tumors and *in vitro* models (Brasó-Maristany *et al.*, 2020).

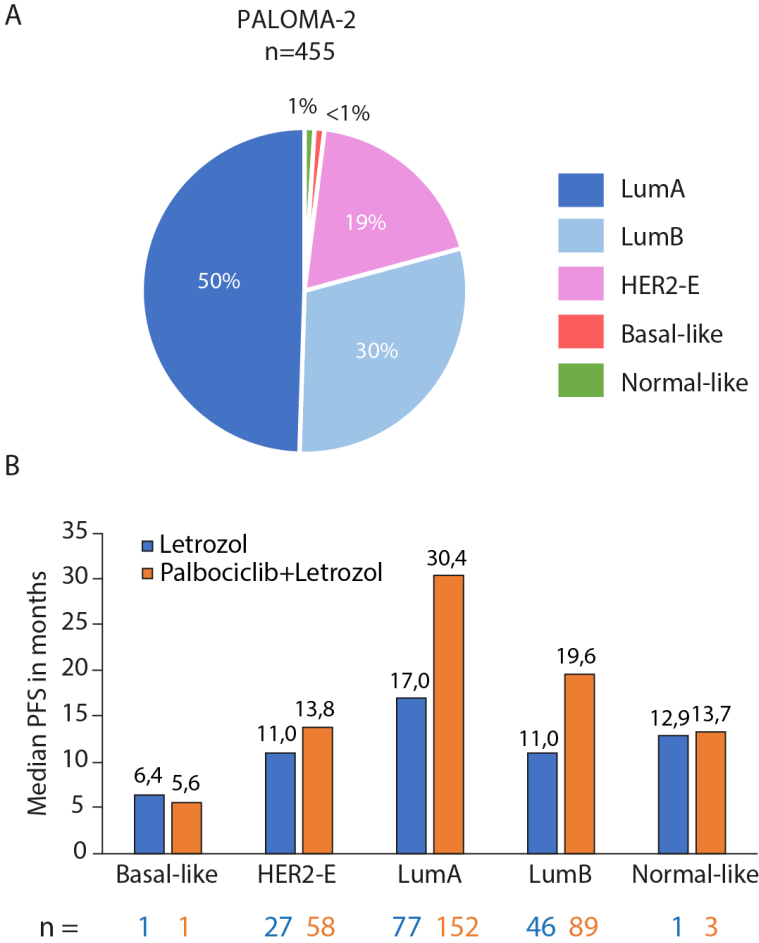


Figure I11. Retrospective analysis of CDK4/6i effect in PALOMA-2.

(A) PAM50 classification of 455 ER+/HER2-negative advanced BCa samples from PALOMA-2 clinical trial. (B) Median PFS in months of each intrinsic subtype after letrozole treatment or Palbociclib plus letrozole. Number of samples analyzed is noted under each condition. Adapted from Finn *et al.*, 2016.

This switch towards the luminal phenotype after anti-HER2 therapy returns sensitivity to CDK4/6i. When HER2 blockade was discontinued *in vitro*, cells switched back to HER2-E intrinsic subtype and increased resistance to CDK4/6i. Moreover, sustained anti-HER2 treatment caused the development of acquired resistance, which abolished subtype switch and sensitivity to CDK4/6i (Brasó-Maristany et al., 2020).

In line with these results, an exploratory study analyzed the PAM50 subtype in 29 samples of NeoPalAna trial that included 50 postmenopausal women with ER+/HER2-negative early BCa treated with neoadjuvant AI plus palbociclib. Non-luminal subtypes, including HER2-E subtype, showed no response in Ki67 reduction. This result reinforces the association of HER2-E subtype with HT resistance phenotype and resistance to CDK4/6 inhibition (Ma et al., 2017).

Collectively, these data suggest that the analysis of intrinsic subtype in patients' samples may become a potential predictor of CDK4/6i response. The molecular subtypes of ER+/HER2-negative BCa tumors correlate with the different CDK4/6i treatment outcomes. Of note, in the case of HER2-E subtype tumors these observations need to be addressed, because they represent a big proportion of ER+/HER2-negative BCa tumors and they present increased resistance to luminal treatments such as endocrine therapy and CDK4/6i. Therefore, understanding which mechanisms drive CDK4/6i resistance in HER2-E subtype ER+/HER2-negative metastatic BCa tumors is key to develop new therapeutic strategies to overcome this resistance.

Objectives

CDK4/6i treatment improves the PFS and OS in ER+/HER2-negative advanced BCa patients, as demonstrated in different clinical trials. This changed the standard of care for treating metastatic ER+/HER2-negative BCa patients. However, an important proportion of ER+/HER2-negative advanced BCa patients are PAM50 classified as HER2-E molecular subtype. In different retrospective analyses, HER2-E subtype has been associated with increased CDK4/6i resistance. Therefore, these patients have no benefit from CDK4/6i treatment. Unraveling which factors determine CDK4/6i response or resistance in ER+/HER2-negative advanced BCa patients classified as HER2-E by PAM50 is central to improve these patients' outcome. In this thesis, we tried to characterize mechanisms that drive CDK4/6i resistance in HER2-E subtype advanced ER+/HER2-negative BCa.

- 1 - To identify gene drivers of CDK4/6i resistance by genome-wide CRISPR-Cas9 screen in palbociclib-resistant cell lines.
- 2 – To integrate the different molecular and clinical analyses and select the candidate gene driver of CDK4/6i resistance.
- 3 – To clinical and functionally validate XXXX-induced CDK4/6i resistance.
- 4 – To unravel the molecular mechanism downstream of XXXX driving CDK4/6i resistance.

- Methods -

Methods

Cell culture

Human metastatic BCa cell lines T47D, MCF7, ZR75, BT474, MDA-231 and SKBr3 and human embryonic kidney 293T cells were purchased from American Type Culture Collection (ATCC, USA). MCF7-derived palbociclib-resistant (MCF7-PR) cell line was generated by treating with increasing doses of palbociclib (#S1116, Selleckchem) in each passage for 6 months. BT474 with acquired resistance to anti-HER2 dual therapies lapatinib or tucatinib, together with trastuzumab were developed in Prat Lab following the protocol described in Brasó-Maristany *et al.*, 2020 (BT474-LTR and BT474-TTR).

All cell lines were cultured in DMEM medium supplemented with 10% Fetal Bovine Serum (Gibco), 100 units/mL Penicillin, 100 ug/mL Streptomycin and 5% L-glutamine at standard conditions (37°C, 5% CO₂). MCF7-derived cell line was maintained in complete medium with 500nM palbociclib. Cells were routinely tested for mycoplasma. Transgene selection in genetically modified cell lines was induced using puromycin (2 µg/ml) or blasticidin (10 µg/ml).

Immunocytochemistry

Cell pellets were embedded in paraffin blocks. For staining with antibodies, paraffin sections were deparaffinized and rehydrated through a series of decreasing alcohol dilutions (Xylene-96-90-80-70-50-25% ethanol and distilled water). For ER staining, antigen retrieval was performed with Tris-EDTA at pH=9 with PTLINK 20 min at 97°C and then, permeabilized with 1X PBS - 0,1% triton 10 min at RT. For HER2 staining, antigen retrieval was performed with citrate at pH=6 with PTLINK 1h 15min at 97°C and then, permeabilized with 3 washes with Tris buffered saline containing 0.1% Tween (TBS-T). Both stainings were blocked with peroxidase-blocking solution (#S2023, Dako) for 10 min at RT. Primary antibody (1/100) were diluted in antibody diluent (#S0809, Dako) for 45 min at RT. Secondary HRP-conjugated antibody was added for 45 min at RT. Sections were incubated with DAB from 10 sec to 3 min. Hematoxylin was used as a counterstaining dye. Slides were dehydrated and mounted with DPX (06522, Merck).

Fluorescent *in situ* hybridization (FISH)

Cell pellets deparaffinated with the described protocol and were autoclaved with citrate pH=6 for 4 min at 120°. Slides were incubated with Proteinase K (Dako) for 5 min at RT. Cells were fixed with 10X formalin 10 min at RT. Formalin was

removed with 2X SSC Pre-hybridization Buffer (20X stock solution consists of 3 M sodium chloride and 300 mM trisodium citrate pH=6,2) and then dehydrated with growing ethanol dilution. Slides were dried and 10 ul of ERBB2/Con17 probe (#ERBB2-CHR17-20-ORGR, BioTrend) was added in a dark and humid chamber. For probe hybridization, samples were denaturated for 5 min at 83°C and incubated O/N at 37°C. Samples were washed first with 0.4X SSC-0.3% NP-40 (#CA-630 Igepal, Sigma) for 2 min at 73°C and then with 2X SSC-0.1%NP-40 for 2 min at RT. Slides were washed with H₂O and dehydrated with growing ethanol concentrations. Finally, ProLong Gold antifade mounting medium with DAPI was added.

Proliferation assay and IC50 estimation

A total of 5.000 tumor cells per well were seeded in 96-well plates. Next day, palbociclib was added in increasing doses for 4 days. Proliferation was assessed with CyQUANT NF (No Freeze) Cell Proliferation (#C35007, ThermoFisher Scientific) according to manufacturer's instructions. Fluorescence measurements were taken using FL800 Fluorescence plate reader with excitation at 485 nm and emission detection at 520 nm. Each reading was normalized with the non-treated value of the appropriate cell line. IC50 was estimated manually.

β-galactosidase staining

Tumor cells were seeded in 24-well plates and treated with palbociclib at different time points. Then, they were washed in PBS, fixed for 15 min at RT in fixing solution (5mM EGTA, 2mM MgCl₂, 0.2% glutaraldehyde in 0,1M phosphate buffer), washed, and incubated O/N at 37°C (without CO₂) with fresh 1mg/ml x-gal in dimethylformamide added to stain solution (40mM Citric acid, 5mM potassium cyanoferrate (II), 5mM potassium cyanoferrate (III), 150mM sodium chloride, 2mM magnesium chloride in phosphate). After a final wash, images were taken with a brightfield microscope. This protocol was adapted from Dimri *et al.*, 1995.

Genome wide CRISPR/Cas9 drop out screening

The Human CRISPR Knock-out Pooled Library (Brunello) (#73178-LV, Addgene, Doench et al., 2016) was used for gene knock-out screen. Viral particles were purchased ready to use.

Screening optimization

We selected ZR75 and BT474 ER+ BCa palbo-resistant cell lines for performing the genome wide CRISPR/Cas9 drop out screening. Following Doench *et al.*, 2016 protocol, we first determined the appropriate multiplicity of infection (MOI) for each

cell line. Three million cells were seeded into each well of a 12-well plate. Viral particles were added at volumes that ranged from 0 to 500 μ L from a 10⁷TU/ml provided stock, supplemented with 8 μ g/ml polybrene (#H9268-5G, Sigma). Cells were then centrifuged at 2000 g for 2 hours at 37°C. After centrifugation the cells were incubated 48h with the virus and then the media was changed. Next day, the cells were trypsinized and treated with 2 μ g/ml puromycin for one week until non-infected cells were dead. Media with fresh puromycin was changed every 48h. We selected the MOI of 0,4 to have one viral particle infecting one single cell. The minimum number of cells seeded in the experiment was determined by:

Min. cells needed = 76,441 sgRNAs x 500 cells/sgRNA x (1/0,4) = 95.5x10⁶ cells

Viral infection was performed in 34 wells of a 12 well plate at 3 \cdot 10⁶cells per well with 8 μ g/mL polybrene and 1,25 \cdot 10⁶ TU/well for ZR75. For BT474, MOI was optimized to 50 wells of a 12 well plate at 2 \cdot 10⁶ cells per well and 1,25 \cdot 10⁶ TU/well for 48h infection. Infected cells containing the pooled sgRNA library were under selection for one week and expanded to 6x10⁷ cells per condition, minimum 500x representation was always maintained. Palbociclib (#S1116, Selleckchem) was added to the medium at a concentration of 50 nM. Vehicle was added to the control condition. After 4 days of drug treatment, cells were trypsinized, pellet, and stored at -80° C.

DNA extraction and library preparation

Genomic DNA was extracted using Genra Puregene Cell Kit (#158788, Qiagen). Frozen pellets containing 5 \cdot 10⁷ cells were lysate and purified using the protocol indicated by manufacturers. The gDNA concentration was measured using NanoDrop One (ThermoFisher).

Two-step PCR reactions were used to amplify and attach sequencing tails. Primer sequences are available in Table M3. Previously to the libraries preparation the sequence of the amplicon from the PCR2 was checked by Sanger sequencing. A custom sequencing primer of 44 nucleotides for the Illumina run was designed from the chromatogram. The low complexity of this kind of libraries is increased with the start of the sequence at the first nucleotide of the sgRNA, so the diversity is high at the 20 first nucleotides and drops later. In the first PCR (PCR1) the region encompassing the integrated sgRNA is amplified from the genomic DNA with custom primers. The forward primer has only the part needed to bind to the flowcell (P5) without the Illumina sequencing primer binding site and vector specific sequence upstream the sgRNA insert. The reverse primer contains a partial adaptor sequence of the NEBNext adaptor and the vector specific sequence downstream the

sgRNA insert. To maintain 500x representation we performed 12X PCR1 reactions per condition, obtaining a total amount of 200 µg of amplified DNA (17 µg DNA per reaction). Premix Ex Taq™ DNA Polymerase Hot Start Version (#RR006A, Takara) was used to amplify the gDNA. The program used for the PCR1 was: 1 min at 95 °C; followed by 30 s at 95 °C, 30 s at 55°C, 30 s at 75 °C, for 18 cycles; and a final 10 min extension at 72 °C. Twelve PCR1 reactions for each condition were pooled in each sample and quantified with Qubit dsDNA HS Assay Kit (#Q32851, Invitrogen). The second PCR reaction (PCR2) was used to add Illumina sequencing tails with unique indexes (Table M3) for each library.

The PCR2 was carried out at similar conditions as PCR1 except for the number of cycles. The optimal number of cycles is determined for each sample by qPCR with SYBR Green in order to maintain the relative representation of each sgRNA avoiding the over-amplification. Amplicons from PCR2 were purified with Mag-Bind® Total Pure NGS (Omega BIO-TEK) beads in a PCR-product-to-bead ratio of 1:1.1. The resulting libraries were quantified with Invitrogen Qubit dsDNA HS Assay and the nmolar concentration and the sizing were determined by electrophoresis with Agilent DNA 1000 chips.

Sequencing and data processing

Cells after selection (time 0), Vehicle-treated cells and Palbociclib-treated cells (three conditions per cell line) were sequenced as a pool on Illumina HiSeq2500 by 50-bp single-end sequencing with the custom sequencing primer (CGATTTCTTGGC TTTATATATCTTGTGGAAAGGACGAAACACCG). The desired output was a library representation threshold of 500X (40 million reads per sample).

All the computational analyses of CRISPR/Cas9 screening data were performed with the MAGeCK-VISPR software (Li *et al.*, 2015). Data pre-processing consisted on i) alignment of sequencing reads to the Brunello sgRNA library, ii) sgRNA count, and iii) sgRNA count normalization using a list of 1000 non-targeting control sgRNAs. Then, we used the MAGeCK-RRA (Li *et al.*, 2014) module from MAGeCK-VISPR to assess the sgRNA count differences between the Palbociclib-treated and the corresponding control sample within each condition (i.e. cell line and sampling time). Namely, MAGeCK-RRA yields, for each gene within a condition, a robust rank aggregation (RRA) score, as well as a consensus sgRNA log₂ fold change. We also employed the MAGeCK-MLE (Li *et al.*, 2015) module to estimate a beta score (β) that indicate a significant (FDR <0.25 after 10 permutations) increase (positive β) or decrease (negative β) in sgRNA counts with respect to the Time 0 sample. Genes that are potential conferrors of resistance to palbociclib have negative β scores in the Palbociclib-treated samples, while in control

samples their β scores are either positive or, in any case, non-significantly different from 0. Both measurements showed whether the treated sample has lower sgRNA counts than the control, which could mean that knocking-out a specific gene is negatively selected exclusively in the presence of palbociclib, therefore suggesting that the gene provides resistance to the drug. GSEA (Subramanian et al., 2005) was determined using the β scores provided before. Using Broad Institute GenePattern (Reich et al., 2006) and Bioconductors' R package `org.Hs.eg.db`, genes were annotated according to GO terms labels.

Statistical analysis of patient's data sets

Patient's data set

CDK patient cohort includes 162 samples from 147 HR+/HER2-negative metastatic BCa patients. Patients were treated with CDK4/6i (including palbociclib, ribociclib and abemaciclib) at Hospital Clinic of Barcelona between 2014 and 2021. Samples collected at baseline (134 samples) included 61 primary tumor and 73 metastatic tissues. Additionally, 28 samples from progressive disease (PD) were available for molecular characterization. The hospital institutional ethics committee approved the study in accordance with the principles of Good Clinical Practice, the Declaration of Helsinki, and other applicable local regulations. The medical records were retrospectively reviewed to obtain the clinical data analyzed in the study.

CORALEEN data set was obtained from patients participating in a phase II clinical trial (completed clinical trial registered with ClinicalTrials.gov, NCT03248427 Prat *et al.*, 2020) that included post-menopausal patients with primary operable LumB subtype HR+/HER2-negative BCa. The clinical trial randomized patients (1:1) to get administered neoadjuvant treatments either six 28-days cycle of ribociclib (oral 600 mg daily for 3 weeks on, 1 week off) plus daily letrozole (twice a day oral 5 mg) or four cycles of chemotherapeutic agents doxorubicin (intravenous 60 mg/m²) and cyclophosphamide (intravenous 600 mg/m²) every 21 days followed by weekly paclitaxel (intravenous 80 mg/m²) for 12 weeks. The neoadjuvant therapy lasted for 24 weeks. Samples were collected at baseline, day 15 of treatment and time of surgery of the primary BCa tumors.

The **TCGA** RNAseqV2 gene expression data (“Comprehensive Molecular Portraits of Human Breast Tumours,,” 2012) and clinical data were obtained from the cBioportal (Gao *et al.*, 2013). Altogether, we collected and analyzed 1,096 female BCa from the TCGA with normalized gene expression and specific clinical status. Molecular subtype based on PAM50 score was available for 981 BCa tumors.

The **METABRIC** cohort includes 1026 ER+/HER2-negative BCa patients. Gene expression was standardized within subtype and ER status (Curtis et al., 2012). This cohort was downloaded from the cBioportal for Cancer Genomics (Cerami et al., 2012).

Statistical analysis

PFS was referred to the period between treatment start and the time of relapse, whereas OS was defined as the period between the start of the treatment and death or last follow-up. Kaplan-Meier curves and the log-rank test determined the survival estimation. Prognostic significance of each variable was assessed using univariate and multivariable Cox models. Significant differences were considered with a p-value <0.05. Differential gene expression was identified using unpaired and paired significance analysis of microarrays (SAM) with a false discovery rate (FDR). Statistical analysis was performed in R 3.6.3. (<http://cran.r-project.org>).

In the TCGA cohort, the correlation between the 11 candidate drivers of CDK4/6i resistance was examined using the Pearson correlation test one by one. P<0.05 was considered to be a significant correlation.

In the METABRIC cohort, the expression of the CDK4/6i resistance candidates' signature was associated with overall survival using Cox proportional hazards models where samples' cohort of origin was included as covariate for statistical control. Hazard Ratios (HR) were computed as measures of association and statistical significance was assessed by means of Wald tests for pairwise comparisons. For creation of gene signatures scores, expression values were centered and scaled gene-wise to produce z-scores, which were then averaged across all genes included in the given gene signature. The resulting scores were in turn centered and scaled across samples that were included in the dataset. For each gene, sample groups of low, medium and high expression levels were defined using tertiles as cutoffs. Also, Cox proportional hazard ratios smoothed by continuous signature expression levels were graphically represented using smoothing splines with a p-spline basis (Eilers and Marx, 1996) as implemented in the R package phenoTest.

Gene expression analysis

RNA samples of the CORALEEN clinical trial and CDK cohort were extracted using High Pure FFPE RNA isolation kit (Roche) following manufacturer's instructions. From 1 to 5 10-um FFPE slides from each tumor sample were used and macrodissected, if needed, to avoid normal tissue contamination. RNA from cell lines was extracted with Pure Link RNA MiniKit (Invitrogen) and quantified with

NanoDrop spectrophotometer (Thermo Fisher Scientific). For clinical samples, a minimum of 100ng of total RNA was analyzed at the nCounter platform (Nanostring Technologies) using the Breast Cancer 360™ Panel, which measures the expression of 771 breast cancer-related genes and 5 housekeeping genes (ACTB, MRPL19, PSMC4, RPLP0, and SF3A1). For cell lines samples, a custom nCounter panel of 72-gene set including PAM50 genes was used to assess the molecular classification (Wallden et al., 2015). Using custom scripts in R 3.6.3, expression counts were normalized and all tumors and cell line samples were assigned to an intrinsic molecular subtype of BCa (LumA, LumB, HER2-E, Basal-like and Normal-like) using PAM50 subtype predictor (Parker et al., 2009)

CRISPR Cas9 genetic knock-out

The CRISPR/Cas 9 backbone plasmid vector used for generating XXXX KO was the lentiCRISPRv2 (#52961, Addgene). All sgRNAs sequences were designed using Synthego crispr design tool (Table M3, <https://design.synthego.com>). The top 4 target sites for XXXX [Eliminated ID sequence – confidential information] were assessed considering exon number, on target and off targets scores. The protocol for cloning the top ranked single guide RNAs (sgRNA) into the lentiviral transfer plasmid followed was the one vector system, described in Sanjana *et al.* (2014) and Shalem *et al.* (2014). We designed oligos carrying a BsmBI digestion site in the 5' end of 20 nucleotide sgRNA sequences for each target site. Each pair of synthesized oligos was annealed, phosphorylated and ligated to BsmBI linearized vector using FastDigest Esp3I kit (#FD0454, ThermoFisher). We checked the final construct by sequencing with hU6 promoter primer. We generated lentivirus carrying the sgRNA-Cas9 plasmid and infected cell lines of interest to generate stable XXXX knock-out cell lines. After puromycin selection, we obtained a pool of mutated cells without XXXX. The pool of XXXX KO GFP+ cells was trypsinized and collected and single sorted for GFP expression by FACS Aria 2.0 into a P96 well plate.

Protein extraction and Western Blot

Cells were lysed with RIPA buffer composed of 25 mM Tris-HCl (pH= 7.5), 150 mM NaCl, 1% NP-40, 1% sodium deoxycholate and 0.1% SDS, 10 mM NaF, 1mM Na₃VO₄, supplemented with protease and phosphatase inhibitors cocktail (Roche) and sonicated 10 minutes on ice with a 30s interval at medium intensity using Bioruptor Standard sonication device (Diagenode). Sonicated samples were centrifuged at maximum speed for 10 min at 4°C and supernatant was stored at -80°C. Protein concentration was assessed by Protein Assay (BioRad), based on the Bradford method. The same amount of protein for all samples was mixed with

sample buffer (45 mM Tris pH 6.8, 10% glycerol, 1% SDS, 52 mM DTT and 1% bromophenol blue) and denaturalized at 95°C for 5 min. Proteins were loaded and separated by standard SDS-PAGE gel and transferred to PVDF membranes (Immobilon-P). In order to avoid unspecific antibody binding membranes were blocked with TBS-T and 5% bovine serum albumin (BSA, #A7906, Sigma) for 1h shaking at RT. Primary antibodies were incubated overnight at 4°C or 1 h at RT (Table M1). Membranes were washed for 5 min 3 times with TBS-T and incubated 1h at RT with animal specific HRP-conjugated secondary antibodies (1/5000). Membranes were washed with TBS-T for 5 min 3 times and 1 min with Pierce™ ECL Western Blotting Substrate (#32106, Thermo Fisher Scientific). HRP activity was developed using super RX-N films (Fujifilm). Protein bands density was calculated using Image J software.

RNA extraction, reverse-transcription and quantitative real-time PCR analysis

RNA was extracted from frozen cell pellets using Pure Link RNA MiniKit (#12183018A, Invitrogen) as indicated by manufacturer's instructions. Concentration and quality of the mRNA was assessed by a NanoDrop spectrophotometer. cDNA was obtained by reverse transcription reaction using 1 µg of total RNA and a high-capacity cDNA reverse transcriptase kit (Applied Biosystems). Quantitative PCR was performed using TaqMan gene expression assay. The expression of different genes of interest was measured with specific TaqMan probes (Table M2) mixed with TaqMan Universal PCR Master Mix (Applied Biosystems) as indicated in the datasheet. Three technical replicates were measured per reaction. Depending on the experiment, B2M or GAPDH were used as housekeeping genes using comparative CT method.

siRNA-induced gene silencing

In order to induce transient silence of XXXX expression siGENOME SMARTpool targeting XXXX (#XXXX, ThermoFisher Scientific) was transfected into the different cell lines. Negative control used was Silencer® Select Negative Control #1 (#4390843, ThermoFisher Scientific). The transfection of the siRNA was performed with 20 nmol/L siRNA using Lipofectamine RNAiMax transfection reagent (#13778-075, Invitrogen), following the manufacturer's instructions.

Viral production and infection with silencing shRNA and overexpression plasmids

pLKOlentiviral vectors with human shRNA sequences were obtained from MISSION TRC1 library (Table M4). Precision LentiORF Human XXXX (#XXXX, Horizon) was used for XXXX overexpression experiments. The amplification of all the plasmids was done in DH5a *E. coli* bacteria strain. After plasmid isolation with PureLink HiPure™ (#K210017, Invitrogen), 3 µg of shRNA/XXXX OE plasmid was mixed in 1:1 ratio with third generation packaging vectors V-SVG, RRE and RSV in NaCl (150 mM) supplemented with PEI (5,8 µg/ml). HEK-293T cells were transfected with the mix and left O/N. Next day, fresh medium was added and the cells were incubated at 37°C for 48h in order to allow viral production. Medium with viral particles was collected, filtrated (0,45µM) and stored at -80°C. Polybrene (8 µg/ml) was added to the medium containing the virus before the transduction. Recipient cells in 50% confluence were incubated with the mix for 24h and passed adding puromycin antibiotic (2 µg/ml) for shRNA infection and blasticidin (10 µg/ml) for XXXX OE infection to the fresh medium to select for stable cell lines.

XXXX side-directed mutagenesis

We mutated XXXX from Precision LentiORF Human XXXX using QuikChange Lightning Multi Site-Directed Mutagenesis Kit (#210515-5, Agilent). We designed the mutagenesis primers per each specific mutation (Table M3). For the XXXX constitutively active (CA) form, we changed XX that is translated into XX mutation. For the XXXX kinase dead (KD), we changed XX that is translated in XX. We performed a PCR according to the kit's datasheet to amplify the plasmid carrying the mutated region. Then, we added *DpnI* restriction enzyme to the PCR product and incubated 5 min at 37°C to digest parental non-mutated ds-DNA. Finally, we transformed the digested PCR product into DH5- α *E. Coli* bacteria and seeded them into agar plates with ampicillin. Next day, we selected different individual colonies, let them grow O/N and extracted the plasmids using Miniprep. We sequenced XXXX gene with sequential primers (Table M3) to validate that the only mutation we generated was the expected one.

Proximity-dependent biotin identification (BioID)

XXXX was amplified by PCR from Precision LentiORF Human XXXX using primers designed to have NheI and HpaI restriction enzyme sites (Table M3) and cloned into MCS-BioID2-HA (#74224, Addgene).

MCF7 cells were transfected with empty myc-BioID2 as a control and XXXX-BioID2-HA plasmids using GenJET DNA transfection reagent for MCF7 cells (#SL100489-MCF7, SignaGen Laboratories) following manufacturer's instructions. Five P150 plates per condition were treated with 50 μ M Biotin in the medium overnight. Next day cells were trypsinized and cell pellets were lysated using 5 ml of lysis buffer (50 mM Tris-HCl pH=8, 150 mM NaCl, 0.1% SDS, 2 mM MgCl₂, 1% Triton X-100, 1 mM EDTA, 1 mM EGTA, 1 mM NaF, 1 mM Na₃VO₄, protease inhibitor cocktail (Roche)) with 1:2000 benzonase (Sigma-Aldrich) by rotating for 1 h at 4°C. Then, samples were sonicated with 3 rounds of 30 sec ON/OFF with Bioruptor (Diagenode) and centrifuged at 15000g for 30 min at 4°C. Biotinylated proteins were captured by immunoprecipitation (IP) protocol using Dynabeads® MyOne Streptavidin C1 beads (#65002, Thermo Fisher Scientific). After isolation, proteins-bead complexes were washed once with lysis buffer and three times with 50 mM NH₄HCO₃ before digestion. Tryptic digestion was performed directly on beads by incubating them with 2 μ g of trypsin dissolved in 300 μ L of 50 mM NH₄HCO₃ at 37°C overnight (200 μ L were added to the delivered 100 μ L volume). The following morning, an additional 1 μ g trypsin was added and incubated for 2 h at 37°C.

Beads were pelleted by centrifugation at 2,000g for 5 min, and the supernatant was transferred to a fresh Eppendorf tube. Beads were washed once with 100 μ L of 50 mM NH₄HCO₃, and then pooled with the first supernatant. Formic acid was added to the eluates to a 1% final concentration. Complete separation of the beads is performed with a little magnet. Samples were cleaned up through C18 tips (polyLC C18 tips) and peptides were eluted with 80% acetonitrile - 1% trifluoroacetic acid. Next, samples were diluted to 20% acetonitrile - 0.25% trifluoroacetic acid, loaded into strong cation exchange columns and peptides were eluted in 5% NH₄OH, 30% methanol. Finally, samples were evaporated to dry, reconstituted in 50 μ L and diluted 1:8 with 3% acetonitrile, 1% formic acid aqueous solution for MS analysis.

The nano-LC-MS/MS set up was as follows. Digested peptides were resuspended in 50 μ L of 3% acetonitrile - 1% formic acid and diluted 1:8 in 0.1% formic acid aqueous solution. Sample was loaded to a Evotip C18 μ -precolumn (Evosep), MSPCF Protocol_70 (SampleLoading_forEvotips). Peptides were separated using a C18 analytical column EV1106 column (150 μ m \times 150 mm, 1.9 μ m) (Evosep) using a Evosep One (EV-1000, Evosep) chromatographic system with an 88 min run. The column outlet was directly connected to an Orbitrap Eclipse™ Tribrid (Thermo Scientific). The mass spectrometer was operated in a data-dependent acquisition (DDA) mode. Survey MS scans were acquired in the Orbitrap with the resolution (defined at 200 m/z) set to 120,000. The lock mass was user-defined at 445.12 m/z

in each Orbitrap scan. The top speed (most intense) ions per scan were fragmented by CID and detected in the linear ion trap. The ion count target value was 400,000 and 10,000 for the survey scan and for the MS/MS scan respectively. Target ions already selected for MS/MS were dynamically excluded for 15 s. RF Lens were tuned to 30%. Minimal signal required to trigger MS to MS/MS switch was set to 5,000. The spectrometer was working in positive polarity mode and singly charge state precursors were rejected for fragmentation.

A DDA label free search was performed using MaxQuant software v1.6.17.0 (MQ) and its Andromeda search engine (Cox *et al.*, 2011, 2014; Cox and Mann, 2008; Schaab *et al.*, 2012; Turner *et al.*, 2019; Tyanova *et al.*, 2015, 2016). Human protein database from SwissProt (released on 2021/06) was used as a database along with our proteins XXXX and BioID2 sequences and the list of common contaminants included by default in MQ. The search was run against the target and the decoy databases in order to determine the false discovery rate (FDR). Only peptides with an FDR below 1% were considered as positive identifications. Some of the most relevant search parameters were trypsin (allowing for two missed cleavage sites) as digesting enzyme; oxidation in methionine and methyl group loss with and without acetylation in protein N-terminus as dynamic modifications; 10 ppm as precursor mass tolerance; and 0.6 Da as MS/MS mass tolerance.

The SAINTq algorithm was used for the interactome analysis (Teo *et al.*, 2014, 2016) using the protein groups MS1 intensities provided by MQ. Contaminant and decoy identifications were removed and only unique peptides for protein groups were sent to SAINTq. The resulting list with potential interactors was initially filtered by requiring a fold change (FC) greater than or equal to 3 and a Bayesian false discovery rate (BFDR) lower than or equal to 0.02. However, in order to get a preliminary (and slightly broader) interactome landscape, we decided to relax the BFRD $\leq 0,21$. This threshold was chosen based on the known XXXX interactor YYYY. In MCF7-PR cell lines the positive control YYYY showed an BFDR=0,21, therefore we decided to relax the variable up to that point.

Immunofluorescence

Cells were seeded in round glass coverslips in 12-well plates and let them attach O/N. Cells were treated with specific protocols depending on the experiment. Then, cells were fixed with formalin for 20 min at RT. Cells were permeabilized with PBS-0,5% Triton X-100 for 10 min and blocked with PBS-1% BSA for 45 min at RT. Coverslips were incubated with specific the primary antibody for 1h at RT or O/N at 4°C. Then, animal specific secondary antibody was incubated 1h at RT. DAPI counterstain for nuclear detection was included in the ProLong Gold antifade

mounting medium (# P36935, Thermo Fisher Scientific). Stack images were taken with confocal Zeiss LSM780 microscope with 63X/1. oil immersion objective.

- Materials -

Materials

Table M1. List of Antibodies.

Antigen	ID	Supplier	Source	Application	Dilution
<i>Primary Antibodies</i>					
HER2	A0485	Dako	Rabbit	ICC	1:200
ER	sc-543	Santa Cruz	Rabbit	ICC	1:100
XXXX	XXXX	Cell Signaling	Rabbit	WB	1:1000
CCNE1	05-363	Merck	Mouse	WB	1:500
Tubulin	T5168	Sigma Aldrich	Mouse	WB	1:5000
GAPDH	G8795	Abnova	Mouse	WB	1:5000
HA-Tag	H3663	Sigma Aldrich	Mouse	WB	1:1000
				IF	1:500
MYC-Tag		Cell Signaling	Rabbit	WB	1:1000
				IF	1:500
<i>Secondary Antibodies</i>					
Rabbit IgG HRP-conjugated	NA934	GE Healthcare	Donkey	WB	1:5000
Mouse IgG HRP-conjugated	31452	ThermoFisher Scientific	Rabbit	WB	1:5000
Streptavidin HRP-conjugated	ab7403	Abcam		WB	1:1000
Streptavidin Alexa Fluor 546-conjugated	S11225	Invitrogen		IF	1:500
Rabbit IgG Alexa Fluor 488-conjugated	A-11008	Invitrogen	Goat		1:500
Mouse IgG Alexa Fluor 488-conjugated	A-11001	Invitrogen	Goat		1:500

Table M2. List of Taqman probes.

Gene Symbol	ID	Supplier
CCNE1	Hs01026536_m1	Applied Biosystems
XXXX	XXXX	Applied Biosystems
GAPDH	Hs02786624_g1	Applied Biosystems

Table M3. List of primers.

Name	Primer sequence (5' to 3')	Information
<i>Primers for CRISPR/Cas9 screening library preparation</i>		
P5+vector	AATGATACGGCGACCACCGAGATCTCGAT TTCTTGGCTTTATATATCTTGTGGAAAGG ACG	Forward PCR1 primer
Adaptor+vector	GTGACTGGAGTTCAGACGTGTGCTCTTCC GATCTCCAATTCCTCAAGACCT	Reverse PCR1 primer
P5	AATGATACGGCGACCACCGAGATCT	Forward PCR2 primer
NEBNext + adaptor	CAAGCAGAAGACGGCATACGAGAT index GTGACTGGACTTCAGACGTGTGCTCTTCC GATC	Reverse PCR2 primer

Index

Time 0 - NEBNext Index 37 - CGGAAT

Vehicle- treated - NEBNext Index 30 - CACCGG

Palbo-treated - NEBNext Index 41 - GACGAC

[Eliminated section - confidential information]

Table M4. List of plasmids.

Name	Supplier	Information
Precision Human XXXX	LentiORF XXXX	Plasmid used for overexpressing XXXX (WT, CA, KD) and clone XXXX in MCS-BioID2-HA
lentiCRISPRv2	Addgene (#52961)	Plasmid to generate CRISPR/Cas9 KO in XXXX
XXXX siGENOME SMARTpool	ThermoFisher Scientific (#XXXX)	Plasmid including siRNA used to silence transiently XXXX
Silencer® Select Negative Control #1	ThermoFisher Scientific (#4390843)	Plasmid used as a negative control for siRNA XXXX silencing
pLKOlentiviral vectors	MISSION TRC1 library	Plasmids including shRNAs used to silence specific genes
pRSV-Rev	Addgene (#12253)	3rd generation lentiviral packaging plasmid
pMDLg/pRRE	Addgene (#12251)	3rd generation lentiviral packaging plasmid
pCMV-VSV-G	Addgene (#8454)	3rd generation lentiviral packaging plasmid
myc-BioID2-MCS	Addgene (#74223)	Plasmid used as a negative control in the BioID experiment
MCS-BioID2-HA	Addgene (#74224)	Plasmid to fuse XXXX to the N-terminus of BioID2
XXXX-BioID2-HA		Plasmid for XXXX-BioID2 fusion protein expression
pLKOlentiviral vectors	MISSION TRC1 library	
Gene	Clone ID	Target Sequence
shXXXX-1	TRCN0000XXXX	XXXX
shXXXX-2	TRCN0000XXXX	XXXX
shCCNE1-1	TRCN0000045301	GCAATTCCTTCTGGATTGGTTA
shCCNE1-2	TRCN0000045302	CGACATAGAGAACTGTGTCAA

- Results -

Experimental design to identify molecular mechanisms involved in CDK4/6i resistance in ER+ BCa

To unravel the molecular mechanisms that confer resistance to CDK4/6i in advanced HER2-E subtype ER+ BCa we designed a workflow integrating molecular and clinical data. The project was subdivided in 5 different parts (Figure R1): (1) Molecular strategy, (2) clinical data analysis, (3) integration of the candidates, (4) validation of the driver, (5) mechanism of resistance. We designed each step to tackle the biological problem (See objectives) in an unbiased and comprehensive manner. Further details will be described in the following sections of the thesis.

The molecular strategy (1) to identify resistance drivers consisted in the performance of a drop out screen. To this, we first had to select the appropriate model that recapitulated CDK4/6i resistance phenotype in HER2-E subtype ER+/HER2-negative BCa. A comprehensive characterization of different metastatic ER+ BCa cell lines was performed to select CDK4/6i-resistant cell lines, showing high HER2-E score. Next, we optimized the technical procedure to perform the screen. We used an unbiased whole genome knock-out screen. This approach is based on the induction of single mutations in each cell that globally targets most of the coding genes. The use of CRISPR/Cas 9 technology allow us to find CDK4/6i resistance driver genes through a functional *in vitro* screen. Importantly, we designed the workflow adjusting time and drug concentration to observe phenotypic effects but without inducing cell toxicity. Finally, we implemented next-generation sequencing coupled to the screen, and through bioinformatic analysis, we deconvoluted the sequenced sgRNA associated with CDK4/6i resistance. In parallel, we analyzed two clinical cohorts (2), using different statistical strategies, and selected the genes associated with poor response to CDK4/6i.

In the third step we consolidated the previous observations. We seek for convergence of the two independent strategies and selected by common candidate drivers. The integration was crucial for the reliability of the selected gene driver of CDK4/6i resistance.

We then functional and clinically validated the effect on CDK4/6i resistance of the selected gene. We designed and optimized different *in vitro* tools to validate the resistance driver. Loss- and gain-of-function strategies and the generation of an acquired resistance cell line were some of the tools used for this purpose. Further analysis using clinical data from well anotated patient samples were performed to interrogate the association of the selected gene with poor response to CDK4/6i.

Finally, in the last step we aimed to understand the molecular mechanism involved in CDK4/6i resistance in advanced HER2-E subtype ER+ BCa. We developed a proximity labeling technique to unravel the interactome of the selected gene in cells with acquired resistance to CDK4/6i.

In sum, the workflow followed had the objective to optimize and explore different perspectives in order to identify the most relevant gene driver responsible for the CDK4/6i resistance in HER2-E molecular subtype metastatic ER+/HER2- BCa tumors.

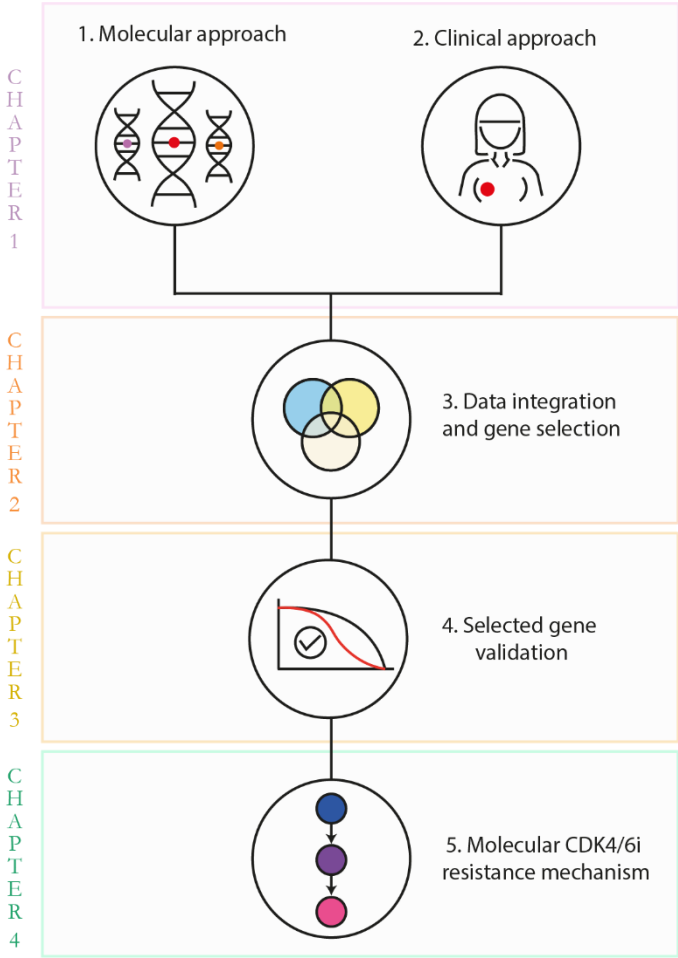


Figure R1. Project design overview.

Five main steps comprise the workflow to interrogate CDK4/6i resistance in metastatic ER+ BCa. (1) First step includes molecular strategies to obtain drivers of resistance *in vitro*. (2) In parallel, interrogation of clinical data from two patient cohorts to find genes associated with worst prognosis. (3) Integration of the different analysis and selection of a driver candidate. (4) Validation of the driver gene using different tools. (5) Exploration of the molecular mechanism leading to CDK4/6i resistance in metastatic HER2-E ER+ BCa.

CHAPTER 1

Identification of CDK4/6i gene drivers using
CRISPR/Cas9 KO screen and clinical data analysis

Genome-wide CRISPR/Cas9-based KO screen identifies potential CDK4/6i resistance drivers

a. Characterization of ER+ BCa cell lines

To study the genes responsible for CDK4/6i resistance *in vitro*, we determined the response of metastatic ER+ BCa cell lines to palbociclib treatment. We characterized different features of MCF7, T47D, ZR75 and BT474 cell lines. First, we verified the ER levels by immunocytochemistry (ICC, Figure R2A). We confirmed that MCF7 cells express the highest amount of ER, followed by T47D cells. ZR75 and BT474 cell lines express ER but at a lower level. As a negative control we used a well established ER- BCa cell line, MDA-231-MD cells (Figure R2A). Next, we tested HER2 amplification, as a main histopathological BCa marker. We used ICC and fluorescent *in situ* hybridization labelling (FISH) to determine HER2 expression in the membrane and *ERBB2* gene amplification, respectively. For performing the FISH method, we hybridize a probe at *ERBB2* genomic loci of the cell nucleus and then detected the fluorescence emitted. We used a probe targeting chromosomal centromeres (*CEN* probe) as a control for chromosomal number in each cell nuclei. As expected, BT474 cells presented more than 10 copies of *ERBB2* in most of the nuclei, translated in a high expression in the cell membrane (Figure R2B/C). The ratio *ERBB2*/*CEN* showed that BT474 cell line had more than 4 times the amount of *ERBB2* per each chromosome. BT474 cells are classified as HER2+ or HER2 amplified, whereas the rest are HER2 non amplified (Figure R2B). The rest of the cell lines did not present *ERBB2* amplification, although ZR75 presented higher expression of HER2 compared to MCF7 and T47D cells (Figure R2A).

Next, we characterized the molecular subtypes and the response to CDK4/6i of ER+ BCa cell lines. Throughout our experiments we used palbociclib, a CDK4/6i that has shown to display cytostatic growth inhibition in a panel of molecularly profiled BCa cells *in vitro* (Finn et al., 2009). Initially, we determined the molecular subtype of BT474, MCF7, T47D and ZR75 cells using nCounter technology and classified them according to PAM50 score. The PAM50 score compares the relative expression of 50 genes related with ER signaling, HER2 function, proliferation and basal-like phenotype. BT474 cells were classified as HER2-E molecular subtype, whereas the rest of the cell lines were classified as LumB subtype. Interestingly, when we focused on T47D and ZR75 PAM50 scores, we observed that HER2-E subtype scored higher than in MCF7 cells, which are the most luminal-like cells (Figure R3A and R3B). This suggests that the gene expression profile of ZR75 and T47D cells

was in a more intermediate state between HER2-E and LumB subtypes than the MCF7 cells. Next, we characterized the BCa cell lines response to CDK4/6i. To this, a palbociclib dose-response assay was performed and the relative half maximal inhibitory concentration (IC50) calculated.

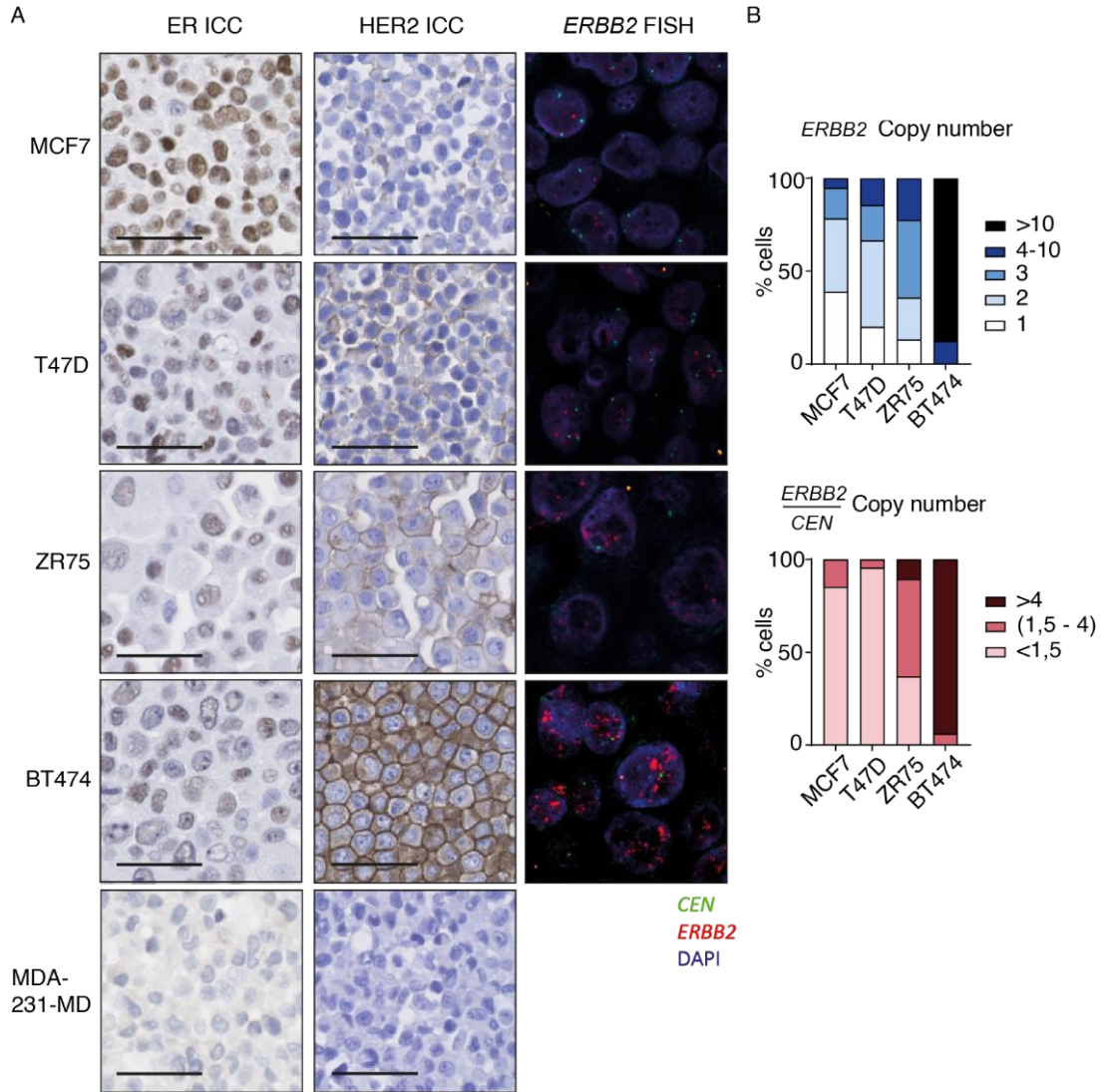


Figure R2. Defining ER and HER2 status in a cell line panel.

(A) ER ICC staining (left), HER2 ICC staining (center) and *ERBB2* (red)/*CEN* (green) FISH detection (right) in paraffin-embedded cell pellets. Nucleus were stained in blue with Hematoxylin counterstaining in ICC and fluorescent DAPI in the FISH experiment. (B) Manual quantification of *ERBB2* signal (up) and *ERBB2*/*CEN* ratio calculation (down). Scale bar: 50 μ m (black line), 10 μ m (white line).

We determined cell viability based on DNA content after 4 days of palbociclib treatment. Then, we established the palbociclib concentration required to inhibit 50% cell growth (IC50). MCF7 cells were the most sensitive cells to the drug (IC50 of 50 nM), followed by T47D cells (IC50 of 80 nM). It was previously described that BCa cell lines classified as HER2+ and TN showed increased resistance to CDK4/6i (Finn *et al.*, 2009), therefore we used BT474 cell line as a control for resistant phenotype in our experimental design. Indeed, BT474 cell line was the most resistant cell line (IC50 = 2 μ M). Unexpectedly, ZR75 cells showed resistance to palbociclib without HER2 amplification with an IC50 of 600 nM (Figure R3C). In summary, we identified palbo-sensitive cell lines (MCF7 and T47D) and palbo-resistant cell lines (BT474 and ZR75), which serve the purpose of the subsequent studies.

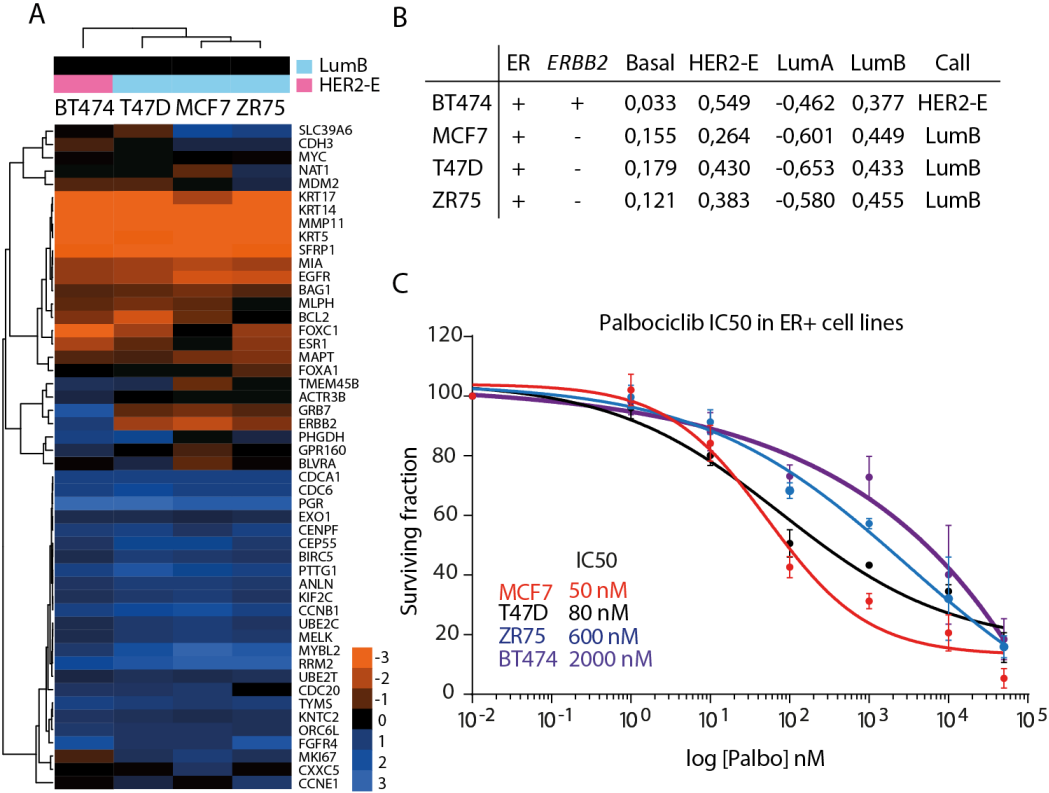


Figure R3. Characterization of molecular classification and palbociclib effect. (A) Molecular classification assessment by PAM50; BT474 cells were classified as HER2-E subtype and T47D, MCF7 and ZR75 cells for LumB subtype. (B) PAM50 scores assessed in every subtype for the four cell lines. (C) Palbociclib dose-response and IC50 measurement in all the cell lines.

Next, we established the Time variable for palbociclib treatment in order to have a functional outcome from the treatment without inducing massive senescence in the cells. To this, we tested the senescence status in our cell lines during palbociclib treatment by means of a time-course approach. Of note, the aim of the project was to identify molecular mechanisms that confer resistance to palbociclib cytostatic effect, but not to CDK4/6i induced senescence. For this reason, we selected a time point that allowed an effect on cell growth without major senescence associated β -galactosidase (β -gal) activity accumulation for our ulterior experiments. We treated the different cell lines with 50 nM palbociclib for 2, 4 and 6 days and compared the

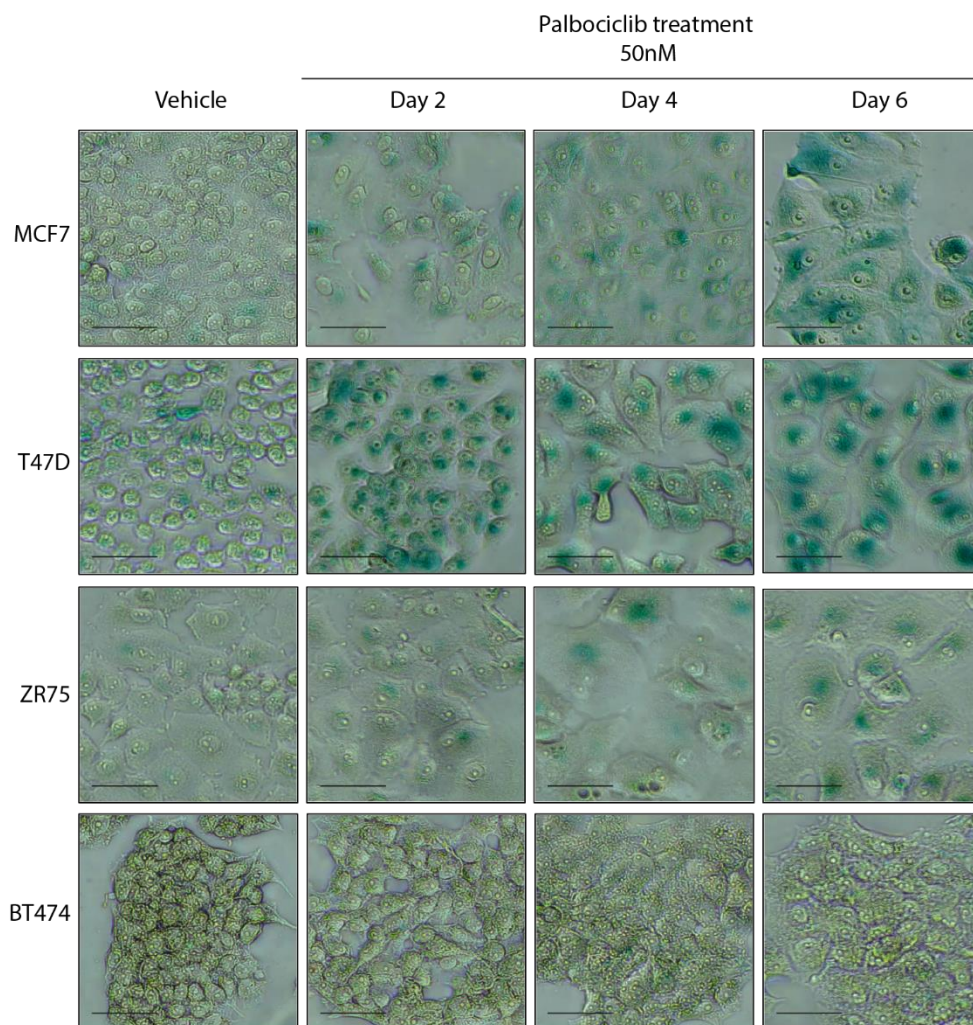


Figure R4. Palbociclib induction of senescence through time.

β -gal staining of the four cell lines at time 2, 4 and 6 days of 50 nM palbociclib treatment incubation compared with a vehicle-treated condition. Scale bar: 50 μ m (black line).

β -gal production to the vehicle condition. There were differences in β -gal staining among cell lines. T47D cells already showed β -gal staining in the vehicle condition and morphological changes with increasing incubation times of palbociclib (Figure R4). The latter cell morphology changes are associated with the acquisition of the senescence features (Collado and Serrano, 2006; Dimri *et al.*, 1995). MCF7 and ZR75 cells also showed increase β -gal activity accumulation with the strongest effect at 6 days of incubation with the drug. Interestingly, palbociclib showed little β -gal activity measured in BT474 cells. We selected the 4 days timepoint as an adequate incubation time for the functional screen.

Taking together all the experiments, MCF7 cells were selected palbo-sensitive and ZR75 and BT474 as palbo-resistant cell lines, respectively.

b. Optimization of screen workflow

High-throughput sequencing screening strategies have been extensively used to study molecular mechanisms related with drug resistance in many human cancers. In the laboratory, we previously took advantage of *in vivo* genome-wide loss-of-function shRNA screen to identified a novel regulator of metastatic dormancy in BCa (Gawrzak *et al.*, 2018). However, shRNA-based screenings present some limitations addressed in the discussion. Recent advances in genome editing technologies that have opened new opportunities in the field of functional genomic research. In 2005, Francisco JM Mojica described for the first time the function of clustered regularly interspaced short palindrome repeats (CRISPR)/Cas9 system. These sequences were used by prokaryotes as an adaptive immune mechanism to fight against viral DNA invasion (Mojica *et al.*, 2005). This finding lead to the development of the CRISPR/Cas9 system. This technology has been improved and modified to become an easy, cheap and an efficient tool to generate specific mutations in genes of interest. Because of all the advantages in using the CRISPR/Cas9 system, it has been implemented and applied for the study of gene function in a variety of biological processes. The most recent advance in CRISPR/Cas9 methodology has been the development of genome-wide libraries carrying pooled sgRNAs that target most protein coding genes (Chen *et al.*, 2015; Shalem *et al.*, 2015; Zhou *et al.*, 2014). Genome-wide CRISPR/Cas9 screen has been implemented for identifying key genes for cancer cell proliferation, survival, transformation and resistance to treatments in different *in vitro* and *in vivo* models (Shalem *et al.*, 2015; Zhou *et al.*, 2014).

In this project, we used a genome-wide CRISPR/Cas9 knock-out screen in metastatic palbo-resistant ER+ BCa cells to unravel the potential drivers of

palbociclib resistance. To this end, ZR75 and BT474 cell lines were selected as palbociclib-resistant *in vitro* model to perform the screen. The human Brunello CRISPR knock-out pooled library containing 76,441 sgRNAs, which targets 19,114 genes (four different shRNA per each gene) was used to generate a mutant cell pool where each cell carried one single mutation. The human Brunello pooled library was optimized to maximize activity and minimize CRISPR/Cas9 off-target effects (Doench et al., 2016). The screening process consisted in four main steps (Figure R5A). ZR75 and BT474 cells were infected with the virus encoding sgRNA pooled library (1). Next, a functional phenotype selection after four days of palbociclib treatment was performed (2). Genomic DNA was isolated and the amplified library was generated (3). Finally, a bioinformatic analysis of the sequencing results was performed to obtain the resistant drivers of palbociclib resistance (4).

First, we assessed the adequate viral concentration for cell transduction to establish a single insertion of each sgRNA in a single tumor cell. The recommended representation is 400 cells per each sgRNA. For optimization purposes, we seeded both palbo-resistant cell lines in 12-well plate with high confluence (3×10^6 cells/well) and infected each cell line with increasing concentrations of viral particles to calculate the appropriate multiplicity of infection (MOI). The infection efficiency increases proportionally to the MOI, therefore we used an MOI of $<0,4$, to infect $\leq 30\%$ of the cells (Figure R5B). The previous proportion of infected cell ensures that only one sgRNA is inserted in each cell. The infection of ZR75 cells was established with the recommended conditions from the manufacturers (Figure R5B). Contrarily, the conditions to infect BT474 cells needed further optimization because of the low infection efficiency. We adjusted the seeding number and the infection time in order to increase the infection rate. BT474 cells showed an appropriate MOI with $1,5 \times 10^6$ seeded cells per well and 48h of incubation time.

The screen was performed in 10^8 tumor cells based on the improved conditions per each cell line at MOI = 0,4 to ensure that we reached around 30% of the cells infected. Next, we used 50 nM palbociclib for the treated condition, a concentration that effectively suppressed cell proliferation in palbo-sensitive cells but did not have any effect in palbo-resistant cell lines (Figure R3C).

We generated the sgRNA library from the isolated genomic DNA using a two-step PCR reaction. This protocol was used to amplify the sgRNA sequence and attach sequencing tails (Figure R5C). In the first PCR, the region encompassing the integrated sgRNA is amplified from the genomic DNA with custom primers.

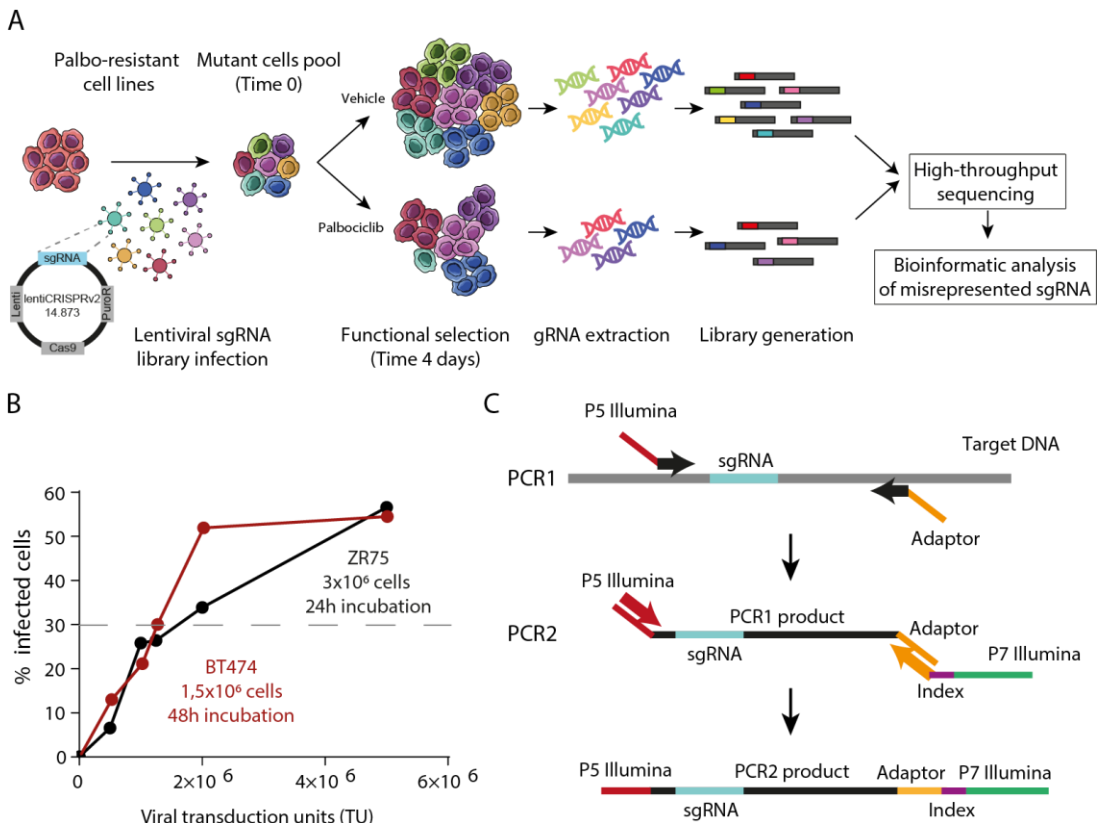


Figure R5. Genome-wide CRISPR/Cas9 screen optimization.

(A) Graphical representation of the screen workflow: (1) Viral infection of palbo-resistant cell lines with the sgRNA pooled library, (2) functional selection after four days palbociclib treatment, (3) genomic DNA isolation and library generation, (4) bioinformatic analysis of the sequencing results. (B) First test for MOI determination for ZR75 and BT474 cell lines (up) and optimization of BT474 conditions to improve infection efficiency (down). (C) Two-PCR library preparation scheme for high-throughput sequencing analysis.

The forward primer provides the binder to the flowcell (P5) and vector specific sequence upstream the sgRNA insert. The reverse primer contains partial adaptor sequence for the NEBNext adaptor and vector specific sequence downstream the sgRNA insert. The second PCR added Illumina sequencing tails (P7), together with unique indexes for each library (Table M3).

Next generation sequencing was performed at the Center for genome regulation (CRG) in Barcelona.

c. Analysis of CRISPR-Cas9 screen results

We compared in each palbo-resistant cell line the abundance of each sgRNA. We had two different conditions: a vehicle-treated condition (Control) and a palbociclib-treated condition (Palbociclib). The aim of the drop-out screen was to detect the sgRNAs that disappeared or decreased from the initial population (Time 0) after palbociclib treatment, with 0 or little effect on the vehicle-treated condition. We analyzed the sequencing results with MAGeCK-VISPR software (Li *et al.*, 2014, 2015). The principal component analysis (PCA) A and B separated the samples according to T0, Control and Palbociclib conditions (Figure R6A). Using MAGeCK-MLE module we estimated the beta score (β). The β score is calculated normalizing each treated condition (Control and Palbociclib) to Time 0. Therefore, this score measures gene selection and provides a similar evaluation than the term of 'log fold change' in differential expression analysis. When the β score is positive ($\beta > 0$) indicates that the cell population carrying one specific sgRNA was enriched in that condition. On the other hand, when the score is negative ($\beta < 0$) indicates that the cells with a mutation in one specific gene are reduced from the initial population. The latter situation in palbociclib-treated cells provided the genes that were conferring resistance to palbociclib in palbo-resistant cell lines. A mutation in resistant driver genes induces a sensitivity to the drug, thus cells carrying mutations on driver genes get arrested. Consequently, we identified all the sgRNAs with a negative β score after palbociclib treatment. The combined analysis for both cell lines showed many candidate gene drivers of resistance based on the negative β score in the treated condition. In order to avoid losing important candidates, we decided to keep a generous threshold: β palbo ≤ -0.9 (palbociclib treated condition) and β control ≤ 0.9 (vehicle treated condition). In ZR75 cells, 1,563 genes were selected and 2,386 genes in BT474 cells. We found 219 genes shared between ZR75 and BT474 cell lines (purple dots, Figure R6B). Notably, gene ontology (GO) analysis of the genes selected in ZR75 cells highlighted pathways associated with PI3K activity, cell adhesion, growth hormone signaling and cell cycle mitosis were conferring resistance (Figure R6C). In BT474 cells the GO pathways associated with resistance were related with FGFR signaling, WNT signaling, nucleotide-excision repair (NER) machinery and CDK activity.

Next, we interrogated GO Biological pathways from common genes in both cell lines, we averaged the β scores of each common gene and we performed the analysis. The highlighted GO biological pathways were a mix of the previous analysis, except for the BMP signaling cascade (Figure R6C).

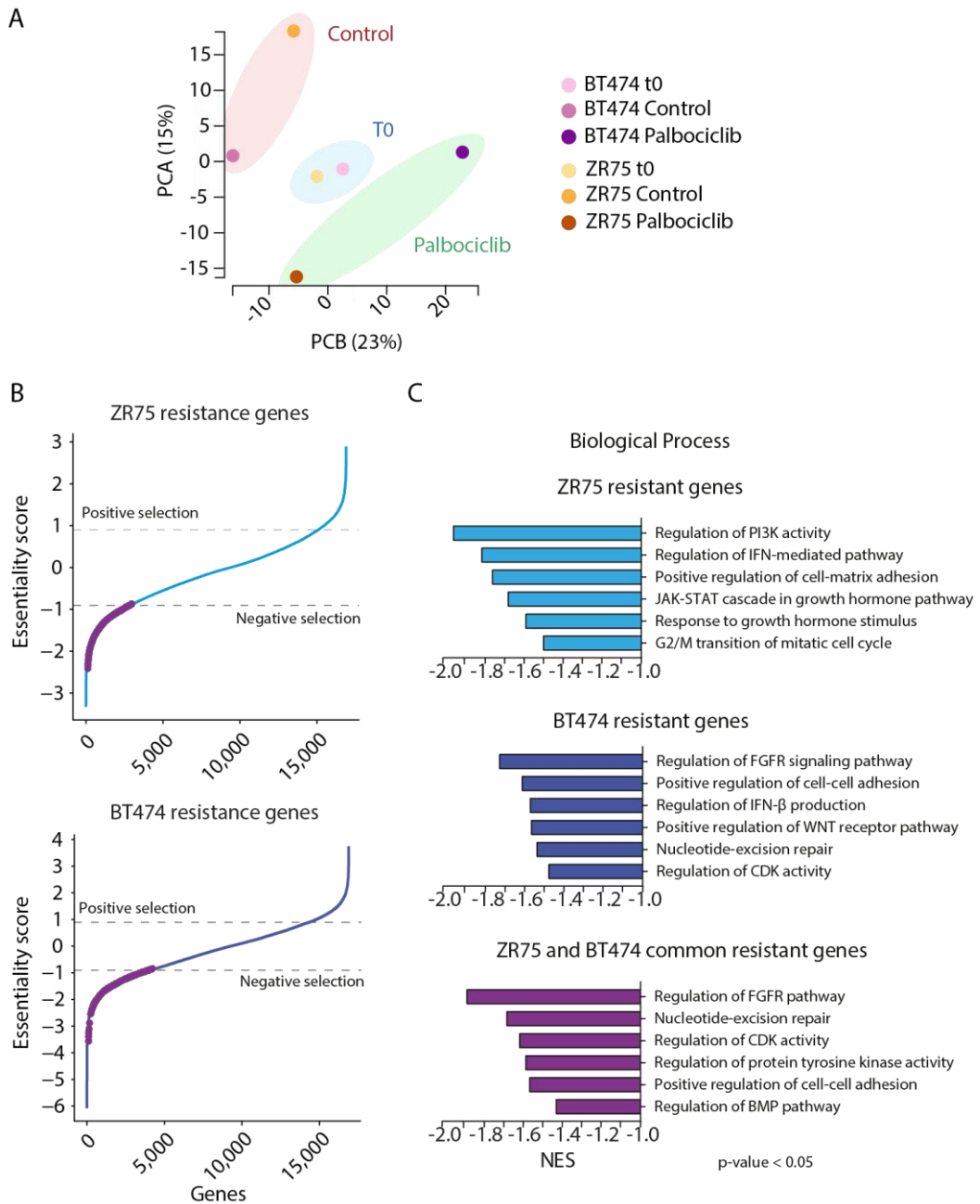


Figure R6. Bioinformatic analysis of CRISPR/Cas9 screening from BT474 and ZR75 palbo-resistant cell lines.

(A) Principal component analysis (PCA) A and B divide the samples depending on conditions T0, Control and Palbociclib both palbo-resistant cell lines. (B) Essentiality score graph showing all the sgRNA plotted according to the β palbo score. Dashed lines indicate the selected threshold. Purple dots indicate common sgRNA negatively selected in ZR75 and BT474. (C) GSEA of GO biological processes associated with resistant candidate genes in ZR75 (top) and BT474 (center) and common genes (bottom).

FGFR and CDK signaling cascades were the most enriched biological pathways in the analysis of the common candidates between both palbo-resistant cells lines. Remarkably, these two pathways, together with PI3K activity, have been previously associated with resistance to CDK4/6i. Consistently, the screening was able to capture previously described CDK4/6i resistance mechanisms.

Genes associated with worse response to CDK4/6i in two different clinical cohorts.

Gene expression changes associated with resistance to CDK4/6i treatment plus endocrine therapy were interrogated in two different clinical cohorts. In both patient data sets, we had access to formalin fixed paraffin embedded (FFPE) tumor tissue from patients treated at early stage and metastasis. We characterized gene expression of 771 genes using the nCounter Breast Cancer 360™ panel (Nanostring Technologies).

The first patient data set includes 134 baseline samples and 28 progressive disease (PD) samples from pre- and post-menopausal metastatic ER+/HER2-negative BCa patients treated with CDK4/6i (including palbociclib, ribociclib or abemaciclib) and endocrine therapy at any line of treatment (named CDK patient cohort, from Hospital Clinic of Barcelona, Figure R7A). To test the prognostic significance of each gene expression, we used univariate Cox models. From the 771 tested genes, we identified 8 genes associated with worse PFS upon high expression and 23 genes whose high expression was associated with worse OS (Supplementary table 1). Then, we performed unpaired and paired significance analysis of microarrays (SAM) to determine differences in gene expression between baseline and progress disease (PD) samples. There were 92 genes upregulated in PD samples compared to baseline samples with unpaired SAM analysis and 44 genes with paired SAM analysis (Supplementary table 2). In summary, 119 genes were highlighted significantly associated with non-responding phenotype.

The second clinical cohort analyzed was obtained from the CORALEEN clinical trial (Prat *et al.*, 2020). Samples from CORALEEN clinical trial included postmenopausal ER+/HER2-negative and LumB by PAM50 early-stage BCa patients treated with ribociclib plus letrozole (Figure R7B). We characterized treatment response in 49 samples at baseline, day 15 of treatment and surgery. Tumors with a Risk of Relapse score (ROR) < 50% after treatment were classified as responders, whereas tumors with ROR ≥ 50% as non-responders. Differential gene expression between responders and non-responder was assessed using unpaired

SAM analyses at baseline, day 15 and surgery samples. At baseline and day 15 any significant gene expression was associated with response to treatment, however 145 genes from the 771 panel were found overexpressed in surgery samples from non-responders compared with responders (Supplementary table 3). In summary, we developed three experimental approaches to identify genes associated with CDK4/6i resistance. We next seek to unravel which genes are common through the three experiments.

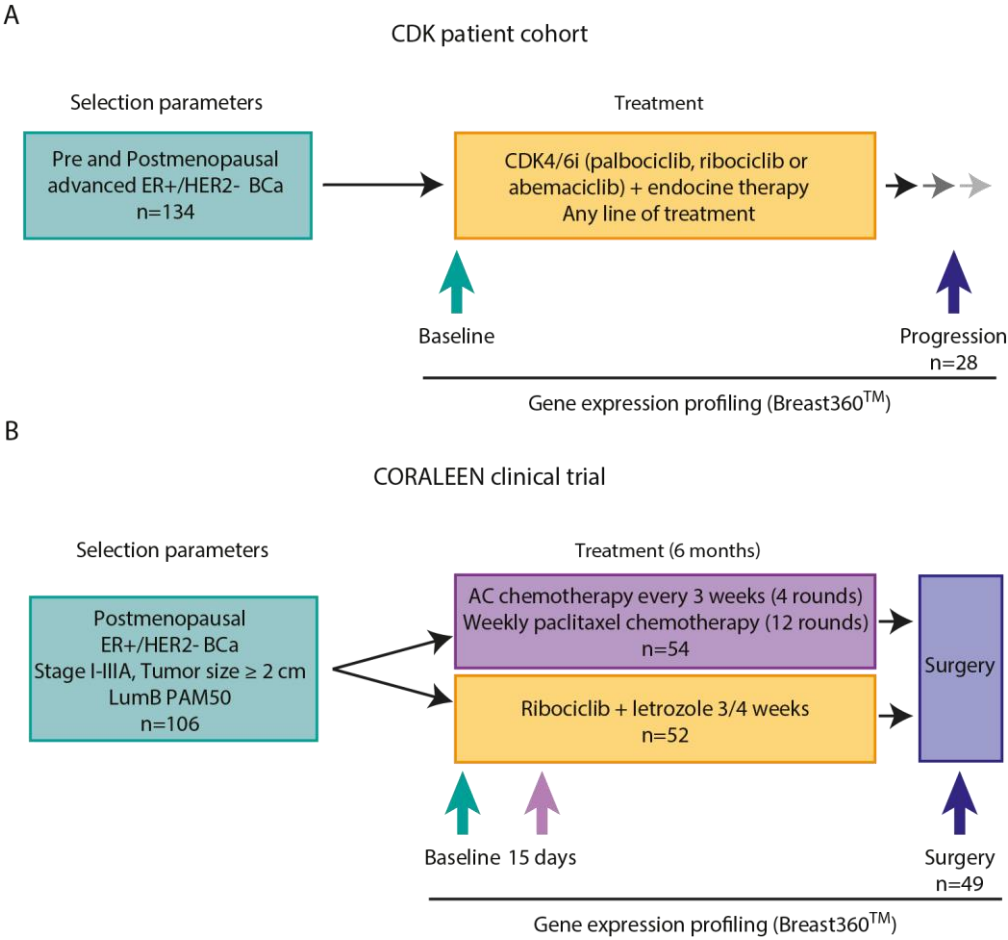


Figure R7. Description of the two clinical cohorts used to obtain candidate genes associated with poor response to CDK4/6i.

(A) CDK patient cohort representation. Samples were extracted at two different points: baseline and during disease progression (green and blue arrows, respectively). (B) CORALEEN clinical trial representation. Samples obtained at baseline, 15 days from the treatment beginning and surgery (green, purple and blue arrows, respectively).

CHAPTER 2

Integration of the CDK4/6i resistance driver candidates from the CRISPR/Cas9 drop out screen and clinical data analysis

Integration of the screen resistant candidates and the genes associated with poor response in patients

The potential resistance drivers obtained through the three analyses were then integrated together to find common candidates that are conferring resistance to CDK4/6i (Figure R8A). Out of 3730 genes identified in CRISPR/Cas9-based screen associated with resistant phenotype (ZR75 and BT474 cell lines together), 152 were interrogated in the clinical cohorts (genes profiled with nCounter Breast360™ panel, Supplementary table 4).

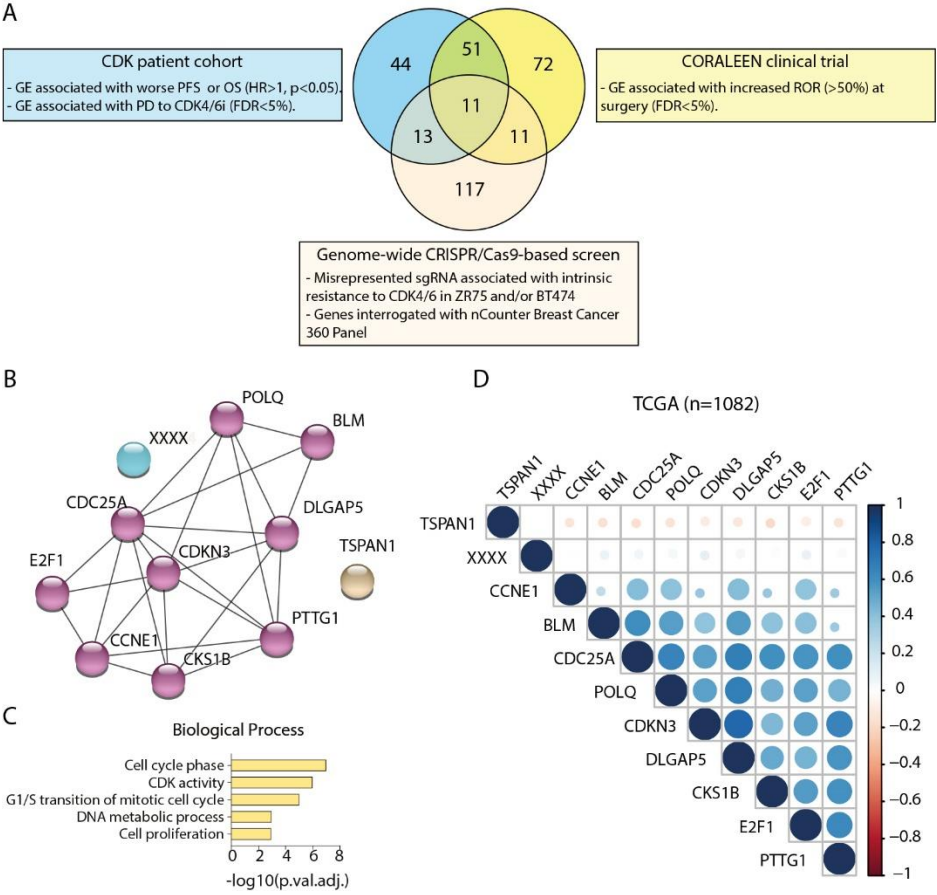


Figure R8. Integration of the candidates obtained with CRISPR/Cas9 screen, CDK and CORALEEN patient cohorts' analysis.

(A) Venn diagram of the common candidates between the different strategies. (B) Search Tool for the Retrieval of Interacting Genes/Proteins (STRING) network graph of the eleven common candidates in the three strategies. Gray lines show high-confidence protein-protein associations. The Markov Cluster (MCL) algorithm was used to cluster the proteins. (C) Hypergeometric test of GO biological pathways for the 4 intersections using BH-adjusted values. (D) Co-expression analysis of the eleven candidates in TCGA BCa tumors dataset.

CDK/ CORALEEN / CRISPR screen (11)	CDK/ CORALEEN (51)		CORALEEN/ CRISPR screen (11)	CDK/ CRISPR screen (13)
BLM	ANLN	KIF23	CDH1	AGT
CCNE1	ASPM	KIF2C	BMP8A	B3GNT3
CDC25A	AURKA	KIFC1	DLL3	BNIP3
CDKN3	BIRC5	KNTC2	IL22RA2	CDH2
CKS1B	CCNA2	MCM2	ITGB6	DSC2
DLGAP5	CCNB1	MCM3	PAX8	EGLN3
E2F1	CCNE2	MELK	SMC1B	HIF1A
xxxx	CDC20	MKI67	DUSP4	LFNG
POLQ	CDC25C	MYBL2	ATP10B	MT1G
PTTG1	CDCA5	MYCN	FZD9	NETO2
TSPAN1	CDK1	PRC1	GNLY	PIK3R3
	CEACAM5	PSAT1		PLCB1
	CEACAM6	RAD51		STAT1
	CHEK2	RAD54L		
	CXCL10	RASGRF1		
	CXCL9	RFC4		
	DEPDC1	RRM2		
	ELF3	SPC25		
	EXO1	SUV39H2		
	FAM83D	TOP2A		
	FOXM1	TRIP13		
	FUT3	TTK		
	GGH	TYMS		
	HIST1H3H	UBE2C		
	HIST3H2BB	UBE2T		
	KIF11			

Table R1. Candidate drivers of CDK4/6i resistance obtained from the integration of the three analyses. These genes form the Union signature.

Eleven genes were found highlighted in the three analyses individually. CDK and CORALEEN patient cohorts had 51 genes in common. CRISPR/Cas9 screen shared 13 candidate genes with CDK patient cohort and 11 genes with CORALEEN clinical trial (Table R1). We mainly focused on the intersection of the three strategies and interrogated the molecular function of the eleven candidates. Nine out of the

eleven genes in the intersection play a role in cell cycle progression and replication determined by an hypergeometric test of GO biological pathways (*BLM*, *CCNE1*, *CDC25A*, *CDKN3*, *CKS1B*, *DLGAP5*, *E2F1*, *POLQ* and *PTTG1*), the other two genes were membrane proteins involved in signaling transduction (*XXXX* and *TSPAN1*) (Figure R8B). We then checked the gene expression correlation between the eleven candidates in primary BCa samples of the TCGA dataset (Figure R8D). We could clearly see a cluster of cell cycle-related genes, but *XXXX* and *TSPAN1* showed a poor correlation with the rest of the candidates. The alteration of cell cycle mediators have been previously associated with resistance to CDK4/6i (reviewed in Álvarez-Fernández and Malumbres, 2020; McCartney *et al.*, 2019; Pandey *et al.*, 2019),

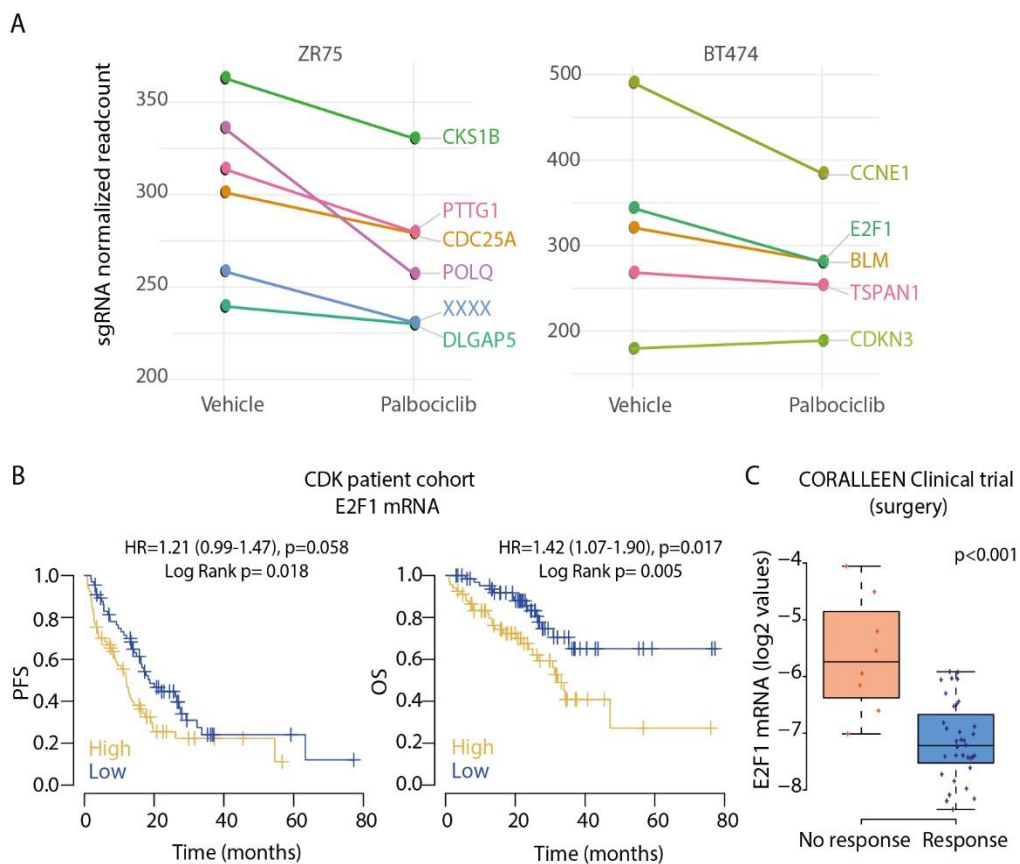


Figure R9. E2F1 gene candidate as positive control of palbociclib resistance in our models.

(A) β scores comparison between control (vehicle) and palbo-treated condition in ZR75 (left) and BT474 (right) cell lines. (B) PFS and OS analysis of CDK patient cohort dividing baseline samples in high and low expression of E2F1 gene. (C) E2F1 expression comparison between tumors that responded to ribociclib plus letrozole and the tumors that did not respond.

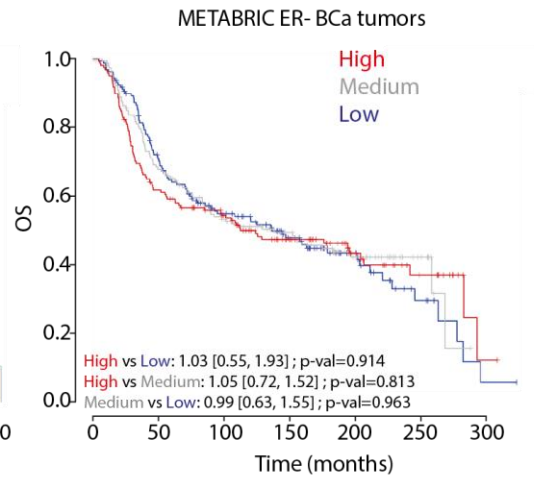
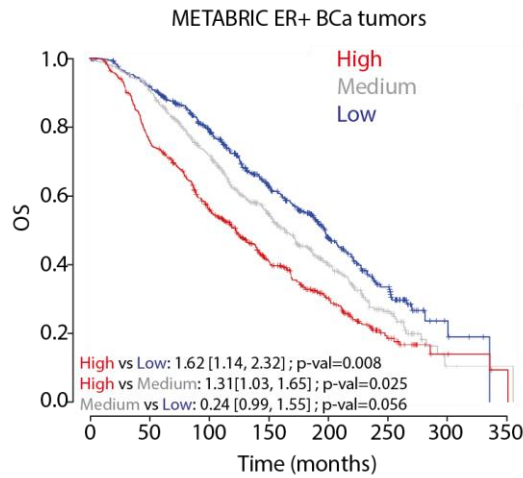
supporting our findings. As a positive control of our results, E2F1 gene was one of the top hits from the CRISPR/Cas9 screen in BT474 cell line (Figure R9A). Corroborating the performance of the unbiased *in vitro* screen, we confirmed that high expression of E2F1 was significantly associated with worst PFS and OS in CDK patient cohort (Figure R9B). In addition, non-responder tumors in CORALEEN clinical trial also showed higher expression of E2F1 compared to responder tumors (Figure R9C). E2F1 is a transcription factor from E2F family downstream of RB, that has an important role in the G1-S phase transition in cell cycle progression (Clark et al., 2016; Diehl, 2002). The phosphorylation of RB by CDK4/6 induces RB inactivation and allows E2F release, leading to the transcription of different proteins required for cell cycle progression, including cyclin E. Then, cyclin E-CDK2 phosphorylates RB, inducing more E2F release and promoting S phase transition. The overexpression of E2F1 bypasses CDK4/6 inhibition and causes the cell to depend on other signaling pathways instead of cyclin D-CDK4/6 for cell cycle progression (Dean et al., 2010). Additionally, we decided to group any gene candidate common in at least two of the three analyses in a gene expression signature, named Union signature (Table R1). The association of this gene signature with OS in METABRIC BCa tumors was interrogated. The expression of this group of genes (classified by their high, medium and low expression) in ER+ BCa tumors showed significant differences in OS (Figure R10A). High expression of these genes was associated with worst OS (Figure R10A). In ER-negative BCa tumors no differences were observed. We next classified the tumors by PAM50 molecular subtypes and tested how this gene signature was associated with the molecular subtypes' outcome. We observed that high expression of these genes is related with worst OS only in LumB subtype BCa tumors (Figure R10B). These results could be explained, in part, by the significant enrichment in cell cycle related genes. Thus, this CDK4/6i resistance gene drivers' signature could be a surrogate of increased proliferation, therefore worst OS. To clarify this, further analysis is needed.

Collectively, the integrative analysis of molecular and clinical strategies identified previously described mechanisms of resistance as well as novel potential CDK4/6i resistance drivers.

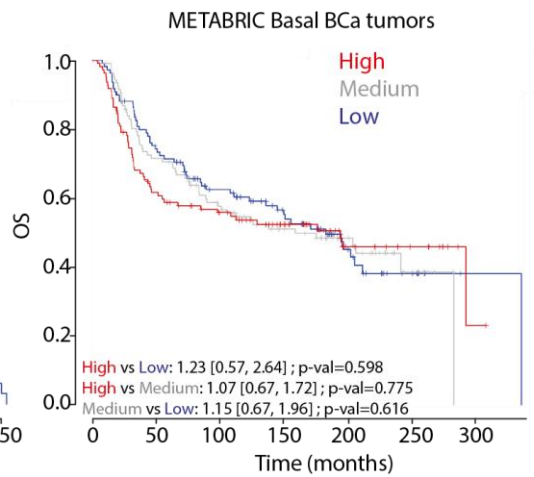
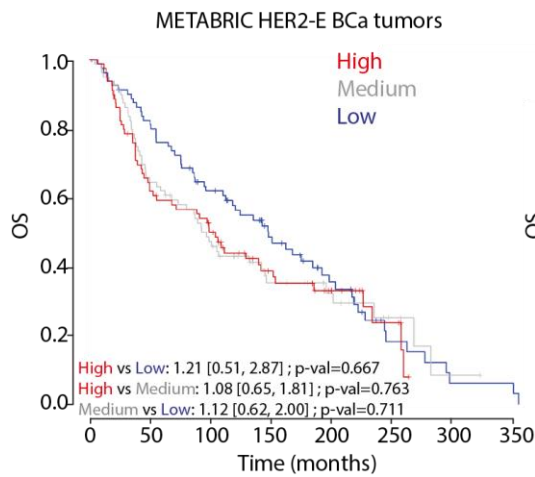
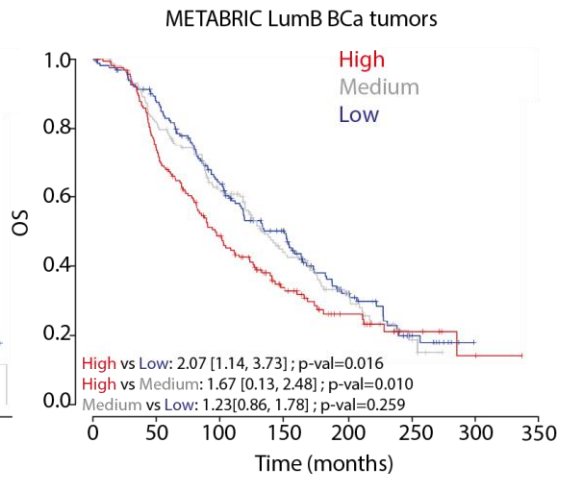
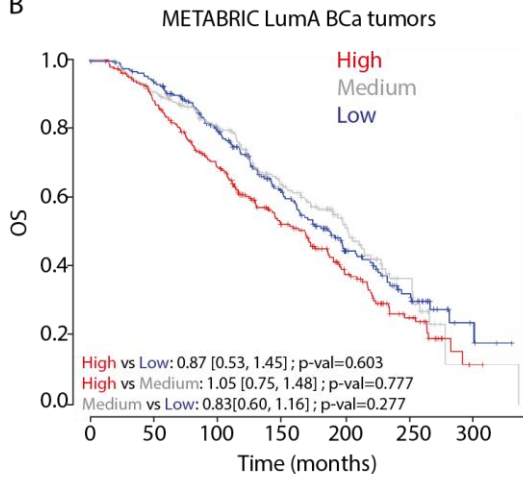
Figure R10. OS analysis of METABRIC BCa tumor data set.

(A) Interrogation of the effect of Union signature expression on OS in METABRIC BCa dataset stratified depending on ER expression (B) Interrogation of the effect of Union signature expression on OS in METABRIC BCa dataset stratified depending on PAM50 molecular subtypes. Cox models on standardized gene expression (centered and scale within subtype) and on gene signature with global signature adjustment.

A



B



CHAPTER 3

Validation of XXXX-driven CDK4/6i resistance

XXXX is associated with HER2-E and worse response in patient cohorts

Nine out of the eleven gene drivers of CDK4/6i resistance obtained with the CRISPR/Cas9 screen and the clinical data analysis are part of the cell cycle machinery. The other two genes are membrane molecules that induce signaling transduction. *TSPAN1* encodes for the Tetraspanin 1 protein, a member of the transmembrane 4 superfamily, that plays a role in many biological processes including proliferation, cell adhesion, migration and motility. *TSPAN1* is upregulated

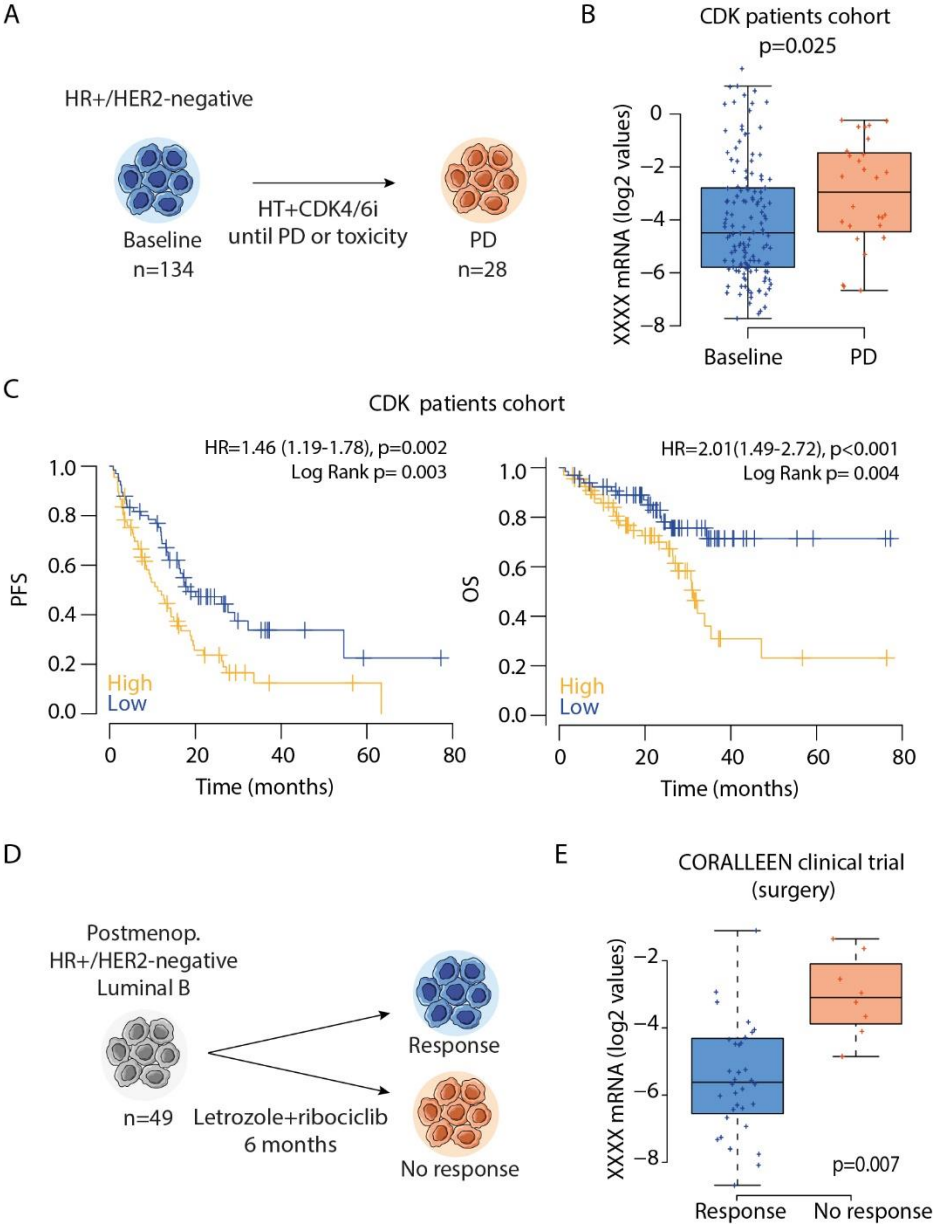


Figure R11. XXXX expression was associated with worse response to CDK4/6i treatment in CDK and CORALEEN clinical cohorts.

(A) CDK patient cohort samples acquisition design. (B) XXXX gene expression in baseline and PD samples in CDK cohort. (C) PFS and OS univariate analysis, dividing high and low XXXX expression in baseline samples in CDK patient cohort. (D) CORALEEN clinical trial samples acquisition design. (E) XXXX gene expression after letrozole plus ribociclib treatment comparing those tumors that responded vs those that did not respond.

in different tumor types such as colorectal adenocarcinoma (Chen *et al.*, 2009) and ovarian carcinoma (Scholz *et al.*, 2009).

[Eliminated section – Confidential Information]

In the CDK patient cohort (Figure R11A), baseline tumor samples with high levels of XXXX expression were significantly associated with worse PFS ([HR]=1.46) and OS (HR=2.01) (Figure R11C). In addition, PD samples showed an increased XXXX expression compared with baseline samples, indicating a positive selection of this protein through the treatment process and a correlation with the non-responder phenotype (Figure R11B). Data from the ribociclib and letrozole arm of the CORALEEN clinical trial showed that XXXX expression was also increased in surgical samples of tumors that did not respond to treatment (Figure R11D/E).

In conclusion, these observations suggest that XXXX plays a relevant role in CDK4/6i resistance in HER2-E molecular subtype tumors.

Validation of XXXX as a CDK4/6i resistance mediator

To interrogate XXXX function during CDK4/6i treatment, we used different *in vitro* models. We first generated an acquired resistance cell line to palbociclib by treating palbo-sensitive MCF7 cells with increasing doses of the drug in every passage (until reaching 1 μ M palbociclib in the media, MCF7-PR, Figure R12A). We characterized the palbociclib dose-response and PAM50 molecular subtype in these cells (Figure R12B/C, respectively).

As expected, MCF7-PR showed increased resistance to palbociclib, together with an increase in XXXX expression (Figure R12C) compared to parental. XXXX gene expression was upregulated. (Figure R12C). Interestingly, the PAM50 score showed

a switch from LumB to HER2-E molecular subtype in MCF7 cells after the resistance acquisition, in line with the previous observations.

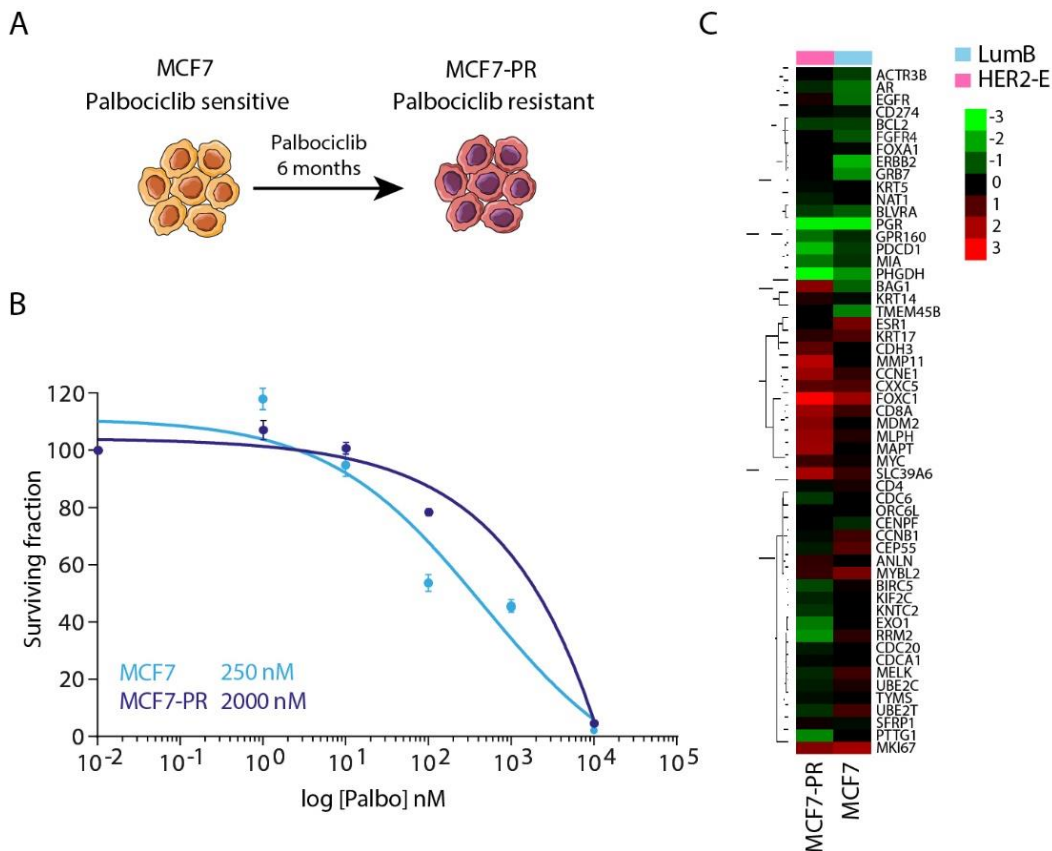


Figure R12. Development of acquired resistance to palbociclib cell model in MCF7 palbo-sensitive cell line.

(A) Acquired resistance cell line model. (B) Dose-response to palbociclib treatment. IC₅₀ measurement is annotated next to the cell lines (C) PAM50 assessment classified parental MCF7 as LumB and derived MCF7-PR as HER2-E.

a. XXXX loss-of-function strategies

Next, we interrogated the effect of XXXX loss in ZR75 and BT474 palbo-resistant cell lines. We designed a CRISPR/Cas9 knock-out (KO) strategy with 4 different sgRNA targeting XXXX gene. We cloned the sgRNAs into lentiCRISPRv2 plasmid (Figure R13A) and selected sgRNA3 as the most efficient sgRNA (Figure R12B left). However, after infection and puromycin selection, we were not able to fully eliminate XXXX protein expression (Figure R13B right).

This strategy was aimed to obtain a pool of XXXX-mutated clones, therefore the efficiency of the process needed to be optimal. XXXX KO cells after different passages adapted to recover XXXX expression, which suggests that not all cells induced a KO mutation in XXXX gene. Clonal selection was not possible due to technical problems. We are repeating this experiment to obtain single XXXX KO clones.

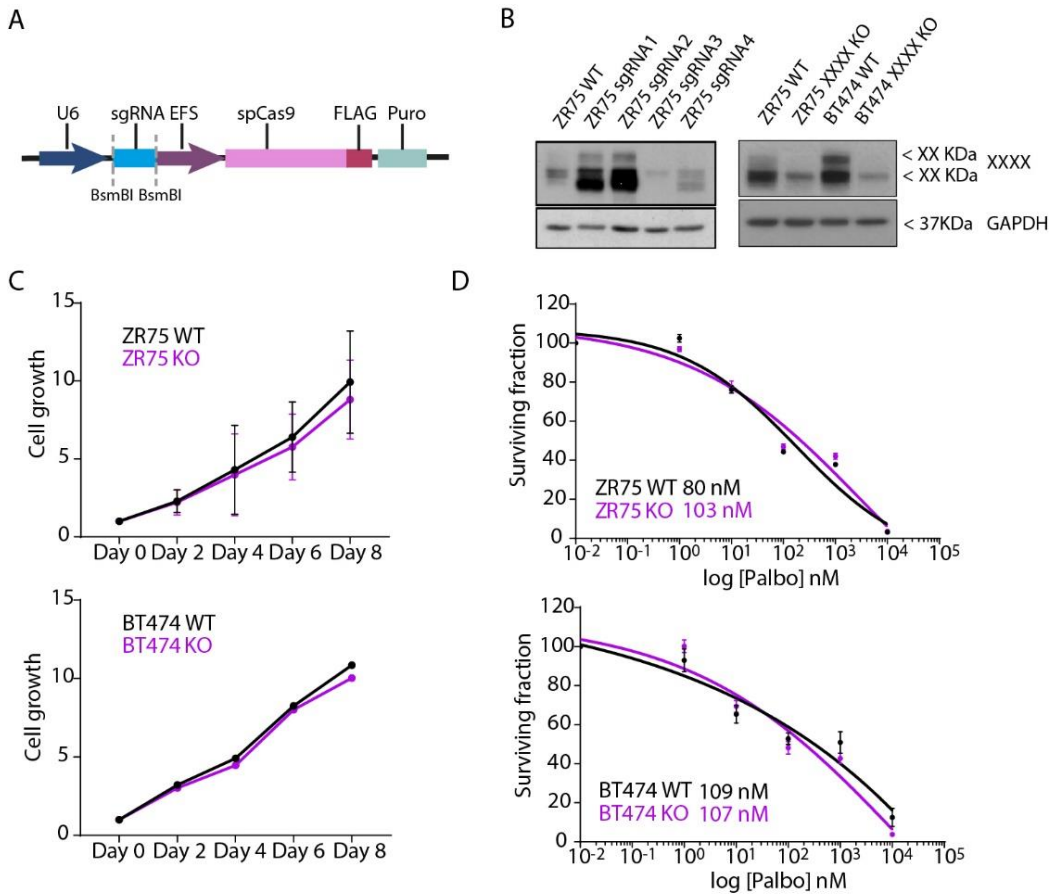


Figure R13. XXXX CRISPR/Cas9 KO generation.

(A) LentiCRISPRv2 plasmid design containing sgRNA for XXXX gene. (B) WB validation of the XXXX expression silencing of the 4 different sgRNA (left). ZR75 and BT474 XXXX KO (sgRNA3) cell lines showed a band at 95 KDa. (C) Cell proliferation assay for ZR75 WT and XXXX KO (up) and BT474 WT and XXXX KO (down). (D) Dose-response assay comparing ZR75 WT and XXXX KO (up) and BT474 WT and XXXX KO (down). IC50 was annotated next to the cell lines.

We determined cell growth (Figure R13C) and palbociclib dose-response (Figure R13D) of the mutated XXXX KO pool cells compared with the WT condition (cells infected with the lentiCRISPRv2 plasmid without sgRNA) for each cell line. There were no differences in cell growth nor response to palbociclib in XXXX KO cells compared to WT.

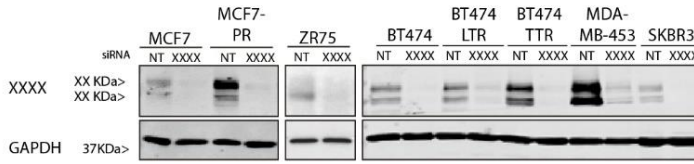
Because of the technical problems we had to completely KO XXXX in palbo-resistant cell lines, we decided to use 2 different downregulation strategies to determine XXXX effect during palbociclib treatment: siRNA and shRNA. We used transient siRNA to analyze the immediate effect of XXXX silencing in cell growth. Apart from the MCF7-PR cells we generated, we took advantage of two BT474-derived cell lines with acquired resistance to well established anti-HER2 therapies (protocol described in Brasó-Maristany *et al.*, 2020): BT474 lapatinib and trastuzumab resistant (BT474-LTR) and BT474 tucatinib and trastuzumab resistant (BT474-TTR). Both cell models are HER2-E by PAM50 and palbociclib resistant (Brasó-Maristany *et al.*, 2020). Non-targeting (NT) siRNA were used as negative controls (Figure R14A-B). XXXX downregulation significantly reduced cell growth in 5 out of 8 cell lines tested: MDA-MB-453 (XXXX-mutated cell line used as positive control for XXXX dependency), ZR75, MCF7-PR, BT474-LTR, BT474-TTR cells (Figure R13B and C). Derived cell lines (MCF7-PR, BT474-LTR, BT474-TTR), which presented an increased resistance to palbociclib effect, had a stronger dependence on XXXX signaling cascade than parental (Figure R14C).

The second downregulation strategy used to help us decipher XXXX role in palbociclib resistance was shRNA. Silencing with shRNA have a stable effect, maintaining the downregulation for several passages. We first tested the downregulation after shRNA infection by WB and then we analyzed the palbociclib dose-response effect in cell lines with different sensitivity to palbociclib (Figure R15A/B, respectively). Cell lines defined as palbo-resistant, showed a reduction in the palbociclib IC50, whereas the palbo-sensitive MCF7 cells showed small or no decrease in this measurement after XXXX silencing. Interestingly, the strongest effect in sensitivity increase upon XXXX downregulation was detected in ZR75 cells.

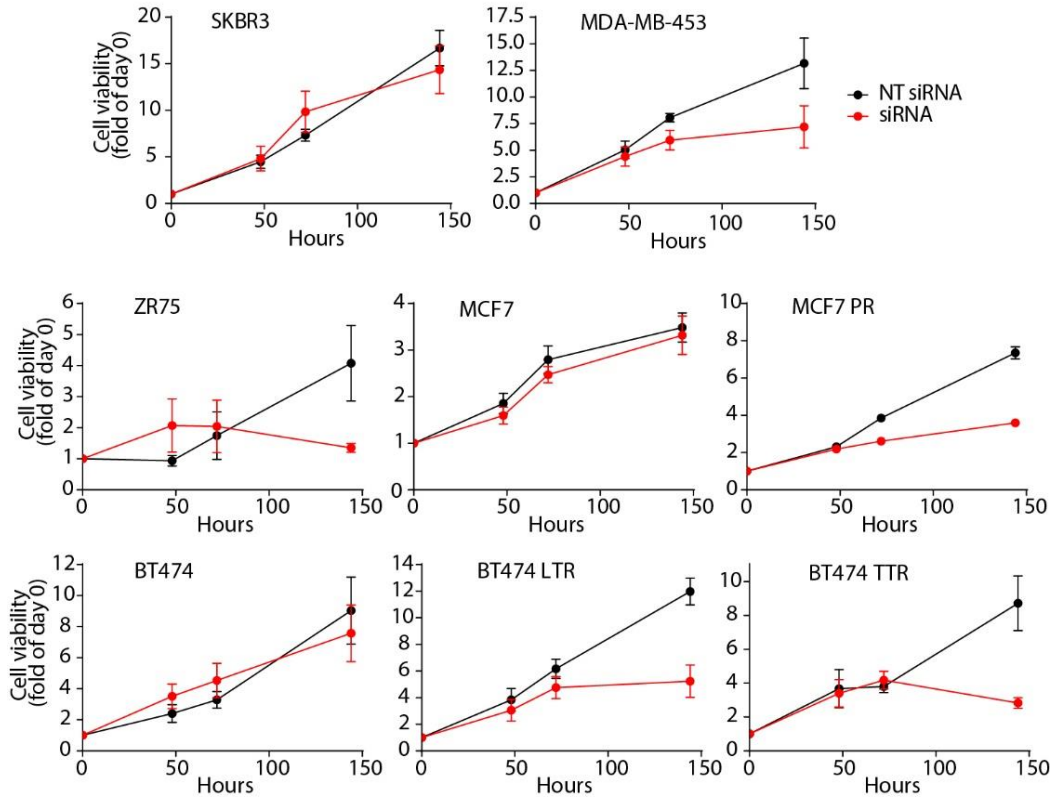
Figure R14. Effect of XXXX silencing with siRNA in cell growth.

(A) Protein validation by WB of XXXX silencing induced by transient siRNA. GAPDH is used as a loading control. (B) Cell proliferation over time, comparing XXXX siRNA with control (NT). (C) Growth arrest waterfall plot comparing XXXX siRNA with control (NT).

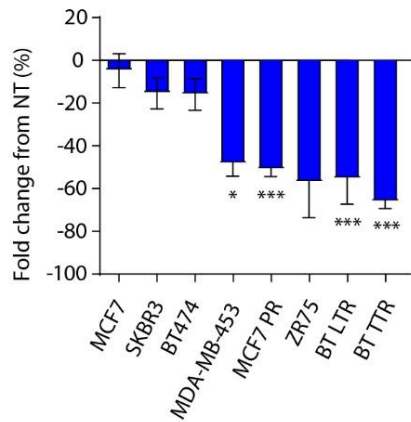
A



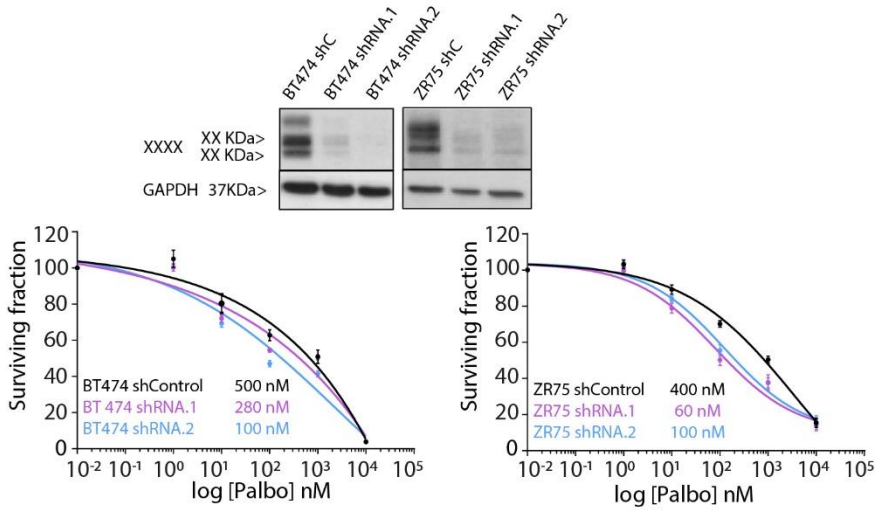
B



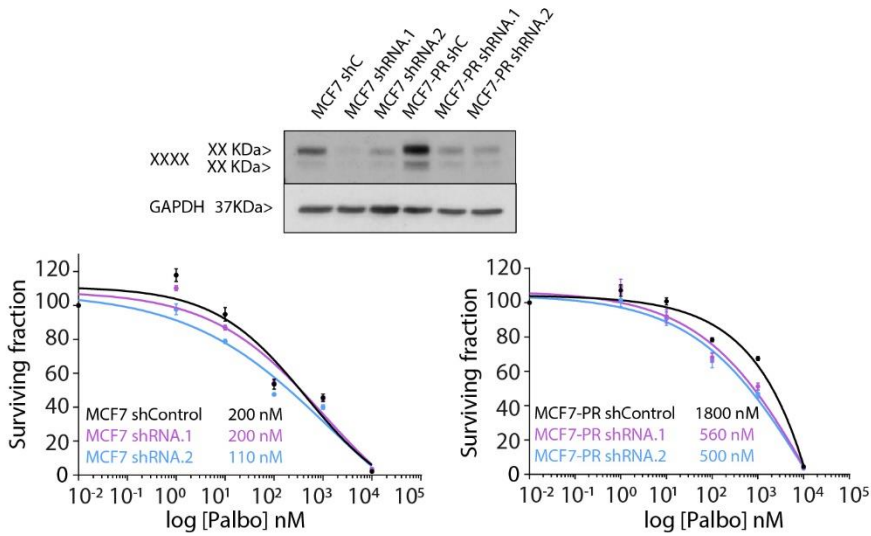
C



A



B



C

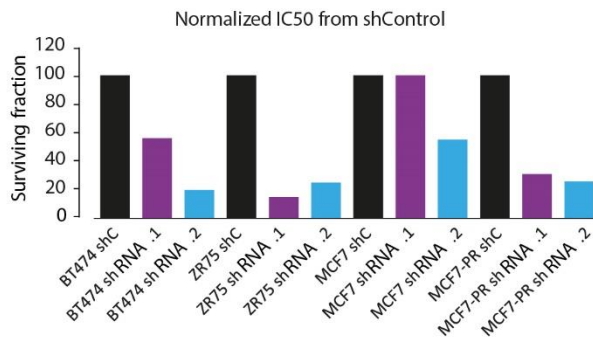


Figure R15. Changes in palbociclib IC50 upon XXXX silencing in different cell lines.

(A) WB validation of XXXX silencing by two independent shRNA. GAPDH is used as a loading control. (B) Dose-response curves and IC50 measurement in each cell lines comparing shScrambled (shC) and shXXXX. (C) Normalization of the IC50 to the shScrambled.

b. Gain-of-function experiments

Next, we developed a gain-of-function approach enhancing the biological function of XXXX. To this, we generated cells that overexpress XXXX (OE), XXXX constitutively active (CA) and XXXX kinase dead (KD) proteins. To generate CA and KD isoforms we induced a point mutation for each condition: Y367C in the case of the CA isoform and K504M for the KD. We infected ZR75 palbo-resistant and MCF7 palbo-sensitive cell lines with the indicated constructs and tested XXXX activation by Y642 phosphorylation (Figure R16A). The control for the infection was the backbone of the plasmid with the RFP molecule. We detected the XXXX overexpression in ZR75 and MCF7 OE, CA and KD cells. Of note, ZR75 showed a higher overexpression of the three isoforms. We also assessed the XXXX activation based on the phosphorylation of TyrXX, a residue located in the

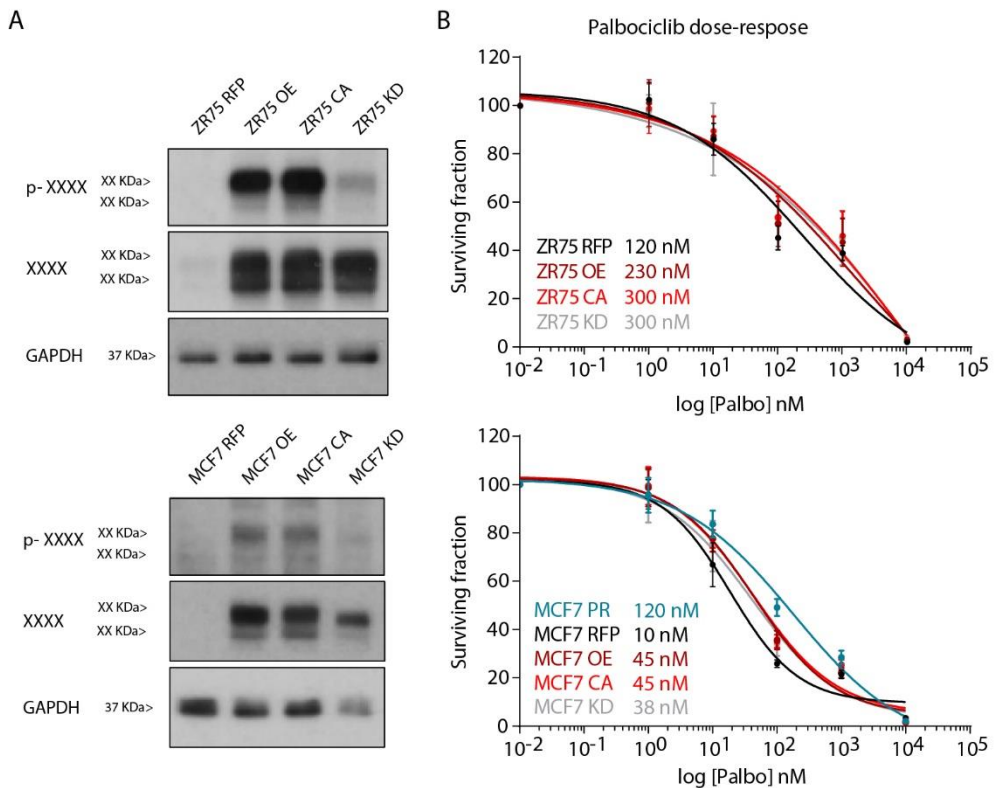


Figure R16. XXXX gain-of-function effect over palbociclib response in ZR75 and MCF7 cells.

(A) XXXX total and phosphorylated XXXX (Tyr642) WB detection. GAPDH is used as a loading control. (B) Response to palbociclib in ZR75 and MCF7 cells control (RFP), overexpressing XXXX (OE), a constitutively active form of XXXX (CA) and a kinase dead form (KD). We measured IC50 per each cell line.

intracellular domain of the protein that gets phosphorylated upon activation of the receptor. Cell lines overexpressing WT and CA XXXX showed increased phosphorylation, whereas the KD isoform had basal XXXX activation. Next, we tested the functional outcome of overexpressing XXXX in the different isoforms. We performed a palbociclib dose-response assay to measure the palbociclib effect in XXXX overexpressing cells compared to parental cells (Figure R16B). In ZR75 palbo-resistant cells, the overexpression of XXXX in any of the three isoforms doubled the palbociclib IC50 (ZR75 RFP IC50 = 120 nM vs. ZR75 OE/CA/KD IC50 = 230-300 nM), suggesting an increase in palbociclib resistance. In MCF7 palbo-sensitive cells, we added a positive control for resistance, the derived MCF7-PR cells. We detected a 4-fold increase in palbociclib IC50 in MCF7 OE,CA and KD (MCF7 RFP IC50=10 nM vs. MCF7 OE/CA/KD = 38-45 nM). However, the increase did not reach the IC50 for the acquired resistance cell lines MCF7-PR (IC50 = 120 nM). Remarkably, KD isoform overexpression showed the same effect on the IC50 than the other two overexpressing isoforms, suggesting that the effect of XXXX in CDK4/6i resistance may be induced through a kinase independent manner. Further experiments have to be performed to unravel the specific molecular mechanism by which XXXX drives CDK4/6i resistance.

Collectively, these results confirm the contribution of XXXX to CDK4/6i resistance.

CHAPTER 4

Characterization of the XXXX-driven mechanism
that induces CDK4/6i resistance

Characterization of the XXXX-driven mechanism that induces CDK4/6i resistance.

For the identification of protein-protein interactions we optimized a unique method called Proximity-dependent biotin identification (BioID). It consists on the fusion of a promiscuous biotin ligase (*Escherichia coli*-derived BirA R118G*) to our protein of interest to covalently label with biotin proteins that are in close proximity. A co-immunoprecipitation with streptavidin beads is performed to purify the proteins that are biotinylated. Finally, protein interactors are identified by mass spectrometry analysis (Figure R17).

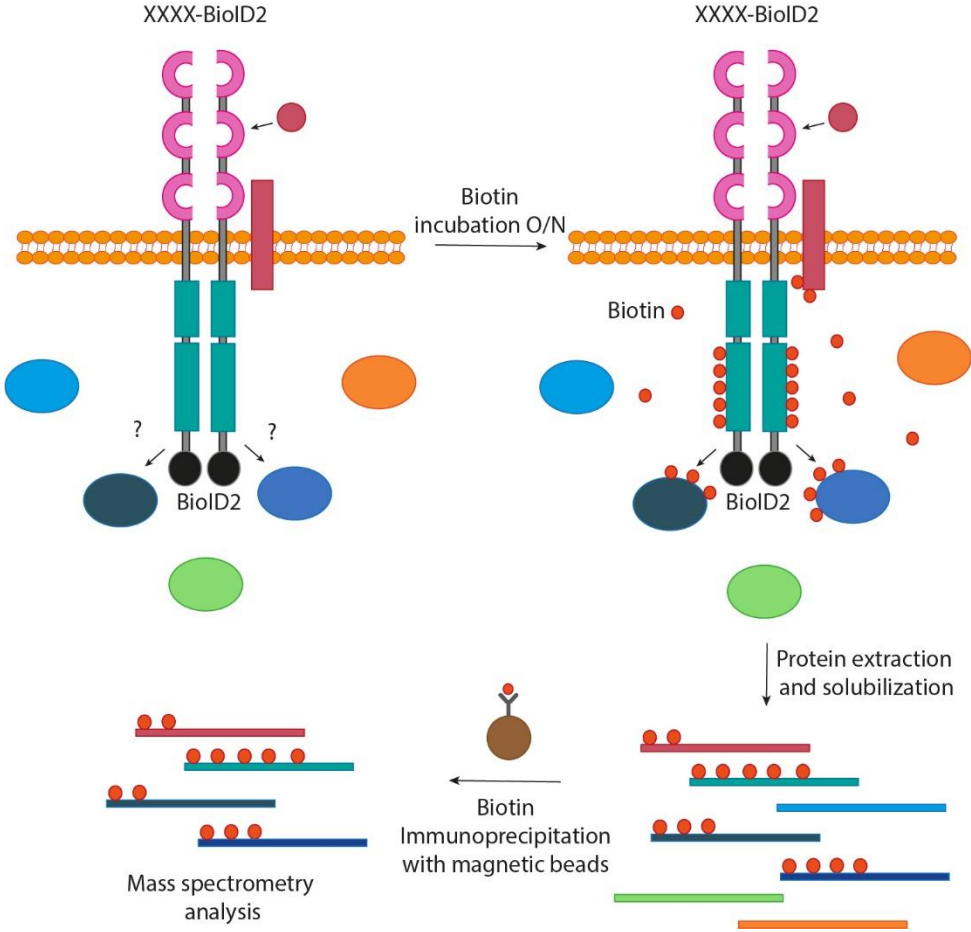


Figure R17. Proximity ligase approach to unravel which signaling cascade is activating XXXX to induce CDK4/6i resistance.

Graphic representation of BioID methodology. Cells are transduced with a plasmid containing the protein of interest fused with a promiscuous biotin ligase. After incubating O/N with biotin, all the molecules that were close to our protein of interest were biotinylated. Then, cells are lysed and protein fraction is obtained. By immunoprecipitation using streptavidin magnetic beads, biotinylated proteins are isolated and purified to further analysis by mass spectrometry (MS).

a. Optimization and validation of XXXX-BioID2 fusion protein.

The first step to adapt the BioID methodology to our setting was to generate the plasmids carrying our protein of interest fused with the BioID2 molecule. To this, we introduced XXXX transcript in frame before the BioID2 protein in MCS-BioID2-HA backbone. Herein, we used second-generation biotin ligase (BioID2), which is smaller and allows a more selective biotinylation (Kim *et al.*, 2016) compared with first generation BirA. BioID2 also needs less biotin in the media than BirA R118G* to perform the labelling, enhancing its function. When applying the BioID technique, the protein of interest is normally fused to N-terminus (myc-BioID2-protein) and C-terminus (protein-BioID2-HA) in parallel to capture all possible interactions and avoid interferences from the BioID molecule. Since XXXX is a membrane protein and we were interested in the intracellular pathways that are activated within palbociclib treatment, we decided to simplify the experimental design and use only the N-terminus construct (XXXX-BioID2-HA). The negative control used for our experiments is myc-BioID2, due to lack of expression of BioID2-HA protein after transfection. We decided to use MCF7 and MCF7-PR to compare the molecular interactors of XXXX that may change upon CDK4/6i resistance. MCF7-PR cells were cultured with 200 nM palbociclib in the medium. MCF7 cells transfection was very efficient, thus suitable for the large number of transfected cells required for performing the BioID experiments. We validated through IF staining the biotinylation function of the BioID2 in both constructs (Figure R18A) upon biotin addition. We also determined the differences in cellular localization of XXXX-BioID2-HA compared to myc-BioID2. XXXX-BioID2-HA was strongly detected in the membrane and vesicle compartments but did not stained the nucleus. Myc-BioID2 was stained spread through all the cell compartments without distinction, which indicated XXXX-BioID2-HA construct specificity.

b. XXXX interactome identification in MCF7 and MCF7-PR cells

We performed the BioID experiment to identify XXXX interactors in MCF7 and MCF7-PR cells. To this, we transfected these cells with myc-BioID2 and XXXX-BioID2-HA plasmids. The myc-BioID2 was used as a control to identify proteins that are randomly biotinylated, therefore excluding unspecific interactions, whereas XXXX-BioID2 was used as a bait. Cells were incubated with 50 μ M biotin O/N, biotinylated proteins were purified using streptavidin-conjugated beads and analyzed by mass spectrometry (MS). Protein cell extracts were obtained after biotin pull down experiments to determine global biotinylation (HRP-streptavidin antibody) and the transfection efficiency (HA/myc tags and XXXX antibodies) (Figure 18B). As observed in the streptavidin WB (Lower panel, Figure R18B), the control plasmid (myc-BioID2) biotinylates more proteins than XXXX-BioID2-HA. These results are explained by the presence of the myc-BioID2 molecule in all the compartments compared with the membrane-specific localization of the XXXX-BioID2-HA protein. Of note, MCF7-PR transfection efficiency was much lower than parental and it translated to lower number of interactors in the MS analysis (Supplementary table 5). Interactors were identified using two biological replicates comparing XXXX-containing conditions with the controls and filtering the interactor candidates with a Bayesian false discovery rate (BFDR) less than 0.02 and a 3-fold enrichment.

The MS analysis identified 86 interactors in MCF7 cells and 9 in MCF7-PR (BFDR < 0,02, fold change > 3, Supplementary table 5). We used YYYYY, a protein related with our candidate, as a BioID positive control. In MCF7 cells it is one of the top identified molecules with a 11262,4-fold change compared with the control condition. In MCF7-PR cells YYYYY show a fold change of 335,3 but a BFDR = 0,21. This result is not significant, however based on the previous information, we decided to relax the BFDR threshold to 0,21 in both cell lines. With the new threshold, 101 proteins were detected in MCF7 and 78 in MCF7-PR cells (Supplementary table 5). Fifteen proteins were common in both cell lines. XXXX interactome characterization identified three signaling cascades in MCF7 and MCF7-PR: RSK, mTOR and PLC γ pathways. Many interactors found in both cell lines were proteins involved in vesicle

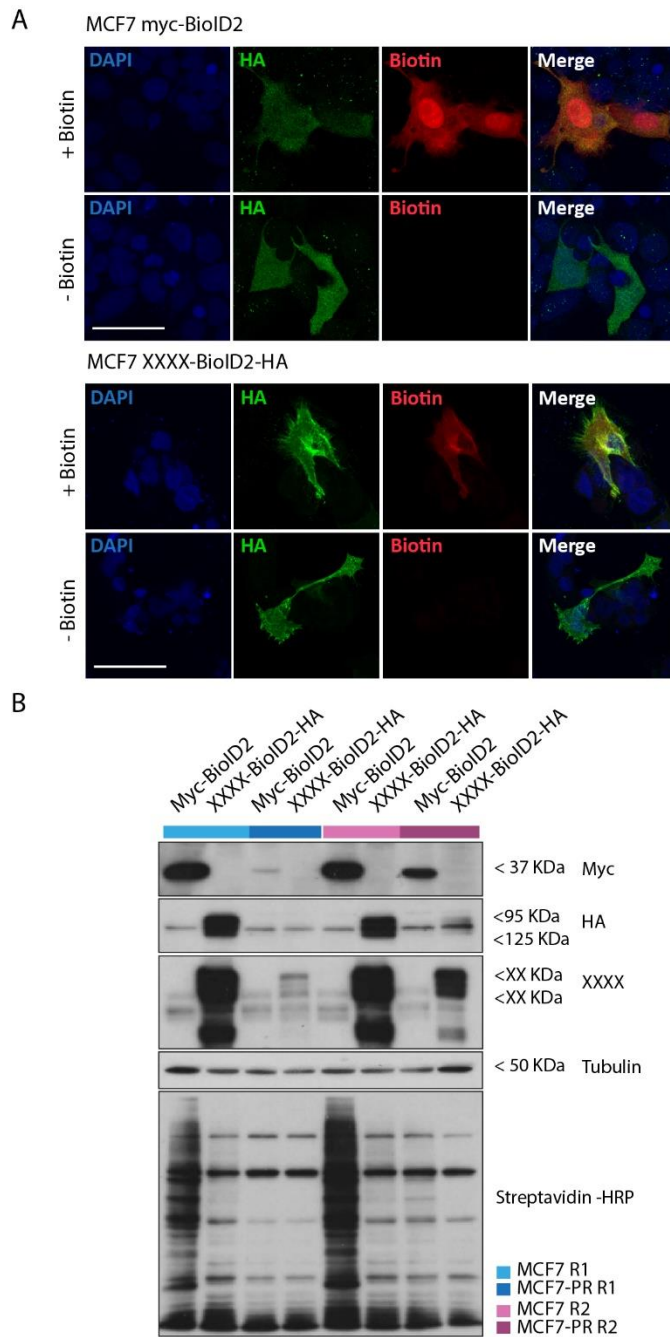


Figure R18. Validation of XXXX-BioID2-HA construct.

(A) Representative images obtained with immunofluorescence labeling of MCF7 cells transfected with the indicated plasmids. Nucleus were stained with DAPI. Scale bar: 50 μ m (white line). (B) WB validation of the BioID experiments (two biological replicates) we performed with MCF7 and MCF7-PR cell lines.

trafficking and membrane functions such as cell-cell interactions. The compartment localization of these interactors fit with the XXXX immunofluorescence signal which situated the receptor specifically in the vesicle-like intracellular organelles and the cell membrane.

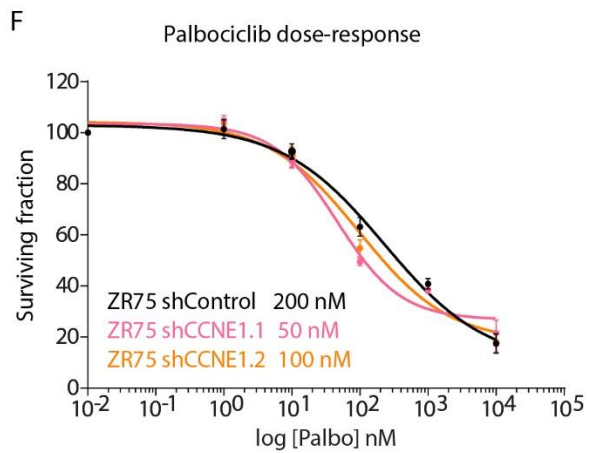
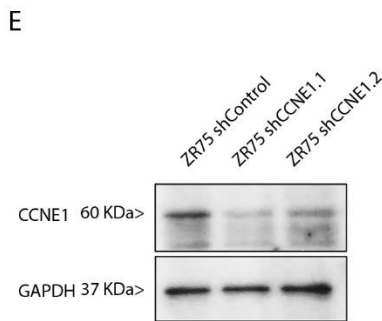
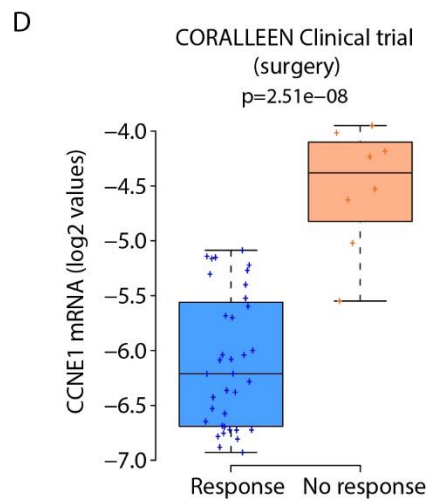
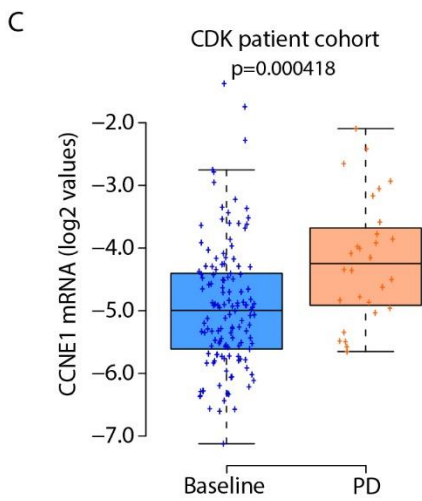
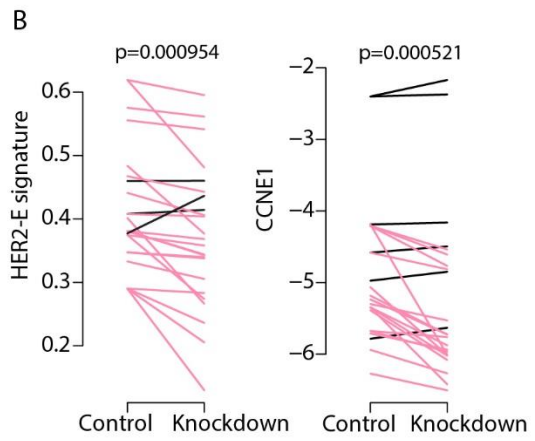
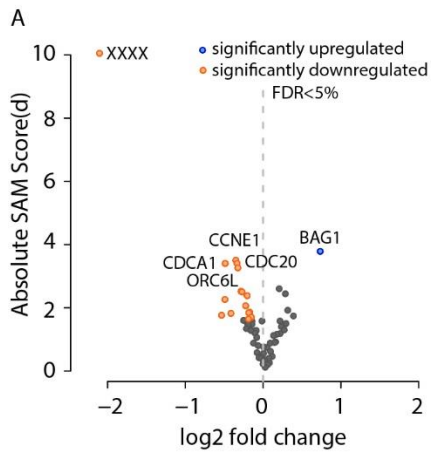
We specifically focused on those interactors with signal transduction function. In both MCF7 cell lines, XXXX was interacting with YYYYY, RSK1, RICTOR, and PLCG1, proteins involved in important biological pathways such as proliferation, differentiation and survival. According to DAVID bioinformatic tool (Huang *et al.*, 2009), the unique proteins identified in MCF7-PR were related with transcription regulation (BRD7, EHMT1, MBD1, LGR4 and UIMC1), rRNA processing (EXOSC5, EXOSC9, MPHOSPH10 and NOL6), mRNA stability (EXOSC5, EXOSC9 and PSMD5), vesicle-mediated transport (AP3S2, JAGN1 and SAR1A) and G2 DNA damage checkpoint (TAOK2 and UIMC1).

XXXX induces *CCNE1* activity promoting cell cycle progression

We further analyze gene expression changes after XXXX silencing, as an alternative method to find interesting downstream mechanisms that explain how XXXX is driving CDK4/6i resistance. We interrogated the expression of a nCounter panel, including the 50 genes of the PAM50 gene signature upon XXXX silencing (knocked down with siRNA and shRNA). Using SAM analysis, we identified 15 genes that were differentially expressed (FDR<5%) without XXXX expression (Supplementary table 6). *CCNE1* was significantly downregulated upon XXXX knock-down (Figure R19A and B), together with other cell cycle associated genes such as *CDCA1* and *CDC20*. Consistent with previous reported data, silencing XXXX reduced the HER2-E signature in these cell lines (Figure R19B). *CCNE1* was a CDK4/6i resis-

Figure R19. *CCNE1* association with CDK4/6i resistance.

(A) Gene expression analysis measured with nCounter panel including PAM50 gene signature from different cell lines that downregulated XXXX expression using siRNA and shRNA. Significantly upregulated genes (blue) and downregulated genes (orange) with FDR<5%. (B) Interrogation of HER2-E signature and *CCNE1* expression levels in the previous cell lines. Upregulation (black) or downregulation (pink) of HER2-E signature (left) and *CCNE1* expression (right) upon XXXX silencing in different cell lines. (C) *CCNE1* gene expression in baseline and PD samples in CDK cohort. (D) *CCNE1* gene expression comparing tumors that responded vs tumors that did not respond to letrozole plus ribociclib treatment. (E) Palbociclib effect on ZR75 cells with and without *CCNE1* silencing.



tance candidate driver gene obtained after the integration of the three analyses (Figure R8A). High expression of *CCNE1* was previously associated with resistance to palbociclib and HT (Guarducci *et al.*, 2017; Herrera-Abreu *et al.*, 2016; Ma *et al.*, 2017; Turner *et al.*, 2019). In the CDK patient cohort, tumors from patients that relapsed after CDK4/6i treatment showed a significantly increased expression of *CCNE1* compared to baseline samples (Figure R19C). Similar results were found when analyzing CORALEEN clinical trial, tumors that did not respond to ribociclib plus letrozole showed a significantly higher expression of *CCNE1* than the responders (Figure R19D). Collectively, these evidences suggest *CCNE1* as a potential downstream effector of XXXX. To this, we measured changes in palbociclib capacity to inhibit proliferation in ZR75 cells with and without *CCNE1* expression. Downregulation of *CCNE1* levels with two independent shRNA showed a reduction in palbociclib IC50 from 200 nM to 50 nM in sh*CCNE1*#1 and 100 nM in sh*CCNE1*#2 (Figure R19E).

CCNE1 encodes for cyclin E1 that generates a complex with CDK2 to phosphorylate RB, among other proteins, in order to induce cell cycle progress (Chandarlapaty and Razavi, 2019). These preliminary results suggest that XXXX might be inducing *CCNE1* expression and therefore bypassing G1 checkpoint, independently of CDK4/6 function. Further experiments are being performed *in vitro* and *in vivo* to confirm this hypothesis.

- Discussion -

Discussion

The development of CDK4/6i has had a substantial impact on luminal advanced BCa therapy. However, some studies have shown differences in treatment efficiency depending on the molecular subtype of the tumor (Finn *et al.*, 2018b; Ma *et al.*, 2017). HER2-E subtype, together with Basal-like, showed little to no response to CDK4/6i therapy compared with the benefits that luminal subtypes obtained from the treatment. Additionally, during the metastatic process around 14% of the luminal tumors evolve towards a HER2-E intrinsic subtype (Cejalvo *et al.*, 2017), which suggests that these tumors are unlikely to benefit from the treatment. Unravelling which mechanisms drive the resistance to CDK4/6i in this situation is pivotal to maximize treatment outcome. Herein, we aimed to underlie these mechanisms in order to eventually overcome CDK4/6i resistance in HER2-E subtype advanced ER+/HER2-negative BCa.

Identification of CDK4/6i gene drivers using CRISPR/Cas9 screen and clinical data analysis.

Since the outstand of the CDK4/6i as a standard of care to treat ER+/HER2-negative BCa, several reports have pointed to resistance as the eventual driver of therapy failure. To this, many studies have identified mechanisms that explain this resistance, mainly pointing at cell cycle proteins. However, although mutations in cell cycle-related genes may account for a subset of the patients, they fail to systematically explain CDK4/6i resistance. To unravel the mechanisms that confer CDK4/6i resistance in HER2-E ER+/HER2-negative BCa tumors we designed different strategies. We implemented a genome-wide screen in CDK4/6i-resistant cell lines and analyzed two different patient data sets in order to identify genes associated with CDK4/6i resistance.

High-throughput sequencing screening strategies are a very powerful tool to identify molecular mechanisms related with drug resistance in cancer research. During the last decade, different whole genome screening technologies have been developed. Gene silencing with shRNA has been commonly used for functional genomics, but with the refinement of the CRISPR/Cas 9 genetic tool, a new genetic strategy for functional screenings has emerged. The main difference between both approaches is that shRNA produces a knock-down of the gene expression, whereas CRISPR/Cas 9 introduces point mutations, generating a knock-out of the targeted gene. ShRNA interferes at the post-transcriptional level targeting mRNAs, yet residual protein

expression could remain after the knock-down, which may mask certain phenotypes. This effect could be prevented with a complete knock-out with CRISPR/Cas 9 which modifies the DNA, inducing permanent effects. Both shRNA and CRISPR/Cas 9 tools produce off-target effects that can introduce false positives. Moreover, shRNA display a sequence-independent off-target effect based on the addition of RNA molecules that trigger the interferon-regulated genes and can alter protein expression (Bridge *et al.*, 2003). The off-target activity produced by CRISPR/Cas 9 has been mitigated by the improvement of sgRNA design tools and selecting the most efficient guides for the libraries. A recent comparative study showed that CRISPR/Cas 9 present lower susceptibility to off-targets than shRNA (Smith *et al.*, 2017). Based on all the previous information, we decided to use CRISPR/Cas 9 screen to identify the drivers of CDK4/6i resistance in palbociclib resistant cell lines. Additionally, we chose a genome wide targeting approach to identify novel candidates that were not previously associated with CDK4/6i resistance. This way, our experimental design could screen for the functional effect of any protein in an unbiased manner.

We chose ER+/HER2-negative ZR75 cell line to perform the screening because of the increased palbociclib IC50 (IC50 = 600nM), compared to sensitive cells MCF7 (IC50 = 50nM) or T47D (IC50 = 80 nM). ZR75 cells sensitivity to palbociclib is in line with resistant cells such as BT474 (IC50 = 2000nM). BT474 cell line was chosen as a positive control of CDK4/6i resistance. BT474 cells are HER2-E by PAM50 and present *ERBB2* amplification. We also performed the screening in BT474 cells to help differentiate those candidates that are associated with HER2 amplification and the ones that are not.

Collectively, we designed an unbiased genome wide CRISPR/Cas 9 screen to functionally identify drivers of CDK4/6i resistance in two ER+ BCa cell lines that showed resistance to palbociclib *in vitro*.

A limitation of whole genome screen are confounders. The functional selection performed to identify driver genes of CDK4/6i resistance needed to be simple enough to rule out genes that are involved in other cellular responses such as senescence. Cell cycle arrest produced by CDK4/6i can result in quiescence, senescence or apoptosis. Senescence is a phenotype acquired by the cell as a response to stress that can be induced by different stimuli such as oncogenic activation, chemotherapy, irradiation and other therapies like CDK4/6i treatment. During senescence, cell cycle is arrested, and cells produce a secretome that boost the microenvironment and engages the immune system. In BCa, senescence has been detected in pre-clinical research, *in vitro* and *in vivo* (Goel *et al.*, 2017; Vijayaraghavan *et al.*, 2017). If senescent cells are found in patients after treatment, is still unknown

due to the lack of appropriate diagnostic tests. Since our focus was not the effect of the senescence phenotype after palbociclib treatment, we explored at which time point ER+ BCa cells express β -gal, a biomarker of senescence, and started to change the morphology. Consequently, we could focus only in the CDK4/6i cytostatic effect in tumor cells. At day 4 after starting palbociclib treatment, ZR75 cells began to show morphological changes and at day 6 of treatment, they increased the expression of β -gal. Considering these observations, we decided to use a 4-day time point to run our functional selection.

For the sequencing analysis of the CRISPR/Cas 9 drop out screen results, we implemented two different methodological approaches using MAGeCK-VISPR: Maximum likelihood estimation (MLE) and Robust rank aggregation (RRA). Based on the straightforward design of our experiment, we could use both modules, yet the new algorithm implemented in the MAGeCK-MLE model also considers the sgRNA KO efficiency. This efficiency can vary depending on different variables such as the sequence content and chromatin structure (Wu *et al.*, 2014; Xu *et al.*, 2015). This information was considered relevant in our context, thus we focused on the results analyzed by MaGECK-MLE module to select our candidate genes. Once we had the β score for all the genes, we selected the genes based on a -0,9 palbociclib β score. We observed that the top hit candidate resistant genes were cell specific. As a result of relaxing the threshold, common candidates between BT474 and ZR75 resistant cell lines were captured. Moreover, the relaxed threshold allowed us to fish out more drivers to explore after integrating the screen results along with the patient data sets. Expression profiles from patient samples was performed using a panel of 771 genes called Breast Cancer 360™. These were the genes that we could interrogate in our three analyses. Only 152 out of 3.730 gene candidates from the screen (when pooling BT474 and ZR75 cells together) were included in Breast Cancer360™ panel, leaving the majority of the candidates obtained out of the analysis.

Integration of the CDK4/6i resistance driver candidates from the CRISPR/Cas9 screen and patients data sets analysis

When integrating the data obtained with the CRISPR/Cas 9 screen with the gene expression analysis of two patient data sets (CDK patient cohort and CORALEEN data set), we identified 11 CDK4/6i resistance candidates: BLM, CCNE1, CDC25A, CDKN3, CKS1B, DLGAP5, E2F1, XXXX, POLQ, PTTG1, TSPAN1. This included nine genes associated with cell cycle progression. Remarkably, some of them were previously characterized as drivers of CDK4/6 resistance. In addition,

the other two candidates were cell signaling proteins involved in the regulation of important cell functions such as growth and migration.

Cell cycle related candidates

BLM, DLGAP5, POLQ, PTTG1, CDKN3, and CDC25A are genes included in a gene expression signature of RB loss-of-function that includes 87 genes, named RBsig (Malorni *et al.*, 2016). This signature have prognostic value in ER+ BCa tumors from the METABRIC dataset (Malorni *et al.*, 2016). Additionally, the RBsig identified which BCa cell lines were resistant or sensitive to palbociclib (Malorni *et al.*, 2016). Consistently, CDC25A was previously associated with HT resistance in luminal BCa tumors. The phosphatase CDC25A dephosphorylates and activates cyclin-CDK complexes. It is an unstable protein generated at G1 and degraded at mitosis. The overexpression of this phosphatase accelerates the G1/S and G2/M transitions, inducing genomic instability and tumor formation. When DNA damage is detected by the DNA damage sensor ATM, CHK2 is activated and phosphorylates CDC25A to be degraded. ATM-CHK2-CDC25A axis has been found crucial for the efficacy of HT in luminal tumors and defects in single strand break repair in ER+ BCa can drive endocrine therapy resistance (Anurag *et al.*, 2018; Haricharan *et al.*, 2017). In addition, CDC25A dephosphorylates CDK4/6 complex inducing its activation, which would suggest a function in controlling CDK4/6i outcome in ER+ BCa tumors. CKS1B is a regulatory subunit of cyclin-dependent kinase and plays an essential role in cell cycle progression. Many studies have associated CKS1B to different cancer types such as myeloma and retinoblastoma. This protein has also been related with chemotherapy resistance through the activation of STAT3 and MEK signaling in multiple mieloma (Huang *et al.*, 2015; Shi *et al.*, 2020).

E2F1 has been widely associated with CDK4/6i resistance in different pre-clinical models and patients' data. CDK-RB-E2F axis is central for cell cycle progression. E2F function is regulated at many levels, such as transcription, mRNA stability, post-translational modifications, interaction with regulatory proteins and protein stability (Kent and Leone, 2019). Cyclin D-CDK4/6 and cyclin E-CDK2 complexes regulate the dissociation of RB-E2F, allowing E2F transcription activity (Johnson *et al.*, 2016). E2F is commonly upregulated in cancer and is associated with poor prognosis (Kent and Leone, 2019). The overexpression of E2F can bypass cyclin D-CDK4/6 function and escape from CDK4/6i-induced cell arrest (Dean *et al.*, 2010).

Another interesting cell cycle-associated candidate was Cyclin E1. As introduced before, cyclin E-CDK2 complex phosphorylate RB after it is phosphorylated by cyclin D-CDK4/6, inducing E2F release. Upon CDK4/6 inhibition, endogenous levels of cyclin E-CDK2 cannot efficiently phosphorylate RB, decreasing E2F

release. To overcome this situation, tumor cells have been found to upregulate cyclin E1, cyclin E2 and CDK2 in different CDK4/6i resistance models (Bollard *et al.*, 2017; Herrera-Abreu *et al.*, 2016; Martin *et al.*, 2017; Taylor-Harding *et al.*, 2015; Yang *et al.*, 2017). Silencing cyclin E1 or CDK2 restores sensitivity in resistant cells to palbociclib-induced cell cycle arrest (Herrera-Abreu *et al.*, 2016).

Collectively, identifying genes that were previously reported to be involved in CDK4/6i resistance validates the results we obtained with the integration of the different strategies. Contrarily, any of these cell cycle-related proteins introduces novel CDK4/6i resistance mechanisms.

Cell cycle non-related candidates

Unexpectedly, genes that are not associated with cell cycle progression machinery were also highlighted. These genes were not previously reported to be drivers of CDK4/6i resistance, hence representing promising unappreciated mechanisms of resistance. This includes TSPAN1 and XXXX membrane proteins.

TSPAN1 is a cell-surface protein member of the tetraspanin family. This molecule mediates signal transduction that regulates cell development, growth and migration. TSPAN1 has been associated with tumor progression in different cancer types such as pancreas, head and neck and prostate cancer (Chen *et al.*, 2009; Garcia-Mayea *et al.*, 2020; Munkley *et al.*, 2017; Ye *et al.*, 2021). TSPAN1 was identified in a proteomic study that interrogated genes involved in cisplatin acquired resistance in head and neck squamous carcinoma (HNSCC) (Garcia-Mayea *et al.*, 2020). They validated TSPAN1 induction of cisplatin resistance HNSCC *in vitro*, *in vivo* and in patients samples. Upon TSPAN1 silencing in cisplatin-resistant cells, proliferation and autophagy were reduced, apoptosis was induced, and cells were sensitized to chemotherapy. Cisplatin-resistant tumors presented EMT phenotype that disappeared after the inhibition of TSPAN1, indicating a relation between TSPAN1, EMT and metastasis (Garcia-Mayea *et al.*, 2020). TSPAN1 has not previously been associated with CDK4/6i resistance, however some evidence suggested that EMT is related with this resistance. The inhibition of CDK4/6 has been reported to induce EMT via Smad-dependent TGF β signaling (Liu and Korc, 2012; Tobin *et al.*, 2011). Consistently, the inhibition of CDK2-mediated phosphorylation of Smad3 decreases cell migration and invasion in TN BCa through modifying EMT signaling (Thomas *et al.*, 2017). Consequently, CDK4/6i resistance may be induced from suppression of Smad3 which is associated with cyclin E-CDK2 and EMT pathways (Franco *et al.*, 2014; Herrera-Abreu *et al.*, 2016; Liu and Korc, 2012).

In summary, TSPAN1 is associated with EMT and chemotherapy resistance, and EMT has been related with CDK4/6i resistance through Smad3 and Cyclin E-CDK2

axis. Therefore, TSPAN1 could be another interesting driver of CDK4/6i resistance to further explore in the future.

XXXX was the second molecule identified that was not part of the cell cycle machinery. Although XXXX was not a top hit in the CRISPR/Cas9 screen, the two clinical cohorts showed a strong significant association between XXXX and poor response to CDK4/6i in patients. Interestingly, in the analysis of the CORALEEN clinical trial, XXXX was the most significantly increased gene in tumors with no response to ribociclib plus letrozole.

[Section eliminated – Confidential information]

Finally, we decided to select XXXX for further validation instead of TSPAN1. We based our decision on the novelty of the association between this gene and CDK4/6i resistance (i), the strong association between XXXX and the HER2-E molecular subtype (ii) and because of the cell membrane localization (iii) that provides an accessible target to develop inhibitors against it.

Validation of XXXX-driven CDK4/6i resistance

Remarkably, HER2-E resistant cells expressing XXXX are refractory to XXXX-depletion. Extended passaging of pool CRISPR/Cas 9 XXXX KO selected cells is not viable and XXXX-expressing clones take out the KO pooled cell population. This suggests that CDK4/6i resistance selects for XXXX addiction. Alternatively, we used XXXX knockdowns (shRNA) to interrogate the effect of the gene in palbociclib response. Downregulation of XXXX showed a partial restorage of palbociclib sensitivity in ZR75, BT474 and MCF7-PR, whereas parental MCF7 were unaffected. On the other hand, overexpression of XXXX in ZR75 cells increased the resistance to CDK4/6i. In MCF7 cells overexpressing XXXX, resistance was increased, but it did not reach MCF7-PR resistance, showing an intermediate state. We could also appreciate that the increased resistance was found in the 3 isoforms (OE, CA, KD), suggesting that XXXX induction of resistance could be independent of its kinase activity. Further experiments to test changes in signal transduction pathways upon XXXX overexpression are ongoing.

Given the different effects that CDK4/6i treatment has in patients, it is challenging to validate XXXX-mediated CDK4/6i resistance *in vitro*. To this, i) we are currently optimizing two xenograft mouse models for testing palbociclib effect *in vivo*. MCF7 cells expressing luciferase are injected intracardially in athymic mice, to avoid immune system clearance of human tumor cells. After malignant cells spread, we

measure bone lesions in the legs through the luciferase activity in the malignant cells using IVIS. When the metastatic outgrowth reaches the 10% from day 0, we start treating the animals with daily gavage administration of palbociclib. Alternatively, we are measuring the palbociclib effect on mammary fat pad injections of MCF7 cells in athymic mice. The optimization of both models is ongoing. We are determining the appropriate time to start the treatment, the palbociclib dosage and frequency of treatment of the mice. ii) We aim to use XXXX-depleted cells or XXXX-directed mAb against XXXX to test the role of XXXX in CDK4/6i resistance. iii) We plan to compare MCF7 and MCF7 XXXX OE cells to see metastatic burden and tumor growth during CDK4/6i treatment.

Characterization of the XXXX-driven mechanism that induces CDK4/6i resistance

To unravel key signaling mediators of XXXX in HER2-E context a protein-protein interaction screening was completed. We used proximity labeling assay BioID approach to identify XXXX interactors in MCF7 cell lines (MCF7 and MCF7-PR). Characterization of XXXX downstream interactome may allow us to better discern what signaling cascades are key to drive palbociclib treatment resistance.

BioID is a unique technique to identify physiologically relevant protein interactions. This method fuses a promiscuous biotin ligase to the protein of interest in order to biotinylate proteins that are in close proximity (Roux *et al.*, 2018). Biotinylation is a physiologically rare protein modification, therefore this method allows a selective isolation and identification of BioID-biotinylated molecules. The interactome of the protein of interest is determined by standard biotin-affinity capture using streptavidin beads and subsequent mass spectrometry peptide analysis. Importantly, interactors must be validated through alternative techniques such as co-IP or proximity-ligation assay (PLA). Remarkably, the BioID enables the detection of low affinity and transient interaction in the cellular context. This has offered a more comprehensive view of the XXXX potential partners.

We used a second-generation biotin ligase (BioID2) for developing our BioID experiments. This molecule is smaller than the first biotin ligase BirA R118G*, which increases selectivity and enhances labeling of close proteins to the fused target molecule (Kim *et al.*, 2016).

We used two different cell lines for the BioID: MCF7 and MCF7-PR (two replicates each). The results showed that in both cell lines XXXX is interacting with RSK1, RICTOR and PLCG1, which were previously reported and serve as positive

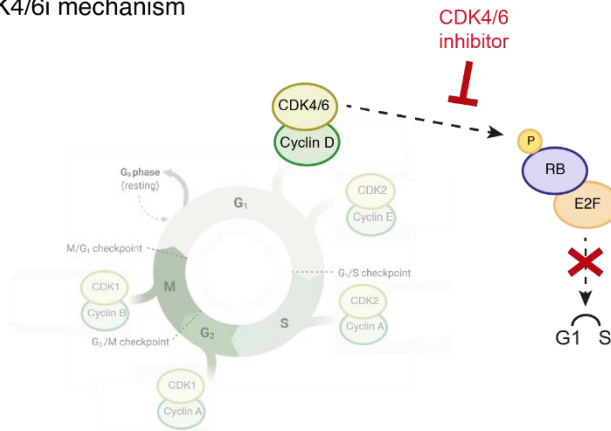
controls. We next focus on XXXX interactome in palbo-resistant cells incubated with palbociclib. Out of the 63 unique interactors in MCF7-PR cells, RHEB and LGR4 were highlighted based on their association with important signaling cascades related with tumor cell growth and metastasis.

RHEB is a conserved small GTPase that belongs to the Ras superfamily and activates cell growth through mTORC1 activation. It requires signals from metabolites such as amino acids, glucose, oxygen, ATP and growth factors (cytokines and hormones like insulin) to stimulate mTORC1 complex (Dibble and Cantley, 2015). RHEB has been found overexpressed in human carcinomas with a crucial function in carcinogenesis (Lu *et al.*, 2010). Interestingly, a study showed that the activation of mTORC1 and mTORC2 induces CDK4/6i resistance in PDAC tumors. They found that the combinatorial effect of both complexes increase cyclin D1 and cyclin E1 expression, therefore enhancing cell cycle in PDAC cells (Knudsen *et al.*, 2019). In our context, XXXX could be activating mTORC1 and 2 through RHEB in MCF7-PR cells, inducing gene expression changes, such as CCNE1 upregulation, and bypassing CDK4/6i effect.

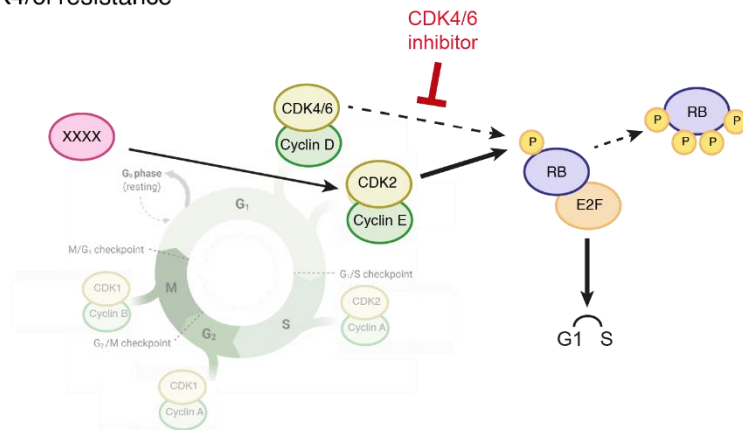
LGR4, together with LGR5 and 6, stabilizes Wnt receptors, inducing Wnt signaling cascade. A recent article showed that LGR4 was able to enhance BCa metastasis independently of Wnt signaling (Yue *et al.*, 2021). In a multiomics screening analysis they identified EGFR as a key mediator of LGR4 activity in BCa progression (Yue *et al.*, 2021). LGR4 interacts with EGFR, avoiding EGFR degradation and enhancing the activation of the molecule. In our CDK4/6i resistant cells, LGR4 interaction with XXXX could be inhibiting its degradation in CDK4/6i resistant cell lines enhancing its function and leading to cell cycle progression.

We hypothesize that XXXX, enhanced by LGR4 function in the membrane, might be activating PI3K/AKT/mTOR signaling to ultimately phosphorylate CDK2. CDK2-cyclin E1 complex might be phosphorylating RB and releasing E2F1 transcription factor. Preliminary experiments have pointed towards a decrease in phospho-RB after silencing XXXX, translated in cell cycle arrest. The XXXX-mediated effect on RB phosphorylation and E2F1 activation may explain CCNE1 expression changes in XXXX-depleted cell lines. Of note, cyclin E1 was one of the candidates found in the integration of the CRISPR/Cas 9 screen and the two clinical cohorts. The expression of this gene was highly associated with PD samples in CDK cohort and with no response to ribociclib plus letrozole in CORALEEN clinical trial. Moreover, downregulation of CCNE1 in ZR75 palbo-resistant cells increased sensitivity to palbociclib. However, CCNE1 has widely studied associated with CDK4/6i resistance

CDK4/6i mechanism



CDK4/6i resistance



Overcoming CDK4/6i resistance

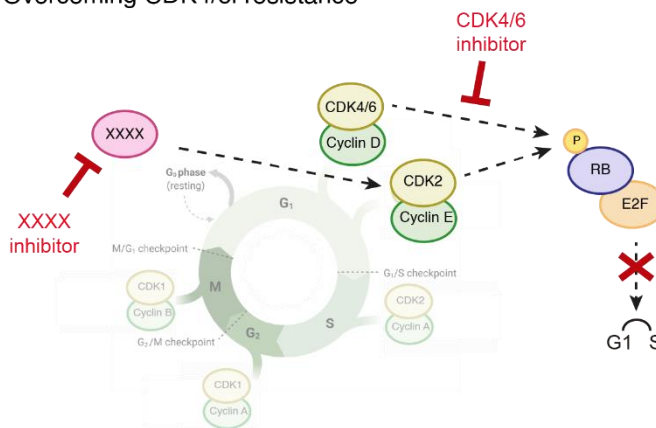


Figure D1. XXXX drives CDK4/6i resistance in HER2-E ER+/HER2-negative BCa tumors.

Schematic representation of the mechanism involved in CDK4/6i resistance in cells that are sensitive (top) and resistant (center) to palbociclib based on our research. XXXX inhibitors would be a new therapeutic strategy (bottom) to overcome XXXX-mediated CDK4/6i resistance.

All together, we suggest a working model in which XXXX is the driver of CDK4/6i resistance in HER2-E ER+/HER2-negative metastatic tumors by increasing cyclin E1-CDK2 function and evading CDK4/6 inhibition. We hypothesize that the inhibition of XXXX would restore CDK4/6i sensitivity in HER2-E subtype metastatic ER+/HER2-negative tumors (Figure D1). Further experiments must be performed to validate the activation of PIP3K/AKT/mTOR and CDK2 upon XXXX activation in the context of CDK4/6i treatment.

[Section eliminated – Confidential information]

In summary, this thesis describes a potential driver of CDK4/6i resistance in HER2-E subtype ER+/HER2-negative BCa tumors. Based on these results, XXXX-directed mAb therapy to treat HER2-E subtype ER+/HER2-negative advanced tumors with poor response to CDK4/6i might be beneficial and could improve treatment outcome. We propose XXXX-targeted therapy in combination with HT and CDK4/6i as a testable therapeutic strategy in metastatic ER+/HER2-negative BCa tumors with HER2-E molecular subtype that have poor response to first line HT plus CDK4/6i.

- Conclusions -

Conclusions

Integration of a genome wide CRISPR/Cas 9 screening in palbo-resistant cell lines, with the analysis of two patients' data sets identified eleven candidate gene drivers of CDK4/6i resistance: BLM, CCNE1, CDC25A, CDKN3, CKS1B, DLGAP5, E2F1, XXXX, POLQ, PTTG1 and TSPAN1. Nine out of the eleven candidates are part of the cell cycle machinery and were previously associated with CDK4/6i resistance.

XXXX was significantly associated with progression disease in the CDK patient cohort that included tumors treated with different CDK4/6i lines.

In patients that did not respond to ribociclib plus letrozole treatment in the CORALEEN clinical trial, XXXX expression was significantly upregulated compared with baseline samples.

XXXX depletion increased sensitivity to palbociclib in palbo-resistant ER+ BCa cell lines.

XXXX interactome in MCF7 parental and palbo-resistant include RSK1, RICTOR and PLCG1 signaling mediators.

XXXX interactome in MCF7 palbo-resistant show 63 unique interactors. LRG4 and RHEB are signaling mediators that could explain XXXX-driven mechanism of CDK4/6i resistance.

XXXX silencing reduces CCNE1 expression in different ER+ BCa cell lines.

CCNE1 silencing increases sensitivity to palbociclib in ZR75 ER+/HER2-negative BCa cell lines.

- Bibliography -

Bibliography

- Aguirre-Ghiso, J. A., Estrada, Y., Liu, D., & Ossowski, L. (2003). ERK(MAPK) activity as a determinant of tumor growth and dormancy; regulation by p38(SAPK). *Cancer Research*, 63(7), 1684–1695.
- Aird, W. C. (2007). Phenotypic heterogeneity of the endothelium: II. Representative vascular beds. *Circulation Research*, 100(2), 174–190. <https://doi.org/10.1161/01.RES.0000255690.03436.ae>
- Ali, S., & Coombes, R. C. (2002). Endocrine-responsive breast cancer and strategies for combating resistance. *Nature Reviews. Cancer*, 2(2), 101–112. <https://doi.org/10.1038/nrc721>
- Allison, K. H. (2012). Molecular pathology of breast cancer: what a pathologist needs to know. *American Journal of Clinical Pathology*, 138(6), 770–780. <https://doi.org/10.1309/AJCPIV9IQ1MRQMOO>
- Álvarez-Fernández, M., & Malumbres, M. (2020). Mechanisms of Sensitivity and Resistance to CDK4/6 Inhibition. *Cancer Cell*, 37(4), 514–529. <https://doi.org/10.1016/j.ccell.2020.03.010>
- André, F., Ciruelos, E., Rubovszky, G., Campone, M., Loibl, S., Rugo, H. S., Iwata, H., Conte, P., Mayer, I. A., Kaufman, B., Yamashita, T., Lu, Y.-S., Inoue, K., Takahashi, M., Pápai, Z., Longin, A.-S., Mills, D., Wilke, C., Hirawat, S., & Juric, D. (2019). Alpelisib for PIK3CA-Mutated, Hormone Receptor-Positive Advanced Breast Cancer. *New England Journal of Medicine*, 380(20), 1929–1940. <https://doi.org/10.1056/NEJMoa1813904>
- Andreopoulou, E., & Sparano, J. A. (2013). Chemotherapy in Patients with Anthracycline- and Taxane-Pretreated Metastatic Breast Cancer: An Overview. *Current Breast Cancer Reports*, 5(1), 42–50. <https://doi.org/10.1007/s12609-012-0097-1>
- Anurag, M., Punturi, N., Hoog, J., Bainbridge, M. N., Ellis, M. J., & Haricharan, S. (2018). Comprehensive Profiling of DNA Repair Defects in Breast Cancer Identifies a Novel Class of Endocrine Therapy Resistance Drivers. *Clinical Cancer Research*, 24(19), 4887 LP – 4899. <https://doi.org/10.1158/1078-0432.CCR-17-3702>
- Barnard, M. E., Boeke, C. E., & Tamimi, R. M. (2015). Established breast cancer risk factors and risk of intrinsic tumor subtypes. *Biochimica et Biophysica Acta*, 1856(1), 73–85. <https://doi.org/10.1016/j.bbcan.2015.06.002>
- Baselga, J., Campone, M., Piccart, M., Burris, H. A. 3rd, Rugo, H. S., Sahmoud, T., Noguchi, S., Gnani, M., Pritchard, K. I., Lebrun, F., Beck, J. T., Ito, Y., Yardley, D., Deleu, I., Perez, A., Bachelot, T., Vittori, L., Xu, Z., Mukhopadhyay, P., ... Hortobagyi, G. N. (2012). Everolimus in postmenopausal hormone-receptor-positive advanced breast cancer. *The New England Journal of Medicine*, 366(6), 520–529. <https://doi.org/10.1056/NEJMoa1109653>

- Begg, A. C., Stewart, F. A., & Vens, C. (2011). Strategies to improve radiotherapy with targeted drugs. *Nature Reviews. Cancer*, 11(4), 239–253. <https://doi.org/10.1038/nrc3007>
- Bidwell, B. N., Slaney, C. Y., Withana, N. P., Forster, S., Cao, Y., Loi, S., Andrews, D., Mikeska, T., Mangan, N. E., Samarajiwa, S. A., de Weerd, N. A., Gould, J., Argani, P., Möller, A., Smyth, M. J., Anderson, R. L., Hertzog, P. J., & Parker, B. S. (2012). Silencing of Irf7 pathways in breast cancer cells promotes bone metastasis through immune escape. *Nature Medicine*, 18(8), 1224–1231. <https://doi.org/10.1038/nm.2830>
- Blackwell, K. L., Pegram, M. D., Tan-Chiu, E., Schwartzberg, L. S., Arbushites, M. C., Maltzman, J. D., Forster, J. K., Rubin, S. D., Stein, S. H., & Burstein, H. J. (2009). Single-agent lapatinib for HER2-overexpressing advanced or metastatic breast cancer that progressed on first- or second-line trastuzumab-containing regimens. *Annals of Oncology: Official Journal of the European Society for Medical Oncology*, 20(6), 1026–1031. <https://doi.org/10.1093/annonc/mdn759>
- Bollard, J., Miguela, V., Ruiz de Galarreta, M., Venkatesh, A., Bian, C. B., Roberto, M. P., Tovar, V., Sia, D., Molina-Sánchez, P., Nguyen, C. B., Nakagawa, S., Llovet, J. M., Hoshida, Y., & Lujambio, A. (2017). Palbociclib (PD-0332991), a selective CDK4/6 inhibitor, restricts tumour growth in preclinical models of hepatocellular carcinoma. *Gut*, 66(7), 1286–1296. <https://doi.org/10.1136/gutjnl-2016-312268>
- Bos, P. D., Zhang, X. H.-F., Nadal, C., Shu, W., Gomis, R. R., Nguyen, D. X., Minn, A. J., van de Vijver, M. J., Gerald, W. L., Foekens, J. A., & Massagué, J. (2009). Genes that mediate breast cancer metastasis to the brain. *Nature*, 459(7249), 1005–1009. <https://doi.org/10.1038/nature08021>
- Brasó-Maristany, F., Griguolo, G., Pascual, T., Paré, L., Nuciforo, P., Llombart-Cussac, A., Bermejo, B., Oliveira, M., Morales, S., Martínez, N., Vidal, M., Adamo, B., Martínez, O., Pernas, S., López, R., Muñoz, M., Chic, N., Galván, P., Garau, I., ... Prat, A. (2020). Phenotypic changes of HER2-positive breast cancer during and after dual HER2 blockade. *Nature Communications*, 11(1), 385. <https://doi.org/10.1038/s41467-019-14111-3>
- Brennan, A., Leech, J. T., Kad, N. M., & Mason, J. M. (2020). Selective antagonism of cJun for cancer therapy. *Journal of Experimental & Clinical Cancer Research: CR*, 39(1), 184. <https://doi.org/10.1186/s13046-020-01686-9>
- Bridge, A. J., Pebernard, S., Ducraux, A., Nicoulaz, A.-L., & Iggo, R. (2003). Induction of an interferon response by RNAi vectors in mammalian cells. *Nature Genetics*, 34(3), 263–264. <https://doi.org/10.1038/ng1173>
- Brisken, C., & O'Malley, B. (2010). Hormone action in the mammary gland. *Cold Spring Harbor Perspectives in Biology*, 2(12), a003178. <https://doi.org/10.1101/cshperspect.a003178>
- Britt, K. (2012). Menarche, menopause, and breast cancer risk. In *The Lancet. Oncology* (Vol. 13, Issue 11, pp. 1071–1072). [https://doi.org/10.1016/S1470-2045\(12\)70456-4](https://doi.org/10.1016/S1470-2045(12)70456-4)
- Budczies, J., von Winterfeld, M., Klauschen, F., Bockmayr, M., Lennerz, J. K., Denkert, C.,

- Wolf, T., Warth, A., Dietel, M., Anagnostopoulos, I., Weichert, W., Wittschieber, D., & Stenzinger, A. (2015). The landscape of metastatic progression patterns across major human cancers. *Oncotarget*, *6*(1), 570–583. <https://doi.org/10.18632/oncotarget.2677>
- Cameron, M. D., Schmidt, E. E., Kerkvliet, N., Nadkarni, K. V, Morris, V. L., Groom, A. C., Chambers, A. F., & MacDonald, I. C. (2000). Temporal progression of metastasis in lung: cell survival, dormancy, and location dependence of metastatic inefficiency. *Cancer Research*, *60*(9), 2541–2546.
- Cannata, D., Lann, D., Wu, Y., Elis, S., Sun, H., Yakar, S., Lazzarino, D. A., Wood, T. L., & Leroith, D. (2010). Elevated circulating IGF-I promotes mammary gland development and proliferation. *Endocrinology*, *151*(12), 5751–5761. <https://doi.org/10.1210/en.2010-0792>
- Cardoso, F., Senkus, E., Costa, A., Papadopoulos, E., Aapro, M., André, F., Harbeck, N., Aguilar Lopez, B., Barrios, C. H., Bergh, J., Biganzoli, L., Boers-Doets, C. B., Cardoso, M. J., Carey, L. A., Cortés, J., Curigliano, G., Diéras, V., El Saghir, N. S., Eniu, A., ... Winer, E. P. (2018). 4th ESO-ESMO International Consensus Guidelines for Advanced Breast Cancer (ABC 4)†. *Annals of Oncology: Official Journal of the European Society for Medical Oncology*, *29*(8), 1634–1657. <https://doi.org/10.1093/annonc/mdy192>
- Cejalvo, J. M., Martínez de Duenas, E., Galvan, P., García-Recio, S., Burgues Gasion, O., Pare, L., Antolin, S., Martinello, R., Blancas, I., Adamo, B., Guerrero-Zotano, A., Muñoz, M., Nuciforo, P., Vidal, M., Perez, R. M., Chacon Lopez-Muniz, J. I., Caballero, R., Peg, V., Carrasco, E., ... Prat, A. (2017). Intrinsic Subtypes and Gene Expression Profiles in Primary and Metastatic Breast Cancer. *Cancer Research*, *77*(9), 2213–2221. <https://doi.org/10.1158/0008-5472.CAN-16-2717>
- Celià-Terrassa, T., & Jolly, M. K. (2020). Cancer Stem Cells and Epithelial-to-Mesenchymal Transition in Cancer Metastasis. *Cold Spring Harbor Perspectives in Medicine*, *10*(7). <https://doi.org/10.1101/cshperspect.a036905>
- Celià-Terrassa, T., & Kang, Y. (2018). Metastatic niche functions and therapeutic opportunities. *Nature Cell Biology*, *20*(8), 868–877. <https://doi.org/10.1038/s41556-018-0145-9>
- Celià-Terrassa, T., Meca-Cortés, O., Mateo, F., Martínez de Paz, A., Rubio, N., Arnal-Estapé, A., Ell, B. J., Bermudo, R., Díaz, A., Guerra-Rebollo, M., Lozano, J. J., Estarás, C., Ulloa, C., Álvarez-Simón, D., Milà, J., Vilella, R., Paciucci, R., Martínez-Balbás, M., de Herrerros, A. G., ... Thomson, T. M. (2012). Epithelial-mesenchymal transition can suppress major attributes of human epithelial tumor-initiating cells. *The Journal of Clinical Investigation*, *122*(5), 1849–1868. <https://doi.org/10.1172/JCI59218>
- Cen, L., Carlson, B. L., Schroeder, M. A., Ostrem, J. L., Kitange, G. J., Mladek, A. C., Fink, S. R., Decker, P. A., Wu, W., Kim, J.-S., Waldman, T., Jenkins, R. B., & Sarkaria, J. N. (2012). p16-Cdk4-Rb axis controls sensitivity to a cyclin-dependent kinase inhibitor PD0332991 in glioblastoma xenograft cells. *Neuro-Oncology*, *14*(7), 870–881. <https://doi.org/10.1093/neuonc/nos114>
- Cerami, E., Gao, J., Dogrusoz, U., Gross, B. E., Sumer, S. O., Aksoy, B. A., Jacobsen, A.,

- Byrne, C. J., Heuer, M. L., Larsson, E., Antipin, Y., Reva, B., Goldberg, A. P., Sander, C., & Schultz, N. (2012). The cBio cancer genomics portal: an open platform for exploring multidimensional cancer genomics data. *Cancer Discovery*, 2(5), 401–404. <https://doi.org/10.1158/2159-8290.CD-12-0095>
- Chaffer, C. L., & Weinberg, R. A. (2011). A perspective on cancer cell metastasis. *Science (New York, N.Y.)*, 331(6024), 1559–1564. <https://doi.org/10.1126/science.1203543>
- Chambers, A. F., Groom, A. C., & MacDonald, I. C. (2002). Dissemination and growth of cancer cells in metastatic sites. *Nature Reviews. Cancer*, 2(8), 563–572. <https://doi.org/10.1038/nrc865>
- Chandarlapaty, S., & Razavi, P. (2019). Cyclin E mRNA: Assessing Cyclin-Dependent Kinase (CDK) Activation State to Elucidate Breast Cancer Resistance to CDK4/6 Inhibitors. In *Journal of clinical oncology: official journal of the American Society of Clinical Oncology* (Vol. 37, Issue 14, pp. 1148–1150). <https://doi.org/10.1200/JCO.19.00090>
- Chaussepied, M., & Ginsberg, D. (2004). Transcriptional regulation of AKT activation by E2F. *Molecular Cell*, 16(5), 831–837. <https://doi.org/10.1016/j.molcel.2004.11.003>
- Cheang, M. C. U., Martin, M., Nielsen, T. O., Prat, A., Voduc, D., Rodriguez-Lescure, A., Ruiz, A., Chia, S., Shepherd, L., Ruiz-Borrego, M., Calvo, L., Alba, E., Carrasco, E., Caballero, R., Tu, D., Pritchard, K. I., Levine, M. N., Bramwell, V. H., Parker, J., ... Carey, L. A. (2015). Defining breast cancer intrinsic subtypes by quantitative receptor expression. *The Oncologist*, 20(5), 474–482. <https://doi.org/10.1634/theoncologist.2014-0372>
- Cheang, M. C. U., Voduc, K. D., Tu, D., Jiang, S., Leung, S., Chia, S. K., Shepherd, L. E., Levine, M. N., Pritchard, K. I., Davies, S., Stjleman, I. J., Davis, C., Ebbert, M. T. W., Parker, J. S., Ellis, M. J., Bernard, P. S., Perou, C. M., & Nielsen, T. O. (2012). Responsiveness of intrinsic subtypes to adjuvant anthracycline substitution in the NCIC.CTG MA.5 randomized trial. *Clinical Cancer Research: An Official Journal of the American Association for Cancer Research*, 18(8), 2402–2412. <https://doi.org/10.1158/1078-0432.CCR-11-2956>
- Chen, L., Zhu, Y.-Y., Zhang, X.-J., Wang, G.-L., Li, X.-Y., He, S., Zhang, J.-B., & Zhu, J.-W. (2009). TSPAN1 protein expression: a significant prognostic indicator for patients with colorectal adenocarcinoma. *World Journal of Gastroenterology*, 15(18), 2270–2276. <https://doi.org/10.3748/wjg.15.2270>
- Chen, M.-T., Sun, H.-F., Zhao, Y., Fu, W.-Y., Yang, L.-P., Gao, S.-P., Li, L.-D., Jiang, H., & Jin, W. (2017). Comparison of patterns and prognosis among distant metastatic breast cancer patients by age groups: a SEER population-based analysis. *Scientific Reports*, 7(1), 9254. <https://doi.org/10.1038/s41598-017-10166-8>
- Chen, S.-H., Gong, X., Zhang, Y., Van Horn, R. D., Yin, T., Huber, L., Burke, T. F., Manro, J., Iversen, P. W., Wu, W., Bhagwat, S. V., Beckmann, R. P., Tiu, R. V., Buchanan, S. G., & Peng, S.-B. (2018). RAF inhibitor LY3009120 sensitizes RAS or BRAF mutant cancer to CDK4/6 inhibition by abemaciclib via superior inhibition of phospho-RB and suppression of cyclin D1. *Oncogene*, 37(6), 821–832. <https://doi.org/10.1038/onc.2017.384>

- Chen, S., Sanjana, N. E., Zheng, K., Shalem, O., Lee, K., Shi, X., Scott, D. A., Song, J., Pan, J. Q., Weissleder, R., Lee, H., Zhang, F., & Sharp, P. A. (2015). Genome-wide CRISPR screen in a mouse model of tumor growth and metastasis. *Cell*, *160*(6), 1246–1260. <https://doi.org/10.1016/j.cell.2015.02.038>
- Choi, Y. J., & Anders, L. (2014). Signaling through cyclin D-dependent kinases. *Oncogene*, *33*(15), 1890–1903. <https://doi.org/10.1038/onc.2013.137>
- Clark, A. S., Karasic, T. B., DeMichele, A., Vaughn, D. J., O'Hara, M., Perini, R., Zhang, P., Lal, P., Feldman, M., Gallagher, M., & O'Dwyer, P. J. (2016). Palbociclib (PD0332991)-a Selective and Potent Cyclin-Dependent Kinase Inhibitor: A Review of Pharmacodynamics and Clinical Development. *JAMA Oncology*, *2*(2), 253–260. <https://doi.org/10.1001/jamaoncol.2015.4701>
- Coleman, R. E., Major, P., Lipton, A., Brown, J. E., Lee, K.-A., Smith, M., Saad, F., Zheng, M., Hei, Y. J., Seaman, J., & Cook, R. (2005). Predictive value of bone resorption and formation markers in cancer patients with bone metastases receiving the bisphosphonate zoledronic acid. *Journal of Clinical Oncology: Official Journal of the American Society of Clinical Oncology*, *23*(22), 4925–4935. <https://doi.org/10.1200/JCO.2005.06.091>
- Coleman, R., Hall, A., Albanell, J., Hanby, A., Bell, R., Cameron, D., Dodwell, D., Marshall, H., Jean-Mairet, J., Tercero, J., Rojo, F., Gregory, W., & Gomis, R. R. (2017). Effect of MAF amplification on treatment outcomes with adjuvant zoledronic acid in early breast cancer: a secondary analysis of the international, open-label, randomised, controlled, phase 3 AZURE (BIG 01/04) trial. *The Lancet Oncology*, *18*(11), 1543–1552. [https://doi.org/10.1016/S1470-2045\(17\)30603-4](https://doi.org/10.1016/S1470-2045(17)30603-4)
- Collado, M., & Serrano, M. (2006). The power and the promise of oncogene-induced senescence markers. *Nature Reviews Cancer*, *6*(6), 472–476. <https://doi.org/10.1038/nrc1884>
- Comprehensive molecular portraits of human breast tumours. (2012). *Nature*, *490*(7418), 61–70. <https://doi.org/10.1038/nature11412>
- Condorelli, R., Spring, L., O'Shaughnessy, J., Lacroix, L., Bailleux, C., Scott, V., Dubois, J., Nagy, R. J., Lanman, R. B., Iafrate, A. J., Andre, F., & Bardia, A. (2018). Polyclonal RB1 mutations and acquired resistance to CDK 4/6 inhibitors in patients with metastatic breast cancer. *Annals of Oncology: Official Journal of the European Society for Medical Oncology*, *29*(3), 640–645. <https://doi.org/10.1093/annonc/mdx784>
- Cortazar, P., Zhang, L., Untch, M., Mehta, K., Costantino, J. P., Wolmark, N., Bonnefoi, H., Cameron, D., Gianni, L., Valagussa, P., Swain, S. M., Prowell, T., Loibl, S., Wickerham, D. L., Bogaerts, J., Baselga, J., Perou, C., Blumenthal, G., Blohmer, J., ... von Minckwitz, G. (2014). Pathological complete response and long-term clinical benefit in breast cancer: the CTNeoBC pooled analysis. *Lancet (London, England)*, *384*(9938), 164–172. [https://doi.org/10.1016/S0140-6736\(13\)62422-8](https://doi.org/10.1016/S0140-6736(13)62422-8)
- Cortes, J., Cescon, D. W., Rugo, H. S., Nowecki, Z., Im, S.-A., Yusof, M. M., Gallardo, C., Lipatov, O., Barrios, C. H., Holgado, E., Iwata, H., Masuda, N., Otero, M. T., Gokmen, E., Loi, S., Guo, Z., Zhao, J., Aktan, G., Karantza, V., & Schmid, P. (2020).

- Pembrolizumab plus chemotherapy versus placebo plus chemotherapy for previously untreated locally recurrent inoperable or metastatic triple-negative breast cancer (KEYNOTE-355): a randomised, placebo-controlled, double-blind, phase 3 clinical trial. *Lancet (London, England)*, 396(10265), 1817–1828. [https://doi.org/10.1016/S0140-6736\(20\)32531-9](https://doi.org/10.1016/S0140-6736(20)32531-9)
- Cox, J., Hein, M. Y., Luber, C. A., Paron, I., Nagaraj, N., & Mann, M. (2014). Accurate proteome-wide label-free quantification by delayed normalization and maximal peptide ratio extraction, termed MaxLFQ. *Molecular & Cellular Proteomics: MCP*, 13(9), 2513–2526. <https://doi.org/10.1074/mcp.M113.031591>
- Cox, J., & Mann, M. (2008). MaxQuant enables high peptide identification rates, individualized p.p.b.-range mass accuracies and proteome-wide protein quantification. *Nature Biotechnology*, 26(12), 1367–1372. <https://doi.org/10.1038/nbt.1511>
- Cox, J., Michalski, A., & Mann, M. (2011). Software lock mass by two-dimensional minimization of peptide mass errors. *Journal of the American Society for Mass Spectrometry*, 22(8), 1373–1380. <https://doi.org/10.1007/s13361-011-0142-8>
- Cox, T. R., Rumney, R. M. H., Schoof, E. M., Perryman, L., Høye, A. M., Agrawal, A., Bird, D., Latif, N. A., Forrest, H., Evans, H. R., Huggins, I. D., Lang, G., Linding, R., Gartland, A., & Erler, J. T. (2015). The hypoxic cancer secretome induces pre-metastatic bone lesions through lysyl oxidase. *Nature*, 522(7554), 106–110. <https://doi.org/10.1038/nature14492>
- Cristofanilli, M., Turner, N. C., Bondarenko, I., Ro, J., Im, S.-A., Masuda, N., Colleoni, M., DeMichele, A., Loi, S., Verma, S., Iwata, H., Harbeck, N., Zhang, K., Theall, K. P., Jiang, Y., Bartlett, C. H., Koehler, M., & Slamon, D. (2016). Fulvestrant plus palbociclib versus fulvestrant plus placebo for treatment of hormone-receptor-positive, HER2-negative metastatic breast cancer that progressed on previous endocrine therapy (PALOMA-3): final analysis of the multicentre, double-blind, phase 3 randomised controlled trial. *The Lancet. Oncology*, 17(4), 425–439. [https://doi.org/10.1016/S1470-2045\(15\)00613-0](https://doi.org/10.1016/S1470-2045(15)00613-0)
- Crowder, R. J., Phommaly, C., Tao, Y., Hoog, J., Luo, J., Perou, C. M., Parker, J. S., Miller, M. A., Huntsman, D. G., Lin, L., Snider, J., Davies, S. R., Olson, J. A. J., Watson, M. A., Saporita, A., Weber, J. D., & Ellis, M. J. (2009). PIK3CA and PIK3CB inhibition produce synthetic lethality when combined with estrogen deprivation in estrogen receptor-positive breast cancer. *Cancer Research*, 69(9), 3955–3962. <https://doi.org/10.1158/0008-5472.CAN-08-4450>
- Curtis, C., Shah, S. P., Chin, S.-F., Turashvili, G., Rueda, O. M., Dunning, M. J., Speed, D., Lynch, A. G., Samarajiwa, S., Yuan, Y., Gräf, S., Ha, G., Haffari, G., Bashashati, A., Russell, R., McKinney, S., Caldas, C., Aparicio, S., Curtis†, C., ... subgroup, D. analysis. (2012). The genomic and transcriptomic architecture of 2,000 breast tumours reveals novel subgroups. *Nature*, 486(7403), 346–352. <https://doi.org/10.1038/nature10983>
- Darby, S., McGale, P., Correa, C., Taylor, C., Arriagada, R., Clarke, M., Cutter, D., Davies, C., Ewertz, M., Godwin, J., Gray, R., Pierce, L., Whelan, T., Wang, Y., & Peto, R. (2011). Effect of radiotherapy after breast-conserving surgery on 10-year recurrence and 15-year breast cancer death: meta-analysis of individual patient data for 10,801

- women in 17 randomised trials. *Lancet (London, England)*, 378(9804), 1707–1716. [https://doi.org/10.1016/S0140-6736\(11\)61629-2](https://doi.org/10.1016/S0140-6736(11)61629-2)
- David, J. M., Dominguez, C., Hamilton, D. H., & Palena, C. (2016). The IL-8/IL-8R Axis: A Double Agent in Tumor Immune Resistance. *Vaccines*, 4(3). <https://doi.org/10.3390/vaccines4030022>
- De Angelis, C., Nardone, A., Cataldo, M. L., Veeraraghavan, J., Fu, X., Giuliano, M., Malorni, L., Jeselsohn, R., Osborne, K. C., & Schiff, R. (2018). Abstract P4-03-05: AP-1 as a potential mediator of resistance to the cyclin-dependent kinase (CDK) 4/6-inhibitor palbociclib in ER-positive endocrine-resistant breast cancer. *Cancer Research*, 78(4 Supplement), P4-03-05 LP-P4-03–05. <https://doi.org/10.1158/1538-7445.SABCS17-P4-03-05>
- de Dueñas, E. M., Hernández, A. L., Zotano, A. G., Carrión, R. M. P., López-Muñiz, J. I. C., Novoa, S. A., Rodríguez, A. L., Fidalgo, J. A. P., Lozano, J. F., Gasión, O. B., Carrascal, E. C., Capilla, A. H., López-Barajas, I. B., Mateu, M. M., de Ceballos Reyna, M. H. L., Ferrando, A. O., Jañez, N. M., Ballerini, V. C., Torres, A. A., ... González-Angulo, A. M. (2014). Prospective evaluation of the conversion rate in the receptor status between primary breast cancer and metastasis: results from the GEICAM 2009-03 ConvertHER study. *Breast Cancer Research and Treatment*, 143(3), 507–515. <https://doi.org/10.1007/s10549-013-2825-2>
- de Leeuw, R., McNair, C., Schiewer, M. J., Neupane, N. P., Brand, L. J., Augello, M. A., Li, Z., Cheng, L. C., Yoshida, A., Courtney, S. M., Hazard, E. S., Hardiman, G., Hussain, M. H., Diehl, J. A., Drake, J. M., Kelly, W. K., & Knudsen, K. E. (2018). MAPK Reliance via Acquired CDK4/6 Inhibitor Resistance in Cancer. *Clinical Cancer Research: An Official Journal of the American Association for Cancer Research*, 24(17), 4201–4214. <https://doi.org/10.1158/1078-0432.CCR-18-0410>
- Dean, J. L., Thangavel, C., McClendon, A. K., Reed, C. A., & Knudsen, E. S. (2010). Therapeutic CDK4/6 inhibition in breast cancer: key mechanisms of response and failure. *Oncogene*, 29(28), 4018–4032. <https://doi.org/10.1038/onc.2010.154>
- Degriolamo, C., Sabbà, C., & Moschetta, A. (2016). Therapeutic potential of the endocrine fibroblast growth factors FGF19, FGF21 and FGF23. *Nature Reviews. Drug Discovery*, 15(1), 51–69. <https://doi.org/10.1038/nrd.2015.9>
- Denicourt, C., & Dowdy, S. F. (2004). Cip/Kip proteins: more than just CDKs inhibitors. *Genes & Development*, 18(8), 851–855. <https://doi.org/10.1101/gad.1205304>
- Di Leo, A., O'Shaughnessy, J., Sledge, G. W. J., Martin, M., Lin, Y., Frenzel, M., Hardebeck, M. C., Smith, I. C., Llombart-Cussac, A., Goetz, M. P., & Johnston, S. (2018). Prognostic characteristics in hormone receptor-positive advanced breast cancer and characterization of abemaciclib efficacy. *NPJ Breast Cancer*, 4, 41. <https://doi.org/10.1038/s41523-018-0094-2>
- Dibble, C. C., & Cantley, L. C. (2015). Regulation of mTORC1 by PI3K signaling. *Trends in Cell Biology*, 25(9), 545–555. <https://doi.org/https://doi.org/10.1016/j.tcb.2015.06.002>

- Dickler, M. N., Tolaney, S. M., Rugo, H. S., Cortés, J., Diéras, V., Patt, D., Wildiers, H., Hudis, C. A., O'Shaughnessy, J., Zamora, E., Yardley, D. A., Frenzel, M., Koustenis, A., & Baselga, J. (2017). MONARCH 1, A Phase II Study of Abemaciclib, a CDK4 and CDK6 Inhibitor, as a Single Agent, in Patients with Refractory HR(+)/HER2(-) Metastatic Breast Cancer. *Clinical Cancer Research: An Official Journal of the American Association for Cancer Research*, 23(17), 5218–5224. <https://doi.org/10.1158/1078-0432.CCR-17-0754>
- Diehl, J. A. (2002). Cycling to cancer with cyclin D1. *Cancer Biology & Therapy*, 1(3), 226–231. <https://doi.org/10.4161/cbt.72>
- Dimri, G. P., Lee, X., Basile, G., Acosta, M., Scott, G., Roskelley, C., Medrano, E. E., Linskens, M., Rubelj, I., & Pereira-Smith, O. (1995). A biomarker that identifies senescent human cells in culture and in aging skin in vivo. *Proceedings of the National Academy of Sciences of the United States of America*, 92(20), 9363–9367. <https://doi.org/10.1073/pnas.92.20.9363>
- Ding, L., Ellis, M. J., Li, S., Larson, D. E., Chen, K., Wallis, J. W., Harris, C. C., McLellan, M. D., Fulton, R. S., Fulton, L. L., Abbott, R. M., Hoog, J., Dooling, D. J., Koboldt, D. C., Schmidt, H., Kalicki, J., Zhang, Q., Chen, L., Lin, L., ... Mardis, E. R. (2010). Genome remodelling in a basal-like breast cancer metastasis and xenograft. *Nature*, 464(7291), 999–1005. <https://doi.org/10.1038/nature08989>
- Disibio, G., & French, S. W. (2008). Metastatic patterns of cancers: results from a large autopsy study. *Archives of Pathology & Laboratory Medicine*, 132(6), 931–939. [https://doi.org/10.1043/1543-2165\(2008\)132\[931:MPOCRF\]2.0.CO;2](https://doi.org/10.1043/1543-2165(2008)132[931:MPOCRF]2.0.CO;2)
- Doench, J. G., Fusi, N., Sullender, M., Hegde, M., Vaimberg, E. W., Donovan, K. F., Smith, I., Tothova, Z., Wilen, C., Orchard, R., Virgin, H. W., Listgarten, J., & Root, D. E. (2016). Optimized sgRNA design to maximize activity and minimize off-target effects of CRISPR-Cas9. *Nature Biotechnology*, 34(2), 184–191. <https://doi.org/10.1038/nbt.3437>
- Dowsett, M., Cuzick, J., Ingle, J., Coates, A., Forbes, J., Bliss, J., Buyse, M., Baum, M., Buzdar, A., Colleoni, M., Coombes, C., Snowdon, C., Gnant, M., Jakesz, R., Kaufmann, M., Boccardo, F., Godwin, J., Davies, C., & Peto, R. (2010). Meta-analysis of breast cancer outcomes in adjuvant trials of aromatase inhibitors versus tamoxifen. *Journal of Clinical Oncology: Official Journal of the American Society of Clinical Oncology*, 28(3), 509–518. <https://doi.org/10.1200/JCO.2009.23.1274>
- Drebin, J. A., Link, V. C., Weinberg, R. A., & Greene, M. I. (1986). Inhibition of tumor growth by a monoclonal antibody reactive with an oncogene-encoded tumor antigen. *Proceedings of the National Academy of Sciences of the United States of America*, 83(23), 9129–9133. <https://doi.org/10.1073/pnas.83.23.9129>
- Dunbier, A. K., Anderson, H., Ghazoui, Z., Salter, J., Parker, J. S., Perou, C. M., Smith, I. E., & Dowsett, M. (2011). Association between breast cancer subtypes and response to neoadjuvant anastrozole. *Steroids*, 76(8), 736–740. <https://doi.org/10.1016/j.steroids.2011.02.025>
- Efeyan, A., Ortega-Molina, A., Velasco-Miguel, S., Herranz, D., Vassilev, L. T., & Serrano,

- M. (2007). Induction of p53-dependent senescence by the MDM2 antagonist nutlin-3a in mouse cells of fibroblast origin. *Cancer Research*, 67(15), 7350–7357. <https://doi.org/10.1158/0008-5472.CAN-07-0200>
- Eilers, P. H. C., & Marx, B. D. (1996). Flexible Smoothing with B-splines and Penalties. *Statistical Science*, 11(2), 89–102.
- Ellis, M. J., Suman, V. J., Hoog, J., Lin, L., Snider, J., Prat, A., Parker, J. S., Luo, J., DeSchryver, K., Allred, D. C., Esserman, L. J., Unzeitig, G. W., Margenthaler, J., Babiera, G. V., Marcom, P. K., Guenther, J. M., Watson, M. A., Leitch, M., Hunt, K., & Olson, J. A. (2011). Randomized phase II neoadjuvant comparison between letrozole, anastrozole, and exemestane for postmenopausal women with estrogen receptor-rich stage 2 to 3 breast cancer: clinical and biomarker outcomes and predictive value of the baseline PAM50-based in. *Journal of Clinical Oncology: Official Journal of the American Society of Clinical Oncology*, 29(17), 2342–2349. <https://doi.org/10.1200/JCO.2010.31.6950>
- Everest, H. M., Hislop, J. N., Harding, T., Uney, J. B., Flynn, A., Millar, R. P., & McArdle, C. A. (2001). Signaling and antiproliferative effects mediated by GnRH receptors after expression in breast cancer cells using recombinant adenovirus. *Endocrinology*, 142(11), 4663–4672. <https://doi.org/10.1210/endo.142.11.8503>
- Fidler, I. J. (2003). The pathogenesis of cancer metastasis: the “seed and soil” hypothesis revisited. *Nature Reviews. Cancer*, 3(6), 453–458. <https://doi.org/10.1038/nrc1098>
- Finak, G., Bertos, N., Pepin, F., Sadekova, S., Souleimanova, M., Zhao, H., Chen, H., Omeroglu, G., Meterissian, S., Omeroglu, A., Hallett, M., & Park, M. (2008). Stromal gene expression predicts clinical outcome in breast cancer. *Nature Medicine*, 14(5), 518–527. <https://doi.org/10.1038/nm1764>
- Finn, R S, Liu, Y., Martin, M., Rugo, H. S., Dieras, V., Im, S.-A., Gelmon, K., Harbeck, N., Zhu, Z., Lu, D., Gauthier, E., Bartlett, C. H., & Slamon, D. J. (2018). Abstract P2-09-10: Comprehensive gene expression biomarker analysis of CDK 4/6 and endocrine pathways from the PALOMA-2 study. *Cancer Research*, 78(4 Supplement), P2-09-10 LP-P2-09-10. <https://doi.org/10.1158/1538-7445.SABCS17-P2-09-10>
- Finn, Richard S, Aleshin, A., & Slamon, D. J. (2016). Targeting the cyclin-dependent kinases (CDK) 4/6 in estrogen receptor-positive breast cancers. *Breast Cancer Research: BCR*, 18(1), 17. <https://doi.org/10.1186/s13058-015-0661-5>
- Finn, Richard S, Crown, J. P., Lang, I., Boer, K., Bondarenko, I. M., Kulyk, S. O., Ettl, J., Patel, R., Pinter, T., Schmidt, M., Shparyk, Y., Thummala, A. R., Voytko, N. L., Fowst, C., Huang, X., Kim, S. T., Randolph, S., & Slamon, D. J. (2015). The cyclin-dependent kinase 4/6 inhibitor palbociclib in combination with letrozole versus letrozole alone as first-line treatment of oestrogen receptor-positive, HER2-negative, advanced breast cancer (PALOMA-1/TRIO-18): a randomised phase 2 study. *The Lancet. Oncology*, 16(1), 25–35. [https://doi.org/10.1016/S1470-2045\(14\)71159-3](https://doi.org/10.1016/S1470-2045(14)71159-3)
- Finn, Richard S, Dering, J., Conklin, D., Kalous, O., Cohen, D. J., Desai, A. J., Ginther, C., Atefi, M., Chen, I., Fowst, C., Los, G., & Slamon, D. J. (2009). PD 0332991, a selective cyclin D kinase 4/6 inhibitor, preferentially inhibits proliferation of luminal estrogen

- receptor-positive human breast cancer cell lines in vitro. *Breast Cancer Research : BCR*, 11(5), R77. <https://doi.org/10.1186/bcr2419>
- Finn, Richard S, Liu, Y., Zhu, Z., Martin, M., Rugo, H. S., Diéras, V., Im, S.-A., Gelmon, K. A., Harbeck, N., Lu, D. R., Gauthier, E., Huang Bartlett, C., & Slamon, D. J. (2020). Biomarker Analyses of Response to Cyclin-Dependent Kinase 4/6 Inhibition and Endocrine Therapy in Women with Treatment-Naïve Metastatic Breast Cancer. *Clinical Cancer Research : An Official Journal of the American Association for Cancer Research*, 26(1), 110–121. <https://doi.org/10.1158/1078-0432.CCR-19-0751>
- Finn, Richard S, Martin, M., Rugo, H. S., Jones, S., Im, S.-A., Gelmon, K., Harbeck, N., Lipatov, O. N., Walshe, J. M., Moulder, S., Gauthier, E., Lu, D. R., Randolph, S., Dieras, V., & Slamon, D. J. (2016). Palbociclib and Letrozole in Advanced Breast Cancer. *The New England Journal of Medicine*, 375(20), 1925–1936. <https://doi.org/10.1056/NEJMoa1607303>
- Fischer, K. R., Durrans, A., Lee, S., Sheng, J., Li, F., Wong, S. T. C., Choi, H., El Rayes, T., Ryu, S., Troeger, J., Schwabe, R. F., Vahdat, L. T., Altorki, N. K., Mittal, V., & Gao, D. (2015). Epithelial-to-mesenchymal transition is not required for lung metastasis but contributes to chemoresistance. *Nature*, 527(7579), 472–476. <https://doi.org/10.1038/nature15748>
- Folkman, J. (2002). Role of angiogenesis in tumor growth and metastasis. *Seminars in Oncology*, 29(6 Suppl 16), 15–18. <https://doi.org/10.1053/sonc.2002.37263>
- Formisano, L., Lu, Y., Servetto, A., Hanker, A. B., Jansen, V. M., Bauer, J. A., Sudhan, D. R., Guerrero-Zotano, A. L., Croessmann, S., Guo, Y., Ericsson, P. G., Lee, K., Nixon, M. J., Schwarz, L. J., Sanders, M. E., Dugger, T. C., Cruz, M. R., Behdad, A., Cristofanilli, M., ... Arteaga, C. L. (2019). Aberrant FGFR signaling mediates resistance to CDK4/6 inhibitors in ER+ breast cancer. *Nature Communications*, 10(1), 1373. <https://doi.org/10.1038/s41467-019-09068-2>
- Förster, C., Mäkela, S., Wärrri, A., Kietz, S., Becker, D., Hultenby, K., Warner, M., & Gustafsson, J.-A. (2002). Involvement of estrogen receptor beta in terminal differentiation of mammary gland epithelium. *Proceedings of the National Academy of Sciences of the United States of America*, 99(24), 15578–15583. <https://doi.org/10.1073/pnas.192561299>
- Frampton, J. E. (2017). Triptorelin: A Review of its Use as an Adjuvant Anticancer Therapy in Early Breast Cancer. *Drugs*, 77(18), 2037–2048. <https://doi.org/10.1007/s40265-017-0849-3>
- Franco, J., Witkiewicz, A. K., & Knudsen, E. S. (2014). CDK4/6 inhibitors have potent activity in combination with pathway selective therapeutic agents in models of pancreatic cancer. *Oncotarget*, 5(15), 6512–6525. <https://doi.org/10.18632/oncotarget.2270>
- Friedl, P., & Gilmour, D. (2009). Collective cell migration in morphogenesis, regeneration and cancer. *Nature Reviews. Molecular Cell Biology*, 10(7), 445–457. <https://doi.org/10.1038/nrm2720>

- Fujii, T., Kogawa, T., Dong, W., Sahin, A. A., Moulder, S., Litton, J. K., Tripathy, D., Iwamoto, T., Hunt, K. K., Pusztai, L., Lim, B., Shen, Y., & Ueno, N. T. (2017). Revisiting the definition of estrogen receptor positivity in HER2-negative primary breast cancer. *Annals of Oncology: Official Journal of the European Society for Medical Oncology*, 28(10), 2420–2428. <https://doi.org/10.1093/annonc/mdx397>
- Gao, J., Aksoy, B. A., Dogrusoz, U., Dresdner, G., Gross, B., Sumer, S. O., Sun, Y., Jacobsen, A., Sinha, R., Larsson, E., Cerami, E., Sander, C., & Schultz, N. (2013). Integrative analysis of complex cancer genomics and clinical profiles using the cBioPortal. *Science Signaling*, 6(269), pl1. <https://doi.org/10.1126/scisignal.2004088>
- Gao, J. J., Cheng, J., Bloomquist, E., Sanchez, J., Wedam, S. B., Singh, H., Amiri-Kordestani, L., Ibrahim, A., Sridhara, R., Goldberg, K. B., Theoret, M. R., Kluetz, P. G., Blumenthal, G. M., Pazdur, R., Beaver, J. A., & Prowell, T. M. (2020). CDK4/6 inhibitor treatment for patients with hormone receptor-positive, HER2-negative, advanced or metastatic breast cancer: a US Food and Drug Administration pooled analysis. *The Lancet. Oncology*, 21(2), 250–260. [https://doi.org/10.1016/S1470-2045\(19\)30804-6](https://doi.org/10.1016/S1470-2045(19)30804-6)
- Garcia-Mayea, Y., Mir, C., Carballo, L., Castellvi, J., Temprana-Salvador, J., Lorente, J., Benavente, S., García-Pedrero, J. M., Allonca, E., Rodrigo, J. P., & LLeonart, M. E. (2020). TSPAN1: A Novel Protein Involved in Head and Neck Squamous Cell Carcinoma Chemoresistance. *Cancers*, 12(11). <https://doi.org/10.3390/cancers12113269>
- Gawrzak, S., Rinaldi, L., Gregorio, S., Arenas, E. J., Salvador, F., Urosevic, J., Figueras-Puig, C., Rojo, F., Del Barco Barrantes, I., Cejalvo, J. M., Palafox, M., Guiu, M., Berenguer-Llargo, A., Symeonidi, A., Bellmunt, A., Kalafatovic, D., Arnal-Estapé, A., Fernández, E., Müllauer, B., ... Gomis, R. R. (2018). MSK1 regulates luminal cell differentiation and metastatic dormancy in ER(+) breast cancer. *Nature Cell Biology*, 20(2), 211–221. <https://doi.org/10.1038/s41556-017-0021-z>
- Gay, L. J., & Felding-Habermann, B. (2011). Contribution of platelets to tumour metastasis. *Nature Reviews. Cancer*, 11(2), 123–134. <https://doi.org/10.1038/nrc3004>
- Giampieri, S., Manning, C., Hooper, S., Jones, L., Hill, C. S., & Sahai, E. (2009). Localized and reversible TGFbeta signalling switches breast cancer cells from cohesive to single cell motility. *Nature Cell Biology*, 11(11), 1287–1296. <https://doi.org/10.1038/ncb1973>
- Gladden, A. B., & Diehl, J. A. (2003). Cell cycle progression without cyclin E/CDK2: breaking down the walls of dogma. *Cancer Cell*, 4(3), 160–162. [https://doi.org/10.1016/s1535-6108\(03\)00217-4](https://doi.org/10.1016/s1535-6108(03)00217-4)
- Goel, S., DeCristo, M. J., Watt, A. C., BrinJones, H., Sceneay, J., Li, B. B., Khan, N., Ubellacker, J. M., Xie, S., Metzger-Filho, O., Hoog, J., Ellis, M. J., Ma, C. X., Ramm, S., Krop, I. E., Winer, E. P., Roberts, T. M., Kim, H.-J., McAllister, S. S., & Zhao, J. J. (2017). CDK4/6 inhibition triggers anti-tumour immunity. *Nature*, 548(7668), 471–475. <https://doi.org/10.1038/nature23465>
- Goetz, M. P., Toi, M., Campone, M., Sohn, J., Paluch-Shimon, S., Huober, J., Park, I. H., Tredan, O., Chen, S.-C., Manso, L., Freedman, O. C., Garnica Jaliffe, G., Forrester, T.,

- Frenzel, M., Barriga, S., Smith, I. C., Bourayou, N., & Di Leo, A. (2017). MONARCH 3: Abemaciclib As Initial Therapy for Advanced Breast Cancer. *Journal of Clinical Oncology: Official Journal of the American Society of Clinical Oncology*, *35*(32), 3638–3646. <https://doi.org/10.1200/JCO.2017.75.6155>
- Gomis, R. R., & Gawrzak, S. (2017). Tumor cell dormancy. *Molecular Oncology*, *11*(1), 62–78. <https://doi.org/10.1016/j.molonc.2016.09.009>
- Grinda, T., Joyon, N., Lusque, A., Lefèvre, S., Arnould, L., Penault-Llorca, F., Macgrogan, G., Treilleux, I., Vincent-Salomon, A., Haudebourg, J., Maran-Gonzalez, A., Charafe-Jauffret, E., Courtinard, C., Franchet, C., Verrielle, V., Brain, E., Tas, P., Blanc-Fournier, C., Leroux, A., ... Lacroix-Triki, M. (2021). Phenotypic discordance between primary and metastatic breast cancer in the large-scale real-life multicenter French ESME cohort. *Npj Breast Cancer*, *7*(1), 41. <https://doi.org/10.1038/s41523-021-00252-6>
- Guarducci, C., Nardone, A., Feiglin, A., Migliaccio, I., Malorni, L., Bonechi, M., Benelli, M., Di Leo, A., Hodgson, G., Shapiro, G., Brown, M., & Jeselsohn, R. (2019). Abstract PD7-12: Inhibition of CDK7 overcomes resistance to CDK4/6 inhibitors in hormone receptor positive breast cancer cells. *Cancer Research*, *79*(4 Supplement), PD7-12 LP-PD7-12. <https://doi.org/10.1158/1538-7445.SABCS18-PD7-12>
- Guarducci, Cristina, Bonechi, M., Benelli, M., Biagioni, C., Boccalini, G., Romagnoli, D., Verardo, R., Schiff, R., Osborne, C. K., De Angelis, C., Di Leo, A., Malorni, L., & Migliaccio, I. (2018). Cyclin E1 and Rb modulation as common events at time of resistance to palbociclib in hormone receptor-positive breast cancer. *NPJ Breast Cancer*, *4*, 38. <https://doi.org/10.1038/s41523-018-0092-4>
- Guarducci, Cristina, Bonechi, M., Boccalini, G., Benelli, M., Risi, E., Di Leo, A., Malorni, L., & Migliaccio, I. (2017). Mechanisms of Resistance to CDK4/6 Inhibitors in Breast Cancer and Potential Biomarkers of Response. *Breast Care (Basel, Switzerland)*, *12*(5), 304–308. <https://doi.org/10.1159/000484167>
- Gupta, G. P., & Massagué, J. (2006). Cancer metastasis: building a framework. *Cell*, *127*(4), 679–695. <https://doi.org/10.1016/j.cell.2006.11.001>
- Haines, E., Chen, T., Kommajosyula, N., Chen, Z., Herter-Sprie, G. S., Cornell, L., Wong, K.-K., & Shapiro, G. I. (2018). Palbociclib resistance confers dependence on an FGFR-MAP kinase-mTOR-driven pathway in KRAS-mutant non-small cell lung cancer. *Oncotarget*, *9*(60), 31572–31589. <https://doi.org/10.18632/oncotarget.25803>
- Hall, A. (2009). The cytoskeleton and cancer. *Cancer Metastasis Reviews*, *28*(1–2), 5–14. <https://doi.org/10.1007/s10555-008-9166-3>
- Ham, I.-H., Oh, H. J., Jin, H., Bae, C. A., Jeon, S.-M., Choi, K. S., Son, S.-Y., Han, S.-U., Brekken, R. A., Lee, D., & Hur, H. (2019). Targeting interleukin-6 as a strategy to overcome stroma-induced resistance to chemotherapy in gastric cancer. *Molecular Cancer*, *18*(1), 68. <https://doi.org/10.1186/s12943-019-0972-8>
- Hammond, M. E. H., Hayes, D. F., Dowsett, M., Allred, D. C., Hagerty, K. L., Badve, S., Fitzgibbons, P. L., Francis, G., Goldstein, N. S., Hayes, M., Hicks, D. G., Lester, S.,

- Love, R., Mangu, P. B., McShane, L., Miller, K., Osborne, C. K., Paik, S., Perlmutter, J., ... Wolff, A. C. (2010). American Society of Clinical Oncology/College Of American Pathologists guideline recommendations for immunohistochemical testing of estrogen and progesterone receptors in breast cancer. *Journal of Clinical Oncology: Official Journal of the American Society of Clinical Oncology*, 28(16), 2784–2795. <https://doi.org/10.1200/JCO.2009.25.6529>
- Haricharan, S., Punturi, N., Singh, P., Holloway, K. R., Anurag, M., Schmelz, J., Schmidt, C., Lei, J. T., Suman, V., Hunt, K., Olson, J. A. J., Hoog, J., Li, S., Huang, S., Edwards, D. P., Kavuri, S. M., Bainbridge, M. N., Ma, C. X., & Ellis, M. J. (2017). Loss of MutL Disrupts CHK2-Dependent Cell-Cycle Control through CDK4/6 to Promote Intrinsic Endocrine Therapy Resistance in Primary Breast Cancer. *Cancer Discovery*, 7(10), 1168–1183. <https://doi.org/10.1158/2159-8290.CD-16-1179>
- Harrell, J. C., Prat, A., Parker, J. S., Fan, C., He, X., Carey, L., Anders, C., Ewend, M., & Perou, C. M. (2012). Genomic analysis identifies unique signatures predictive of brain, lung, and liver relapse. *Breast Cancer Research and Treatment*, 132(2), 523–535. <https://doi.org/10.1007/s10549-011-1619-7>
- Harris, L. N., Ismaila, N., McShane, L. M., Andre, F., Collyar, D. E., Gonzalez-Angulo, A. M., Hammond, E. H., Kuderer, N. M., Liu, M. C., Mennel, R. G., Van Poznak, C., Bast, R. C., & Hayes, D. F. (2016). Use of Biomarkers to Guide Decisions on Adjuvant Systemic Therapy for Women With Early-Stage Invasive Breast Cancer: American Society of Clinical Oncology Clinical Practice Guideline. *Journal of Clinical Oncology: Official Journal of the American Society of Clinical Oncology*, 34(10), 1134–1150. <https://doi.org/10.1200/JCO.2015.65.2289>
- He, X., & Xu, C. (2020). Immune checkpoint signaling and cancer immunotherapy. *Cell Research*, 30(8), 660–669. <https://doi.org/10.1038/s41422-020-0343-4>
- Helsten, T., Elkin, S., Arthur, E., Tomson, B. N., Carter, J., & Kurzrock, R. (2016). The FGFR Landscape in Cancer: Analysis of 4,853 Tumors by Next-Generation Sequencing. *Clinical Cancer Research*, 22(1), 259 LP – 267. <https://doi.org/10.1158/1078-0432.CCR-14-3212>
- Hennighausen, L., & Robinson, G. W. (1998). Think globally, act locally: the making of a mouse mammary gland. *Genes & Development*, 12(4), 449–455. <https://doi.org/10.1101/gad.12.4.449>
- Hennighausen, Lothar, & Robinson, G. W. (2005). Information networks in the mammary gland. *Nature Reviews. Molecular Cell Biology*, 6(9), 715–725. <https://doi.org/10.1038/nrm1714>
- Herrera-Abreu, M. T., Palafox, M., Asghar, U., Rivas, M. A., Cutts, R. J., Garcia-Murillas, I., Pearson, A., Guzman, M., Rodriguez, O., Grueso, J., Bellet, M., Cortés, J., Elliott, R., Pancholi, S., Lord, C. J., Baselga, J., Dowsett, M., Martin, L.-A., Turner, N. C., & Serra, V. (2016). Early Adaptation and Acquired Resistance to CDK4/6 Inhibition in Estrogen Receptor–Positive Breast Cancer. *Cancer Research*, 76(8), 2301 LP – 2313. <https://doi.org/10.1158/0008-5472.CAN-15-0728>
- Hess, K. R., Pusztai, L., Buzdar, A. U., & Hortobagyi, G. N. (2003). Estrogen receptors and

- distinct patterns of breast cancer relapse. *Breast Cancer Research and Treatment*, 78(1), 105–118. <https://doi.org/10.1023/a:1022166517963>
- Hinck, L., & Silberstein, G. B. (2005). Key stages in mammary gland development: the mammary end bud as a motile organ. *Breast Cancer Research: BCR*, 7(6), 245–251. <https://doi.org/10.1186/bcr1331>
- Hortobagyi, G. N., Stemmer, S. M., Burris, H. A., Yap, Y. S., Sonke, G. S., Paluch-Shimon, S., Campone, M., Petrakova, K., Blackwell, K. L., Winer, E. P., Janni, W., Verma, S., Conte, P., Arteaga, C. L., Cameron, D. A., Mondal, S., Su, F., Miller, M., Elmeliegy, M., ... O'Shaughnessy, J. (2018). Updated results from MONALEESA-2, a phase III trial of first-line ribociclib plus letrozole versus placebo plus letrozole in hormone receptor-positive, HER2-negative advanced breast cancer. *Annals of Oncology: Official Journal of the European Society for Medical Oncology*, 29(7), 1541–1547. <https://doi.org/10.1093/annonc/mdy155>
- Howell, A., Anderson, A. S., Clarke, R. B., Duffy, S. W., Evans, D. G., Garcia-Closas, M., Gescher, A. J., Key, T. J., Saxton, J. M., & Harvie, M. N. (2014). Risk determination and prevention of breast cancer. *Breast Cancer Research: BCR*, 16(5), 446. <https://doi.org/10.1186/s13058-014-0446-2>
- Howlader, N., Forjaz, G., Mooradian, M. J., Meza, R., Kong, C. Y., Cronin, K. A., Mariotto, A. B., Lowy, D. R., & Feuer, E. J. (2020). The Effect of Advances in Lung-Cancer Treatment on Population Mortality. *The New England Journal of Medicine*, 383(7), 640–649. <https://doi.org/10.1056/NEJMoa1916623>
- Huang, D. W., Sherman, B. T., & Lempicki, R. A. (2009). Systematic and integrative analysis of large gene lists using DAVID bioinformatics resources. *Nature Protocols*, 4(1), 44–57. <https://doi.org/10.1038/nprot.2008.211>
- Huang, J., Zhou, Y., Thomas, G. S., Gu, Z., Yang, Y., Xu, H., Tricot, G., & Zhan, F. (2015). NEDD8 Inhibition Overcomes CKS1B-Induced Drug Resistance by Upregulation of p21 in Multiple Myeloma. *Clinical Cancer Research: An Official Journal of the American Association for Cancer Research*, 21(24), 5532–5542. <https://doi.org/10.1158/1078-0432.CCR-15-0254>
- Huerta-Reyes, M., Maya-Núñez, G., Pérez-Solis, M. A., López-Muñoz, E., Guillén, N., Olivo-Marin, J.-C., & Aguilar-Rojas, A. (2019). Treatment of Breast Cancer With Gonadotropin-Releasing Hormone Analogs. *Frontiers in Oncology*, 9, 943. <https://doi.org/10.3389/fonc.2019.00943>
- Hurvitz, S. A., Martin, M., Press, M. F., Chan, D., Fernandez-Abad, M., Petru, E., Rostorfer, R., Guarneri, V., Huang, C.-S., Barriga, S., Wijayawardana, S., Brahmachary, M., Ebert, P. J., Hossain, A., Liu, J., Abel, A., Aggarwal, A., Jansen, V. M., & Slamon, D. J. (2020). Potent Cell-Cycle Inhibition and Upregulation of Immune Response with Abemaciclib and Anastrozole in neoMONARCH, Phase II Neoadjuvant Study in HR(+)/HER2(-) Breast Cancer. *Clinical Cancer Research: An Official Journal of the American Association for Cancer Research*, 26(3), 566–580. <https://doi.org/10.1158/1078-0432.CCR-19-1425>
- Iida, M., Nakamura, M., Tokuda, E., Niwa, T., Ishida, T., & Hayashi, S.-I. (2018). Abstract P6-04-02: CDK6 might be a key factor for efficacy of CDK4/6 inhibitor and the

- hormone sensitivity following acquired resistance. *Cancer Research*, 78(4 Supplement), P6-04-02 LP-P6-04-02. <https://doi.org/10.1158/1538-7445.SABCS17-P6-04-02>
- Iida, Masafumi, Toyosawa, D., Nakamura, M., Tsuboi, K., Tokuda, E., Niwa, T., Ishida, T., & Hayashi, S.-I. (2020). Decreased ER dependency after acquired resistance to CDK4/6 inhibitors. *Breast Cancer (Tokyo, Japan)*, 27(5), 963–972. <https://doi.org/10.1007/s12282-020-01090-3>
- Janku, F., Yap, T. A., & Meric-Bernstam, F. (2018). Targeting the PI3K pathway in cancer: are we making headway? *Nature Reviews. Clinical Oncology*, 15(5), 273–291. <https://doi.org/10.1038/nrclinonc.2018.28>
- Jansen, V. M., Bhola, N. E., Bauer, J. A., Formisano, L., Lee, K.-M., Hutchinson, K. E., Witkiewicz, A. K., Moore, P. D., Estrada, M. V., Sánchez, V., Ericsson, P. G., Sanders, M. E., Pohlmann, P. R., Pishvaian, M. J., Riddle, D. A., Dugger, T. C., Wei, W., Knudsen, E. S., & Arteaga, C. L. (2017). Kinome-Wide RNA Interference Screen Reveals a Role for PDK1 in Acquired Resistance to CDK4/6 Inhibition in ER-Positive Breast Cancer. *Cancer Research*, 77(9), 2488 LP – 2499. <https://doi.org/10.1158/0008-5472.CAN-16-2653>
- Johnson, J., Thijssen, B., McDermott, U., Garnett, M., Wessels, L. F. A., & Bernards, R. (2016). Targeting the RB-E2F pathway in breast cancer. *Oncogene*, 35(37), 4829–4835. <https://doi.org/10.1038/onc.2016.32>
- Joyce, J. A., & Pollard, J. W. (2009). Microenvironmental regulation of metastasis. *Nature Reviews. Cancer*, 9(4), 239–252. <https://doi.org/10.1038/nrc2618>
- Kalluri, R., & Zeisberg, M. (2006). Fibroblasts in cancer. *Nature Reviews. Cancer*, 6(5), 392–401. <https://doi.org/10.1038/nrc1877>
- Kang, Y., Siegel, P. M., Shu, W., Drobnjak, M., Kakonen, S. M., Cordon-Cardo, C., Guise, T. A., & Massagué, J. (2003). A multigenic program mediating breast cancer metastasis to bone. *Cancer Cell*, 3(6), 537–549. [https://doi.org/10.1016/s1535-6108\(03\)00132-6](https://doi.org/10.1016/s1535-6108(03)00132-6)
- Karagiannis, G. S., Condeelis, J. S., & Oktay, M. H. (2018). Chemotherapy-induced metastasis: mechanisms and translational opportunities. *Clinical & Experimental Metastasis*, 35(4), 269–284. <https://doi.org/10.1007/s10585-017-9870-x>
- Katoh, M. (2019). Fibroblast growth factor receptors as treatment targets in clinical oncology. *Nature Reviews Clinical Oncology*, 16(2), 105–122. <https://doi.org/10.1038/s41571-018-0115-y>
- Kennecke, H., Yerushalmi, R., Woods, R., Cheang, M. C. U., Voduc, D., Speers, C. H., Nielsen, T. O., & Gelmon, K. (2010). Metastatic behavior of breast cancer subtypes. *Journal of Clinical Oncology : Official Journal of the American Society of Clinical Oncology*, 28(20), 3271–3277. <https://doi.org/10.1200/JCO.2009.25.9820>
- Kent, L. N., & Leone, G. (2019). The broken cycle: E2F dysfunction in cancer. *Nature Reviews. Cancer*, 19(6), 326–338. <https://doi.org/10.1038/s41568-019-0143-7>
- Kessenbrock, K., Plaks, V., & Werb, Z. (2010). Matrix metalloproteinases: regulators of the

- tumor microenvironment. *Cell*, 141(1), 52–67.
<https://doi.org/10.1016/j.cell.2010.03.015>
- Kim, D. I., Jensen, S. C., Noble, K. A., Kc, B., Roux, K. H., Motamedchaboki, K., & Roux, K. J. (2016). An improved smaller biotin ligase for BioID proximity labeling. *Molecular Biology of the Cell*, 27(8), 1188–1196. <https://doi.org/10.1091/mbc.E15-12-0844>
- Kleinberg, D. L. (1998). Role of IGF-I in normal mammary development. *Breast Cancer Research and Treatment*, 47(3), 201–208. <https://doi.org/10.1023/a:1005998832636>
- Knudsen, E. S., Kumarasamy, V., Ruiz, A., Sivinski, J., Chung, S., Grant, A., Vail, P., Chauhan, S. S., Jie, T., Riall, T. S., & Witkiewicz, A. K. (2019). Cell cycle plasticity driven by MTOR signaling: integral resistance to CDK4/6 inhibition in patient-derived models of pancreatic cancer. *Oncogene*, 38(18), 3355–3370. <https://doi.org/10.1038/s41388-018-0650-0>
- Kollmann, K., Heller, G., Schneckenleithner, C., Warsch, W., Scheicher, R., Ott, R. G., Schäfer, M., Fajmann, S., Schleder, M., Schiefer, A.-I., Reichart, U., Mayerhofer, M., Hoeller, C., Zöchbauer-Müller, S., Kerjaschki, D., Bock, C., Kenner, L., Hoefler, G., Freissmuth, M., ... Sexl, V. (2013). A kinase-independent function of CDK6 links the cell cycle to tumor angiogenesis. *Cancer Cell*, 24(2), 167–181. <https://doi.org/10.1016/j.ccr.2013.07.012>
- Kouhara, H., Hadari, Y. R., Spivak-Kroizman, T., Schilling, J., Bar-Sagi, D., Lax, I., & Schlessinger, J. (1997). A lipid-anchored Grb2-binding protein that links FGF-receptor activation to the Ras/MAPK signaling pathway. *Cell*, 89(5), 693–702. [https://doi.org/10.1016/s0092-8674\(00\)80252-4](https://doi.org/10.1016/s0092-8674(00)80252-4)
- Krook, M. A., Reeser, J. W., Ernst, G., Barker, H., Wilberding, M., Li, G., Chen, H.-Z., & Roychowdhury, S. (2021). Fibroblast growth factor receptors in cancer: genetic alterations, diagnostics, therapeutic targets and mechanisms of resistance. *British Journal of Cancer*, 124(5), 880–892. <https://doi.org/10.1038/s41416-020-01157-0>
- Kuchenbaecker, K. B., Hopper, J. L., Barnes, D. R., Phillips, K.-A., Mooij, T. M., Roos-Blom, M.-J., Jervis, S., van Leeuwen, F. E., Milne, R. L., Andrieu, N., Goldgar, D. E., Terry, M. B., Rookus, M. A., Easton, D. F., Antoniou, A. C., & Consortium, and the B. and B. C. (2017). Risks of Breast, Ovarian, and Contralateral Breast Cancer for BRCA1 and BRCA2 Mutation Carriers. *JAMA*, 317(23), 2402–2416. <https://doi.org/10.1001/jama.2017.7112>
- Kunwor, R., Baniya, R., & Abu-Khalaf, M. M. (2020). Meta-analysis of cyclin-dependent kinase (CDK) 4/6 inhibitors with endocrine therapy versus endocrine therapy alone on progression-free survival (PFS) and overall survival (OS) for metastatic breast cancer (MBC). *Journal of Clinical Oncology*, 38(15_suppl), 1060. https://doi.org/10.1200/JCO.2020.38.15_suppl.1060
- Labelle, M., Begum, S., & Hynes, R. O. (2011). Direct signaling between platelets and cancer cells induces an epithelial-mesenchymal-like transition and promotes metastasis. *Cancer Cell*, 20(5), 576–590. <https://doi.org/10.1016/j.ccr.2011.09.009>
- Laroche-Clary, A., Chaire, V., Algeo, M.-P., Derieppe, M.-A., Loarer, F. L., & Italiano, A.

- (2017). Combined targeting of MDM2 and CDK4 is synergistic in dedifferentiated liposarcomas. *Journal of Hematology & Oncology*, 10(1), 123. <https://doi.org/10.1186/s13045-017-0482-3>
- Le Gal, K., Ibrahim, M. X., Wiel, C., Sayin, V. I., Akula, M. K., Karlsson, C., Dalin, M. G., Akyürek, L. M., Lindahl, P., Nilsson, J., & Bergo, M. O. (2015). Antioxidants can increase melanoma metastasis in mice. *Science Translational Medicine*, 7(308), 308re8. <https://doi.org/10.1126/scitranslmed.aad3740>
- Lewis Phillips, G. D., Li, G., Dugger, D. L., Crocker, L. M., Parsons, K. L., Mai, E., Blättler, W. A., Lambert, J. M., Chari, R. V. J., Lutz, R. J., Wong, W. L. T., Jacobson, F. S., Koeppen, H., Schwall, R. H., Kenkare-Mitra, S. R., Spencer, S. D., & Sliwkowski, M. X. (2008). Targeting HER2-positive breast cancer with trastuzumab-DM1, an antibody-cytotoxic drug conjugate. *Cancer Research*, 68(22), 9280–9290. <https://doi.org/10.1158/0008-5472.CAN-08-1776>
- Li, J., Huo, X., Zhao, F., Ren, D., Ahmad, R., Yuan, X., Du, F., & Zhao, J. (2020). Association of Cyclin-Dependent Kinases 4 and 6 Inhibitors With Survival in Patients With Hormone Receptor-Positive Metastatic Breast Cancer: A Systematic Review and Meta-analysis. *JAMA Network Open*, 3(10), e2020312. <https://doi.org/10.1001/jamanetworkopen.2020.20312>
- Li, W., Köster, J., Xu, H., Chen, C.-H., Xiao, T., Liu, J. S., Brown, M., & Liu, X. S. (2015). Quality control, modeling, and visualization of CRISPR screens with MAGeCK-VISPR. *Genome Biology*, 16(1), 281. <https://doi.org/10.1186/s13059-015-0843-6>
- Li, W., Xu, H., Xiao, T., Cong, L., Love, M. I., Zhang, F., Irizarry, R. A., Liu, J. S., Brown, M., & Liu, X. S. (2014). MAGeCK enables robust identification of essential genes from genome-scale CRISPR/Cas9 knockout screens. *Genome Biology*, 15(12), 554. <https://doi.org/10.1186/s13059-014-0554-4>
- Liu, F., & Korc, M. (2012). Cdk4/6 inhibition induces epithelial-mesenchymal transition and enhances invasiveness in pancreatic cancer cells. *Molecular Cancer Therapeutics*, 11(10), 2138–2148. <https://doi.org/10.1158/1535-7163.MCT-12-0562>
- Lord, C. J., & Ashworth, A. (2017). PARP inhibitors: Synthetic lethality in the clinic. *Science (New York, N.Y.)*, 355(6330), 1152–1158. <https://doi.org/10.1126/science.aam7344>
- Lu, Z. H., Shvartsman, M. B., Lee, A. Y., Shao, J. M., Murray, M. M., Kladney, R. D., Fan, D., Krajewski, S., Chiang, G. G., Mills, G. B., & Arbeit, J. M. (2010). Mammalian Target of Rapamycin Activator RHEB Is Frequently Overexpressed in Human Carcinomas and Is Critical and Sufficient for Skin Epithelial Carcinogenesis. *Cancer Research*, 70(8), 3287 LP – 3298. <https://doi.org/10.1158/0008-5472.CAN-09-3467>
- Luzzi, K. J., MacDonald, I. C., Schmidt, E. E., Kerkvliet, N., Morris, V. L., Chambers, A. F., & Groom, A. C. (1998). Multistep nature of metastatic inefficiency: dormancy of solitary cells after successful extravasation and limited survival of early micrometastases. *The American Journal of Pathology*, 153(3), 865–873. [https://doi.org/10.1016/S0002-9440\(10\)65628-3](https://doi.org/10.1016/S0002-9440(10)65628-3)
- Ma, C. X., Gao, F., Luo, J., Northfelt, D. W., Goetz, M., Forero, A., Hoog, J., Naughton,

- M., Ademuyiwa, F., Suresh, R., Anderson, K. S., Margenthaler, J., Aft, R., Hobday, T., Moynihan, T., Gillanders, W., Cyr, A., Eberlein, T. J., Hieken, T., ... Ellis, M. J. (2017). NeoPalAna: Neoadjuvant Palbociclib, a Cyclin-Dependent Kinase 4/6 Inhibitor, and Anastrozole for Clinical Stage 2 or 3 Estrogen Receptor-Positive Breast Cancer. *Clinical Cancer Research: An Official Journal of the American Association for Cancer Research*, 23(15), 4055–4065. <https://doi.org/10.1158/1078-0432.CCR-16-3206>
- Makino, H., Seki, S., Yahara, Y., Shiozawa, S., Aikawa, Y., Motomura, H., Nogami, M., Watanabe, K., Sainoh, T., Ito, H., Tsumaki, N., Kawaguchi, Y., Yamazaki, M., & Kimura, T. (2017). A selective inhibition of c-Fos/activator protein-1 as a potential therapeutic target for intervertebral disc degeneration and associated pain. *Scientific Reports*, 7(1), 16983. <https://doi.org/10.1038/s41598-017-17289-y>
- Malanchi, I., Santamaria-Martínez, A., Susanto, E., Peng, H., Lehr, H.-A., Delaloye, J.-F., & Huelsken, J. (2011). Interactions between cancer stem cells and their niche govern metastatic colonization. *Nature*, 481(7379), 85–89. <https://doi.org/10.1038/nature10694>
- Malladi, S., Macalinao, D. G., Jin, X., He, L., Basnet, H., Zou, Y., de Stanchina, E., & Massagué, J. (2016). Metastatic Latency and Immune Evasion through Autocrine Inhibition of WNT. *Cell*, 165(1), 45–60. <https://doi.org/10.1016/j.cell.2016.02.025>
- Malorni, L., Piazza, S., Ciani, Y., Guarducci, C., Bonechi, M., Biagioni, C., Hart, C. D., Verardo, R., Di Leo, A., & Migliaccio, I. (2016). A gene expression signature of retinoblastoma loss-of-function is a predictive biomarker of resistance to palbociclib in breast cancer cell lines and is prognostic in patients with ER positive early breast cancer. *Oncotarget*, 7(42), 68012–68022. <https://doi.org/10.18632/oncotarget.12010>
- Mani, S. A., Guo, W., Liao, M.-J., Eaton, E. N., Ayyanan, A., Zhou, A. Y., Brooks, M., Reinhard, F., Zhang, C. C., Shipitsin, M., Campbell, L. L., Polyak, K., Brisken, C., Yang, J., & Weinberg, R. A. (2008). The epithelial-mesenchymal transition generates cells with properties of stem cells. *Cell*, 133(4), 704–715. <https://doi.org/10.1016/j.cell.2008.03.027>
- Mantovani, A., Allavena, P., Sica, A., & Balkwill, F. (2008). Cancer-related inflammation. *Nature*, 454(7203), 436–444. <https://doi.org/10.1038/nature07205>
- Mao, P., Cohen, O., Kowalski, K. J., Kusiel, J. G., Buendia-Buendia, J. E., Cuoco, M. S., Exman, P., Wander, S. A., Waks, A. G., Nayar, U., Chung, J., Freeman, S., Rozenblatt-Rosen, O., Miller, V. A., Piccioni, F., Root, D. E., Regev, A., Winer, E. P., Lin, N. U., & Wagle, N. (2020). Acquired FGFR and FGF Alterations Confer Resistance to Estrogen Receptor (ER) Targeted Therapy in ER+ Metastatic Breast Cancer. *Clinical Cancer Research*, 26(22), 5974 LP – 5989. <https://doi.org/10.1158/1078-0432.CCR-19-3958>
- Martin, L.-A., Pancholi, S., Ribas, R., Gao, Q., Simigdala, N., Nikitorowicz-Buniak, J., Johnston, S. R., & Dowsett, M. (2017). Abstract P3-03-09: Resistance to palbociclib depends on multiple targetable mechanisms highlighting the potential of drug holidays and drug switching to improve therapeutic outcome. *Cancer Research*, 77(4 Supplement), P3-03-09 LP-P3-03–09. <https://doi.org/10.1158/1538-7445.SABCS16-P3-03-09>

- Massagué, J., & Obenauf, A. C. (2016). Metastatic colonization by circulating tumour cells. *Nature*, *529*(7586), 298–306. <https://doi.org/10.1038/nature17038>
- Matheson, C. J., Backos, D. S., & Reigan, P. (2016). Targeting WEE1 Kinase in Cancer. *Trends in Pharmacological Sciences*, *37*(10), 872–881. <https://doi.org/10.1016/j.tips.2016.06.006>
- Matsen, C. B., & Neumayer, L. A. (2013). Breast cancer: a review for the general surgeon. *JAMA Surgery*, *148*(10), 971–979. <https://doi.org/10.1001/jamasurg.2013.3393>
- Mauri, D., Pavlidis, N., Polyzos, N. P., & Ioannidis, J. P. A. (2006). Survival with aromatase inhibitors and inactivators versus standard hormonal therapy in advanced breast cancer: meta-analysis. *Journal of the National Cancer Institute*, *98*(18), 1285–1291. <https://doi.org/10.1093/jnci/djj357>
- McAllister, S. S., & Weinberg, R. A. (2014). The tumour-induced systemic environment as a critical regulator of cancer progression and metastasis. *Nature Cell Biology*, *16*(8), 717–727. <https://doi.org/10.1038/ncb3015>
- McCartney, A., Migliaccio, I., Bonechi, M., Biagioni, C., Romagnoli, D., De Luca, F., Galardi, F., Risi, E., De Santo, I., Benelli, M., Malorni, L., & Di Leo, A. (2019). Mechanisms of Resistance to CDK4/6 Inhibitors: Potential Implications and Biomarkers for Clinical Practice. *Frontiers in Oncology*, *9*, 666. <https://doi.org/10.3389/fonc.2019.00666>
- McConnell, B. B., Gregory, F. J., Stott, F. J., Hara, E., & Peters, G. (1999). Induced expression of p16(INK4a) inhibits both CDK4- and CDK2-associated kinase activity by reassortment of cyclin-CDK-inhibitor complexes. *Molecular and Cellular Biology*, *19*(3), 1981–1989. <https://doi.org/10.1128/MCB.19.3.1981>
- Meloche, S., & Pouységur, J. (2007). The ERK1/2 mitogen-activated protein kinase pathway as a master regulator of the G1- to S-phase transition. *Oncogene*, *26*(22), 3227–3239. <https://doi.org/10.1038/sj.onc.1210414>
- Meric-Bernstam, F., Frampton, G. M., Ferrer-Lozano, J., Yelensky, R., Pérez-Fidalgo, J. A., Wang, Y., Palmer, G. A., Ross, J. S., Miller, V. A., Su, X., Eroles, P., Barrera, J. A., Burgues, O., Lluch, A. M., Zheng, X., Sahin, A., Stephens, P. J., Mills, G. B., Cronin, M. T., & Gonzalez-Angulo, A. M. (2014). Concordance of genomic alterations between primary and recurrent breast cancer. *Molecular Cancer Therapeutics*, *13*(5), 1382–1389. <https://doi.org/10.1158/1535-7163.MCT-13-0482>
- Michaloglou, C., Crafter, C., Siersbaek, R., Delpuech, O., Curwen, J. O., Carnevalli, L. S., Staniszewska, A. D., Polanska, U. M., Cheraghchi-Bashi, A., Lawson, M., Chernukhin, I., McEwen, R., Carroll, J. S., & Cosulich, S. C. (2018). Combined Inhibition of mTOR and CDK4/6 Is Required for Optimal Blockade of E2F Function and Long-term Growth Inhibition in Estrogen Receptor-positive Breast Cancer. *Molecular Cancer Therapeutics*, *17*(5), 908–920. <https://doi.org/10.1158/1535-7163.MCT-17-0537>
- Miller, T. W., Balko, J. M., & Arteaga, C. L. (2011). Phosphatidylinositol 3-kinase and antiestrogen resistance in breast cancer. *Journal of Clinical Oncology: Official Journal of the American Society of Clinical Oncology*, *29*(33), 4452–4461. <https://doi.org/10.1200/JCO.2010.34.4879>

- Miller, T. W., Hennessy, B. T., González-Angulo, A. M., Fox, E. M., Mills, G. B., Chen, H., Higham, C., García-Echeverría, C., Shyr, Y., & Arteaga, C. L. (2010). Hyperactivation of phosphatidylinositol-3 kinase promotes escape from hormone dependence in estrogen receptor-positive human breast cancer. *The Journal of Clinical Investigation*, *120*(7), 2406–2413. <https://doi.org/10.1172/JCI41680>
- Minn, A. J., Gupta, G. P., Siegel, P. M., Bos, P. D., Shu, W., Giri, D. D., Viale, A., Olshen, A. B., Gerald, W. L., & Massagué, J. (2005). Genes that mediate breast cancer metastasis to lung. *Nature*, *436*(7050), 518–524. <https://doi.org/10.1038/nature03799>
- Mojica, F. J. M., Díez-Villaseñor, C., García-Martínez, J., & Soria, E. (2005). Intervening sequences of regularly spaced prokaryotic repeats derive from foreign genetic elements. *Journal of Molecular Evolution*, *60*(2), 174–182. <https://doi.org/10.1007/s00239-004-0046-3>
- Morales, M., Arenas, E. J., Urosevic, J., Guiu, M., Fernández, E., Planet, E., Fenwick, R. B., Fernández-Ruiz, S., Salvatella, X., Reverter, D., Carracedo, A., Massagué, J., & Gomis, R. R. (2014). RARRES3 suppresses breast cancer lung metastasis by regulating adhesion and differentiation. *EMBO Molecular Medicine*, *6*(7), 865–881. <https://doi.org/10.15252/emmm.201303675>
- Morris, L., Allen, K. E., & La Thangue, N. B. (2000). Regulation of E2F transcription by cyclin E-Cdk2 kinase mediated through p300/CBP co-activators. *Nature Cell Biology*, *2*(4), 232–239. <https://doi.org/10.1038/35008660>
- Mueller, S. O., Clark, J. A., Myers, P. H., & Korach, K. S. (2002). Mammary gland development in adult mice requires epithelial and stromal estrogen receptor alpha. *Endocrinology*, *143*(6), 2357–2365. <https://doi.org/10.1210/endo.143.6.8836>
- Munkley, J., McClurg, U. L., Livermore, K. E., Ehrmann, I., Knight, B., McCullagh, P., McGrath, J., Crundwell, M., Harries, L. W., Leung, H. Y., Mills, I. G., Robson, C. N., Rajan, P., & Elliott, D. J. (2017). The cancer-associated cell migration protein TSPAN1 is under control of androgens and its upregulation increases prostate cancer cell migration. *Scientific Reports*, *7*(1), 5249. <https://doi.org/10.1038/s41598-017-05489-5>
- Murphy, B. L., Day, C. N., Hoskin, T. L., Habermann, E. B., & Boughey, J. C. (2018). Neoadjuvant Chemotherapy Use in Breast Cancer is Greatest in Excellent Responders: Triple-Negative and HER2+ Subtypes. *Annals of Surgical Oncology*, *25*(8), 2241–2248. <https://doi.org/10.1245/s10434-018-6531-5>
- Narod, S. A., & Foulkes, W. D. (2004). BRCA1 and BRCA2: 1994 and beyond. *Nature Reviews. Cancer*, *4*(9), 665–676. <https://doi.org/10.1038/nrc1431>
- Navid, S., Fan, C., O Flores-Villanueva, P., Generali, D., & Li, Y. (2020). The Fibroblast Growth Factor Receptors in Breast Cancer: from Oncogenesis to Better Treatments. *International Journal of Molecular Sciences*, *21*(6). <https://doi.org/10.3390/ijms21062011>
- Neoplastic Diseases: A Treatise on Tumours. By James Ewing, A.M., M.D., Sc.D., Professor of Pathology at Cornell University Medical College, N.Y.; Pathologist to the Memorial Hospital. Third edition. Royal 8vo. Pp. 1127, with 546 illustrations. 1928. Phil. (1928). *BJS (British Journal of Surgery)*, *16*(61), 174–175.

<https://doi.org/https://doi.org/10.1002/bjs.1800166126>

- Nguyen, D. X., Bos, P. D., & Massagué, J. (2009). Metastasis: from dissemination to organ-specific colonization. *Nature Reviews. Cancer*, 9(4), 274–284. <https://doi.org/10.1038/nrc2622>
- Niavarani, S.-R., Lawson, C., Boudaud, M., Simard, C., & Tai, L.-H. (2020). Oncolytic vesicular stomatitis virus-based cellular vaccine improves triple-negative breast cancer outcome by enhancing natural killer and CD8(+) T-cell functionality. *Journal for Immunotherapy of Cancer*, 8(1). <https://doi.org/10.1136/jitc-2019-000465>
- O’Leary, B., Cutts, R., Huang, X., Hrebien, S., Liu, Y., Garcia-Murillas, I., Andre, F., Loi, S., Loibl, S., Cristofanilli, M., Bartlett, C. H., & Turner, N. C. (2019). Genomic markers of early progression on fulvestrant with or without palbociclib for ER+ advanced breast cancer in the PALOMA-3 trial. *Journal of Clinical Oncology*, 37(15_suppl), 1010. https://doi.org/10.1200/JCO.2019.37.15_suppl.1010
- O’Brien, T., Xiao, Y., Ong, C., Daemen, A., & Friedman, L. (2017). Abstract P3-04-24: Identification of preclinical mechanisms driving acquired resistance to selective ERa degraders (SERDs), CDK4/6 inhibitors, or to combinations of both agents. *Cancer Research*, 77(4 Supplement), P3-04-24 LP-P3-04-24. <https://doi.org/10.1158/1538-7445.SABCS16-P3-04-24>
- Obenauf, A. C., & Massagué, J. (2015). Surviving at a Distance: Organ-Specific Metastasis. *Trends in Cancer*, 1(1), 76–91. <https://doi.org/10.1016/j.trecan.2015.07.009>
- Ohtani, K., DeGregori, J., & Nevins, J. R. (1995). Regulation of the cyclin E gene by transcription factor E2F1. *Proceedings of the National Academy of Sciences of the United States of America*, 92(26), 12146–12150. <https://doi.org/10.1073/pnas.92.26.12146>
- Olanich, M. E., Sun, W., Hewitt, S. M., Abdullaev, Z., Pack, S. D., & Barr, F. G. (2015). CDK4 Amplification Reduces Sensitivity to CDK4/6 Inhibition in Fusion-Positive Rhabdomyosarcoma. *Clinical Cancer Research: An Official Journal of the American Association for Cancer Research*, 21(21), 4947–4959. <https://doi.org/10.1158/1078-0432.CCR-14-2955>
- Oskarsson, T., Acharyya, S., Zhang, X. H.-F., Vanharanta, S., Tavazoie, S. F., Morris, P. G., Downey, R. J., Manova-Todorova, K., Brogi, E., & Massagué, J. (2011). Breast cancer cells produce tenascin C as a metastatic niche component to colonize the lungs. *Nature Medicine*, 17(7), 867–874. <https://doi.org/10.1038/nm.2379>
- Pack, C. D., Bommireddy, R., Munoz, L. E., Patel, J. M., Bozeman, E. N., Dey, P., Radhakrishnan, V., Vartabedian, V. F., Venkat, K., Ramachandiran, S., Reddy, S. J. C., & Selvaraj, P. (2020). Tumor membrane-based vaccine immunotherapy in combination with anti-CTLA-4 antibody confers protection against immune checkpoint resistant murine triple-negative breast cancer. *Human Vaccines & Immunotherapeutics*, 16(12), 3184–3193. <https://doi.org/10.1080/21645515.2020.1754691>
- Padua, D., Zhang, X. H.-F., Wang, Q., Nadal, C., Gerald, W. L., Gomis, R. R., & Massagué, J. (2008). TGFbeta primes breast tumors for lung metastasis seeding through angiopoietin-like 4. *Cell*, 133(1), 66–77. <https://doi.org/10.1016/j.cell.2008.01.046>

- Paget, S. (1989). The distribution of secondary growths in cancer of the breast. 1889. *Cancer Metastasis Reviews*, 8(2), 98–101.
- Pancholi, S., Ribas, R., Simigdala, N., Schuster, E., Nikitorowicz-Buniak, J., Ressa, A., Gao, Q., Leal, M. F., Bhamra, A., Thornhill, A., Morisset, L., Montaudon, E., Sourd, L., Fitzpatrick, M., Altelaar, M., Johnston, S. R., Marangoni, E., Dowsett, M., & Martin, L.-A. (2020). Tumour kinome re-wiring governs resistance to palbociclib in oestrogen receptor positive breast cancers, highlighting new therapeutic modalities. *Oncogene*, 39(25), 4781–4797. <https://doi.org/10.1038/s41388-020-1284-6>
- Pandey, K., An, H.-J., Kim, S. K., Lee, S. A., Kim, S., Lim, S. M., Kim, G. M., Sohn, J., & Moon, Y. W. (2019). Molecular mechanisms of resistance to CDK4/6 inhibitors in breast cancer: A review. *International Journal of Cancer*, 145(5), 1179–1188. <https://doi.org/10.1002/ijc.32020>
- Panera, N., Ceccarelli, S., Nobili, V., & Alisi, A. (2015). Targeting FGF19 binding to its receptor system: a novel therapeutic approach for hepatocellular carcinoma. In *Hepatology (Baltimore, Md.)* (Vol. 62, Issue 4, p. 1324). <https://doi.org/10.1002/hep.27741>
- Parker, J. S., Mullins, M., Cheang, M. C. U., Leung, S., Voduc, D., Vickery, T., Davies, S., Fauron, C., He, X., Hu, Z., Quackenbush, J. F., Stijleman, I. J., Palazzo, J., Marron, J. S., Nobel, A. B., Mardis, E., Nielsen, T. O., Ellis, M. J., Perou, C. M., & Bernard, P. S. (2009). Supervised risk predictor of breast cancer based on intrinsic subtypes. *Journal of Clinical Oncology: Official Journal of the American Society of Clinical Oncology*, 27(8), 1160–1167. <https://doi.org/10.1200/JCO.2008.18.1370>
- Paterson, A. H. G., Lucas, P. C., Anderson, S. J., Mamounas, E. P., Brufsky, A., Baez-Diaz, L., King, K. M., Lad, T., Robidoux, A., Finnigan, M., Sampayo, M., Tercero, J. C., Mairet, J. J., Wolff, A. C., Fehrenbacher, L., Wolmark, N., & Gomis, R. R. (2021). MAF Amplification and Adjuvant Clodronate Outcomes in Early-Stage Breast Cancer in NSABP B-34 and Potential Impact on Clinical Practice. *JNCI Cancer Spectrum*, 5(4). <https://doi.org/10.1093/jncics/pkab054>
- Pavlovic, M., Arnal-Estapé, A., Rojo, F., Bellmunt, A., Tarragona, M., Guiu, M., Planet, E., Garcia-Albéniz, X., Morales, M., Urosevic, J., Gawrzak, S., Rovira, A., Prat, A., Nonell, L., Lluch, A., Jean-Mairet, J., Coleman, R., Albanell, J., & Gomis, R. R. (2015). Enhanced MAF Oncogene Expression and Breast Cancer Bone Metastasis. *Journal of the National Cancer Institute*, 107(12), djv256. <https://doi.org/10.1093/jnci/djv256>
- Peinado, H., Alečković, M., Lavotshkin, S., Matei, I., Costa-Silva, B., Moreno-Bueno, G., Hergueta-Redondo, M., Williams, C., García-Santos, G., Ghajar, C., Nitoro-Hoshino, A., Hoffman, C., Badal, K., Garcia, B. A., Callahan, M. K., Yuan, J., Martins, V. R., Skog, J., Kaplan, R. N., ... Lyden, D. (2012). Melanoma exosomes educate bone marrow progenitor cells toward a pro-metastatic phenotype through MET. *Nature Medicine*, 18(6), 883–891. <https://doi.org/10.1038/nm.2753>
- Piezzo, M., Chiodini, P., Riemma, M., Cocco, S., Caputo, R., Cianniello, D., Di Gioia, G., Di Lauro, V., Rella, F. D., Fusco, G., Iodice, G., Nuzzo, F., Pacilio, C., Pensabene, M., & Laurentiis, M. D. (2020). Progression-Free Survival and Overall Survival of CDK 4/6 Inhibitors Plus Endocrine Therapy in Metastatic Breast Cancer: A Systematic

Review and Meta-Analysis. In *International Journal of Molecular Sciences* (Vol. 21, Issue 17). <https://doi.org/10.3390/ijms21176400>

- Polyak, K. (2007). Breast cancer: origins and evolution. *The Journal of Clinical Investigation*, *117*(11), 3155–3163. <https://doi.org/10.1172/JCI33295>
- Prat, A, Ortega, V., Villagrasa, P., Paré, L., Galván, P., Oliveira, M., Nuciforo, P., Lluch, A., Morales, S., Amillano, K., Lopez, R., Gonzalez, R., Manso, L., Martinez, J., Llombart, A., De la Peña, L., Di Cosimo, S., Rubio, I. T., Harbeck, N., ... Cortés, J. (2017). Abstract P1-09-09: Efficacy and gene expression results from SOLTI1007 NEOERIBULIN phase II clinical trial in HER2-negative early breast cancer. *Cancer Research*, *77*(4 Supplement), P1-09-09 LP-P1-09-09. <https://doi.org/10.1158/1538-7445.SABCS16-P1-09-09>
- Prat, A, Parker, J. S., Fan, C., Cheang, M. C. U., Miller, L. D., Bergh, J., Chia, S. K. L., Bernard, P. S., Nielsen, T. O., Ellis, M. J., Carey, L. A., & Perou, C. M. (2012). Concordance among gene expression-based predictors for ER-positive breast cancer treated with adjuvant tamoxifen. *Annals of Oncology: Official Journal of the European Society for Medical Oncology*, *23*(11), 2866–2873. <https://doi.org/10.1093/annonc/mds080>
- Prat, Aleix, Cheang, M. C. U., Galván, P., Nuciforo, P., Paré, L., Adamo, B., Muñoz, M., Viladot, M., Press, M. F., Gagnon, R., Ellis, C., & Johnston, S. (2016). Prognostic Value of Intrinsic Subtypes in Hormone Receptor-Positive Metastatic Breast Cancer Treated With Letrozole With or Without Lapatinib. *JAMA Oncology*, *2*(10), 1287–1294. <https://doi.org/10.1001/jamaoncol.2016.0922>
- Prat, Aleix, Cheang, M. C. U., Martín, M., Parker, J. S., Carrasco, E., Caballero, R., Tyldesley, S., Gelmon, K., Bernard, P. S., Nielsen, T. O., & Perou, C. M. (2013). Prognostic significance of progesterone receptor-positive tumor cells within immunohistochemically defined luminal A breast cancer. *Journal of Clinical Oncology: Official Journal of the American Society of Clinical Oncology*, *31*(2), 203–209. <https://doi.org/10.1200/JCO.2012.43.4134>
- Prat, Aleix, Ellis, M. J., & Perou, C. M. (2011). Practical implications of gene-expression-based assays for breast oncologists. *Nature Reviews. Clinical Oncology*, *9*(1), 48–57. <https://doi.org/10.1038/nrclinonc.2011.178>
- Prat, Aleix, Fan, C., Fernández, A., Hoadley, K. A., Martinello, R., Vidal, M., Viladot, M., Pineda, E., Arance, A., Muñoz, M., Paré, L., Cheang, M. C. U., Adamo, B., & Perou, C. M. (2015). Response and survival of breast cancer intrinsic subtypes following multi-agent neoadjuvant chemotherapy. *BMC Medicine*, *13*, 303. <https://doi.org/10.1186/s12916-015-0540-z>
- Prat, Aleix, Galván, P., Jimenez, B., Buckingham, W., Jeiranian, H. A., Schaper, C., Vidal, M., Álvarez, M., Díaz, S., Ellis, C., Nuciforo, P., Ferree, S., Ribelles, N., Adamo, B., Ramón Y Cajal, S., Peg, V., & Alba, E. (2016). Prediction of Response to Neoadjuvant Chemotherapy Using Core Needle Biopsy Samples with the Prosigna Assay. *Clinical Cancer Research: An Official Journal of the American Association for Cancer Research*, *22*(3), 560–566. <https://doi.org/10.1158/1078-0432.CCR-15-0630>
- Prat, Aleix, Lluch, A., Turnbull, A. K., Dunbier, A. K., Calvo, L., Albanell, J., de la Haba-

- Rodríguez, J., Arcusa, A., Chacón, J. I., Sánchez-Rovira, P., Plazaola, A., Muñoz, M., Paré, L., Parker, J. S., Ribelles, N., Jimenez, B., Bin Aiderus, A. A., Caballero, R., Adamo, B., ... Alba, E. (2017). A PAM50-Based Chemoendocrine Score for Hormone Receptor-Positive Breast Cancer with an Intermediate Risk of Relapse. *Clinical Cancer Research: An Official Journal of the American Association for Cancer Research*, 23(12), 3035–3044. <https://doi.org/10.1158/1078-0432.CCR-16-2092>
- Prat, Aleix, Pineda, E., Adamo, B., Galván, P., Fernández, A., Gaba, L., Díez, M., Viladot, M., Arance, A., & Muñoz, M. (2015). Clinical implications of the intrinsic molecular subtypes of breast cancer. *Breast (Edinburgh, Scotland)*, 24 Suppl 2, S26-35. <https://doi.org/10.1016/j.breast.2015.07.008>
- Prat, Aleix, Saura, C., Pascual, T., Hernando, C., Muñoz, M., Paré, L., González Farré, B., Fernández, P. L., Galván, P., Chic, N., González Farré, X., Oliveira, M., Gil-Gil, M., Arumi, M., Ferrer, N., Montañó, A., Izarzugaza, Y., Llombart-Cussac, A., Bratos, R., ... Gavilá, J. (2020). Ribociclib plus letrozole versus chemotherapy for postmenopausal women with hormone receptor-positive, HER2-negative, luminal B breast cancer (CORALLEEN): an open-label, multicentre, randomised, phase 2 trial. *The Lancet. Oncology*, 21(1), 33–43. [https://doi.org/10.1016/S1470-2045\(19\)30786-7](https://doi.org/10.1016/S1470-2045(19)30786-7)
- Qian, B.-Z., & Pollard, J. W. (2010). Macrophage diversity enhances tumor progression and metastasis. *Cell*, 141(1), 39–51. <https://doi.org/10.1016/j.cell.2010.03.014>
- Rabindran, S. K., Discafani, C. M., Rosfjord, E. C., Baxter, M., Floyd, M. B., Golas, J., Hallett, W. A., Johnson, B. D., Nilakantan, R., Overbeek, E., Reich, M. F., Shen, R., Shi, X., Tsou, H.-R., Wang, Y.-F., & Wissner, A. (2004). Antitumor activity of HKI-272, an orally active, irreversible inhibitor of the HER-2 tyrosine kinase. *Cancer Research*, 64(11), 3958–3965. <https://doi.org/10.1158/0008-5472.CAN-03-2868>
- Razavi, P., dos Anjos, C. H., Brown, D. N., Qing, L., Ping, C., Herbert, J., Colon, J., Liu, D., Mao, M., Norton, L., Scaltriti, M., Solit, D. B., Robson, M. E., Reis-Filho, J. S., Jhaveri, K. L., & Chandarlapaty, S. (2019). Molecular profiling of ER+ metastatic breast cancers to reveal association of genomic alterations with acquired resistance to CDK4/6 inhibitors. *Journal of Clinical Oncology*, 37(15_suppl), 1009. https://doi.org/10.1200/JCO.2019.37.15_suppl.1009
- Rebbeck, T. R., Friebel, T. M., Friedman, E., Hamann, U., Huo, D., Kwong, A., Olah, E., Olopade, O. I., Solano, A. R., Teo, S.-H., Thomassen, M., Weitzel, J. N., Chan, T. L., Couch, F. J., Goldgar, D. E., Kruse, T. A., Palmero, E. I., Park, S. K., Torres, D., ... Nathanson, K. L. (2018). Mutational spectrum in a worldwide study of 29,700 families with BRCA1 or BRCA2 mutations. *Human Mutation*, 39(5), 593–620. <https://doi.org/10.1002/humu.23406>
- Reich, M., Liefeld, T., Gould, J., Lerner, J., Tamayo, P., & Mesirov, J. P. (2006). GenePattern 2.0. In *Nature genetics* (Vol. 38, Issue 5, pp. 500–501). <https://doi.org/10.1038/ng0506-500>
- Rivenbark, A. G., O'Connor, S. M., & Coleman, W. B. (2013). Molecular and cellular heterogeneity in breast cancer: challenges for personalized medicine. *The American Journal of Pathology*, 183(4), 1113–1124. <https://doi.org/10.1016/j.ajpath.2013.08.002>

- Robinson, G. W. (2007). Cooperation of signalling pathways in embryonic mammary gland development. *Nature Reviews. Genetics*, 8(12), 963–972. <https://doi.org/10.1038/nrg2227>
- Romagosa, C., Simonetti, S., López-Vicente, L., Mazo, A., Lleonart, M. E., Castellvi, J., & Ramon y Cajal, S. (2011). p16(Ink4a) overexpression in cancer: a tumor suppressor gene associated with senescence and high-grade tumors. *Oncogene*, 30(18), 2087–2097. <https://doi.org/10.1038/onc.2010.614>
- Roux, K. J., Kim, D. I., Burke, B., & May, D. G. (2018). BioID: A Screen for Protein-Protein Interactions. *Current Protocols in Protein Science*, 91, 19.23.1-19.23.15. <https://doi.org/10.1002/cpps.51>
- Russo, J., & Russo, I. H. (2004). Development of the human breast. *Maturitas*, 49(1), 2–15. <https://doi.org/10.1016/j.maturitas.2004.04.011>
- Salvador, F., Llorente, A., & Gomis, R. R. (2019). From latency to overt bone metastasis in breast cancer: potential for treatment and prevention. *The Journal of Pathology*, 249(1), 6–18. <https://doi.org/10.1002/path.5292>
- Sanjana, N. E., Shalem, O., & Zhang, F. (2014). Improved vectors and genome-wide libraries for CRISPR screening. *Nature Methods*, 11(8), 783–784. <https://doi.org/10.1038/nmeth.3047>
- Saura, C., Oliveira, M., Feng, Y.-H., Dai, M.-S., Chen, S.-W., Hurvitz, S. A., Kim, S.-B., Moy, B., Delalogue, S., Gradishar, W., Masuda, N., Palacova, M., Trudeau, M. E., Mattson, J., Yap, Y. S., Hou, M.-F., De Laurentis, M., Yeh, Y.-M., Chang, H.-T., ... Brufsky, A. (2020). Neratinib Plus Capecitabine Versus Lapatinib Plus Capecitabine in HER2-Positive Metastatic Breast Cancer Previously Treated With ≥ 2 HER2-Directed Regimens: Phase III NALA Trial. *Journal of Clinical Oncology: Official Journal of the American Society of Clinical Oncology*, 38(27), 3138–3149. <https://doi.org/10.1200/JCO.20.00147>
- Schaab, C., Geiger, T., Stoehr, G., Cox, J., & Mann, M. (2012). Analysis of high accuracy, quantitative proteomics data in the MaxQB database. *Molecular & Cellular Proteomics: MCP*, 11(3), M111.014068. <https://doi.org/10.1074/mcp.M111.014068>
- Scheiblecker, L., Kollmann, K., & Sexl, V. (2020). CDK4/6 and MAPK-Crosstalk as Opportunity for Cancer Treatment. *Pharmaceuticals (Basel, Switzerland)*, 13(12). <https://doi.org/10.3390/ph13120418>
- Schettini, F., Giudici, F., Giuliano, M., Cristofanilli, M., Arpino, G., Del Mastro, L., Puglisi, F., De Placido, S., Paris, I., De Placido, P., Venturini, S., De Laurentis, M., Conte, P., Juric, D., Llombart-Cussac, A., Pusztai, L., Prat, A., Jerusalem, G., Di Leo, A., & Generali, D. (2020). Overall Survival of CDK4/6-Inhibitor-Based Treatments in Clinically Relevant Subgroups of Metastatic Breast Cancer: Systematic Review and Meta-Analysis. *JNCI: Journal of the National Cancer Institute*, 112(11), 1089–1097. <https://doi.org/10.1093/jnci/djaa071>
- Schmid, P., Adams, S., Rugo, H. S., Schneeweiss, A., Barrios, C. H., Iwata, H., Diéras, V., Hegg, R., Im, S.-A., Shaw Wright, G., Henschel, V., Molinero, L., Chui, S. Y., Funke,

- R., Husain, A., Winer, E. P., Loi, S., & Emens, L. A. (2018). Atezolizumab and Nab-Paclitaxel in Advanced Triple-Negative Breast Cancer. *New England Journal of Medicine*, 379(22), 2108–2121. <https://doi.org/10.1056/NEJMoa1809615>
- Schmid, P., Rugo, H. S., Adams, S., Schneeweiss, A., Barrios, C. H., Iwata, H., Diéras, V., Henschel, V., Molinero, L., Chui, S. Y., Maiya, V., Husain, A., Winer, E. P., Loi, S., & Emens, L. A. (2020). Atezolizumab plus nab-paclitaxel as first-line treatment for unresectable, locally advanced or metastatic triple-negative breast cancer (IMpassion130): updated efficacy results from a randomised, double-blind, placebo-controlled, phase 3 trial. *The Lancet. Oncology*, 21(1), 44–59. [https://doi.org/10.1016/S1470-2045\(19\)30689-8](https://doi.org/10.1016/S1470-2045(19)30689-8)
- Scholz, C.-J., Kurzeder, C., Koretz, K., Windisch, J., Kreienberg, R., Sauer, G., & Deissler, H. (2009). Tspan-1 is a tetraspanin preferentially expressed by mucinous and endometrioid subtypes of human ovarian carcinomas. *Cancer Letters*, 275(2), 198–203. <https://doi.org/10.1016/j.canlet.2008.10.014>
- Senkus, E., Kyriakides, S., Ohno, S., Penault-Llorca, F., Poortmans, P., Rutgers, E., Zackrisson, S., & Cardoso, F. (2015). Primary breast cancer: ESMO Clinical Practice Guidelines for diagnosis, treatment and follow-up. *Annals of Oncology: Official Journal of the European Society for Medical Oncology*, 26 Suppl 5, v8-30. <https://doi.org/10.1093/annonc/mdv298>
- Seoane, J., & Gomis, R. R. (2017). TGF- β Family Signaling in Tumor Suppression and Cancer Progression. *Cold Spring Harbor Perspectives in Biology*, 9(12). <https://doi.org/10.1101/cshperspect.a022277>
- Shalem, O., Sanjana, N. E., Hartenian, E., Shi, X., Scott, D. A., Mikkelsen, T., Heckl, D., Ebert, B. L., Root, D. E., Doench, J. G., & Zhang, F. (2014). Genome-scale CRISPR-Cas9 knockout screening in human cells. *Science (New York, N.Y.)*, 343(6166), 84–87. <https://doi.org/10.1126/science.1247005>
- Shalem, O., Sanjana, N. E., & Zhang, F. (2015). High-throughput functional genomics using CRISPR-Cas9. *Nature Reviews. Genetics*, 16(5), 299–311. <https://doi.org/10.1038/nrg3899>
- Sharma, P., & Allison, J. P. (2015). Immune checkpoint targeting in cancer therapy: toward combination strategies with curative potential. *Cell*, 161(2), 205–214. <https://doi.org/10.1016/j.cell.2015.03.030>
- Shaulian, E., & Karin, M. (2001). AP-1 in cell proliferation and survival. *Oncogene*, 20(19), 2390–2400. <https://doi.org/10.1038/sj.onc.1204383>
- Shi, W., Huang, Q., Xie, J., Wang, H., Yu, X., & Zhou, Y. (2020). CKS1B as Drug Resistance-Inducing Gene—A Potential Target to Improve Cancer Therapy . In *Frontiers in Oncology* (Vol. 10, p. 1978). <https://www.frontiersin.org/article/10.3389/fonc.2020.582451>
- Siegel, D. A., O'Neil, M. E., Richards, T. B., Dowling, N. F., & Weir, H. K. (2020). Prostate Cancer Incidence and Survival, by Stage and Race/Ethnicity - United States, 2001-2017. *MMWR. Morbidity and Mortality Weekly Report*, 69(41), 1473–1480.

<https://doi.org/10.15585/mmwr.mm6941a1>

- Siegel, R. L., Miller, K. D., Fedewa, S. A., Ahnen, D. J., Meester, R. G. S., Barzi, A., & Jemal, A. (2017). Colorectal cancer statistics, 2017. *CA: A Cancer Journal for Clinicians*, *67*(3), 177–193. <https://doi.org/10.3322/caac.21395>
- Sinn, H.-P., & Kreipe, H. (2013). A Brief Overview of the WHO Classification of Breast Tumors, 4th Edition, Focusing on Issues and Updates from the 3rd Edition. *Breast Care*, *8*(2), 149–154. <https://doi.org/10.1159/000350774>
- Slamon, D J, Leyland-Jones, B., Shak, S., Fuchs, H., Paton, V., Bajamonde, A., Fleming, T., Eiermann, W., Wolter, J., Pegram, M., Baselga, J., & Norton, L. (2001). Use of chemotherapy plus a monoclonal antibody against HER2 for metastatic breast cancer that overexpresses HER2. *The New England Journal of Medicine*, *344*(11), 783–792. <https://doi.org/10.1056/NEJM200103153441101>
- Slamon, Dennis J, Neven, P., Chia, S., Fasching, P. A., De Laurentiis, M., Im, S.-A., Petrakova, K., Bianchi, G. V., Esteva, F. J., Martín, M., Nusch, A., Sonke, G. S., De la Cruz-Merino, L., Beck, J. T., Pivot, X., Vidam, G., Wang, Y., Rodriguez Lorenc, K., Miller, M., ... Jerusalem, G. (2018). Phase III Randomized Study of Ribociclib and Fulvestrant in Hormone Receptor–Positive, Human Epidermal Growth Factor Receptor 2–Negative Advanced Breast Cancer: MONALEESA-3. *Journal of Clinical Oncology*, *36*(24), 2465–2472. <https://doi.org/10.1200/JCO.2018.78.9909>
- Sledge, G. W., Toi, M., Neven, P., Sohn, J., Inoue, K., Pivot, X., Burdaeva, O., Okera, M., Masuda, N., Kaufman, P. A., Koh, H., Grischke, E.-M., Frenzel, M., Lin, Y., Barriga, S., Smith, I. C., Bourayou, N., & Llombart-Cussac, A. (2017). MONARCH 2: Abemaciclib in Combination With Fulvestrant in Women With HR+/HER2–Advanced Breast Cancer Who Had Progressed While Receiving Endocrine Therapy. *Journal of Clinical Oncology*, *35*(25), 2875–2884. <https://doi.org/10.1200/JCO.2017.73.7585>
- Smalley, M., & Ashworth, A. (2003). Stem cells and breast cancer: A field in transit. *Nature Reviews. Cancer*, *3*(11), 832–844. <https://doi.org/10.1038/nrc1212>
- Smid, M., Wang, Y., Klijn, J. G. M., Siewerts, A. M., Zhang, Y., Atkins, D., Martens, J. W. M., & Foekens, J. A. (2006). Genes Associated With Breast Cancer Metastatic to Bone. *Journal of Clinical Oncology*, *24*(15), 2261–2267. <https://doi.org/10.1200/JCO.2005.03.8802>
- Smith, I., Greenside, P. G., Natoli, T., Lahr, D. L., Wadden, D., Tirosh, I., Narayan, R., Root, D. E., Golub, T. R., Subramanian, A., & Doench, J. G. (2017). Evaluation of RNAi and CRISPR technologies by large-scale gene expression profiling in the Connectivity Map. *PLoS Biology*, *15*(11), e2003213. <https://doi.org/10.1371/journal.pbio.2003213>
- Smith, L. M., Wise, S. C., Hendricks, D. T., Sabichi, A. L., Bos, T., Reddy, P., Brown, P. H., & Birrer, M. J. (1999). cJun overexpression in MCF-7 breast cancer cells produces a tumorigenic, invasive and hormone resistant phenotype. *Oncogene*, *18*(44), 6063–6070. <https://doi.org/10.1038/sj.onc.1202989>
- Smyth, M. J., Thia, K. Y., Cretney, E., Kelly, J. M., Snook, M. B., Forbes, C. A., & Scalzo, A.

- A. (1999). Perforin is a major contributor to NK cell control of tumor metastasis. *Journal of Immunology (Baltimore, Md. : 1950)*, *162*(11), 6658–6662.
- Sobhani, N., Fassl, A., Mondani, G., Generali, D., & Otto, T. (2021). Targeting Aberrant FGFR Signaling to Overcome CDK4/6 Inhibitor Resistance in Breast Cancer. *Cells*, *10*(2). <https://doi.org/10.3390/cells10020293>
- Soni, A., Ren, Z., Hameed, O., Chanda, D., Morgan, C. J., Siegal, G. P., & Wei, S. (2015). Breast cancer subtypes predispose the site of distant metastases. *American Journal of Clinical Pathology*, *143*(4), 471–478. <https://doi.org/10.1309/AJCPYO5FSV3UPEXS>
- Sternlicht, M. D. (2006). Key stages in mammary gland development: the cues that regulate ductal branching morphogenesis. *Breast Cancer Research: BCR*, *8*(1), 201. <https://doi.org/10.1186/bcr1368>
- Subramanian, A., Tamayo, P., Mootha, V. K., Mukherjee, S., Ebert, B. L., Gillette, M. A., Paulovich, A., Pomeroy, S. L., Golub, T. R., Lander, E. S., & Mesirov, J. P. (2005). Gene set enrichment analysis: a knowledge-based approach for interpreting genome-wide expression profiles. *Proceedings of the National Academy of Sciences of the United States of America*, *102*(43), 15545–15550. <https://doi.org/10.1073/pnas.0506580102>
- Sun, Y.-S., Zhao, Z., Yang, Z.-N., Xu, F., Lu, H.-J., Zhu, Z.-Y., Shi, W., Jiang, J., Yao, P.-P., & Zhu, H.-P. (2017). Risk Factors and Preventions of Breast Cancer. *International Journal of Biological Sciences*, *13*(11), 1387–1397. <https://doi.org/10.7150/ijbs.21635>
- Swain, S. M., Kim, S.-B., Cortés, J., Ro, J., Semiglazov, V., Campone, M., Ciruelos, E., Ferrero, J.-M., Schneeweiss, A., Knott, A., Clark, E., Ross, G., Benyunes, M. C., & Baselga, J. (2013). Pertuzumab, trastuzumab, and docetaxel for HER2-positive metastatic breast cancer (CLEOPATRA study): overall survival results from a randomised, double-blind, placebo-controlled, phase 3 study. *The Lancet. Oncology*, *14*(6), 461–471. [https://doi.org/10.1016/S1470-2045\(13\)70130-X](https://doi.org/10.1016/S1470-2045(13)70130-X)
- Takeshita, T., Yamamoto, Y., Yamamoto-Ibusuki, M., Tomiguchi, M., Sueta, A., Murakami, K., & Iwase, H. (2018). Clinical significance of plasma cell-free DNA mutations in PIK3CA, AKT1, and ESR1 gene according to treatment lines in ER-positive breast cancer. *Molecular Cancer*, *17*(1), 67. <https://doi.org/10.1186/s12943-018-0808-y>
- Tarella, C., Passera, R., Magni, M., Benedetti, F., Rossi, A., Gueli, A., Patti, C., Parvis, G., Ciceri, F., Gallamini, A., Cortelazzo, S., Zoli, V., Corradini, P., Carobbio, A., Mulé, A., Bosa, M., Barbui, A., Di Nicola, M., Sorio, M., ... Rambaldi, A. (2010). Risk Factors for the Development of Secondary Malignancy After High-Dose Chemotherapy and Autograft, With or Without Rituximab: A 20-Year Retrospective Follow-Up Study in Patients With Lymphoma. *Journal of Clinical Oncology*, *29*(7), 814–824. <https://doi.org/10.1200/JCO.2010.28.9777>
- Taylor-Harding, B., Aspuria, P.-J., Agadjanian, H., Cheon, D.-J., Mizuno, T., Greenberg, D., Allen, J. R., Spurka, L., Funari, V., Spiteri, E., Wang, Q., Orsulic, S., Walsh, C., Karlan, B. Y., & Wiedemeyer, W. R. (2015). Cyclin E1 and RTK/RAS signaling drive CDK inhibitor resistance via activation of E2F and ETS. *Oncotarget*, *6*(2), 696–714. <https://doi.org/10.18632/oncotarget.2673>

- Teo, G., Koh, H., Fermin, D., Lambert, J.-P., Knight, J. D. R., Gingras, A.-C., & Choi, H. (2016). SAINTq: Scoring protein-protein interactions in affinity purification - mass spectrometry experiments with fragment or peptide intensity data. *Proteomics*, *16*(15–16), 2238–2245. <https://doi.org/10.1002/pmhc.201500499>
- Teo, G., Liu, G., Zhang, J., Nesvizhskii, A. I., Gingras, A.-C., & Choi, H. (2014). SAINTexpress: Improvements and additional features in Significance Analysis of INTeractome software. *Journal of Proteomics*, *100*, 37–43. <https://doi.org/https://doi.org/10.1016/j.jprot.2013.10.023>
- Thomas, A. L., Lind, H., Hong, A., Dokic, D., Oppat, K., Rosenthal, E., Guo, A., Thomas, A., Hamden, R., & Jeruss, J. S. (2017). Inhibition of CDK-mediated Smad3 phosphorylation reduces the Pin1-Smad3 interaction and aggressiveness of triple negative breast cancer cells. *Cell Cycle (Georgetown, Tex.)*, *16*(15), 1453–1464. <https://doi.org/10.1080/15384101.2017.1338988>
- Thull, D. L., & Vogel, V. G. (2004). Recognition and management of hereditary breast cancer syndromes. *The Oncologist*, *9*(1), 13–24. <https://doi.org/10.1634/theoncologist.9-1-13>
- Tiede, B., & Kang, Y. (2011). From milk to malignancy: the role of mammary stem cells in development, pregnancy and breast cancer. *Cell Research*, *21*(2), 245–257. <https://doi.org/10.1038/cr.2011.11>
- Tigan, A.-S., Bellutti, F., Kollmann, K., Tebb, G., & Sexl, V. (2016). CDK6-a review of the past and a glimpse into the future: from cell-cycle control to transcriptional regulation. *Oncogene*, *35*(24), 3083–3091. <https://doi.org/10.1038/onc.2015.407>
- Tobin, N. P., Sims, A. H., Lundgren, K. L., Lehn, S., & Landberg, G. (2011). Cyclin D1, Id1 and EMT in breast cancer. *BMC Cancer*, *11*, 417. <https://doi.org/10.1186/1471-2407-11-417>
- Tolaney, S. M., Cicin, I., Betancourt, R., Chan, A., Kaen, D., Kaufman, P. A., Delalogue, S., Liu, Q., Cartot-Cotton, S., Amrate, A., Pelekanou, V., & Cuff, K. E. (2020). Phase II trial of SAR439859 vs endocrine monotherapy in pre- and post-menopausal, estrogen receptor-positive (ER+)/human epidermal growth factor receptor 2-negative (HER2-), locally advanced or metastatic breast cancer (BC) with prior exposure to hormonal. *Journal of Clinical Oncology*, *38*(15_suppl), TPS1107–TPS1107. https://doi.org/10.1200/JCO.2020.38.15_suppl.TPS1107
- Torrano, V., Valcarcel-Jimenez, L., Cortazar, A. R., Liu, X., Urosevic, J., Castillo-Martin, M., Fernández-Ruiz, S., Morciano, G., Caro-Maldonado, A., Guiu, M., Zúñiga-García, P., Graupera, M., Bellmunt, A., Pandya, P., Lorente, M., Martín-Martín, N., Sutherland, J. D., Sanchez-Mosquera, P., Bozal-Basterra, L., ... Carracedo, A. (2016). The metabolic co-regulator PGC1 α suppresses prostate cancer metastasis. *Nature Cell Biology*, *18*(6), 645–656. <https://doi.org/10.1038/ncb3357>
- Toste, P. A., Nguyen, A. H., Kadera, B. E., Duong, M., Wu, N., Gawlas, I., Tran, L. M., Bikhchandani, M., Li, L., Patel, S. G., Dawson, D. W., & Donahue, T. R. (2016). Chemotherapy-Induced Inflammatory Gene Signature and Protumorigenic Phenotype in Pancreatic CAFs via Stress-Associated MAPK. *Molecular Cancer Research: MCR*, *14*(5), 437–447. <https://doi.org/10.1158/1541-7786.MCR-15-0348>

- Tripathy, D., Im, S.-A., Colleoni, M., Franke, F., Bardia, A., Harbeck, N., Hurvitz, S. A., Chow, L., Sohn, J., Lee, K. S., Campos-Gomez, S., Villanueva Vazquez, R., Jung, K. H., Babu, K. G., Wheatley-Price, P., De Laurentiis, M., Im, Y.-H., Kuemmel, S., El-Saghir, N., ... Lu, Y.-S. (2018). Ribociclib plus endocrine therapy for premenopausal women with hormone-receptor-positive, advanced breast cancer (MONALEESA-7): a randomised phase 3 trial. *The Lancet. Oncology*, *19*(7), 904–915. [https://doi.org/10.1016/S1470-2045\(18\)30292-4](https://doi.org/10.1016/S1470-2045(18)30292-4)
- Tsuji, T., Ibaragi, S., Shima, K., Hu, M. G., Katsurano, M., Sasaki, A., & Hu, G. (2008). Epithelial-mesenchymal transition induced by growth suppressor p12CDK2-AP1 promotes tumor cell local invasion but suppresses distant colony growth. *Cancer Research*, *68*(24), 10377–10386. <https://doi.org/10.1158/0008-5472.CAN-08-1444>
- Turner, N. C., Liu, Y., Zhu, Z., Loi, S., Colleoni, M., Loibl, S., DeMichele, A., Harbeck, N., André, F., Bayar, M. A., Michiels, S., Zhang, Z., Giorgetti, C., Arnedos, M., Huang Bartlett, C., & Cristofanilli, M. (2019). Cyclin E1 Expression and Palbociclib Efficacy in Previously Treated Hormone Receptor-Positive Metastatic Breast Cancer. *Journal of Clinical Oncology: Official Journal of the American Society of Clinical Oncology*, *37*(14), 1169–1178. <https://doi.org/10.1200/JCO.18.00925>
- Turner, N. C., Slamon, D. J., Ro, J., Bondarenko, I., Im, S.-A., Masuda, N., Colleoni, M., DeMichele, A., Loi, S., Verma, S., Iwata, H., Harbeck, N., Loibl, S., André, F., Puyana Theall, K., Huang, X., Giorgetti, C., Huang Bartlett, C., & Cristofanilli, M. (2018). Overall Survival with Palbociclib and Fulvestrant in Advanced Breast Cancer. *The New England Journal of Medicine*, *379*(20), 1926–1936. <https://doi.org/10.1056/NEJMoa1810527>
- Turner, N., & Grose, R. (2010). Fibroblast growth factor signalling: from development to cancer. *Nature Reviews. Cancer*, *10*(2), 116–129. <https://doi.org/10.1038/nrc2780>
- Turner, N., Pearson, A., Sharpe, R., Lambros, M., Geyer, F., Lopez-Garcia, M. A., Natrajan, R., Marchio, C., Iorns, E., Mackay, A., Gillett, C., Grigoriadis, A., Tutt, A., Reis-Filho, J. S., & Ashworth, A. (2010). FGFR1 Amplification Drives Endocrine Therapy Resistance and Is a Therapeutic Target in Breast Cancer. *Cancer Research*, *70*(5), 2085 LP – 2094. <https://doi.org/10.1158/0008-5472.CAN-09-3746>
- Tyanova, S., Temu, T., Carlson, A., Sinitcyn, P., Mann, M., & Cox, J. (2015). Visualization of LC-MS/MS proteomics data in MaxQuant. *Proteomics*, *15*(8), 1453–1456. <https://doi.org/10.1002/pmic.201400449>
- Tyanova, S., Temu, T., & Cox, J. (2016). The MaxQuant computational platform for mass spectrometry-based shotgun proteomics. *Nature Protocols*, *11*(12), 2301–2319. <https://doi.org/10.1038/nprot.2016.136>
- Urosevic, J., Blasco, M. T., Llorente, A., Bellmunt, A., Berenguer-Llargo, A., Guiu, M., Cañellas, A., Fernandez, E., Burkov, I., Clapés, M., Cartanà, M., Figueras-Puig, C., Batlle, E., Nebreda, A. R., & Gomis, R. R. (2020). ERK1/2 Signaling Induces Upregulation of ANGPT2 and CXCR4 to Mediate Liver Metastasis in Colon Cancer. *Cancer Research*, *80*(21), 4668 LP – 4680. <https://doi.org/10.1158/0008-5472.CAN-19-4028>

- Urosevic, J., Garcia-Albéniz, X., Planet, E., Real, S., Céspedes, M. V., Guiu, M., Fernandez, E., Bellmunt, A., Gawrzak, S., Pavlovic, M., Mangués, R., Dolado, I., Barriga, F. M., Nadal, C., Kemeny, N., Batlle, E., Nebreda, A. R., & Gomis, R. R. (2014). Colon cancer cells colonize the lung from established liver metastases through p38 MAPK signalling and PTHLH. *Nature Cell Biology*, *16*(7), 685–694. <https://doi.org/10.1038/ncb2977>
- Valastyan, S., & Weinberg, R. A. (2011). Tumor metastasis: molecular insights and evolving paradigms. *Cell*, *147*(2), 275–292. <https://doi.org/10.1016/j.cell.2011.09.024>
- Valiente, M., Obenauf, A. C., Jin, X., Chen, Q., Zhang, X. H.-F., Lee, D. J., Chaft, J. E., Kris, M. G., Huse, J. T., Brogi, E., & Massagué, J. (2014). Serpins Promote Cancer Cell Survival and Vascular Co-Option in Brain Metastasis. *Cell*, *156*(5), 1002–1016. <https://doi.org/https://doi.org/10.1016/j.cell.2014.01.040>
- Vernieri, C., Corti, F., Nichetti, F., Ligorio, F., Manglaviti, S., Zattarin, E., Rea, C. G., Capri, G., Bianchi, G. V., & de Braud, F. (2020). Everolimus versus alpelisib in advanced hormone receptor-positive HER2-negative breast cancer: targeting different nodes of the PI3K/AKT/mTORC1 pathway with different clinical implications. *Breast Cancer Research : BCR*, *22*(1), 33. <https://doi.org/10.1186/s13058-020-01271-0>
- Veronesi, U., Boyle, P., Goldhirsch, A., Orecchia, R., & Viale, G. (2005). Breast cancer. *Lancet (London, England)*, *365*(9472), 1727–1741. [https://doi.org/10.1016/S0140-6736\(05\)66546-4](https://doi.org/10.1016/S0140-6736(05)66546-4)
- Vijayaraghavan, S., Karakas, C., Doostan, I., Chen, X., Bui, T., Yi, M., Raghavendra, A. S., Zhao, Y., Bashour, S. I., Ibrahim, N. K., Karuturi, M., Wang, J., Winkler, J. D., Amaravadi, R. K., Hunt, K. K., Tripathy, D., & Keyomarsi, K. (2017). CDK4/6 and autophagy inhibitors synergistically induce senescence in Rb positive cytoplasmic cyclin E negative cancers. *Nature Communications*, *8*, 15916. <https://doi.org/10.1038/ncomms15916>
- von Minckwitz, G., Huang, C.-S., Mano, M. S., Loibl, S., Mamounas, E. P., Untch, M., Wolmark, N., Rastogi, P., Schneeweiss, A., Redondo, A., Fischer, H. H., Jacot, W., Conlin, A. K., Arce-Salinas, C., Wapnir, I. L., Jackisch, C., DiGiovanna, M. P., Fasching, P. A., Crown, J. P., ... Geyer, C. E. (2018). Trastuzumab Emtansine for Residual Invasive HER2-Positive Breast Cancer. *New England Journal of Medicine*, *380*(7), 617–628. <https://doi.org/10.1056/NEJMoa1814017>
- Wagner, K. U., Young, W. S. 3rd, Liu, X., Ginns, E. I., Li, M., Furth, P. A., & Hennighausen, L. (1997). Oxytocin and milk removal are required for post-partum mammary-gland development. *Genes and Function*, *1*(4), 233–244. <https://doi.org/10.1046/j.1365-4624.1997.00024.x>
- Waks, A. G., & Winer, E. P. (2019). Breast Cancer Treatment: A Review. *JAMA*, *321*(3), 288–300. <https://doi.org/10.1001/jama.2018.19323>
- Walden, P. D., Ruan, W., Feldman, M., & Kleinberg, D. L. (1998). Evidence that the mammary fat pad mediates the action of growth hormone in mammary gland development. *Endocrinology*, *139*(2), 659–662. <https://doi.org/10.1210/endo.139.2.5718>

- Wallden, B., Storhoff, J., Nielsen, T., Dowidar, N., Schaper, C., Ferree, S., Liu, S., Leung, S., Geiss, G., Snider, J., Vickery, T., Davies, S. R., Mardis, E. R., Gnant, M., Sestak, I., Ellis, M. J., Perou, C. M., Bernard, P. S., & Parker, J. S. (2015). Development and verification of the PAM50-based Prosigna breast cancer gene signature assay. *BMC Medical Genomics*, 8, 54. <https://doi.org/10.1186/s12920-015-0129-6>
- Warburton, M. J., Mitchell, D., Ormerod, E. J., & Rudland, P. (1982). Distribution of myoepithelial cells and basement membrane proteins in the resting, pregnant, lactating, and involuting rat mammary gland. *The Journal of Histochemistry and Cytochemistry: Official Journal of the Histochemistry Society*, 30(7), 667–676. <https://doi.org/10.1177/30.7.6179984>
- Wculek, S. K., & Malanchi, I. (2015). Neutrophils support lung colonization of metastasis-initiating breast cancer cells. *Nature*, 528(7582), 413–417. <https://doi.org/10.1038/nature16140>
- Weinberg, R. A. (1995). The retinoblastoma protein and cell cycle control. *Cell*, 81(3), 323–330. [https://doi.org/10.1016/0092-8674\(95\)90385-2](https://doi.org/10.1016/0092-8674(95)90385-2)
- Wiseman, B. S., & Werb, Z. (2002). Stromal effects on mammary gland development and breast cancer. *Science (New York, N.Y.)*, 296(5570), 1046–1049. <https://doi.org/10.1126/science.1067431>
- Wu, A., Wu, B., Guo, J., Luo, W., Wu, D., Yang, H., Zhen, Y., Yu, X., Wang, H., Zhou, Y., Liu, Z., Fang, W., & Yang, Z. (2011). Elevated expression of CDK4 in lung cancer. *Journal of Translational Medicine*, 9, 38. <https://doi.org/10.1186/1479-5876-9-38>
- Wu, X., Scott, D. A., Kriz, A. J., Chiu, A. C., Hsu, P. D., Dadon, D. B., Cheng, A. W., Trevino, A. E., Konermann, S., Chen, S., Jaenisch, R., Zhang, F., & Sharp, P. A. (2014). Genome-wide binding of the CRISPR endonuclease Cas9 in mammalian cells. *Nature Biotechnology*, 32(7), 670–676. <https://doi.org/10.1038/nbt.2889>
- Wyckoff, J. B., Wang, Y., Lin, E. Y., Li, J., Goswami, S., Stanley, E. R., Segall, J. E., Pollard, J. W., & Condeelis, J. (2007). Direct visualization of macrophage-assisted tumor cell intravasation in mammary tumors. *Cancer Research*, 67(6), 2649–2656. <https://doi.org/10.1158/0008-5472.CAN-06-1823>
- Xu, H., Xiao, T., Chen, C.-H., Li, W., Meyer, C. A., Wu, Q., Wu, D., Cong, L., Zhang, F., Liu, J. S., Brown, M., & Liu, X. S. (2015). Sequence determinants of improved CRISPR sgRNA design. *Genome Research*, 25(8), 1147–1157. <https://doi.org/10.1101/gr.191452.115>
- Yager, J. D., & Davidson, N. E. (2006). Estrogen carcinogenesis in breast cancer. *The New England Journal of Medicine*, 354(3), 270–282. <https://doi.org/10.1056/NEJMra050776>
- Yamamoto, T., Ebisuya, M., Ashida, F., Okamoto, K., Yonehara, S., & Nishida, E. (2006). Continuous ERK activation downregulates antiproliferative genes throughout G1 phase to allow cell-cycle progression. *Current Biology: CB*, 16(12), 1171–1182. <https://doi.org/10.1016/j.cub.2006.04.044>
- Yang, C., Li, Z., Bhatt, T., Dickler, M., Giri, D., Scaltriti, M., Baselga, J., Rosen, N., &

- Chandarlapaty, S. (2017). Acquired CDK6 amplification promotes breast cancer resistance to CDK4/6 inhibitors and loss of ER signaling and dependence. *Oncogene*, *36*(16), 2255–2264. <https://doi.org/10.1038/onc.2016.379>
- Ye, H., Li, T., Wang, H., Wu, J., Yi, C., Shi, J., Wang, P., Song, C., Dai, L., Jiang, G., Huang, Y., Yu, Y., & Li, J. (2021). TSPAN1, TMPRSS4, SDR16C5, and CTSE as Novel Panel for Pancreatic Cancer: A Bioinformatics Analysis and Experiments Validation . In *Frontiers in Immunology* (Vol. 12, p. 706).
- Ye, N., Ding, Y., Wild, C., Shen, Q., & Zhou, J. (2014). Small molecule inhibitors targeting activator protein 1 (AP-1). *Journal of Medicinal Chemistry*, *57*(16), 6930–6948. <https://doi.org/10.1021/jm5004733>
- Yue, F., Jiang, W., Ku, A. T., Young, A. I. J., Zhang, W., Souto, E. P., Gao, Y., Yu, Z., Wang, Y., Creighton, C. J., Nagi, C., Wang, T., Hilsenbeck, S. G., Feng, X.-H., Huang, S., Coarfa, C., Zhang, X. H.-F., Liu, Q., Lin, X., & Li, Y. (2021). A Wnt-Independent LGR4–EGFR Signaling Axis in Cancer Metastasis. *Cancer Research*, *81*(17), 4441 LP – 4454. <https://doi.org/10.1158/0008-5472.CAN-21-1112>
- Zhang, X. H.-F., Giuliano, M., Trivedi, M. V, Schiff, R., & Osborne, C. K. (2013). Metastasis dormancy in estrogen receptor-positive breast cancer. *Clinical Cancer Research: An Official Journal of the American Association for Cancer Research*, *19*(23), 6389–6397. <https://doi.org/10.1158/1078-0432.CCR-13-0838>
- Zhang, X. H.-F., Wang, Q., Gerald, W., Hudis, C. A., Norton, L., Smid, M., Foekens, J. A., & Massagué, J. (2009). Latent bone metastasis in breast cancer tied to Src-dependent survival signals. *Cancer Cell*, *16*(1), 67–78. <https://doi.org/10.1016/j.ccr.2009.05.017>
- Zheng, X., Carstens, J. L., Kim, J., Scheible, M., Kaye, J., Sugimoto, H., Wu, C.-C., LeBleu, V. S., & Kalluri, R. (2015). Epithelial-to-mesenchymal transition is dispensable for metastasis but induces chemoresistance in pancreatic cancer. *Nature*, *527*(7579), 525–530. <https://doi.org/10.1038/nature16064>
- Zhou, Y., Zhu, S., Cai, C., Yuan, P., Li, C., Huang, Y., & Wei, W. (2014). High-throughput screening of a CRISPR/Cas9 library for functional genomics in human cells. *Nature*, *509*(7501), 487–491. <https://doi.org/10.1038/nature13166>
- Zupkovitz, G., Grausenburger, R., Brunmeir, R., Senese, S., Tischler, J., Jurkin, J., Rembold, M., Meunier, D., Egger, G., Lagger, S., Chiocca, S., Propst, F., Weitzer, G., & Seiser, C. (2010). The cyclin-dependent kinase inhibitor p21 is a crucial target for histone deacetylase 1 as a regulator of cellular proliferation. *Molecular and Cellular Biology*, *30*(5), 1171–1181. <https://doi.org/10.1128/MCB.01500-09>

- Supplementary Tables -

Supplementary tables

Supplementary table 1. List of genes from Breast Cancer 360™ whose high expression is associated with worst PFS (up) and OS (down) in CDK patient cohort. p-value < 0,05.

UNIVARIATE PFS

GENE	HR (95% CI)	p-value
XXXX	1.46 (1.19-1.78)	0,0002
RASGRF1	1.4 (1.16-1.71)	0,0006
LAD1	1.37 (1.09-1.71)	0,0063
BAIAP2L1	1.3 (1.02-1.65)	0,0309
SUV39H2	1.29 (1.06-1.58)	0,0129
PLCB1	1.26 (1.03-1.55)	0,022
ELF3	1.25 (1.01-1.56)	0,0434
SHMT2	1.25 (1.03-1.53)	0,0262

UNIVARIATE OS

GENE	HR (95% CI)	p-value
XXXX	2.01 (1.49-2.72)	0,0000
SFN	1.65 (1.18-2.31)	0,0036
LAD1	1.65 (1.14-2.38)	0,0081
BNIP3	1.52 (1.12-2.07)	0,0073
RPS6KB2	1.48 (1.11-1.96)	0,0073
VEGFA	1.46 (1.1-1.95)	0,0086
MYCN	1.44 (1.06-1.96)	0,0191
GPR160	1.43 (1.01-2.03)	0,0459
E2F1	1.42 (1.07-1.9)	0,0169
TWIST1	1.42 (1.01-1.99)	0,0459

CXCL9	1.4 (1-1.96)	0,0473
DLL4	1.4 (1.02-1.92)	0,0374
TMEM45B	1.4 (1.01-1.94)	0,0451
EIF4E2	1.4 (1.05-1.85)	0,0201
FST	1.39 (1.04-1.88)	0,0284
OCLN	1.39 (1.03-1.87)	0,0302
INHBB	1.38 (1.01-1.9)	0,0445
RASGRF1	1.38 (1.05-1.81)	0,0218
SHMT2	1.37 (1.02-1.85)	0,0373
LFNG	1.37 (1-1.87)	0,0467
MT1G	1.37 (1.02-1.83)	0,0343
CTSW	1.36 (1.03-1.81)	0,0329
MS4A2	1.36 (1.01-1.83)	0,0407

Supplementary table 2. List of genes with increased expression in PD compared to Baseline samples in CDK patient cohort. Unpaired (up) and paired (down) SAM analysis. q-value < 5%.

UNPAIRED SAM ANALYSIS OF CDK BASELINE VS PD

GENE ID	Score(d)	Numerator (r)	Denominator (s+s0)	Fold Change	q-value(%)
GGH	4,1600	1,6580	0,3986	3,1559	0,0000
DLGAP5	3,4514	1,2275	0,3557	2,3416	0,0000
CYP4F3	3,3356	2,0731	0,6215	4,2078	0,0000
DSC2	3,2957	1,1330	0,3438	2,1931	0,0000
PCK1	3,2736	2,3919	0,7307	5,2486	0,0000
CDC25C	3,1679	1,0441	0,3296	2,0620	0,0000
KIF2C	3,1490	1,1672	0,3707	2,2458	0,0000
PGK1	3,1194	0,8063	0,2585	1,7488	0,0000
FAM83D	3,0718	1,0840	0,3529	2,1199	0,0000
RRM2	3,0313	1,1160	0,3682	2,1675	0,0000
UBE2C	3,0031	1,1336	0,3775	2,1941	0,0000
PTTG1	2,9754	0,9956	0,3346	1,9939	0,0000
CCNB1	2,9260	0,8720	0,2980	1,8302	0,0000
SPC25	2,8406	0,9605	0,3382	1,9460	0,0000
DEPDC1	2,8264	0,8788	0,3109	1,8389	0,0000
ALDH1A1	2,8194	1,3371	0,4743	2,5265	0,0000
MCM2	2,7567	0,7728	0,2803	1,7085	0,2416
CCNA2	2,7448	0,8739	0,3184	1,8326	0,2416
ASPM	2,7417	0,9835	0,3587	1,9772	0,2416
CDK1	2,7333	0,9821	0,3593	1,9754	0,2416
PRC1	2,7261	0,8909	0,3268	1,8544	0,2416

PSMB7	2,7215	0,5910	0,2172	1,5063	0,2416
CEACAM6	2,7070	1,9467	0,7192	3,8550	0,2416
CKS1B	2,6764	0,6532	0,2441	1,5726	0,2416
RAD51	2,6552	0,8003	0,3014	1,7415	0,2416
TYMS	2,6165	0,9146	0,3496	1,8851	0,2416
TSPAN1	2,6159	1,3727	0,5247	2,5895	0,2416
CDKN3	2,6041	0,8244	0,3166	1,7708	0,2416
CCNE2	2,5226	0,8272	0,3279	1,7742	0,2416
EGLN3	2,4768	0,9654	0,3898	1,9525	0,2416
TRIP13	2,4703	0,7515	0,3042	1,6836	0,2416
TTK	2,4646	0,8224	0,3337	1,7683	0,2416
CCNE1	2,4253	0,7463	0,3077	1,6775	0,2416
EXO1	2,4130	0,8150	0,3378	1,7594	0,2416
TOP2A	2,4103	0,9190	0,3813	1,8909	0,2416
ENO1	2,4083	0,5482	0,2276	1,4623	0,2416
AURKA	2,3338	0,7172	0,3073	1,6440	0,5759
STAT1	2,3227	0,6826	0,2939	1,6051	0,5759
BLM	2,3026	0,6960	0,3023	1,6200	0,5759
HGF	2,2995	0,8478	0,3687	1,7998	0,5759
PIK3R3	2,2940	0,6859	0,2990	1,6087	0,5759
HIST3H2BB	2,2910	0,7020	0,3064	1,6268	0,5759
CXCL10	2,2814	0,9572	0,4196	1,9416	0,5759
MKI67	2,2741	0,7997	0,3517	1,7408	0,5759
MCM3	2,2718	0,5562	0,2448	1,4704	0,5759
ANLN	2,2693	0,7726	0,3404	1,7083	0,5759
MELK	2,2406	0,7341	0,3276	1,6634	0,5759
FUT3	2,2059	0,9782	0,4435	1,9701	0,8377
UBE2T	2,1801	0,7007	0,3214	1,6253	0,8377
MET	2,1540	0,8484	0,3938	1,8004	0,8377

SLPI	2,1399	1,1801	0,5515	2,2659	0,8377
POLQ	2,1346	0,7007	0,3282	1,6252	0,8377
FOXM1	2,1217	0,7176	0,3382	1,6445	0,8377
LAD1	2,1171	0,8556	0,4041	1,8095	0,8377
CDC20	2,1018	0,7004	0,3332	1,6250	0,8377
CDC25A	2,0739	0,7341	0,3539	1,6633	1,5321
UBB	2,0628	0,4896	0,2373	1,4040	1,5321
PSAT1	2,0511	0,8634	0,4210	1,8194	1,5321
HER2	2,0196	0,3061	0,1516	1,2364	1,5321
HDAC1	2,0184	0,4883	0,2419	1,4028	1,5321
MARCO	2,0144	1,0806	0,5364	2,1148	1,5321
AGT	1,9903	1,1493	0,5775	2,2181	1,5321
HIF1A	1,9705	0,5573	0,2828	1,4715	1,9591
PLA2G2A	1,9561	1,1173	0,5712	2,1694	1,9591
CLDN1	1,9460	0,8625	0,4432	1,8181	1,9591
ORC6	1,9424	0,6116	0,3149	1,5279	1,9591
CXCL8	1,8937	0,9783	0,5166	1,9702	1,9591
ITGB1	1,8653	0,4733	0,2537	1,3882	2,8188
CEACAM5	1,8648	1,2058	0,6466	2,3066	2,8188
OAZ1	1,8555	0,3798	0,2047	1,3012	2,8188
XXXX	1,8549	1,0248	0,5525	2,0347	2,8188
RFC4	1,8504	0,4650	0,2513	1,3803	2,8188
CXADR	1,8439	0,8352	0,4529	1,7841	2,8188
CDH2	1,8415	0,8635	0,4689	1,8194	2,8188
KNTC2	1,8276	0,6137	0,3358	1,5302	2,8188
FGFR2	1,8141	0,7025	0,3873	1,6274	2,8188
FLRT3	1,7898	0,8585	0,4797	1,8132	2,8188
CHEK2	1,7719	0,4504	0,2542	1,3664	3,9689
RAD54L	1,7641	0,5628	0,3190	1,4771	3,9689

KIF23	1,7509	0,5469	0,3123	1,4609	3,9689
IL13RA1	1,7419	0,3757	0,2157	1,2974	3,9689
BIRC5	1,6815	0,6515	0,3875	1,5708	4,9513
CDCA5	1,6718	0,5270	0,3152	1,4409	4,9513
SUV39H2	1,6672	0,3987	0,2391	1,3183	4,9513
TMEM45B	1,6592	0,7651	0,4611	1,6995	4,9513
PREP	1,6484	0,3704	0,2247	1,2927	4,9513
SKP2	1,6405	0,3652	0,2226	1,2880	4,9513
TFRC	1,6348	0,4746	0,2903	1,3895	4,9513
B3GNT3	1,6064	0,6638	0,4132	1,5842	4,9513
NETO2	1,5922	0,6058	0,3805	1,5219	4,9513
KIF11	1,5867	0,5127	0,3231	1,4267	4,9513

PAIRED SAM ANALYSIS OF CDK BASELINE VS PD

GENE ID	Score(d)	Numerator (r)	Denominator (s+s0)	Fold Change	q-value(%)
UBE2C	2,2494	1,4884	0,6617	2,8057	1,2462
GGH	2,1562	1,6431	0,7620	3,1234	1,2462
DLGAP5	2,1347	1,5199	0,7120	2,8676	1,2462
FAM83D	2,0646	1,3821	0,6694	2,6066	1,2462
CDK1	1,9979	1,2640	0,6327	2,4017	1,2462
RRM2	1,9869	1,2430	0,6256	2,3668	1,2462
TYMS	1,9775	1,2278	0,6209	2,3420	1,2462
SPC25	1,9516	1,2387	0,6347	2,3598	1,2462
TOP2A	1,9410	1,3281	0,6842	2,5107	1,2462
PTTG1	1,9366	1,3123	0,6776	2,4834	1,2462

CCNB1	1,9130	1,0927	0,5712	2,1327	1,2462
PRC1	1,9044	1,1696	0,6141	2,2495	1,2462
CYP4F3	1,8881	2,3376	1,2381	5,0547	1,2462
ASPM	1,8770	1,2886	0,6865	2,4428	1,2462
CDC25C	1,7799	1,1837	0,6650	2,2716	1,7361
EXO1	1,7738	1,0834	0,6108	2,1191	1,7361
MKI67	1,7272	1,1639	0,6738	2,2406	2,2477
CXCL8	1,6967	1,4994	0,8837	2,8272	2,2477
MCM2	1,6788	0,8791	0,5237	1,8392	2,2477
CDKN3	1,6602	1,0580	0,6373	2,0820	3,0403
TTK	1,6424	1,0767	0,6556	2,1093	3,0403
TRIP13	1,6394	0,9959	0,6075	1,9944	3,0403
AURKA	1,6134	1,0749	0,6662	2,1065	3,0403
HIST1H3H	1,6133	1,0460	0,6484	2,0648	3,0403
FOXM1	1,5573	1,0140	0,6512	2,0196	3,0403
DEPDC1	1,5446	1,0141	0,6565	2,0196	3,0403
SFN	1,5378	0,9631	0,6263	1,9495	3,0403
CXADR	1,5373	0,8044	0,5232	1,7464	3,0403
CCNA2	1,5314	0,9478	0,6189	1,9289	3,0403
BLM	1,5206	0,9128	0,6003	1,8827	3,7992
PGK1	1,5174	0,7998	0,5271	1,7408	3,7992
CCNE2	1,5088	0,9620	0,6376	1,9479	3,7992
ANLN	1,5041	1,0089	0,6708	2,0124	3,7992
KIF2C	1,5016	0,9998	0,6658	1,9997	3,7992
MYBL2	1,4967	0,9901	0,6615	1,9864	3,7992
CCNE1	1,4959	0,9297	0,6215	1,9049	3,7992
S100A7	1,4917	1,5891	1,0653	3,0087	3,7992
KIF11	1,4842	1,0078	0,6790	2,0109	3,7992
CKS1B	1,4750	0,7466	0,5062	1,6779	3,7992

UBE2T	1,4735	0,9066	0,6153	1,8747	3,7992
RFC4	1,4617	0,7504	0,5134	1,6823	3,7992
CDC25A	1,4527	0,9350	0,6436	1,9119	3,7992
KIFC1	1,4385	0,9539	0,6631	1,9371	3,7992
PCK1	1,4357	1,9974	1,3912	3,9928	3,7992

Supplementary table 3. List of genes whose high expression is associated with increased risk of relapse (up) and worse response to ribociclib plus letrozole (down) in CORALEEN clinical trial. q-value < 5%.

HIGH EXPRESSION:

INCREASED RISK OF RECURRENCE

GENE ID	Score(d)	Fold Change	q-value(%)
CENPF	-3,2391	0,4890	0,0000
TSPAN1	-3,2220	0,3235	0,0000
CDCA1	-3,1979	0,4806	0,0000
DLGAP5	-3,1073	0,4658	0,0000
MKI67	-3,0521	0,4623	0,0000
CDC25C	-3,0493	0,4584	0,0000
HIST1H3H	-2,9973	0,5371	0,0000
KIFC1	-2,9925	0,4705	0,0000
HIST1H2BH	-2,9736	0,6062	0,0000
CDK1	-2,9660	0,4408	0,0000
TTK	-2,8726	0,5351	0,0000
BIRC5	-2,8401	0,4152	0,0000
E2F1	-2,8277	0,5323	0,0000
CEP55	-2,7886	0,5001	0,0000
CCNB1	-2,7839	0,5610	0,0000
UBE2C	-2,7820	0,4076	0,0000
ANLN	-2,7708	0,4430	0,0000
FOXM1	-2,7524	0,4735	0,0000
CDH1	-2,7351	0,4173	0,0000
ASPM	-2,7335	0,4316	0,0000
AURKB	-2,6526	0,5273	0,0000

RAD54L	-2,5888	0,5509	0,0000
PKMYT1	-2,5594	0,4770	0,0000
KNTC2	-2,5557	0,5380	0,0000
RRM2	-2,5278	0,4962	0,0000
KIF23	-2,5275	0,5132	0,0000
MELK	-2,5205	0,5758	0,0000
UBE2T	-2,4992	0,5176	0,0000
MYBL2	-2,4825	0,5031	0,0000
MMP11	-2,4804	0,3690	0,0000
KIF11	-2,4529	0,6017	0,0000
EXO1	-2,4522	0,5014	0,0000
HIST3H2BB	-2,4356	0,5688	0,0000
ST6GALNAC2	-2,4224	0,4558	0,0000
TOP2A	-2,4192	0,5098	1,6504
KIF2C	-2,4179	0,5435	1,6504
PRC1	-2,4084	0,5767	1,6504
TFF3	-2,3961	0,3775	1,6504
SPDEF	-2,3629	0,5993	1,6504
FXYD3	-2,3133	0,4518	1,6504
EFNA3	-2,2547	0,6197	1,6504
ESPL1	-2,2374	0,5529	1,6504
LRP2	-2,2345	0,3585	1,6504
CKMT1A	-2,2158	0,4632	2,7183
AURKA	-2,2059	0,5721	2,7183
XRCC2	-2,1585	0,6068	2,7183
RAD51	-2,1447	0,5892	2,7183
CDC20	-2,1423	0,6038	2,7183
XXXX	-2,1265	0,3711	2,7183
CLDN7	-2,0969	0,6278	2,7183

CCNA2	-2,0950	0,6304	2,7183
CDC25A	-2,0809	0,4679	2,7183
CCNE1	-2,0690	0,6563	3,3540
RAC3	-2,0562	0,6659	3,3540
SPC25	-2,0493	0,5334	3,3540
FAM83D	-2,0374	0,5635	3,3540
CDCA5	-2,0342	0,6320	3,3540
SLC39A6	-2,0298	0,5389	3,3540
MAD2L1	-2,0064	0,7090	3,3540
S100A14	-1,9716	0,4165	3,3540
HIST1H1C	-1,9444	0,7114	4,0184
CACNA1H	-1,9264	0,5746	4,0184
FOXA1	-1,9222	0,5335	4,0184
SLC44A4	-1,9180	0,5334	4,0184
PTTG1	-1,9137	0,6236	4,0184
ELF3	-1,9101	0,5335	4,0184
DNAJC12	-1,9006	0,4662	4,0184
BMP8A	-1,8781	0,5918	4,0184

**HIGH EXPRESSION: WORSE RESPONSE
(CHANGE OF ROR)**

GENE ID	Score(d)	Fold Change	q-value(%)
AGR2	-2,1867	0,2201	0,0000
ANLN	-4,0616	0,1686	0,0000
ASPM	-4,5378	0,1405	0,0000
ATAD2	-1,6544	0,4870	0,6006
ATP10B	-1,1587	0,5277	3,8765
AURKA	-3,9124	0,2218	0,0000
AURKB	-3,4464	0,2546	0,0000

BIRC5	-4,3676	0,1433	0,0000
BLM	-2,6624	0,3350	0,0000
BMP5	-1,4265	0,4343	1,0823
BMP8A	-1,6128	0,4477	0,6006
BRCA2	-2,5540	0,4069	0,0000
CACNG6	-1,3935	0,4274	1,0823
CALML5	-2,4628	0,1353	0,0000
CCL7	-1,1726	0,4693	3,8765
CCNA2	-3,7333	0,2710	0,0000
CCNB1	-3,1434	0,3144	0,0000
CCNE1	-3,0172	0,3408	0,0000
CCNE2	-1,2622	0,5909	1,9178
CD1E	-1,6431	0,4561	0,6006
CDC20	-3,6846	0,2543	0,0000
CDC25A	-3,3085	0,1656	0,0000
CDC25C	-3,4793	0,2305	0,0000
CDC6	-3,1520	0,3299	0,0000
CDCA1	-3,0195	0,2909	0,0000
CDCA5	-3,5930	0,2729	0,0000
CDH1	-1,2736	0,4804	1,9178
CDK1	-3,5917	0,2051	0,0000
CDKN2D	-1,2621	0,6228	1,9178
CDKN3	-2,5798	0,3470	0,0000
CEACAM5	-2,5542	0,1321	0,0000
CEACAM6	-1,2463	0,3352	1,9178
CENPF	-3,0524	0,2972	0,0000
CEP55	-4,0055	0,2136	0,0000
CHEK2	-2,0599	0,4954	0,0000
CKMT1A	-1,6776	0,3724	0,6006

CKS1B	-1,7692	0,5775	0,0000
CXCL10	-1,2649	0,4909	1,9178
CXCL9	-2,0943	0,3249	0,0000
DEPDC1	-3,1776	0,2613	0,0000
DLGAP5	-3,0942	0,2676	0,0000
DLL3	-2,2386	0,3304	0,0000
DUSP4	-1,1985	0,4950	3,8765
E2F1	-2,4840	0,3575	0,0000
EFNA3	-2,0110	0,4415	0,0000
ESPL1	-3,7373	0,2184	0,0000
ETV7	-1,2852	0,5942	1,9178
EXO1	-4,0743	0,1832	0,0000
EYA1	-1,3679	0,4625	1,9178
EYA4	-1,3682	0,4940	1,9178
FAM83D	-2,9039	0,2638	0,0000
FGF13	-1,5936	0,4558	0,6006
FGF9	-1,1634	0,4783	3,8765
XXXX	-1,7209	0,2818	0,0000
FLT3	-1,1071	0,5804	3,8765
FOXM1	-4,2957	0,1788	0,0000
FOXP3	-1,6565	0,4951	0,6006
FREM2	-1,3857	0,4387	1,9178
FUT3	-1,2853	0,4831	1,9178
FZD9	-1,0915	0,5923	3,8765
GATA4	-2,0732	0,3006	0,0000
GGH	-2,2863	0,4165	0,0000
GNLY	-1,0904	0,5966	3,8765
HAPLN1	-1,6287	0,4482	0,6006
HELLS	-2,0161	0,4896	0,0000

HIST1H1C	-1,4797	0,5789	1,0823
HIST1H2BH	-2,6486	0,4095	0,0000
HIST1H3H	-3,3076	0,2990	0,0000
HIST3H2BB	-1,7021	0,4699	0,0000
HOXB13	-1,5646	0,4599	0,6006
IBSP	-1,0949	0,5365	3,8765
IDO1	-2,1005	0,3586	0,0000
IGF1R	-1,2446	0,4532	1,9178
IL12RB2	-1,2202	0,5499	3,8765
IL20RB	-1,5481	0,5114	0,6006
IL22RA2	-1,7461	0,3856	0,0000
ITGB6	-1,3122	0,4657	1,9178
KIF11	-2,7310	0,3563	0,0000
KIF14	-3,6531	0,2188	0,0000
KIF23	-4,1138	0,1969	0,0000
KIF2C	-3,8687	0,2220	0,0000
KIFC1	-2,4102	0,3316	0,0000
KNTC2	-3,1073	0,2791	0,0000
LRP2	-1,1570	0,4214	3,8765
MAD2L1	-2,4538	0,4398	0,0000
MCM2	-2,0988	0,4937	0,0000
MCM3	-1,4069	0,6562	1,0823
MELK	-2,7119	0,3424	0,0000
MIS18A	-1,4331	0,6370	1,0823
MKI67	-3,8907	0,2104	0,0000
MMP11	-1,4162	0,3856	1,0823
MYBL2	-3,4819	0,2185	0,0000
MYCN	-1,8255	0,3925	0,0000
NEIL3	-3,2440	0,2701	0,0000

NRXN1	-1,3134	0,3928	1,9178
NRXN3	-2,0936	0,3436	0,0000
NUDT1	-1,1964	0,6961	3,8765
ORC6L	-2,3948	0,4063	0,0000
PALB2	-1,2624	0,6437	1,9178
PAX8	-1,2597	0,4966	1,9178
PCNA	-1,2395	0,6811	1,9178
PKMYT1	-3,7787	0,1890	0,0000
PLA2G4F	-1,7091	0,4687	0,0000
POLQ	-4,1987	0,1835	0,0000
PRC1	-3,7565	0,2547	0,0000
PSAT1	-1,0747	0,6152	3,8765
PTTG1	-4,2762	0,2166	0,0000
RAD51	-3,8249	0,2341	0,0000
RAD54L	-3,5010	0,2646	0,0000
RASAL1	-1,6540	0,4069	0,6006
RASGRF1	-2,2227	0,3457	0,0000
RBL1	-1,1524	0,6900	3,8765
RFC4	-1,4119	0,6572	1,0823
RNASE2	-1,1646	0,5544	3,8765
RPS6KB1	-1,1803	0,6409	3,8765
RRM2	-4,2255	0,1796	0,0000
SKA3	-3,3805	0,2017	0,0000
SMC1B	-1,2205	0,5570	3,8765
SPC25	-3,3173	0,2085	0,0000
SUV39H2	-1,4674	0,6121	1,0823
TFF1	-2,1506	0,2320	0,0000
TFF3	-1,5376	0,3552	1,0823
TLX1	-1,5560	0,4281	0,6006

TOP2A	-2,8664	0,2650	0,0000
TRIP13	-2,5718	0,3931	0,0000
TTK	-2,8532	0,3247	0,0000
TYMS	-2,4837	0,4026	0,0000
UBE2C	-4,3480	0,1353	0,0000
UBE2T	-3,6248	0,2224	0,0000
WNT2	-1,3644	0,5259	1,9178
WT1	-1,8774	0,3235	0,0000
XRCC2	-2,5734	0,3476	0,0000
XRCC3	-1,5828	0,5919	0,6006
ZIC2	-1,2827	0,4368	1,9178

Supplementary table 4. List of palbociclib resistant drivers identified by genome wide CRISPR/Cas9 screen in ZR75 (up) and BT474 (down) cells (Threshold: β palbo < -0,9; β control <0,9; genes interrogated in Breast Cancer360™).

ZR75 CRISPR/CAS9 SCREEN CANDIDATES

GENE	β control	β palbociclib	Difference
BMP6	-0,6447	-2,1631	-1,5184
TCF4	0,0919	-2,1419	-2,2338
GADD45A	0,5254	-2,1275	-2,6529
DSC2	0,1783	-1,9817	-2,1600
HDC	0,5610	-1,9810	-2,5420
BCAS1	0,0897	-1,8446	-1,9343
PIK3R3	-0,4280	-1,8157	-1,3877
SOCS2	-0,3704	-1,8031	-1,4327
ATP10B	-0,0620	-1,7463	-1,6843
PIK3R2	0,2466	-1,7195	-1,9661
PIK3CG	0,8194	-1,6720	-2,4914
SMAD3	-0,2542	-1,6168	-1,3626
PDCD1	-0,1082	-1,6109	-1,5027
STC1	-0,0524	-1,5962	-1,5438
CAV1	0,0063	-1,5793	-1,5856
CSF3R	0,2089	-1,5619	-1,7707
CDH1	-0,4340	-1,5040	-1,0700
ID4	0,1250	-1,4847	-1,6097

CDC25A	-0,2999	-1,4608	-1,1609
CCL21	0,1462	-1,4358	-1,5820
PDK4	-0,2767	-1,4240	-1,1473
LEF1	-0,3762	-1,3907	-1,0145
CD19	0,1347	-1,3895	-1,5242
CXCL5	0,1557	-1,3819	-1,5376
LTB	0,1783	-1,3660	-1,5442
ECM2	0,1289	-1,3505	-1,4794
POLQ	0,2965	-1,3460	-1,6425
GJB2	0,3139	-1,3436	-1,6575
PSMB9	0,3682	-1,3400	-1,7082
BMP4	0,5244	-1,3140	-1,8384
TNKS2	-0,1915	-1,2944	-1,1030
NOD2	-0,0137	-1,2722	-1,2584
ERBB4	0,5394	-1,2608	-1,8001
DUSP4	0,4121	-1,2568	-1,6689
LIF	0,1723	-1,2544	-1,4267
AGTR1	-0,0415	-1,2382	-1,1967
ROCK2	0,0674	-1,2222	-1,2896
ADAM12	0,2880	-1,2055	-1,4935
FAM214A	-0,1395	-1,1591	-1,0196
PTTG1	-0,1494	-1,1535	-1,0041
PBX3	0,2853	-1,1387	-1,4240
CDH2	0,2943	-1,1243	-1,4186

HDAC11	0,5354	-1,1170	-1,6524
TNFAIP6	0,3763	-1,1006	-1,4769
CLDN3	0,8191	-1,0850	-1,9041
MUS81	0,0031	-1,0647	-1,0679
PRKACA	0,2824	-1,0511	-1,3335
SMURF2	0,7638	-1,0173	-1,7811
HBB	0,6435	-1,0137	-1,6572
DHRS2	0,4970	-1,0078	-1,5048
FGL2	0,0592	-0,9951	-1,0543
CKS1B	0,5349	-0,9833	-1,5182
RASGRF2	0,5796	-0,9794	-1,5590
TYK2	0,2910	-0,9352	-1,2262
DLGAP5	0,3614	-0,9276	-1,2890
CCR5	0,3504	-0,9256	-1,2759
FHL1	0,6820	-0,9140	-1,5960
GZMB	0,7285	-0,9097	-1,6382
XXXX	0,0220	-0,9048	-0,9267

BT474 CRISPR/CAS9 SCREEN CANDIDATES

GENE	β control	β palbociclib	Difference
ACVRL1	0,1713	-3,2936	-3,4649
ID1	0,0426	-2,7496	-2,7921
PLCB1	-0,7178	-2,7268	-2,0090
ITGB6	0,4241	-2,7255	-3,1496
TP53	0,4702	-2,5961	-3,0663

ADAM12	-0,3117	-2,5855	-2,2738
PAX5	0,6374	-2,5589	-3,1963
THBS4	-0,3923	-2,5220	-2,1297
TIMP4	0,1003	-2,5102	-2,6105
PDCD1	-0,2287	-2,3210	-2,0922
COL27A1	0,2302	-2,2729	-2,5031
CD8A	0,0718	-2,2151	-2,2869
SNAI1	-0,5516	-2,1831	-1,6316
NSD1	-0,3682	-2,1543	-1,7860
DUSP4	-0,2546	-2,1400	-1,8855
SCARA5	-0,5271	-2,0830	-1,5558
B3GNT3	-0,8971	-2,0588	-1,1617
PYCARD	0,8000	-2,0345	-2,8345
TLR4	-0,7293	-2,0281	-1,2988
LEF1	0,0431	-1,9715	-2,0146
CDKN1A	0,8528	-1,9139	-2,7667
PIK3CA	0,2185	-1,8978	-2,1163
AGT	-0,0906	-1,8937	-1,8031
TTYH1	0,3140	-1,8785	-2,1924
CACNG1	0,7505	-1,8779	-2,6284
LTB	0,4988	-1,7950	-2,2938
LEPR	-0,7507	-1,7667	-1,0160
TSPAN7	-0,1810	-1,7255	-1,5445
MAPK1	0,4274	-1,7176	-2,1450
SMC1B	0,3824	-1,6822	-2,0646
HSPA2	0,7346	-1,6769	-2,4114
MSR1	-0,2141	-1,6735	-1,4594
LFNG	-0,2494	-1,6679	-1,4185
TCF4	-0,5407	-1,6631	-1,1224

PIK3R2	0,2071	-1,6578	-1,8649
HOXA9	0,1710	-1,6516	-1,8226
PSMB10	0,4817	-1,6372	-2,1190
GJB2	0,2548	-1,6330	-1,8878
BLM	0,8374	-1,6209	-2,4583
CNTFR	0,7374	-1,5650	-2,3024
LAMA3	0,8332	-1,5426	-2,3758
PRF1	-0,0078	-1,5325	-1,5247
COLEC12	0,5761	-1,5310	-2,1071
EFNA5	0,6351	-1,5290	-2,1640
SOCS1	-0,4358	-1,5286	-1,0928
EPAS1	0,7702	-1,5214	-2,2916
PAX8	-0,4283	-1,5083	-1,0800
ITPR1	-0,4245	-1,4765	-1,0519
DTX3	0,5474	-1,4418	-1,9892
DKK2	0,5572	-1,4274	-1,9846
RASGRP1	0,2340	-1,4169	-1,6510
CCNE1	0,6778	-1,4008	-2,0786
LTBP1	-0,0083	-1,3985	-1,3903
GRIN1	0,4357	-1,3983	-1,8340
NEIL2	-0,4662	-1,3884	-0,9222
PARP1	0,2333	-1,3815	-1,6148
GNLY	-0,1887	-1,3691	-1,1803
BNIP3	-0,2466	-1,3663	-1,1197
HLA-DQB1	0,7798	-1,3601	-2,1399
AREG	0,4575	-1,3497	-1,8071
HLA-DMB	-0,1560	-1,3367	-1,1807
BBOX1	0,7520	-1,3327	-2,0847
PDE9A	0,7356	-1,3316	-2,0672

E2F1	0,4787	-1,3074	-1,7861
TUBA4A	-0,0702	-1,2837	-1,2135
DLL3	0,5326	-1,2816	-1,8141
HLA-B	0,4298	-1,2472	-1,6770
TPSAB1	0,8141	-1,2168	-2,0309
EGLN3	0,2485	-1,2148	-1,4633
IL22RA2	-0,0087	-1,2009	-1,1921
SLC2A11	0,5938	-1,1831	-1,7769
PTEN	0,3215	-1,1685	-1,4901
FSTL1	0,3205	-1,1590	-1,4795
BTG2	-0,0232	-1,1589	-1,1357
NETO2	0,1102	-1,1540	-1,2643
CCL5	0,5687	-1,1505	-1,7192
IL1B	0,5442	-1,1414	-1,6856
RORA	0,2910	-1,1381	-1,4291
SFRP1	0,7031	-1,1019	-1,8050
CDKN3	0,3272	-1,0928	-1,4201
GSK3B	0,6228	-1,0922	-1,7150
MT1G	0,3344	-1,0910	-1,4254
DDR2	0,6747	-1,0797	-1,7544
CD27	0,1610	-1,0779	-1,2389
LAMB3	0,2954	-1,0662	-1,3616
MMP3	0,4573	-1,0534	-1,5107
STAT1	0,3204	-1,0396	-1,3601
CPA3	-0,0542	-1,0234	-0,9692
TSPAN1	-0,0623	-1,0173	-0,9550
NOTCH3	-0,0980	-1,0136	-0,9156
HLA-E	0,0672	-1,0086	-1,0758
RPS6KA5	0,6884	-1,0007	-1,6891

CCND2	0,0963	-0,9861	-1,0823
NFATC1	0,5800	-0,9810	-1,5610
FZD9	-0,0246	-0,9805	-0,9560
IFT140	0,0793	-0,9767	-1,0560
CD19	0,5581	-0,9750	-1,5331
CCR5	0,1372	-0,9639	-1,1011
BMP8A	0,3478	-0,9638	-1,3116
WNT11	0,4119	-0,9613	-1,3732
HIF1A	0,2683	-0,9390	-1,2074
IDO1	0,3840	-0,9290	-1,3130
IL2RA	0,1083	-0,9277	-1,0359

Supplementary table 5. List of XXXX interactors identified with the BioID experiments in MCF7 cells (up) and MCF7-PR (down). BFDR < 0,2109; fold change > 3).

MCF7 XXXX-BIOID-HA VS CONTROL			
Prey	Gene	Fold Change	BFDR
P22455	XXXX	369170,3	0
Q9UFC0	LRWD1	18614,8	0
Q8WVV4	POF1B	14594,1	0
Q8WU20	YYYY	11262,4	0
P19174	PLCG1	8993,4	0
Q07617	SPAG1	8060,9	0
Q9H1K0	RBSN	4391,7	0
P51812	RPS6KA3	3734,1	0
Q86X29	LSR	3219,0	0
Q8IZ21	PHACTR4	3147,1	0
Q9BPZ7	MAPKAP1	2457,8	0
Q96QD8	SLC38A2	2397,3	0
Q6R327	RICTOR	2261,4	0
Q5W0Z9	ZDHHC20	1686,0	0
Q8WVX9	FAR1	1643,7	0
Q9H267	VPS33B	1581,4	0
O75781	PALM	1361,8	0
O75396	SEC22B	1243,2	0
Q9NQS7	INCENP	1234,9	0
Q15835	GRK1	1230,0	0
Q9BZE1	MRPL37	990,6	0
Q9C0B5	ZDHHC5	987,1	0
Q13439	GOLGA4	901,8	0

Q8N4C8	MINK1	840,6	0
Q5M775	SPECC1	820,0	0
Q9UBI6	GNG12	747,1	0
Q8NFA0	USP32	693,1	0
Q6P996	PDXDC1	692,7	0
Q92665	MRPS31	627,7	0
P82673	MRPS35	609,3	0
Q9Y3P9	RABGAP1	496,9	0
Q16625	OCLN	490,5	0
P52569	SLC7A2	487,4	0
Q96Q05	TRAPPC9	453,1	0
O14683	TP53I11	436,9	0
Q2TAY7	SMU1	422,3	0
Q16698	DECR1	410,4	0
Q9NR48	ASH1L	408,6	0
O14924	RGS12	388,4	0
P35789	ZNF93	383,1	0
Q12788	TBL3	335,3	0
Q7Z7K6	CENPV	321,7	0
Q15633	TARBP2	242,6	0
Q9UNX4	WDR3	240,9	0
Q2M389	WASHC4	212,5	0
Q7Z3T8	ZFYVE16	194,0	0
Q86UU1	PHLDB1	186,8	0
Q53GA4	PHLDA2	92,8	0
O15126	SCAMP1	45,1	0
Q7L7X3	TAOK1	40,8	0
P02786	TFRC	36,4	0
O75110	ATP9A	33,3	0

Q96RT1	ERBIN	33,2	0
Q92609	TBC1D5	16,7	0
Q8N884	CGAS	16,2	0
Q9BV40	VAMP8	12,3	0
Q9NVF7	FBXO28	12,3	0
Q9NRW7	VPS45	10,6	0
Q12768	WASHC5	8,3	0
Q9HCU4	CELSR2	8,1	0
P50416	CPT1A	7,6	0
Q01831	XPC	7,5	0
P55327	TPD52	7,4	0
O00767	SCD	5,0	0
Q9H6F5	CCDC86	4,7	0
P11233	RALA	4,7	0
Q8TDM6	DLG5	4,5	0
Q07960	ARHGAP1	4,5	0
Q96SB3	PPP1R9B	4,4	0
Q5T0W9	FAM83B	4,4	0
Q15361	TTF1	3,7	0
Q14160	SCRIB	3,6	0
Q7KZI7	MARK2	3,3	0
O43399	TPD52L2	3,2	0
Q9H4M9	EHD1	3,1	0
Q13601	KRR1	3,2	0,0002
O60716	CTNND1	4,7	0,0003
Q8WYL5	SSH1	7,1	0,0005
Q96ME7	ZNF512	3,3	0,0018
O15417	TNRC18	3,7	0,0027
O15049	N4BP3	7,3	0,004

Q15418	RPS6KA1	5,8	0,0063
P49757	NUMB	10,9	0,0084
Q9Y446	PKP3	7,3	0,0135
Q9UPX8	SHANK2	4,6	0,0151
Q9Y2Q9	MRPS28	3,4	0,0168
Q2TB10	ZNF800	3,8	0,0256
Q8WVM8	SCFD1	3,3	0,0341
Q96FF7	MISP3	4,2	0,0502
Q96QD9	FYTTD1	3,3	0,0594
O43581	SYT7	4,4	0,0618
Q9H7N4	SCAF1	11,2	0,0644
Q99549	MPHOSPH8	4,5	0,0773
Q9Y2R9	MRPS7	5,8	0,0823
Q96EY7	PTCD3	5,1	0,0848
Q92552	MRPS27	3,8	0,0897
O94880	PHF14	4,2	0,0921
P82930	MRPS34	4,3	0,0992
Q9UHA3	RSL24D1	3,1	0,1319
Q9Y676	MRPS18B	3,1	0,1473
Q12933	TRAF2	3,5	0,1649

MCF7-PR XXXX-BIOID-HA VS CONTROL

Prey	Gene	Fold Change	BFDR
Q9UGI0	ZRANB1	6780,3	0
A1L170	C1orf226	2948,7	0
Q68D10	SPTY2D1	2015,0	0
P07339	CTSD	837,8	0

O75110	ATP9A	532,2	0
P22455	XXXX	270,3	0
Q9UHB7	AFF4	241,0	0
O00566	MPHOSPH10	2,6	0
Q9H2U1	DHX36	6,5	0,014
Q09161	NCBP1	3,6	0,0344
Q16401	PSMD5	2,4	0,1092
Q6P161	MRPL54	2,2	0,1906
Q93052	LPP	56406,7	0,2109
Q96GW7	BCAN	11279,3	0,2109
P59780	AP3S2	7421,7	0,2109
Q8WVV4	POF1B	5803,3	0,2109
P52943	CRIP2	4547,3	0,2109
Q9HCU4	CELSR2	2927,6	0,2109
Q8N0Z8	PUSL1	2517,5	0,2109
Q9UPQ3	AGAP1	2489,0	0,2109
Q15382	RHEB	2409,0	0,2109
Q6P6C2	ALKBH5	1761,9	0,2109
O95427	PIGN	1543,5	0,2109
Q9H0C5	BTBD1	1534,4	0,2109
O75363	BCAS1	1429,0	0,2109
O15126	SCAMP1	1317,4	0,2109
Q06265	EXOSC9	1315,5	0,2109
Q96GC5	MRPL48	1177,1	0,2109
Q7Z4S6	KIF21A	1170,5	0,2109
Q9UIS9	MBD1	1117,8	0,2109
Q9Y450	HBS1L	1103,2	0,2109
Q8WVM8	SCFD1	1063,5	0,2109
Q9H9B1	EHMT1	1011,9	0,2109

P57772	EEFSEC	914,3	0,2109
Q96FX7	TRMT61A	902,6	0,2109
Q8N5M9	JAGN1	812,2	0,2109
P10253	GAA	773,6	0,2109
Q96K37	SLC35E1	758,8	0,2109
Q6AHZ1	ZNF518A	725,5	0,2109
O60524	NEMF	683,7	0,2109
Q13029	PRDM2	678,0	0,2109
Q9NTI5	PDS5B	654,6	0,2109
Q8IV04	TBC1D10C	626,0	0,2109
Q9NQT4	EXOSC5	624,8	0,2109
Q8N8U2	CDYL2	561,1	0,2109
P40222	TXLNA	550,8	0,2109
Q9UL54	TAOK2	539,1	0,2109
P02792	FTL	447,0	0,2109
P55327	TPD52	429,2	0,2109
Q5T9C2	FAM102A	401,9	0,2109
Q6R327	RICTOR	393,4	0,2109
Q9BY44	EIF2A	381,9	0,2109
Q9NVZ3	NECAP2	360,4	0,2109
Q8WU20	YYYY	335,3	0,2109
P08651	NFIC	289,4	0,2109
Q15418	RPS6KA1	282,8	0,2109
P49590	HARS2	247,7	0,2109
Q8NFV4	ABHD11	241,1	0,2109
P78356	PIP4K2B	216,7	0,2109
P19174	PLCG1	194,5	0,2109
Q96RL1	UIMC1	181,8	0,2109
Q96Q05	TRAPPC9	143,2	0,2109

Q9UPX8	SHANK2	130,2	0,2109
Q8N1G2	CMTR1	117,9	0,2109
Q9BXB1	LGR4	33,1	0,2109
Q14244	MAP7	18,0	0,2109
O75083	WDR1	14,0	0,2109
Q13618	CUL3	10,9	0,2109
Q8TBA6	GOLGA5	10,0	0,2109
Q9P2J8	ZNF624	8,2	0,2109
Q8TF76	HASPIN	5,9	0,2109
O76062	TM7SF2	5,8	0,2109
Q9NPI1	BRD7	5,6	0,2109
Q9H6R4	NOL6	5,4	0,2109
Q9NR31	SAR1A	5,4	0,2109
Q96RT1	ERBIN	5,2	0,2109
P09972	ALDOC	4,9	0,2109
Q86U06	RBM23	4,9	0,2109

Supplementary table 6. List of genes differentially expressed in cell lines with XXXX downregulated. Genes interrogated with nCounter included PAM50 signature. Seventeen genes were found significantly changed upon XXXX silencing with p-value < 0,05.

GENE	SCORE(D)	NUMERATOR(R)	P-VALUE
BAG1	3,7166	0,7074	0
XXXX	-9,9806	-2,1275	0
CCNE1	-3,4347	-0,3770	0
CDCA1	-3,3380	-0,5130	0
CDC20	-3,3369	-0,3612	0
ORC6L	-3,1988	-0,3499	0
EGFR	-2,4720	-0,3094	0
CDC6	-2,4363	-0,2981	0
ANLN	-2,3238	-0,2300	0
SLC39A6	-2,2086	-0,5177	0
EXO1	-1,9942	-0,2511	0
MELK	-1,7932	-0,1992	0
AR	-1,7866	-0,2105	0
MMP11	-1,7614	-0,4391	0
PHGDH	-1,6969	-0,5591	0
UBE2C	-1,6330	-0,1761	0
TYMS	-1,5800	-0,2144	0
MYBL2	-1,5439	-0,2766	0,0656
PTTG1	-1,5150	-0,1683	0,0656
RRM2	-1,4390	-0,2273	0,0656
CENPF	-1,4167	-0,1690	0,0656
KIF2C	-1,4064	-0,2185	0,0656
MKI67	-1,2869	-0,2403	0,0656

CCNB1	-1,2305	-0,1238	0,0656
UBE2T	-1,2258	-0,1136	0,0656
BIRC5	-1,2218	-0,1814	0,0656
CEP55	-1,1312	-0,1305	0,0656
GPR160	2,5466	0,1806	0,0888
MDM2	2,3819	0,2597	0,0888
ERBB2	-1,0071	-0,1086	0,0888
CD274	-0,8185	-0,1488	0,1620
KNTC2	-0,7387	-0,0866	0,1620
TMEM45B	-0,5223	-0,1045	0,1620
ACTR3B	-0,4064	-0,0662	0,1620
BCL2	-0,3656	-0,0797	0,1620
NAT1	-0,3326	-0,0498	0,1620
FOXA1	-0,2341	-0,0194	0,1620
MYC	-0,1699	-0,0273	0,1620
PGR	1,8574	0,2908	0,1705
CD8A	1,6791	0,3640	0,1705
KRT14	1,5178	0,1917	0,1705
MAPT	1,4374	0,2692	0,2001
CXXC5	1,3456	0,2105	0,2001
KRT17	1,2504	0,2462	0,2001
MIA	1,1287	0,1920	0,2135
MLPH	1,1068	0,1510	0,2135
ESR1	1,0569	0,1074	0,2135
GRB7	0,8703	0,1337	0,2395
FOXC1	0,8441	0,1218	0,2395
BLVRA	0,8147	0,0659	0,2395
CDH3	0,5573	0,0683	0,2869
PDCD1	0,3919	0,0920	0,2869

SFRP1	0,3459	0,0487	0,2869
KRT5	0,2086	0,0551	0,2869
CD4	0,1317	0,0320	0,2869